University of Tennessee, Knoxville

TRACE: Tennessee Research and Creative Exchange

Doctoral Dissertations

Graduate School

12-2016

Synthesis and Behavior of Stimuli-Responsive Shape-Changing Linear Molecular Bottlebrushes

Daniel Mark Henn
University of Tennessee, Knoxville, dhenn@vols.utk.edu

Follow this and additional works at: https://trace.tennessee.edu/utk_graddiss

Part of the Polymer Chemistry Commons

Recommended Citation

Henn, Daniel Mark, "Synthesis and Behavior of Stimuli-Responsive Shape-Changing Linear Molecular Bottlebrushes. " PhD diss., University of Tennessee, 2016.
https://trace.tennessee.edu/utk_graddiss/4096

This Dissertation is brought to you for free and open access by the Graduate School at TRACE: Tennessee Research and Creative Exchange. It has been accepted for inclusion in Doctoral Dissertations by an authorized administrator of TRACE: Tennessee Research and Creative Exchange. For more information, please contact trace@utk.edu.

To the Graduate Council:

I am submitting herewith a dissertation written by Daniel Mark Henn entitled "Synthesis and Behavior of Stimuli-Responsive Shape-Changing Linear Molecular Bottlebrushes." I have examined the final electronic copy of this dissertation for form and content and recommend that it be accepted in partial fulfillment of the requirements for the degree of Doctor of Philosophy, with a major in Chemistry.

Bin Zhao, Major Professor

We have read this dissertation and recommend its acceptance:

Mark D. Dadmun, George K. Schweitzer, Hong Guo

Accepted for the Council:

Carolyn R. Hodges

Vice Provost and Dean of the Graduate School

(Original signatures are on file with official student records.)

Synthesis and Behavior of Stimuli-Responsive Shape-Changing Linear Molecular Bottlebrushes

A Dissertation Presented for the

Doctor of Philosophy

Degree

The University of Tennessee, Knoxville

Daniel Mark Henn

December 2016

Acknowledgements

I would first like to express my gratitude to Professor Bin Zhao for your invaluable advice, support, and instruction throughout my graduate school career. You taught me how to be a scientist, how to solve problems and how to learn from setbacks. Your excitement for chemistry and dedication to learning and teaching is an inspiration, and the high standard that you set for not only scientific research but also professionalism I'm sure will benefit me for my entire life.

Additionally, this would not have been possible without the help of my committee members: Professor Mark Dadmun, Professor George Schweitzer, and Professor Hong Guo. Each of you have been generous with your time and advice, and I appreciate the expertise and insight you all bring to our conversations. I would like to give a special thanks to Professor Schweitzer, who has been an early mentor in my chemistry career. Thank you for the opportunity to work as an undergraduate student in your lab, where I was introduced to how scientific research is done and how rewarding it can be. Your enthusiasm and encouragement both in the lab and the classroom I will be forever grateful for.

Thanks to our collaborators, Professor Christopher Li and Shan Mei, for your suggestions and help with AFM.

Thank you to Dr. Ke An; learning from and working with you was a great experience.

I also thank the Department of Chemistry and the National Science Foundation, without which this work could not have been accomplished.

I want to acknowledge both past and present group members whose advice, help, and kinship have been so valuable: Dr. Niaxiong Jin, Dr. Jeremiah Woodcock, Dr. Jonathan Horton, Dr. Chunhui Bao, Dr. Xueguang Jiang, Dr. Roger Wright, Dr. Bin Hu, Sisi Jiang, Bryan Seymour, Ethan Kent, Jessica Holmes, Maggie Lau, Dr. Wenxin Fu, Dr. Chunhui Luo, and Dr. Kewei Wang.

I have to thank my family for whose support has been unwavering. Thanks to my father Mark Henn and my step mother Ann Avery. Without you, this could not have been possible. You both have given me so much encouragement and advice during this time and throughout my life. Thank you to my mother Jan Henn who was my first lab partner. I couldn't possibly repay you all for what you have done for me. Thanks also to my mother and father in law, Joy and Kirk Parrott, who have been so supportive.

Finally, I want to thank my favorite person of all, my wife, Taylor. Your presence in this cannot be described.

Abstract

Molecular bottlebrushes are composed of polymer side chains densely grafted to a macromolecular backbone. The main focus of this dissertation work is the synthesis and behavior of linear molecular brushes that can undergo unimolecular size and shape changes in response to environmental stimuli in dilute aqueous solution. Chapter 1 provides an introduction to molecular bottlebrushes and stimuli-responsive polymers.

Chapter 2 presents the development of a robust method for the synthesis of well-defined molecular brushes by a "grafting to" approach using copper-catalyzed azide-alkyne cycloaddition "click" reactions. Well-defined, new azide-containing backbone polymers with different lengths and high degrees of azide functionality were synthesized. Using alkyne end-functionalized poly(ethylene oxide) (PEO) as model side chain polymer, homografted molecular brushes with nearly quantitative grafting densities were prepared when a molar ratio of approximately 1 : 2 for backbone monomer units to side chains was adopted, and the grafting density can be readily tuned by adjusting this ratio.

Chapters 3 and 4 extend the methodology to stimuli-responsive molecular bottlebrushes. Homografted molecular brushes were prepared with side chains composed of either thermosensitive poly(di(ethylene glycol) ethyl ether acrylate) (PDEGEA), thermo- and light-responsive poly((di(ethylene glycol) methyl ether acrylate)-*co*-(*o*-nitrobenzyl acrylate)) (P(DEGMA-*co*-NBA)), or pH-responsive poly(*N*,*N*-diethylaminoethyl methacrylate) (PDEAEMA). High grafting density brushes were achieved, and their dramatic size changes were observed in response to applied stimuli in aqueous solution. Chapter 4 details the preparation of binary heterografted molecular brushes containing PEO and stimuli-responsive PDEGEA, PDEAEMA, or PNBA side chains randomly distributed along the backbone. Compared with

homografted brushes, the collapsed state was stabilized by PEO side chains. These brushes underwent size and shape transitions from an extended worm-like state to a collapsed, roughly spherical state, and we demonstrated that this shape-changing can be exploited to control binding between biotin-containing molecular brushes and avidin.

Chapter 5 focuses on stimuli-responsive hydrogels based on tertiary amine-containing ABA triblock copolymers containing a PEO central block and thermo- and pH-sensitive outer blocks. The effect of different tertiary amines on thermally induced sol-gel transitions of moderately concentrated aqueous solutions was investigated. Chapter 6 provides a summary this dissertation work and future prospects.

Table of Contents

Chapter 1: Introduction……1

1.1. Introduction…….....……...2

1.1.1. Introduction to Polymer Brushes…….…….2

1.1.2. Introduction to Molecular Brushes…….…….…….5

1.1.3. Stimuli-Responsive Molecular Brushes…...……..……...9

1.1.3.1. Stimuli-Responsive Polymers……..…….9

1.1.3.2. Synthesis and Behavior of Stimuli-Responsive Molecular Brushes……..….13

1.1.3.3. The Von Willibrand Factor (VWF) as an Intriguing Biopolymer and an inspiration for Stimuli-Responsive Shape Changing of Synthetic Macromolecules...18

1.1.4. Thermosensitive Hydrophilic Block Copolymer Hydrogels……..21

1.2. Dissertation Overview……26

References…….30

Chapter 2: Water-Soluble Poly(ethylene oxide) Homografted Linear Molecular Brushes with High and Tunable Grafting Densities Synthesized by a "Grafting To" Method…..35

Abstract…….36

2.1. Introduction……38

2.2. Experimental Section…….41

2.2.1. Materials…….41

2.2.2. General Characterization……43

2.2.3. Synthesis of Tri(ethylene glycol) Mono(*t*-butyldimethylsilyl) Ether (TEGSi)….….43

2.2.4. Synthesis of Tri(ethylene glycol) Mono(*t*-butyldimethylsilyl) Ether Methacrylate (TEGSiMA)……..44

2.2.5. Synthesis of Silyl Ether-Protected Backbone Polymers: Poly(tri(ethylene glycol) mono(*t*-butyldimethylsilyl) ether methacrylate) (PTEGSiMA)……...45

2.2.6. Synthesis of Azide-Functionalized Backbone Polymers: PTEGN_3MA…….46

2.2.7. Synthesis of Alkyne End-Functionalized Water-Soluble PEO Side Chain Polymers……...47

2.2.8. Synthesis of Water-Soluble PEO Homografted Molecular Brushes……..48

2.2.9. Atomic Force Microscopy (AFM) of PEO Molecular Brushes……..49

2.3. Results and Discussion……...49

2.3.1. Synthesis of Azide-Functionalized Backbone Polymers (PTEGN_3MA)……....49

2.3.2. Synthesis of Alkyne-End Functionalized Water Soluble PEO Side Chain Polymers……...…59

2.3.3. Synthesis of Water-Soluble PEO Homografted Molecular Brushes from PEO-45....59

2.3.4. Synthesis of Water-Soluble PEO Homografted Molecular Brushes from PEO-114..67

2.3.5. AFM of Water-Soluble PEO Homografted Molecular Brushes…….…75

2.4. Conclusions……78

References…….80

Appendix A……...83

A.1. Example Calculation of Grafting Density of PEO Homografted Molecular Brushes..84

A.2. Supplemental Figures……...…....85

Chapter 3: Synthesis and Characterization of Stimuli-Responsive Homografted Linear Molecular Brushes with High and Tunable Grafting Densities……..91

Abstract……...……..92

3.1. Introduction……94

3.2. Experimental Section…….…99

3.2.1. Materials…….…99

3.2.2. General Characterization……..100

3.2.3. Synthesis of Propargyl 2-Bromoisobutyrate (PBiB)……....101

3.2.4. Synthesis of Propargyl 4-Cyano-4-(phenylcarbonothioylthio)pentanoate PCPP)...101

3.2.5. Synthesis of Thermosensitive Side Chain Polymers by ATRP……102

3.2.6. Synthesis of Dual Thermo- and Light-Responsive Side Chain Polymer by ATRP.103

3.2.7. Synthesis of pH-Responsive Side Chain Polymer by RAFT Polymerization……..103

3.2.8. Synthesis of Stimuli-Responsive Homografted Molecular Brushes…….104

3.2.9. Atomic Force Microscopy of PDEGEA Molecular Brushes……....105

3.2.10. Dynamic Light Scattering Study of Stimuli-Responsive Molecular Brushes in Water…….….105

3.3. Results and Discussion…….106

3.3.1. Synthesis of Azide-Functionalized Backbone Polymers (PTEGN_3MA)……..106

3.3.2. Synthesis of Alkyne End-Functionalized Stimuli-Responsive Side Chain Polymers…….107

3.3.3. Synthesis of Thermosensitive PDEGEA Homografted Molecular Brushes…….110

3.3.4. Thermosensitive Properties of PDEGEA Homografted Molecular Brushes…...….118

3.3.5. Synthesis of Dual Thermo- and Light-Responsive P(DEGEA-*co*-NBA) Homografted Molecular Brushes……...……..120

3.3.6. Thermo- and Light-Responsive Properties of P(DEGEA-*co*-NBA) Homografted Molecular Brushes…….……123

3.3.7. Synthesis of pH-Responsive PDEAEMA Homografted Molecular Brushes…...…127

3.3.8. pH-Responsive Properties of PDEAEMA Homografted Molecular Brushes……..130

3.4. Conclusions……...……..132

References……...135

Appendix B…...……139

B.1. Example Calculation of Grafting Density of Stimuli-Responsive Homografted Molecular Brushes…….....140

B.2. Supplemental Figures……...…...141

Chapter 4: Synthesis and Behavior of Stimuli-Responsive Shape-Changing Binary Heterografted Linear Molecular Brushes……...……....148

Abstract……...149

4.1. Introduction……..151

4.2. Experimental Section……...……157

4.2.1. Materials……...…157

4.2.2. General Characterization……..158

4.2.3. Synthesis of 2-(Acryloyloxyethyl) 5-((3a*S*,4*S*,6a*R*)-2-oxohexahydro-1*H*-thieno[3,4-*d*]imidazole-4-yl)penanoate (D-Biotin Oxyethyl Acrylate, BA)…….…..159

4.2.4. Synthesis of 4-(2-Acryloyloxyethylamino)-7-nitro-2,1,3-benzoxodiazole (NBDA)……...…160

4.2.5. Synthesis of Thermosensitive PDEGEA Side Chain Polymer……...…..161

4.2.6. Synthesis of Light-Responsive PNBA Side Chain Polymer……...….161

4.2.7. Synthesis of Thermosensitive P(DEGEA-*co*-BA-*co*-NBDA) Side Chain Polymer.162

4.2.8. Synthesis of Stimuli-Responsive Binary Heterografted Molecular Brushes……..…163

4.2.9. Dynamic Light Scattering Study of Stimuli-Responsive Binary Heterografted

Molecular Brushes in Water……...……164

4.2.10. Atomic Force Microscopy Study of Binary Heterografted Molecular Brushes…..165

4.2.11. FRET Study of PEO/P(DEGEA-*co*-BA-*co*-NBDA) Binary Heterografted Molecular Brushes and Rhodamine-Labelled Avidin D…….165

4.3. Results and Discussion…….166

4.3.1. Synthesis of Azide-Functionalized Backbone Polymers PTEGN_3MA……....166

4.3.2. Synthesis of Alkyne End-Functionalized Stimuli-Responsive and Water-Soluble Side Chain Polymers……..……167

4.3.3. Synthesis of Thermosensitive PEO/PDEGEA Binary Heterografted Molecular Brushes……...172

4.3.4. Thermosensitive Properties of PEO/PDEGEA Binary Heterografted Molecular Brushes……...177

4.3.5. Synthesis of pH-Responsive PEO/PDEAEMA Binary Heterografted Molecular Brushes……...181

4.3.6. pH-Responsive Properties of PEO/PDEAEMA Binary Heterografted Molecular Brushes……...189

4.3.7. Synthesis of Light-Responsive PEO/PNBA Binary Heterografted Molecular Brushes……...193

4.3.8. Light-Responsive Properties of PEO/PNBA Binary Heterografted Molecular Brushes……..…198

4.3.9. Synthesis of Thermosensitive Binary Heterografted Molecular Brushes Composed of PEO and Biotin- and Fluorescent Dye NBD-Containing P(DEGEA-*co*-BA-*co*-NBDA)……...204

4.3.10. Thermosensitive Properties of PEO/P(DEGEA-*co*-BA-*co*-NBDA) Binary Heterografted Molecular Brushes…….……..…209

4.3.11. FRET Study of Thermo-Regulated Binding Between Biotin-Containing PEO/P(DEGEA-*co*-BA-*co*-NBDA) Binary Heterografted Molecular Brushes and Avidin…….218

4.4. Conclusions……..224

References……...226

Appendix C…...…….229

C.1. Example Calculation of Grafting Density of Binary Heterografted Molecular Brushes……...230

C.2. Supplemental Figures……...…...231

Chapter 5: Tertiary Amine-Containing Thermo- and pH-Sensitive Hydrophilic ABA Triblock Copolymers: Effect of Tertiary Amines on Thermally Induced Sol-Gel Transitions…….243

Abstract……...244

5.1. Introduction……..246

5.2. Experimental Section……...…250

5.2.1. Materials……...250

5.2.2. General Characterization……..251

5.2.3. Synthesis of P(DEGMMA-*co*-DEGEMA-*co*-DEAEMA)-*b*-PEO-*b*-P(DEGMMA-*co*-DEGEMA-*co*-DEAEMA) (ABA DEA-1)…….251

5.2.4. Preparation of 10 wt % Aqueous Solutions of Tertiary Amine-Containing, Thermo- and pH-Responsive ABA Triblock Copolymers……..…..252

5.2.5. Rheological Measurements……...253

5.2.6. Controlled Release of FITC-Dextran from 10 wt % Thermo- and pH-Responsive ABA Triblock Copolymer Hydrogels……253

5.3. Results and Discussion…….254

5.3.1. Synthesis and Characterization of Tertiary Amine-Containing Thermo- and pH-Responsive Hydrophilic ABA Triblock Copolymers……254

5.3.2. pH Dependence of Sol-Gel Transition of 10 wt % Aqueous Solution of ABA-DEA-1……..259

5.3.3. pH Dependence of $T_{\text{sol-gel}}$ of 10 wt % aqueous solutions of ABA-DPA-2 and ABA-DBA-3 and Comparison with ABA-DEA-1……....264

5.3.4. Controlled Release of FITC-Dextran from 10 wt % Thermo- and pH-Responsive ABA Triblock Copolymer Micellar Hydrogels of ABA-DEA-1, ABA-DPA-2, and ABA-DBA-3……..…271

5.3.5. Stability of a 10 wt % Aqueous Solution of ABA-DEA-1 at low pH……..274

5.4. Conclusions……..274

References……...278

Appendix D…….281

Chapter 6: Conclusions and Future Work……..286

References……...…292

Vita……..…294

List of Tables

2.1. Characterization Data for Azide-Functionalized Backbone PTEGN_3MA Polymers and Their PTEGSiMA Precursors…….……58

2.2. Characterization Data for Alkyne End-Functionalized Water-Soluble PEO Side Chain Polymers……..……..62

2.3. PEO Molecular Brushes from PEO-45 with Different Grafting Densities and Backbone Lengths Synthesized by "Grafting To" Using CuAAC "Click" Reactions……..……...64

2.4. PEO Molecular Brushes from PEO-114 with Different Grafting Densities and Backbone Lengths Synthesized by "Grafting To" Using CuAAC "Click" Reactions……..……...69

3.1. Characterization Data for Alkyne End-Functionalized Stimuli-Responsive Side Chain Polymers Synthesized by ATRP and RAFT Polymerization…..……..111

3.2. PDEGEA Molecular Brushes with Different Grafting Densities and Side Chain Lengths Synthesized by "Grafting To" Using CuAAC "Click" Reactions……..…...114

3.3. Characterization Data for P(DEGMA-*co*-NBA) and PDEAEMA Molecular Brushes.....124

4.1. Characterization Data for Alkyne End-Functionalized Stimuli-Responsive and Water-Soluble Side Chain Polymers……...171

4.2. Characterization Data for Stimuli-Responsive Binary Heterografted Molecular Brushes…….174

5.1. Characterization Data for Tertiary Amine-Containing Thermo- and pH-Sensitive Hydrophilic ABA Triblock Copolymers……..260

5.2. The Fitted Values of A_1, A_2, x_0, and dx from Fitting the pH Dependences of $T_{sol\text{-}gel}$ for ABA Triblock Copolymers Using Boltzmann Function……...….266

List of Figures

1.1. (A) Optical photographs showing the reversible clear-to-cloudy transition of a solution of a thermosensitive polymer in water. (B) Illustration of the thermo-induced coil-to-globule transition of PNIPAAm accompanied by "melting" of ordered water around hydrophobic moieties. ……....12

1.2. AFM height images showing the worm-to-sphere transition of thermosensitive homografted molecular brushes with PNIPAM side chains cast from water at 20 ^{o}C (left) and 38 ^{o}C (right)…….……15

1.3. (Top) Optical photographs showing sol-gel-sol-cloudy transitions 20 wt % aqueous solutions of a doubly thermo- and pH-responsive P(TEGMA-*co*-AA)-*b*-P(DEGEA-*co*-AA) diblock copolymer. (Bottom) Schematic illustration of the transitions from a clear molecular solution to a clear molecular sol, clear micellar close-pack gel, back to a clear micellar sol, and finally a cloudy phase-separated mixture upon increases in temperature……24

1.4. Sol-gel-sol transitions of ABA triblock copolymers with doubly thermo- and light-responsive outer blocks……..…25

2.1. (A) ^{1}H NMR and (B) ^{13}C NMR spectra of TEGSiMA monomer in $CDCl_3$……...……..53

2.2. (A) SEC traces and (B) ^{1}H NMR spectra ($CDCl_3$ solvent) of PTEGSiMA-527 and PTEGSiMA-800 backbone polymer precursors. SEC analysis was carried out using a PL GPC-20 system with THF as the mobile phase……...……55

2.3. (A) SEC traces of azide-functionalized backbone polymers PTEGN_3MA-527 and PTEGN_3MA-800. SEC analysis was performed using PL GPC-50 Plus system with Agilent Mixed-B columns and DMF containing 50 mM LiBr as solvent. (B) ^{1}H NMR spectra in

$CDCl_3$ of $PTEGN_3MA$-527, PTESiGMA-527, and the tosylated backbone intermediate PTEGTsMA-527…….……...57

2.4. (A) SEC trace of alkyne-end-functionalized PEO side chain polymers with a DP's of 45 (PEO-45) and 114 (PEO-114). (B) ^1H NMR spectrum of PEO-45 in $CDCl_3$. (C) Zoomed in portion of the ^1H NMR spectrum of PEO-45 showing peaks from end groups. SEC analysis was carried out on PL GPC-20 system using THF as carrier solvent……...…..…61

2.5. Plot of grafting density versus the molar ratio of PEO-45 side chains to backbone monomer units in the feed for PEO molecular brushes prepared from PEO-45……..64

2.6. SEC traces of the reaction mixture at different reaction times from the synthesis of (A) PEO MB-1 as well as $PTEGN_3MA$-527 backbone polymer and (B) PEO MB-2 as well as $PTEGN_3MA$-800 backbone polymer. SEC analysis was performed using PL GPC-50 Plus system with Agilent Mixed-B columns in DMF with 50 mM LiBr……..……...65

2.7. Plot of grafting density versus the molar ratio of PEO-114 side chains to backbone monomer units in the feed for PEO molecular brushes prepared from PEO-114 and (A) $PTEGN_3MA$-527 and (B) $PTEGN_3MA$-800……..69

2.8. (A) SEC traces of PEO MB-6 before and after purification by centrifugal filtration. (B) ^1H NMR spectrum of purified PEO MB-6 (in $CDCl_3$). (C) SEC traces of PEO MB-10 before and after purification by centrifugal filtration. SEC analysis was performed using PL GPC-50 Plus system with Agilent Mixed-B columns in DMF with 50 mM LiBr……....70

2.9. SEC traces before and after centrifugal filtration for (A) PEO MB-11, which was not capped with propargyl alcohol, and (B) PEO MB-12, which was capped with propargyl alcohol. SEC analysis was performed using PL GPC-50 Plus system with Agilent Mixed-B columns in DMF with 50 mM LiBr…….....……74

2.10. Representative AFM height images of PEO MB-6 spin cast onto freshly cleaved mica from a 0.1 mg/g solution in water……...…76

2.11. Representative AFM height images of PEO MB-6 spin cast onto freshly cleaved mica from a 0.01 mg/g solution in water……..……....77

A1. ^{1}H NMR spectra of (A) PTEGTsMA-800 and (B) PTEGN_3MA-800 ($CDCl_3$ solvent)…...85

A2. ^{1}H NMR spectrum of PEO-114 in $CDCl_3$…….……..85

A3. SEC traces of mixtures of 152 kDa and 8 kDa polystyrene polymers with different compositions (top) and summary of composition by mass and peak area ratio, determined by SEC, for each sample. SEC analysis was carried out on PL GPC-20 system using THF as carrier solvent…….……....86

A4. SEC traces of the reaction mixture for the synthesis of PEO MB-3 after 2 h and 4 h reaction time. SEC analysis was carried out on PL GPC-50 Plus system with Agilent Mixed-B columns using DMF containing 50 mM LiBr as carrier solvent…….....87

A5. SEC trace of the reaction mixture for the synthesis of PEO MB-4 after 24 h reaction time. SEC analysis was carried out on PL GPC-50 Plus system with Agilent Mixed-B columns using DMF containing 50 mM LiBr as carrier solvent……..……..87

A6. SEC traces of the reaction mixture for the synthesis of PEO MB-5 after 2 h and 4 h reaction time. SEC analysis was carried out on PL GPC-50 Plus system with Agilent Mixed-B columns using DMF containing 50 mM LiBr as carrier solvent…….……88

A7. SEC trace of the reaction mixture for the synthesis of PEO MB-7 after 24 h reaction time. SEC analysis was carried out on PL GPC-50 Plus system with Agilent Mixed-B columns using DMF containing 50 mM LiBr as carrier solvent……..……..88

A8. SEC traces of the reaction mixture for the synthesis of PEO MB-8 (not capped with propargyl alcohol) before and after six rounds of centrifugal filtration. SEC analysis was carried out on PL GPC-50 Plus system with Agilent Mixed-B columns using DMF containing 50 mM LiBr as carrier solvent…….……89

A9. SEC traces of the reaction mixture for the synthesis of PEO MB-9 (not capped with propargyl alcohol) before and after six rounds of centrifugal filtration. SEC analysis was carried out on PL GPC-50 Plus system with Agilent Mixed-B columns using DMF containing 50 mM LiBr as carrier solvent……..…….89

A10. SEC traces of the reaction mixture for the synthesis of PEO MB-13 (not capped with propargyl alcohol) before and after six rounds of centrifugal filtration. SEC analysis was carried out on PL GPC-50 Plus system with Agilent Mixed-B columns using DMF containing 50 mM LiBr as carrier solvent……..…….90

3.1. (A) SEC trace of side chain polymer PDEGEA-36 from SEC analysis using PL GPC-20 system with THF as mobile phase and (B) ^{1}H NMR spectrum of PDEGEA-36 in $CDCl_3$……...109

3.2. (A) SEC traces of the reaction mixture at different reaction times from the reaction for the synthesis of PDEGEA MB-1 molecular brushes and PTEGN_3MA-527 backbone polymer as well as the purified PDEGEA MB-1 after the removal of excess side chain polymer PDEGEA-36 by fractionation. SEC analysis was performed using PL GPC-50 Plus system with Agilent Mixed-B columns in DMF with 50 mM LiBr. (B) ^{1}H NMR spectrum of the purified PDEGEA MB-1 in $CDCl_3$. ……...….…113

3.3. (A) Plot of grafting density versus the molar ratio of PDEGEA-36 to backbone monomer units for PDEGEA molecular brushes prepared from PDEGEA-36 side chains and

PTEGN$_3$MA-527 or PTEGN$_3$MA-800 backbone. (B) Plot of grafting density versus PDEGEA side chain length for PDEGEA molecular brushes prepared from PTEGN$_3$MA-527 backbone and PDEGEA-36, PDEGEA-59, or PDEGEA-82 side chains……..….114

3.4. AFM height images of PDEGEA MB-8 spin cast onto a silicon wafer from a 0.1 mg/g aqueous solution at 0 °C…….……..117

3.5. Apparent hydrodynamic diameter (D_h) of PDEGEA MB-1 (A) and PDEGEA MB-8 (B) in a 0.2 mg/g aqueous solution at different temperatures obtained from dynamic light scattering experiments……...……119

3.6. (A) SEC traces of P(DEGMA-*co*-NBA) MB-9 before and after the removal of excess P(DEGMA-*co*-NBA)-47 side chains by fractionation. (B) ^{1}H NMR spectrum of purified P(DEGMA-*co*-NBA) MB-9 in CDCl$_3$. SEC analysis was performed using PL GPC-50 Plus system with Agilent Mixed-B columns and DMF with 50 mM LiBr as carrier solvent…….….122

3.7. Apparent hydrodynamic diameter of (A) P(DEGMA-*co*-NBA) MB-9 and (B) MB-10, obtained from DLS studies of 0.2 mg/g aqueous solutions, as a function of temperatures before and after irradiation with 365 nm UV light at ambient temperature for 1 h...…….125

3.8. (A) ^{1}H NMR spectra of PDEAEMA-43 and the final reaction mixture for the synthesis of PDEAEMA MB-11 in CDCl$_3$. (B) ^{1}H NMR spectrum of PDEAEMA MB-11 in CDCl$_3$ after purification by fractionation…….…....129

3.9. Apparent hydrodynamic size of (A) PDEAEMA MB-11 and (B) PDEAEMA MB-12 in 5 mM KH$_2$PO$_4$ aqueous buffer with a concentration of 0.2 mg/g at different pH values obtained from dynamic light scattering studies…….…...131

B1. (A) SEC trace of PDEGEA side chain polymer with a DP of 59 (PDEGEA-59). (B) ^{1}H NMR spectrum of PDEGEA-59 in $CDCl_3$. SEC analysis was carried out on PL GPC-20 system using THF as carrier solvent…….…....141

B2. (A) SEC trace of PDEGEA-82 side chain polymer with a DP of 82. (B) ^{1}H NMR spectrum of PDEGEA-82 in $CDCl_3$. SEC analysis was carried out on PL GPC-20 system using THF as carrier solvent……...……141

B3. (A) SEC trace of PDEAEMA-43 side chain polymer and (B) ^{1}H NMR spectrum of PDEAEMA-43 in $CDCl_3$. SEC analysis was carried out on PL GPC-50 Plus system with PSS GRAL columns using DMF containing 50 mM LiBr as carrier solvent…..…….…142

B4. (A) SEC trace of P(DEGMA-*co*-NBA)-47 side chain polymer and (B) ^{1}H NMR spectrum of P(DEGMA-*co*-NBA)-47 in $CDCl_3$. SEC analysis was carried out on PL GPC-20 system using THF as carrier solvent……...…….….142

B5. SEC trace of PDEGEA MB-2 after 96 h reaction time. SEC analysis was carried out on PL GPC-50 Plus system with Agilent Mixed-B columns using DMF containing 50 mM LiBr as carrier solvent…….……..143

B6. SEC trace of PDEGEA MB-3 after 48 h reaction time. SEC analysis was carried out on PL GPC-50 Plus system with Agilent Mixed-B columns using DMF containing 50 mM LiBr as carrier solvent…….…..143

B7. SEC trace of PDEGEA MB-4 after 72 h reaction time. SEC analysis was carried out on PL GPC-50 Plus system with Agilent Mixed-B columns using DMF containing 50 mM LiBr as carrier solvent…….……..144

B8. SEC trace of PDEGEA MB-5 after 78 h reaction time. SEC analysis was carried out on PL GPC-50 Plus system with Agilent Mixed-B columns using DMF containing 50 mM LiBr as carrier solvent……..……..…144

B9. SEC traces of PDEGEA MB-6 before and after removal of the excess side chain polymer PDEGEA-59 by fractionation. After purification: $M_{n,\ SEC}$ = 1,147,500; PDI = 1.11. SEC analysis was carried out on PL GPC-50 Plus system with Agilent Mixed-B columns using DMF containing 50 mM LiBr as carrier solvent……..…….145

B10. SEC traces of PDEGEA MB-7 before and after the removal of excess PDEGEA-82 side chains by fractionation. After purification: $M_{n,\ SEC}$ = 1,450,400; PDI = 1.13. SEC analysis was carried out on PL GPC-50 Plus system with Agilent Mixed-B columns using DMF containing 50 mM LiBr as carrier solvent…….....……145

B11. SEC traces of PDEGEA MB-8 before and after the removal of excess PDEGEA-36 side chains by fractionation. SEC analysis was carried out on PL GPC-50 Plus system with Agilent Mixed-B columns using DMF containing 50 mM LiBr as carrier solvent…..…146

B12. SEC traces of P(DEGMA-*co*-NBA) MB-10 before and after removal of excess P(DEGMA-*co*-NBA)-47 side chains by fractionation. After purification: $M_{n,SEC}$ = 1,380,800 Da; PDI = 1.14. SEC analysis was carried out on PL GPC-50 Plus system with Agilent Mixed-B columns using DMF containing 50 mM LiBr as carrier solvent……..….146

B13. ^{1}H NMR spectra of PDEAEMA MB-12 (A) before purification and (B) after purification by fractionation in $CDCl_3$…….....147

4.1. (A) SEC trace of side chain polymer PNBA with a DP of 36 (PNBA-36) and (B) ^{1}H NMR spectrum of PNBA-36 in $CDCl_3$. SEC analysis was carried out on PL GPC-20 system using THF as carrier solvent……..…170

4.2. (A) SEC trace of PEO/PDEGEA MMB-1 before and after removal of excess side chains as well as PTEGN$_3$MA-800 backbone polymer for comparison. (B) ^{1}H NMR spectrum of PEO/PDEGEA MMB-1 in $CDCl_3$. SEC analysis was carried out on PL GPC-50 Plus system with Agilent Mixed-B columns using DMF containing 50 mM LiBr as carrier solvent……..……175

4.3. Digital optical photograph of solutions of PDEGEA MB-1 homografted bottlebrush (on left) and PEO/PDEGEA MMB-1 binary heterografted bottlebrush (on right) in water with a polymer concentration of 1.0 mg/g at room temperature……..……....178

4.4. (A) Results of DLS at different temperatures for a 0.2 mg/g aqueous solution of PEO/PDEGEA MMB-1. (B) Size distribution by intensity from DLS of PEO/PDEGEA MMB-1 at 25 °C for different polymer concentrations……....……180

4.5. AFM height images of PEO/DEGEA MMB-1 brush molecules spin coated onto freshly cleaved mica at 0 °C from an aqueous solution with a polymer concentration of 0.1 mg/g…….182

4.6. AFM height images of PEO/DEGEA MMB-1 brush molecules spin coated onto freshly cleaved mica at 40 °C from an aqueous solution with a polymer concentration of 0.01 mg/g…….183

4.7. (A) SEC trace of PEO/PDEAEMA MMB-2 before and after removal of excess side chains. (B) ^{1}H NMR spectrum of PEO/PDEAEMA MMB-2 in $CDCl_3$. SEC analysis was carried out on PL GPC-50 Plus system with PSS GRAL columns using DMF containing 50 mM LiBr as carrier solvent…….....185

4.8. AFM height images of PEO/PDEAEMA MMB-2 spin coated onto freshly cleaved mica from a 0.1 mg/g solution in acetone…….….188

4.9. (A) Optical photograph of PEO/PDEAEMA MMB-2 in 5 mM KH_2PO_4 aqueous buffer at pH = 4.92 (left) and pH = 9.93 (right) with a polymer concentration of 0.2 mg/g. (B) DLS results at different pH values for PEO/PDEAEMA MMB-2 in 5 mM KH_2PO_4 aqueous buffer with a polymer concentration of 0.2 mg/g……..…190

4.10. AFM height images of PEO/PDEAEMA MMB-2 spin coated onto mica from an aqueous 1.25 mM KH_2PO_4 solution at pH = 4.99 with a polymer concentration of 0.05 mg/g……192

4.11. AFM height images of PEO/PDEAEMA MMB-2 spin coated onto mica from an aqueous 0.5 mM KH_2PO_4 solution at pH = 9.79 with a polymer concentration of 0.01 mg/g.....…194

4.12. AFM height images of a 5 mM KH_2PO_4 buffer solution spin cast onto mica as a control……..195

4.13. (A) SEC trace of PEO/PNBA MMB-3 before and after removal of unreacted side chains by fractionation (B) ^{1}H NMR spectrum of purified PEO/PNBA MMB-3 in $CDCl_3$. SEC analysis was carried out on PL GPC-50 Plus system with Agilent Mixed-B columns using DMF containing 50 mM LiBr as carrier solvent……..…….197

4.14. (A) Size distributions by intensity from DLS of PEO/PNBA MMB-3 in DMF (0.2 mg/g), water (0.1 mg/g) after dialysis, and in water (0.1 mg/g) after irradiation with 365 nm UV light for 24 h. (B) Apparent hydrodynamic diameter vs. irradiation time for a 0.1 mg/g aqueous solution of PEO/PNBA MMB-3…….……....199

4.15. AFM height images of PEO/PNBA MMB-3 spin coated onto mica from a 0.01 mg/g solution in chloroform……..202

4.16. AFM height images of PEO/PNBA MMB-3 drop cast onto mica from a 0.1 mg/g solution in water obtained by dialysis against water……..…….203

4.17. AFM height images of PEO/PNBA MMB-3 spin coated onto mica from an aqueous 2 mM KH_2PO_4 solution at pH = 7.06 with a polymer concentration of 0.05 mg/g that had been irradiated with 365 nm UV light for 22 h……..…205

4.18. (A) SEC traces of PEO/P(DEGEA-*co*-BA-*co*-NBDA) MMB-4 before and after removal of unreacted side chains by centrifugal filtration. (B) ^{1}H NMR spectrum of PEO/P(DEGEA-*co*-BA-*co*-NBDA) MMB-4 in $CDCl_3$. SEC analysis was carried out on PL GPC-50 Plus system with Agilent Mixed-B columns using DMF containing 50 mM LiBr as carrier solvent……..……208

4.19. Results of DLS for a 0.2 mg/g aqueous solution of PEO/P(DEGEA-*co*-BA-*co*-NBDA) MMB-4 at different temperatures…….……210

4.20. AFM height images of PEO/P(DEGEA-*co*-BA-*co*-NBDA) MMB-4 spin coated onto mica from an aqueous solution at 0 ºC with a polymer concentration of 0.05 mg/g……...212

4.21. AFM height images of PEO/P(DEGEA-*co*-BA-*co*-NBDA) MMB-4 spin coated onto mica from an aqueous solution at 40 ºC with a polymer concentration of 0.05 mg/g…….213

4.22. AFM height images of PEO/P(DEGEA-*co*-BA-*co*-NBDA) MMB-4 drop cast onto mica-PS from an aqueous solution at 0 ºC with a polymer concentration of 0.05 mg/g……..215

4.23. AFM height images of PEO/P(DEGEA-*co*-BA-*co*-NBDA) MMB-4 drop cast onto mica from an aqueous solution at 45 ºC with a polymer concentration of 0.01 mg/g……...…..216

4.24. AFM height images of a mica-PS control sample that had been spin coated with Milli-Q water…….217

4.25. Fluorescence emission spectra recorded at various time intervals at 40 ºC and 0 ºC for aqueous solutions of (A) 0.005 mg/g MMB-4 as a control sample, (B) 0.025 mg/g avidin

as a control sample, and (C) a mixture containing 0.005 mg/g MMB-4 and 0.025 mg/g avidin……....220

4.26. Plot of the ratio of fluorescence emission intensity for the peaks at 570 nm and 520 nm from the fluorescence emission spectra recorded at various time intervals at 40 ^{o}C and 0 ^{o}C for aqueous solutions containing a mixture of 0.005 mg/g MMB-4 and 0.025 mg/g avidin (Solution **3**) as well as solutions containing 0.005 mg/g MMB-4 alone (Solution **1**) and 0.025 mg/g avidin alone (Solution **2**) as control samples…….....222

4.27. Graph from Figure 4.26 split into three separate plots. (A) Plot of the ratio of fluorescence emission intensity for the peaks at 570 nm and 520 nm (I_{570}/I_{520}) from the fluorescence emission spectra recorded at various time intervals at 40 ^{o}C and 0 ^{o}C for aqueous solutions containing a mixture of 0.005 mg/g MMB-4 and 0.025 mg/g avidin (Solution **3**). (B) Plot of (I_{570}/I_{520}) from the sum of the fluorescence emission spectra for the control samples containing 0.005 mg/g MMB-4 alone (Solution **1**) and 0.025 mg/g avidin alone (Solution **2**). (C) Plot of (I_{570}/I_{520}) from the separate fluorescence emission spectra for the control samples containing 0.005 mg/g MMB-4 alone (Solution **1**) and 0.025 mg/g avidin alone (Solution **2**)…….…..223

C1. (A) SEC trace of PDEGEA side chains with a DP of 46 (PDEGEA-46) and (B) ^{1}H NMR spectrum of PDEGEA-46 in $CDCl_3$. SEC analysis was carried out on PL GPC-20 system using THF as carrier solvent…….…231

C2. (A) SEC trace of PDEAEMA side chains with a DP of 43 (PDEAEMA-43) and (B) ^{1}H NMR spectrum of PDEAEMA-43 in $CDCl_3$. SEC analysis was carried out on PL GPC-50 Plus system with PSS GRAL columns using DMF containing 50 mM LiBr as carrier solvent……...……..…….231

C3. (A) SEC trace of P(DEGEA-*co*-BA-*co*-NBDA) side chains with a DP of 50 (P(DEGEA-*co*-BA-*co*-NBDA)-50) and (B) ^{1}H NMR spectrum of P(DEGEA-*co*-BA-*co*-NBDA)-50 in $CDCl_3$. SEC analysis was carried out on PL GPC-20 system using THF as carrier solvent……..232

C4. (A) SEC trace of PDEGEA MB-1 homografted molecular brushes prepared from PTEGN$_3$MA-800 backbone with PDEGEA-46 side chains before and after removal of unreacted side chains by fractionation. (B) ^{1}H NMR spectrum of PDEGEA 800-46 homograft molecular brushes in $CDCl_3$. SEC analysis was carried out on PL GPC-50 Plus system with Agilent Mixed-B columns using DMF containing 50 mM LiBr as carrier solvent. Before purification: $M_{n,\,SEC}$ = 1,086,000; PDI = 1.12. After purification: $M_{n,\,SEC}$ = 1,190,100; PDI = 1.14……..232

C5. Additional AFM height image of PEO/DEGEA MMB-1 spin coated onto mica from an aqueous solution at 0 ^{o}C with a polymer concentration of 0.1 mg/g……...……...233

C6. Additional AFM height images of PEO/DEGEA MMB-1 spin coated onto mica from an aqueous solution at 40 ^{o}C with a polymer concentration of 0.01 mg/g……...……...…234

C7. Additional AFM height images of PEO/PDEAEMA MMB-2 spin coated onto mica from an aqueous 1.25 mM KH_2PO_4 solution at pH = 4.99 with a polymer concentration of 0.05 mg/g…….235

C8. Additional AFM height images of PEO/PDEAEMA MMB-2 spin coated onto mica from an aqueous 0.5 mM KH_2PO_4 solution at pH = 9.79 with a polymer concentration of 0.01 mg/g…….....236

C9. ^{1}H NMR spectrum of PEO/PNBA MMB-3 obtained from a 0.1 mg/g solution in water that was irradiated with 365 nm UV light for 24 h (DMSO-d_6 solvent for NMR)……...….237

C10. Additional AFM height images of PEO/PNBA MMB-3 spin coated onto mica from a 0.01 mg/g solution in chloroform…….....238

C11. Additional AFM height image of PEO/PNBA MMB-3 spin coated onto mica from an aqueous 2 mM KH_2PO_4 solution at pH = 7.06 with a polymer concentration of 0.05 mg/g after 22 h of irradiation with 365 nm UV light……..…239

C12. Additional AFM height images of PEO/P(DEGEA-*co*-BA-*co*-NBDA) MMB-4 spin coated onto mica from an aqueous solution at 0 ^{o}C with a polymer concentration of 0.05 mg/g…….....240

C13. Additional AFM height images of PEO/P(DEGEA-*co*-BA-*co*-NBDA) MMB-4 drop cast onto mica-PS from an aqueous solution at 0 ^{o}C with a polymer concentration of 0.05 mg/g…….....241

C14. Additional AFM height images of PEO/P(DEGEA-*co*-BA-*co*-NBDA) MMB-4 drop cast onto mica-PS from an aqueous solution at 45 ^{o}C with a polymer concentration of 0.01 mg/g…….....242

5.1. (A) SEC traces of difunctional macroinitiator Br-PEO-Br and P(DEGMMA-*co*-DEGEMA-*co*-DEAEMA)-*b*-PEO-*b*-P(DEGMMA-*co*-DEGEMA-*co*-DEAEMA) (ABA-DEA-1). (B) ^{1}H NMR spectrum of ABA-DEA-1 ($CDCl_3$ as solvent)……...……....256

5.2. (A) SEC traces of difunctional macroinitiator Br-PEO-Br and P(DEGMMA-*co*-DEGEMA-*co*-DPAEMA)-*b*-PEO-*b*-P(DEGMMA-*co*-DEGEMA-*co*-DPAEMA) (ABA-DPA-2). (B) ^{1}H NMR spectrum of ABA-DPA-2 ($CDCl_3$ as solvent)……..…….257

5.3. (A) SEC traces of difunctional macroinitiator Br-PEO-Br and P(DEGMMA-*co*-DEGEMA-*co*-DBAEMA)-*b*-PEO-*b*-P(DEGMMA-*co*-DEGEMA-*co*-DBAEMA) (ABA-DBA-3). (B) ^{1}H NMR spectrum of ABA-DBA-3 ($CDCl_3$ as solvent)……..……258

5.4. (A) Plot of dynamic storage modulus G' (■) and dynamic loss modulus G'' (□) versus temperature for a 10 wt % aqueous solution of ABA-DEA-1 with pH of 10.73. The data were collected from a temperature ramp experiment performed by using a fixed frequency of 1 Hz, a strain amplitude of 1 %, and a heating rate of 3 °C/min. (B) Frequency dependences of G' (■) and G'' (□) at 21.9 °C of the gel formed from the sample with pH of 10.73, collected using a strain amplitude of 1 %.....262

5.5. (A) Plot of dynamic storage modulus G' (■) and loss modulus G'' (□) versus temperature for a 10 wt % aqueous solution of ABA-DEA-1 with pH of 5.18. The data were collected from a heating ramp experiment performed at a frequency of 1 Hz, a strain amplitude of 1 %, and a heating rate of 3 °C/min. (B) Frequency dependences of G' (■) and G'' (□) of the gel from the sample with pH of 5.18 at 47.4 °C, collected using a strain amplitude of 1 %.....263

5.6. The sol-gel transition ($T_{\text{sol-gel}}$) of the 10 wt % solution of ABA-DEA-1 (■), ABA-DPA-2 (●), and ABA-DBA-3 (♦) in the 20 mM phosphate buffer as a function of solution pH fitted to a Boltzmann function as well as the $T_{\text{sol-gel}}$ values at pH = 3.78 and 10.67 of a 10 wt % aqueous solution of ABA-DEA-1 after storage at room temperature and pH = 3.20 for 8 months (■). The two $T_{\text{sol-gel}}$ values at pH = 3.78 and 10.67 for ABA-DEA-1 were not included in the fitting……...…….....265

5.7. The sol-gel transition ($T_{\text{sol-gel}}$) of the 10 wt % aqueous solution of ABA-DEA-1 (■), ABA-DEA-4 (□), ABA-DPA-2 (●), ABA-DPA-5 (○), and ABA-DBA-3 (♦) in the 20 mM phosphate buffer as a function of solution pH fitted to a Boltzmann function. The data for ABA-DEA-1 (■), ABA-DPA-2 (●), and ABA-DBA-3 (♦) are from Figure 5.6…….270

5.8. Cumulative release of FITC-dextran (%) over time from 10 wt % ABA-DEA-1 (■), **A**BA-DPA-2 (●), and ABA-DBA-3 (♦) micellar hydrogels at 37 °C (a) and 27 °C (b)……..272

5.9. Optical photographs showing the sol-gel transitions at pH = 4.78 and pH = 10.67 of a 10 wt % aqueous solution of ABA-DEA-1 in a 20 mM phosphate buffer upon temperature changes. The solution had been stored for eight months at pH = 3.20 before the pH was adjusted to 4.78 and 10.67……....275

D1. (A) SEC traces of difunctional macroinitiator Br-PEO-Br and P(DEGMMA-*co*-DEGEMA-*co*-DEAEMA)-*b*-PEO-*b*-P(DEGMMA-*co*-DEGEMA-*co*-DEAEMA) (ABA-DEA-4). (B) ^{1}H NMR spectrum of ABA-DEA-4 ($CDCl_3$ as solvent)……...……282

D2. (A) SEC traces of difunctional macroinitiator Br-PEO-Br and P(DEGMMA-*co*-DEGEMA-*co*-DPAEMA)-*b*-PEO-*b*-P(DEGMMA-*co*-DEGEMA-*co*-DPAEMA) (ABA-DPA-5). (B) ^{1}H NMR spectrum of ABA-DPA-5 ($CDCl_3$ as solvent)……..…….282

D3. Plot of dynamic storage modulus *G′* (■) and dynamic loss modulus *G″* (□) versus temperature for a 10 wt % aqueous solution of ABA-DPA-2 with (a) pH = 10.48 and (b) pH = 4.93. The data were collected from temperature ramp experiments performed by using a fixed frequency of 1 Hz, a strain amplitude of 1.0 %, and a heating rate of 3 °C/min……..283

D4. Plot of dynamic storage modulus *G′* (■) and dynamic loss modulus *G″* (□) versus temperature for a 10 wt % aqueous solution of ABA-DBA-3 with (a) pH = 9.14 and (b) pH = 5.30. The data were collected from temperature ramp experiments performed by using a fixed frequency of 1 Hz, a strain amplitude of 1.0 %, and a heating rate of 3 °C/min……..283

D5. Plot of dynamic storage modulus *G′* (■) and dynamic loss modulus *G″* (□) versus temperature for a 10 wt % aqueous solution of ABA-DEA-4 with (a) pH = 10.79 and (b) pH = 5.20. The data were collected from temperature ramp experiments performed by using a fixed frequency of 1 Hz, a strain amplitude of 1.0 %, and a heating rate of 3 °C/min……..284

D6. Plot of dynamic storage modulus *G′* (■) and dynamic loss modulus *G″* (□) versus temperature for a 10 wt % aqueous solution of ABA-DPA-5 with (a) pH = 9.74 and (b) pH = 5.65. The data were collected from temperature ramp experiments performed by using a fixed frequency of 1 Hz, a strain amplitude of 1.0 %, and a heating rate of 3 °C/min……..……284

D7. Plot of dynamic storage modulus *G′* (■) and dynamic loss modulus *G″* (□) versus temperature for a 10 wt % aqueous solution of ABA-DEA-1 with (a) pH = 10.67 and (b) pH = 4.78 after storage at pH = 3.20 and room temperature for eight months. The data were collected from temperature ramp experiments performed by using a fixed frequency of 1 Hz, a strain amplitude of 1.0 %, and a heating rate of 3 °C/min……...……..285

D8. ^{1}H NMR spectrum of ABA-DEA-1 from a 10 wt % aqueous solution of ABA-DEA-1 in a 20 mM phosphate buffer after storage at pH = 3.20 and room temperature for eight months ($CDCl_3$ as solvent)…….…..….285

List of Schemes

1.1. Various polymer systems comprising polymer brushes……..……..3

1.2. Different classifications of molecular brushes…….……6

1.3. Three general strategies for the synthesis of molecular brushes: grafting to, grafting from, and grafting through…….7

1.4. Unimolecular shape-changing of stimuli-responsive homografted molecular brushes in dilute solution…….……14

1.5. Simplified sketch of the different stages of blood clotting which highlights the critical role of the von Willibrand Factor (VWF)……..20

2.1. Synthesis of Water-Soluble PEO Molecular Brushes by "Grafting To" CuAAC "Click" Reaction…….…42

2.2. Synthesis of Azide-Functionalized Backbone Polymer PTEGN_3MA by Atom Transfer Radical Polymerization and Subsequent Post-Polymerization Reactions Including Removal of Protective Silyl Ether, Reaction with Tosyl Chloride, and Substitution with Azide……..50

2.3. Synthesis of Monomer TEGSiMA via a Two-Step Process……..…..52

2.4. Synthesis of Alkyne End-Functionalized Water-Soluble Side Chain Polymer PEO by End-Group Modification of Commercially Available PEO with 4-Pentynoic acid……....60

3.1. Synthesis of Stimuli-Responsive Molecular Brushes by "Grafting To" CuAAC "Click" Reactions……....98

3.2. Synthesis of Alkyne End-Functionalized Stimuli-Responsive Side Chain Polymers by Atom Transfer Radical Polymerization (ATRP) and Reversible Addition-Fragmentation Chain Transfer (RAFT) Polymerization…….……..……108

4.1. Shape-Changing of Stimuli-Responsive Binary Heterografted Molecular Brushes...….155

4.2. Synthesis of Stimuli-Responsive Binary Heterografted Molecular Brushes by "Grafting To" CuAAC "Click" Reactions…….……..156

4.3. Synthesis of Alkyne End-Functionalized Stimuli-Responsive Side Chain Polymers by ATRP and RAFT Polymerization…….…....168

5.1. Synthesis of Tertiary Amine-Containing, Thermo- and pH-Sensitive Hydrophilic ABA Triblock Copolymers by Atom Transfer Radical Polymerization (ATRP)……..….…249

List of Abbreviations

2-D: Two-dimensional

3-D: Three-dimensional

AFM: Atomic force microscopy

AIBN: 2,2'-Azobis(2-methylpropionitrile)

ATRP: Atom transfer radical polymerization

BA: 2-(Acryloyloxyethyl) 5-((3a*S*,4*S*,6a*R*)-2-oxohexahydro-1*H*-thieno[3,4-*d*]imidazole-4-yl)pentanoate; alternative: D-Biotin oxyethyl acrylate

Br-PEO-Br: Poly(ethylene glycol) di(2-bromoisobutyrate)

CH_3O-PEO-OH: Poly(ethylene glycol) monomethyl ether

CMC: Critical micelle concentration

Cryo-TEM: Cryogenic transmission electron microscopy

CuAAC: Copper-catalyzed azide-alkyne cycloaddition

DBAEMA: *N*,*N*-Di(*n*-butyl)aminoethyl methacrylate

DEAEMA: *N*,*N*-Diethylaminoethyl methacrylate

DEGEA: Ethoxydi(ethylene glycol) acrylate); alternative: Di(ethylene glycol) ethyl ether acrylate)

DEGEMA: Ethoxydi(ethylene glycol) methacylate); alternative: Di(ethylene glycol) ethyl ether methacrylate)

DEGMA: Methoxydi(ethylene glycol) acrylate); alternative: Di(ethylene glycol) methyl ether acrylate)

DEGMMA: Methoxydi(ethylene glycol) methacrylate; alternative: Di(ethylene glycol) methyl ether methacrylate)

D_h: Apparent hydrodynamic diameter

DLS: Dynamic light scattering

DMAP: 4-(*N*,*N*-Dimethylamino)pyridine

DMF: *N*,*N*-Dimethylformamide

DP: Degree of polymerization

DPAEMA: *N*,*N*-Diisopropylaminoethyl methacrylate

EBiB: Ethyl 2-bromoisobutyrate

EDC-HCl: *N*-(3-dimethylaminopropyl)-*N*′-ethylcarbodiimide hydrochloride

F_{el}: Elastic free energy

F_{int}: Interaction free energy

FITC: Fluorescein isothiocyanate

FRET: Fluorescence resonance energy transfer

G': dynamic storage modulus

G": dynamic loss modulus

GMA: gylcidyl methacrylate

GPC: Gel permeation chromatography; synonymous with SEC

HMTETA: 1,1,4,7,10,10-Hexamethyltriethylenetetramine

HRMS: High resolution mass spectrometry

LCST: Lower critical solution temperature

MB: Molecular brush; Molecular Bottlebrush

Mica-PS: Polystyrene-coated mica

MMB: Mixed (heterografted) molecular brush

MOAB: *cis*- or *trans*-4-Methacryloyloxyazobenzene

MWCO: Molecular weight cut-off

NBA: *o*-Nitrobenzyl acrylate

NBDA: 4-(2-Acryloyloxyethylamino)-7-nitro-2,1,3-benzoxodiazole

NBD-Cl: 4-Chloro-7-nitro-2,1,3-benzoxadiazole

NBD-OH: 4-(2-Hydroxyethylamino)-7-nitro-2,1,3-benzoxadiazole

NMR: Nuclear magnetic resonance

PAA: Poly(acrylic acid)

PBiB: Propargyl 2-bromoisobutyrate

PCPP: Propargyl 4-cyano-4-(phenylcarbonothioylthio)pentanoate

PCL: Poly(carprolactone)

PDEAEMA: Poly(*N*,*N*-diethylaminoethyl methacrylate)

PDEGEA: Poly(ethoxydi(ethylene glycol) acrylate); alternative: Poly(di(ethylene glycol) ethyl ether acrylate)

PDEGEMA: Poly(ethoxydi(ethylene glycol) methacylate); alternative: Poly(di(ethylene glycol) ethyl ether methacrylate)

PDEGMA: Poly(methoxydi(ethylene glycol) acrylate); alternative: Poly(di(ethylene glycol) methyl ether acrylate)

PDEGMMA: Poly(methoxydi(ethylene glycol) methacylate); alternative: Poly(di(ethylene glycol) methyl ether methacrylate)

PDI: Polydispersity index

PDMA: Poly(*N*,*N*-dimethylacrylamide)

PDMAEMA: Poly(*N*,*N*-(dimethylamino)ethyl methacrylate)

PDMAPS: Poly(3-dimethyl(methacryloyloxyethyl) ammonium propane sulfonate

PEO: Poly(ethylene oxide); alternative: Poly(ethylene glycol)

PGMA: Poly(gylcidyl methacrylate)

PMDETA: *N,N,N',N'',N''*-pentamethyldiethylenetriamine

PNAGA: Poly(*N*-acryloylglycinamide)

P*n*BA: poly(*n*-butyl acrylate)

PNBA: Poly(*o*-nitrobenzyl acrylate)

PNIPAM: Poly(*N*-isopropylacrylamide)

POEGMA: Poly(oligo(ethylene glycol)methyl ether methacrylate)

PPO: Poly(propylene oxide)

PS: Polystyrene

P*t*BA: poly(*t*-butyl acrylate)

PTEGEA: Poly(ethoxytri(ethylene glycol) acrylate)

PTEGMA: Poly(methoxytri(ethylene glycol) acrylate)

PTEGMMA: Poly(methoxytri(ethylene glycol) methacrylate)

PTEGN_3MA: Poly(tri(ethylene glycol) azido methacrylate)

PTEGSiMA: Poly(tri(ethylene glycol) mono(*t*-butyldimethylsilyl) ether methacrylate)

PTEGTsMA: Poly(tri(ethylene glycol) *p*-toluenesulfonyl methacrylate)

PTFE: Poly(tetrafluoroethylene)

RAFT: Radical addition-fragmentation chain transfer

R_h: Apparent hydrodynamic radius

ROMP: Ring opening metathesis polymerization

RXN: Reaction

SDS: Sodium dodecyl sulfate

SEC: Size exclusion chromatography; synonymous with GPC

TEGSi: Tri(ethylene glycol) mono(*t*-butyldimethylsilyl) ether

TEGSiMA: Tri(ethylene glycol) mono(*t*-butyldimethylsilyl) ether methacrylate

TEM: Transmission electron microscopy

T_g: Glass transition temperature

THF: Tetrahydrofuran

TMRITC: Tetramethyl-rhodamine isothiocyanate

TOF: Time of flight

$T_{sol\text{-}gel}$: Sol-gel transition temperature

UCST: Upper critical solution temperature

UV: Ultraviolet

VWF: Von Willibrand factor

Chapter 1: Introduction

1.1. Introduction

This dissertation work is generally concerned with stimuli-responsive macromolecules in water, with a major focus on the synthesis and behavior of linear molecular bottlebrushes that can respond to environmental stimuli in dilute aqueous solution. These brushes are composed of stimuli-responsive side chain polymers that are densely tethered at one end to a flexible polymer backbone. Section 1.1.1 offers a brief introduction to polymer brushes, of which molecular bottlebrushes are a subset. Section 1.1.2 provides a more detailed description of molecular brushes as well as general strategies for their synthesis. In Section 1.1.3, we focus on responsive molecular brushes, with an introduction to stimuli-responsive polymers in the beginning of this section. Section 1.1.4 is a slight departure from the main focus of molecular brushes, where we discuss thermosensitive hydrophilic block copolymer hydrogels in order to provide context for Chapter 5. Finally, an overview of the dissertation work, presented in the following Chapters 2 through 5, is provided at the end of Chapter 1 in Section 1.2.

1.1.1. Introduction to Polymer Brushes

Polymer brushes refer to an assembly of polymer chains which are tethered to a substrate at one end with a sufficiently high tethering density such that the chains in their equilibrium state are stretched relative to their unperturbed dimensions.[1-4] Such deformed polymer chains are in fact found in a wide variety of polymeric systems, including end-grafted linear polymers on a substrate, block copolymer micelles, physically absorbed block copolymers on an interface, microphase separated block copolymers in bulk, etc. Polymer brushes end-grafted on a substrate are commonly used as model systems. The substrate to which polymer brushes are grafted can be three-, two-, one-, or zero-dimensional (Scheme 1.1). One notable example of polymer brushes on 3-D substrates is polymer-grafted particles (i.e., hairy particles) where the particle size in comparable

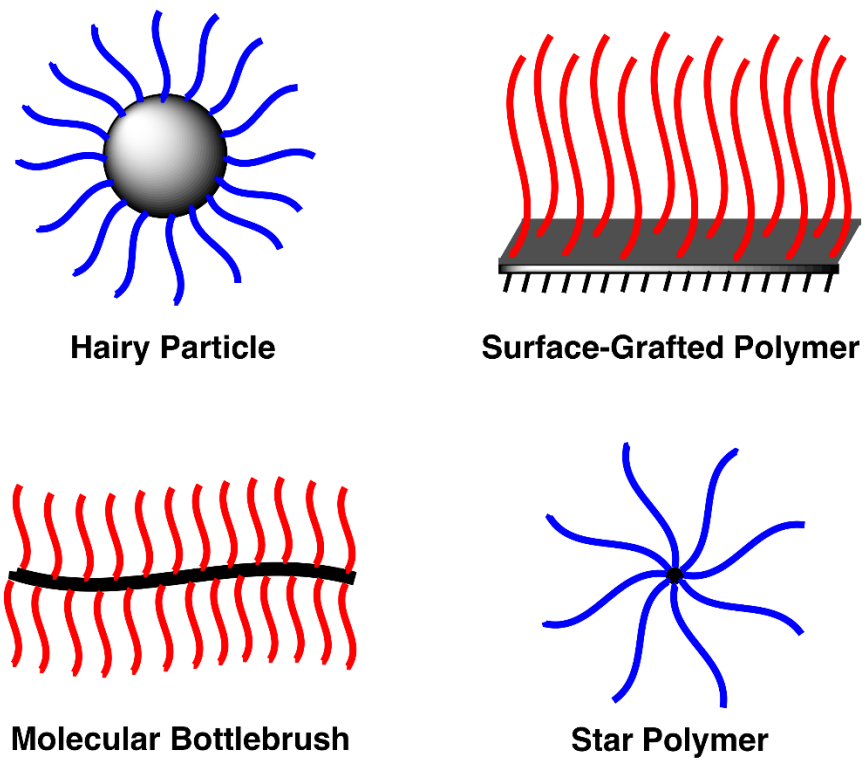

Scheme 1.1. Various polymer systems comprising polymer brushes.

or larger than the size of the end-tethered polymers. Hairy particles are a vastly diverse category of hybrid nanostructured materials that includes polymers, either covalently grafted or physically absorbed to inorganic (silica, titania, gold, silver, etc) or organic (e.g. crosslinked polymer) particles with a variety of shapes, such as spherical, cylindrical, cubic, etc. Examples of polymer brushes on 2-D substrates include polymer chains densely end-grafted by a covalent bond or physically absorbed by one block of a block copolymer on a flat solid substrate. Molecular brushes, also called molecular bottlebrushes and the main focus of this dissertation work, are a type of polymer brushes tethered to a polymer chain/backbone, which can be considered as a one-dimensional substrate when the brushes are in the highly stretched worm-like morphology.[5-7] Multi-arm star copolymers and polymer-grafted small nanoparticles, where the core is a "point" significantly smaller than the size of tethered polymer chains, are often viewed as polymer brushes on zero-dimensional substrates.

The central feature common to all brush systems is that the polymer chains are fixed on a substrate with sufficiently high grafting density, causing the chains to be stretched in the direction normal to the interface. In the absence of solvent, the polymer chains must extend away from the interface in order to avoid overlapping. In a good solvent, the polymer chains become further stretched in order to maximize interactions with the solvent and decrease interactions among polymer segments. Thus, the polymer chains are deformed with respect to an untethered chain, which would assume a random coil conformation. The equilibrium conformation of tethered polymer chains in polymer brushes, either with or without the presence of solvent, is a balance between minimizing the free energy of interactions between polymer segments (F_{int}) and the elastic free energy (F_{el}) per chain.[4] Due to spatial restrictions, the chains stretch away from the tethering substrate in order to reduce the interaction energy between segments at the expense of increased

elastic free energy.

1.1.2. Introduction to Molecular Brushes

Molecular brushes (i.e., molecular bottlebrushes) are a type of graft copolymers where polymer side chains are densely tethered at one end to a polymer backbone. The conformation of molecular brushes is dictated by steric crowding of the side chains, which are separated between grafting sites by a distance that is much less than their unperturbed dimensions. In order to avoid overlapping, both the backbone and the side chains adopt highly stretched conformations, where the backbone resides in the core and the side chains are extended radially outward from the core.[6] Thus, the dimensions of molecular brushes are determined by the length of the backbone and side chains.[7] If the backbone is much longer than the side chains, as is typically the case, the brush molecules resemble a semi-flexible cylinder, commonly referred to as a "worm-like" morphology.

Using controlled polymerization techniques, it is possible to obtain molecular brushes with precisely controlled architectures and functionalities that are rarely seen in other systems and can be useful for applications in a diverse range of areas, such as biomedicine, lubrication, and nanoengineering.[6] Scheme 1.2 illustrates just some examples of the vast array of available molecular brush structures, depending on the composition and arrangement side chains as well as, in the case of star and cyclic brushes, the topology of the backbone and/or side chains. This dissertation focuses mainly on two types: (i) homografted molecular brushes, which are composed of a single type of homopolymer or copolymer side chains, and (ii) binary heterografted (mixed) molecular brushes, where two types of side chains are randomly distributed along the backbone.

There are three general approaches for the synthesis of molecular brushes: "grafting to," "grafting from," and "grafting through" (Scheme 1.3).[5] The synthetic route employed often depends on the desired brush architecture. With the grafting to approach, end-functionalized side

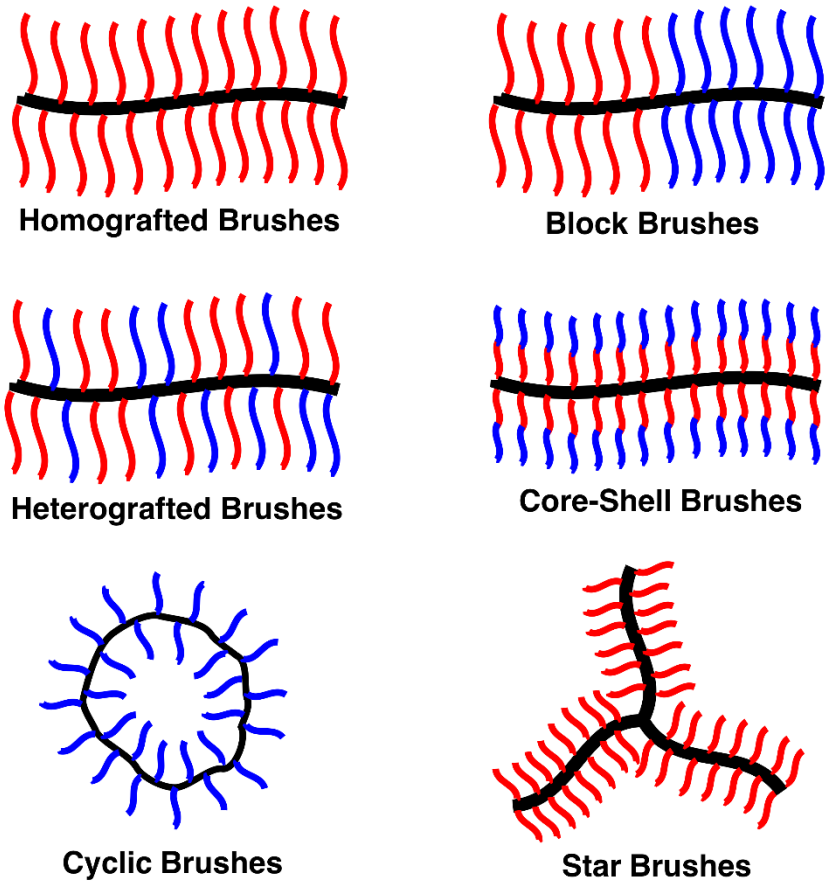

Scheme 1.2. Different classifications of molecular brushes.

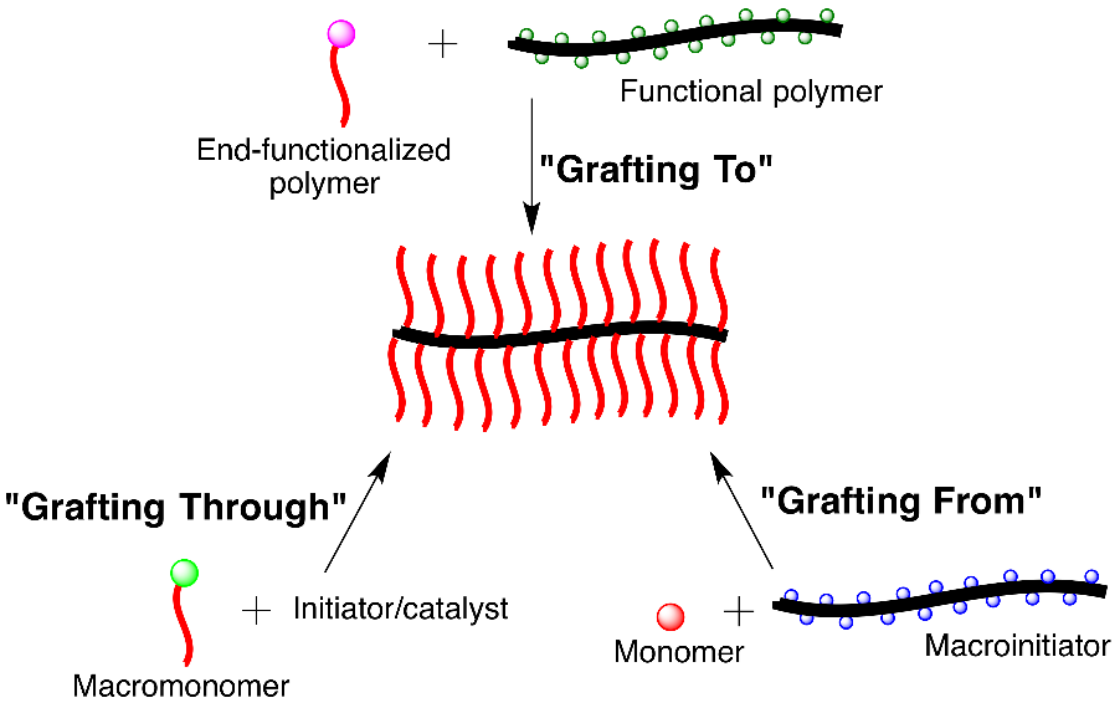

Scheme 1.3. Three general strategies for the synthesis of molecular brushes: grafting to, grafting from, and grafting through. (Adapted/reprinted from Ref. 5 with permission from Elsevier)

chains are attached to a backbone via reactive sites along the backbone. This approach has the benefit of allowing for the backbone and side chains to be prepared and characterized separately, which would be ideal for the synthesis of heterografted molecular brushes. However, low grafting densities are traditionally obtained due to steric crowding between side chains unless a high-yielding coupling reaction is employed. Recent advances in the combination of highly efficient "click" reactions, such as copper-catalyzed azide-alkyne cycloaddition (CuAAC), with macromolecular synthetic techniques have allowed for high grafting densities to be achieved using the "grafting to" route.[8-12] For the grafting from approach, a backbone polymer containing a number of initiation sites is used as a macroinitiator for the polymerization of side chains. Because the growth of side chains is gradual, the grafting from technique alleviates the complication due to steric repulsions of side chains, allowing for high grafting densities to be obtained, provided that high initiation efficiency can be achieved. This approach is well suited for the synthesis of homografted molecular brushes.[13-15] Finally, the grafting through, or "macromonomer" approach, involves the direct polymerization of side chain polymers that bear a polymerizable end group. This technique allows for the greatest control over grafting density, and is well suited for the preparation of block copolymer brushes. However, polymerizations of macromonomers are often slow and proceed to low conversions, due to the low concentration of polymerizable end groups and high steric hindrance at the propagating chain end. Recent developments have shown that in many cases these drawbacks can be alleviated through the use of ring opening metathesis polymerization (ROMP) of norbornenyl macromonomers using highly active Grubbs catalysts, due to the high degree of ring strain in the monomer which provides a strong thermodynamic driving force for polymerization and the relatively large spacing between side chains in the resulting brush.[16-23]

1.1.3. Stimuli-Responsive Molecular Brushes

The physical properties of molecular brushes are, for the most part, determined by the composition of the side chains and, if the side chains are not all identical, the arrangement of different side chains along the backbone. Often times, the only relevant characteristic of the backbone is its length, or degree of polymerization (DP), and is treated as a generic (semi)flexible chain that serves only as a tethering interface for the side chains. This is a consequence of the fact that the backbone: (i) is responsible for only a small portion of both the mass and volume of the brush as a whole, (ii) resides in the core of the brush and is thus somewhat insulated from the environment, and (iii) is generally in a highly restricted conformation which is predominately determined by a balance between the steric interactions among side chains and the interactions (favorable or nonfavorable) between the side chains and the environment. Although it is certainly possible to impart responsive properties into the backbone (e.g., main-chain scission or some cleavage reaction that results in degrafting of side chains upon application of a certain stimulus), it is overwhelmingly the case that any stimuli-responsiveness of molecular brushes is imparted by, and in reference to, the side chains. With this in mind, we will preface the discussion of stimuli-responsive molecular brushes with an overview of stimuli-responsive polymers.

1.1.3.1. Stimuli-Responsive Polymers

Stimuli-responsive polymers are a class of soft materials that undergo dramatic conformational and solubility changes in a solvent in response to changes in environmental conditions.[24] The stimulus can be either chemical (such as pH or the presence of ions, redox agents, enzymes, etc.) or physical (e.g., temperature, light, magnetic fields, or mechanical stress) in nature. Of all the available stimuli, temperature and pH are probably the most widely studied, due to the ability to easily apply the stimuli in situ as well as by virtue of the reversibility of the responsive

property. Although polymers can exhibit responsive properties in a variety of environments, such as organic solvents or even the bulk, water is by far the most studied and applicable medium, and thus, aqueous properties will be our focus here. These types of materials, often called "smart" polymers, have attracted a great amount of interest due to their promising applicability to biomedical challenges such as drug delivery and tissue engineering as well as other uses such as switchable surfaces or regulation of fluid flow through microchannels.

Thermosensitive water-soluble polymers can be divided into two categories: those exhibiting a lower critical solution temperature (LCST) and those exhibiting an upper critical solution temperature (UCST).[25] LCST-type polymers undergo an abrupt soluble-to-insoluble transition upon increasing the temperature above a certain value. The temperature at which phase separation occurs is commonly referred to as the cloud point and is dependent upon molecular weight and concentration among other factors. The LCST refers to the minimum temperature at which phase separation occurs in the phase diagram obtained by plotting the cloud point versus polymer concentration. LCST-type polymers are by far the most common and most widely studied class of thermosensitive polymers. Among them, poly(*N*-isopropylacrylamide) (PNIPAM) is perhaps the most well-known, possessing a biologically relevant LCST of 32 ^{o}C (between room temperature and body temperature) and is often used as a model for LCST-type polymers.[26] Another common type of LCST polymers is a family of (meth)acrylate and styrenic polymers containing oligo(ethylene glycol) pendant groups.[27] These polymers exhibit a wide range of transition temperatures depending on the specific molecular structure. Similar to all LCST-type polymers, PNIPAM contains both hydrophobic moieties as well as hydrophilic portions that are capable of participating in hydrogen bonding with water. At temperatures below the cloud point, such polymers are solubilized by hydrogen bonding between water and the hydrophilic moiety (i.e.,

amide bond) as the hydrophobic portions are surrounded by an ice-like layer of ordered water molecules (Figure 1.1).[28] This ordering of water has the effect of decreasing the overall entropy of the system even though the polymer chains are molecularly dissolved. The entropic penalty is not sustainable thermodynamically at higher temperatures, inducing a conformational transition of polymer chains from a solvated random coil to a collapsed globular state as the protective layer of ordered water around the hydrophobic moieties is "melted" by absorbed heat. In fact, this has been confirmed by the presence of an endothermic peak in differential scanning calorimetry. Thus, the transition is an entropy-driven process. The intra-chain coil-to-globule transition is followed by inter-chain aggregation which is manifested macroscopically by turbidity in the solution.

In contrast to LCST-type polymers, the opposite behavior is exhibited by UCST-type polymers, which undergo a soluble-to-insoluble transition upon decreasing the temperature. In this case, the transition is governed by competing interactions between polymer segments and between polymer segments and water solvent molecules, the relative strengths of which vary with temperature. Polymers that show UCST-type behavior can be further divided into two classes: those whose thermosensitive behavior is due to electrostatic interactions and those whose UCST behavior is based on hydrogen bonding.[25] Examples of the first class are poly(3-dimethyl(methacryloyloxyethyl) ammonium propane sulfonate (PDMAPS), exhibiting a cloud point usually around 30 ^{o}C, and its derivatives. Intragroup, intrachain, and interchain coulombic interactions between zwitterionic repeat units are responsible for the temperature-dependent solubility. Of the second class, which is based on hydrogen bonding between repeat units (often containing multiple donor-acceptor pairs), poly(*N*-acryloylglycinamide) (PNAGA) and its derivatives are probably the most common. Compared to LCST-type polymers, examples of

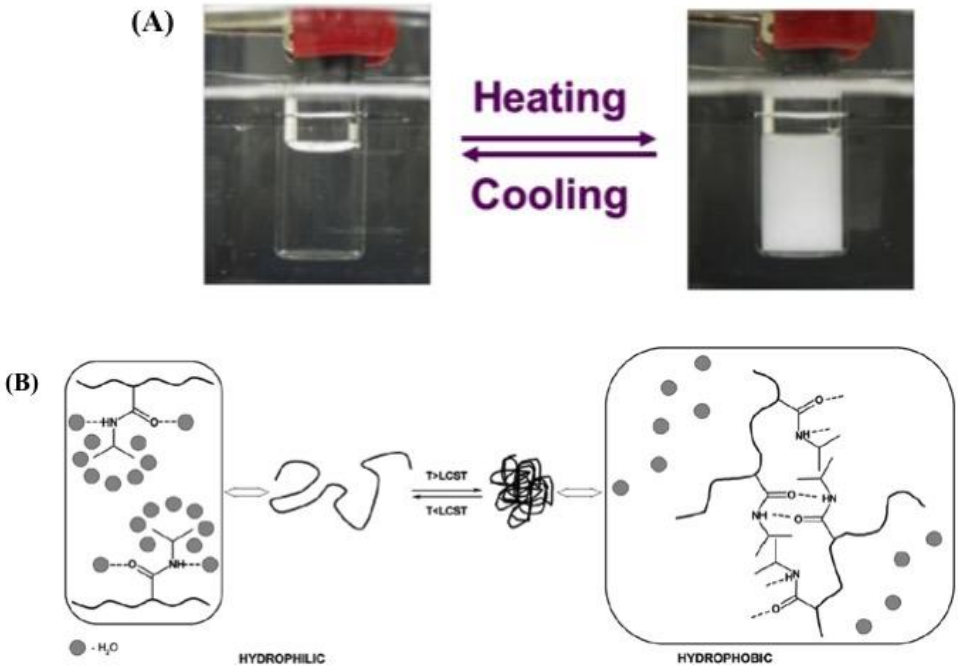

Figure 1.1. (A) Optical photographs showing the reversible clear-to-cloudy transition of a solution of a thermosensitive polymer in water. (B) Illustration of the thermo-induced coil-to-globule transition of PNIPAM accompanied by "melting" of ordered water around hydrophobic moieties. (Reprinted from Ref. 29 with permission from Elsevier)

UCST-type polymers are less numerous, less studied, and are often more sensitive to polymer concentration as well as environmental factors such as the presence of salt and pH.

1.1.3.2. Synthesis and Behavior of Stimuli-Responsive Molecular Brushes

The field of stimuli-responsive molecular brushes has seen a growing amount of research activity in recent years, due in part to advances in controlled polymerization techniques as well as the maturation of highly efficient grafting methodologies which allow for precise control over macromolecular structure. Although there are numerous and interesting studies focusing on stimuli-induced self-assembly of molecular brushes,[30-33] usually based on block copolymer or mixed heterografted brushes, into larger multimolecular nanoobjects of various morphologies, we are especially interested in the stimuli-triggered shape-changing of single bottlebrush molecules (Scheme 1.4). Thus, that will be our main focus here.

The first report of such behavior was by Schmidt et al. in 2004 with thermosensitive PNIPAM brushes that were synthesized using a grafting from technique in which atom transfer radical polymerization (ATRP) was used to grow PNIPAM chains from a macroinitiator backbone.[34] Using dynamic light scattering (DLS) and atomic force microscopy (AFM), they observed a unimolecular shape transition upon increasing temperature above the LCST of PNIPAM from an extended worm-like conformation to a collapsed globular state that was roughly spherical (Figure 1.2). However, the collapsed brushes were unstable at higher temperatures, which resulted in aggregation and eventually precipitation. McCarley et al. prepared PNIPAM brushes from a conducting poly(thiophene) backbone by grafting from using ATRP.[35] They observed a similar decrease in size upon heating that was also accompanied by a blue shift in the UV-Vis absorption spectra as the brushes underwent an extended-to-globular transition. Further

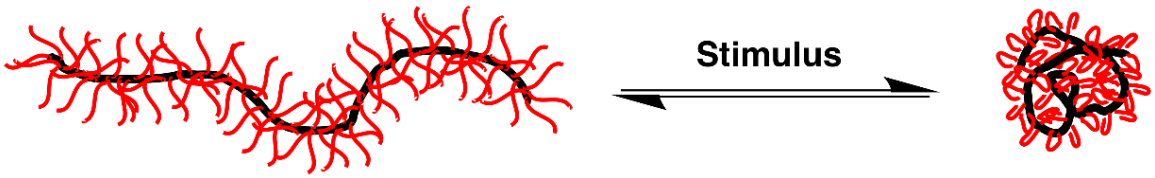

Scheme 1.4. Unimolecular shape-changing of stimuli-responsive homografted molecular brushes in dilute solution.

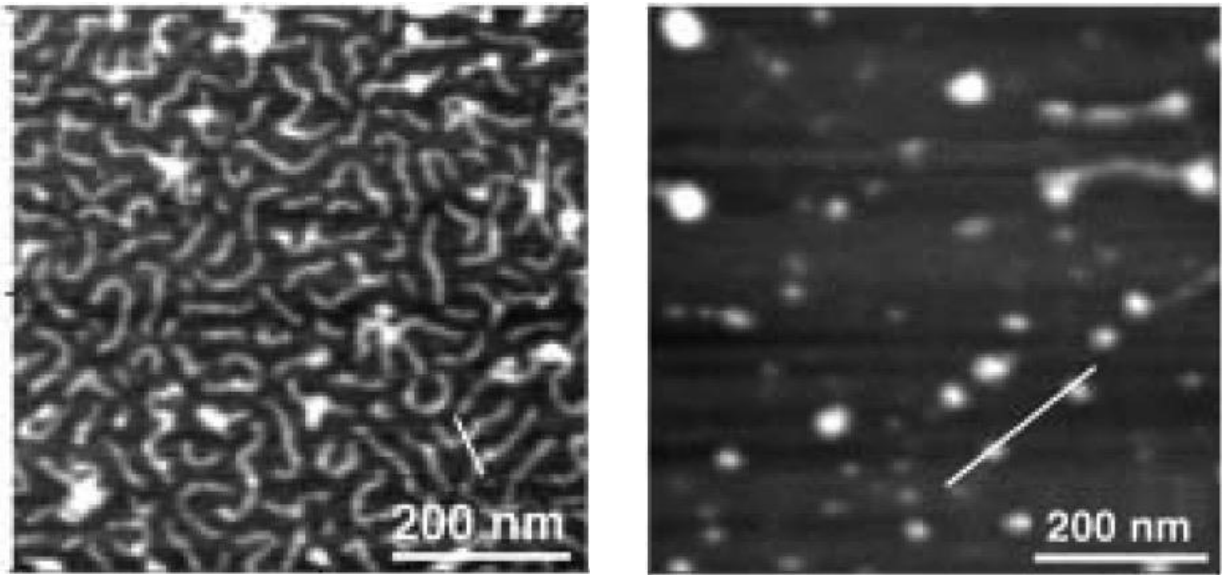

Figure 1.2. AFM height images showing the worm-to-sphere transition of thermosensitive homografted molecular brushes with PNIPAM side chains cast from water at 20 ºC (left) and 38 ºC (right). (Reprinted from Ref. 34 with permission from John Wiley and Sons)

increasing the temperature resulted in aggregation. Matyjaszewski et al. used grafting from ATRP to prepare thermosensitive brushes with a variety of side chain compositions, such as poly(methoxydi(ethylene glycol) methacylate) (PDEGMMA), poly(methoxytri(ethylene glycol) methacrylate) (PTEGMMA), poly(2-(dimethylamino)ethyl methacrylate) (PDMAEMA), poly(*N*,*N*-dimethylacrylamide) (PDMA), as well as statistical copolymers of DMAEMA and DMA with hydrophobic monomers to adjust the LCST of the side chains.[36-38] They also investigated doubly thermosensitive "core-shell" molecular brushes in which the side chains were diblock copolymers of DEGMMA (LCST = 26 ºC) and TEGMMA (LCST = 52 ºC).[37] For brushes with diblock copolymer side chains composed of an inner PDEGMMA block and a PTEGMMA outer shell, the brushes decreased in size as temperature is increased to above the LCST of PDEGMMA and remained stable up to 50 ºC, at which precipitation occurs. This indicates that the brushes are stabilized by the PTEGMMA corona after the core PDEGMMA segments undergo collapse as long as the temperature does not surpass the LCST of the PTEGMMA block. Jordan et al. prepared thermosensitive molecular brushes with side chains composed of poly(2-oxazoline)s by grafting from using a combination of anionic and cationic polymerizations.[39-41] They investigated the effect of side chain composition as well as backbone and side chain length on the LCST transitions.

Matyjaszewski and coworkers prepared pH-responsive poly(acrylic acid) (PAA) brushes with both high and low grafting densities.[42] They observed a globule-to-wormlike transition with increasing pH for the loosely grafted brushes using AFM on a mica substrate. The densely grafted brushes remained in the extended conformation over a wide range of pH values possibly due to increased steric effects which were enhance by absorption onto the substrate. Mueller et al prepared dual thermo- and pH- responsive PDMAEMA brushes by grafting from using ATRP.[43]

At pH = 2, the brushes were highly protonated and exhibited a highly stretched morphology. At pH = 7, the brushes were worm-like but more curved and became highly contracted at pH = 14. Additionally, they found that PDMAEMA brushes that were quarternized with methyl iodide underwent conformational changes in the presence of salts with different valencies.[44] The addition of monovalent salts induced a collapse of the brushes in solution, while an intermediate helical state was observed using di- or trivalent salts. A worm-to-sphere transition was observed upon complexation of the brushes with the anionic surfactant sodium dodecyl sulfate (SDS).[45] The brushes could be switched back to the worm-like state upon addition of α- or β-cyclodextrin, which form inclusion complexes with SDS, and β-cyclodextrin could subsequently be removed by addition of a more competitive inclusion agent, triggering a transition back to the spherical state. However, even at brush concentrations as low as 0.2 mg/g, the solutions became turbid immediately upon collapse of the brushes due to complexation with SDS. In order observe unimolecular collapse by AFM, a very low brush concentration of 0.02 mg/g was used. Matyjaszewski et al. added light responsive properties to PDMAEMA brushes by incorporating *trans*-4-methacryloyloxyazobenzene (MOAB) units, which isomerize to the less hydrophobic *cis* form upon irradiation with UV light.[46] They found that brushes containing MOAB in the *trans* form exhibited regular LCST behavior, which was eliminated after photoisomerization. Tang and coworkers synthesized salt-responsive, cationic poly(caprolactone) (PCL) brushes using a grafting through technique.[47] Macromonomers were prepared by ring-opening copolymerization of ε-caprolactone and α-chloro-ε-caprolactone from a norbornenyl initiator. Grubbs 3rd generation catalyst was used to polymerize the macromonomers by ROMP, and the cationic moieties were installed into the brush side chains by substitution of chlorine by sodium azide followed by CuAAC "click" reactions with an alkyne containing quarternized ammonium salt. The cationic

PCL brushes dissolved in water with a brush concentration of 1 mg/g to form clear solutions, but they became increasingly more turbid as the ionic strength was increased by the addition of sodium chloride. When the brush concentration was decreased to 0.1 mg/g, a gradual morphological transition from worms to spheres was observed by AFM as the concentration of NaCl was increased from 0 to 0.4 M. Although, the brushes still aggregated and precipitated at this concentration as the ionic strength was increased.

It is important to mention that in the examples described above, the stimuli responsive brushes are not stabilized toward aggregation upon collapse, and as a result, the worm-to-sphere transition can typically only be observed under very specific conditions. Otherwise, clouding or precipitation occurs upon application of the stimulus. In Chapter 3, we discuss the synthesis of homografted molecular brushes that respond to variety of stimuli using a grafting to technique that utilizes highly efficient "click" chemistry to obtain high grafting densities. Unimolecular collapse can be achieved at low concentration, while aggregation and clouding is observed at higher concentration. In Chapter 4, we expand this technique to the synthesis of binary heterografted molecular brushes that contain stimuli-responsive chains as well as water soluble chains that are capable of stabilizing the collapsed globular state.

1.1.3.3. The Von Willibrand Factor (VWF) as an Intriguing Biopolymer and an Inspiration for Stimuli-Responsive Shape-Changing of Synthetic Macromolecules.

The work presented in Chapter 4 was mainly inspired by the behavior of the von Willibrand Factor (VWF) in the blood clotting process. The VWF is a glycoprotein that plays a crucial role in the cascade of events that comprise the blood clotting process.[48-50] Its structure is commonly described as a "complex homopolymer," where the monomer units are made up of 4100 amino acids and are assembled into large multimers via disulfide linkages. At least 10 monomer subunits

are required for VWF proteins to function normally, and multimers can reach molecular weights of up ~ 20 million Da. Additionally, each monomer subunit itself contains approximately 15 different folded domains and are heavily glycosylated with oligosaccarrides; thus VWF resembles a molecular bottlebrush in some respects. Although, the role of the pendant sugar chains is not well-known, it is likely that they play a role in regulating interactions with platelets and other cells. Indeed, perhaps crucial to its biological role is the diversity of structure that VWF displays at different length scales, allowing for complex interactions with itself and the environment, both mechanically and chemically.

VWF is interesting because it provides an inspiration for the design of complex macromolecules whose functions can be triggered by environmental changes. For VWF, the environmental trigger is the mechanical shear forces and chemical changes that occur in the bloodstream when a vessel wall is ruptured, exposing collagen (Scheme 1.5).[48] Upon activation, VWF proteins unfold to expose numerous binding sites for collagen. At the same time, VWF promotes the agglomeration of platelets at the site of the rupture, behaving somewhat like a "stimuli-responsive glue" which acts as a temporary seal. After the VWF protein becomes extended and adhered to the vessel wall, it releases a hydrophobic payload, called Factor VIII, which is necessary for the polymerization of fibrinogen into fibrin strands. These fibrin strands form a permanently cross-linked network which plugs the lesion until the vessel wall can heal. Although the mechanism by which VWF operates is highly complex, we think that certain aspects can be applied to the conception of functional synthetic materials. We are especially interested in the possibility of designing molecular brushes that have the ability to fold or unfold upon application of a stimulus, and expose previously hidden moieties that are capable of specific interactions with other macromolecules in the environment. In this vein, we explore the possibility

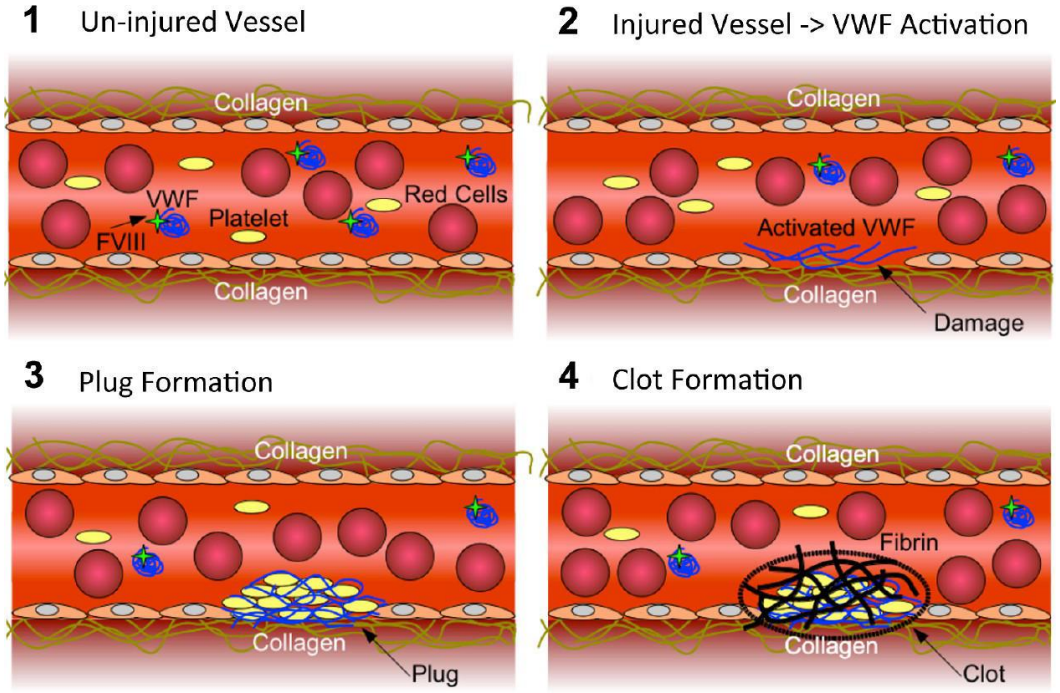

Scheme 1.5. Simplified sketch of the different stages of blood clotting which highlights the critical role of the von Willibrand Factor (VWF). (Reprinted from Ref. 48 with permission from The American Chemical Society)

of exploiting thermo-triggered shape-changing of heterografted molecular brushes to hide and expose "sticky" groups within side chains at the end of Chapter 4.

1.1.4. Thermosensitive Hydrophilic Block Copolymer Hydrogels

Although the incorporation of stimuli-responsive polymers into molecular brushes offers exciting possibilities for unique functional materials, the principal utility of responsive materials to date has been micelles and hydrogels based largely on thermosensitive block copolymers. A great deal of effort has been thrust into this area because of its great promise for biomedical applications, namely drug delivery and injectable hydrogels.[51-55] Thermosensitive polymer micelles in dilute solution can be formed through the self-assembly of diblock copolymers composed of one thermosensitive block and one water-soluble block.[24] Below the transition temperature of the responsive block, both blocks are solvated, and the copolymers exist as unimers. If the polymer concentration is above a critical value – the critical micelle concentration (CMC), when the temperature is increased above the LCST of the responsive block, the unimers assemble into micelles, in which the hydrophobic core is comprised of the now-insoluble responsive block, and the water-soluble block forms a corona. A dynamic equilibrium exists between unimers and micelles, where the concentration of unimers equals the CMC, and results in a constant exchange of polymer chains between micelles. At sufficiently high polymer concentration, the volume fraction of micelles becomes large enough such that a transition from a free-flowing liquid to a free-standing gel occurs due to close-packing of micelles.[56] This type of hydrogel is commonly formed from AB diblock copolymers and ABA triblock copolymers where the B block is thermosensitive. One such example is ABA triblock copolymers composed of water-soluble poly(ethylene oxide) outer blocks and a thermosensitive poly(propylene oxide) inner block (PEO-*b*-PPO-*b*-PEO), known as Pluronics.[57,58] Upon increasing the temperature through the LCST of

the PPO block, a unimer-micelle transition occurs, and the micelles continue to grow as the temperature is increased until they become closely packed such that the solution can no longer flow, resulting in a sol-gel transition. A typical polymer concentration for this type of gel is ~20 wt %. Interestingly, as the temperature is increased further, the volume of the PEO corona decreases due to a reduction in solvent quality, and a second transition from a gel to a free-flowing micellar sol occurs. A second type of hydrogel can be formed from ABA triblock copolymers in which the inner B block is water-soluble and the outer A blocks are thermosensitive. In dilute solution, block copolymers of this type form "flower-like" micelles above the LCST of the A blocks, where the B blocks form loops in the corona. At sufficiently high concentration, the triblock copolymers self-assemble into 3-dimensional networks upon increasing the temperature above the LCST of the A blocks, with the central block forming bridges among micelle cores, which act as physical cross-links.[59-63] Network gels of this type are typically stronger than their close-packed counterparts and form gels at lower polymer concentrations, typically <10 wt %.

An important feature of thermosensitive polymers is that the transition temperature, and thus the micellization and sol-gel temperatures of block copolymers, can be adjusted through copolymerization. The LCST can be increased or decreased via the incorporation of hydrophilic or hydrophobic monomers, respectively, allowing the LCST to be adjusted continuously over a wide range. Alternatively, the LCST can be adjusted through the incorporation of a second type of stimulus-responsive units.[64-69] The most common example is the copolymerization of a small amount of weak acid or base into the thermosensitive block, allowing the LCST to be tuned in situ by changing the solution pH. Our group has done extensive research on tuning of sol-gel transitions of thermosensitve AB diblock and ABA triblock copolymers using a variety of secondary stimuli, including pH, light, and the presence of enzymes.[70-76] Jin et al. showed that doubly thermosensitive

diblock copolymers based on poly(methoxytri(ethylene glycol) acrylate)-*b*-poly(ethoxydi(ethylene glycol) acrylate) (PTEGMA-*b*-PDEGEA) undergo in situ sol-gel-sol-cloudy transitions in water at moderate concentrations (Figure 1.3).[70-72] PTEGMA and PDEGEA homopolymers have LCSTs of approximately 58 ^{o}C and 9 ^{o}C, respectively. At low temperatures, the diblock copolymers exist as unimers in solution. Above the LCST of the PDEGEA block, they undergo self-assembly to form a gel via close-packing of micelles. As the temperature is further increased, a gel-to-sol transition is observed due to shrinking of the PTEGMA corona. Yet higher temperatures above the LCST of PTEGMA result in clouding of the solution. Both the sol-to-gel and gel-to-sol transitions could be tuned on the basis of pH through the incorporation of acrylic acid (AA) groups into the PDEGEA or PTEGMA blocks.

Woodcock et al. prepared 3D network gels from ABA triblock copolymers composed of a long, water-soluble PEO middle B block and doubly thermo- and light-responsive outer A blocks composed of poly(ethoxytri(ethylene glycol) acrylate-*co*-*o*-nitrobenzyl acrylate) (PTEGEA-*co*-NBA).[74] As the temperature was increased through the LCST of the A blocks, moderately concentrated aqueous solutions underwent a sol-gel transition, and remained a free-standing gel at higher temperatures (Figure 1.4). The gel was then exposed to long-wave UV light, which triggered the photocleavage of hydrophobic *o*-nitrobenzyl groups, resulting in an increase in the LCST of the A blocks and thus a transition from a gel to a sol. The gel was reformed at higher temperatures above the new LCST of the A block.

The diversity of responsiveness and functionalities available to stimuli-responsive hydrogels offers a unique opportunity to develop systems tailored to the specific needs of a given application. For example, certain diseased tissues often exhibit abnormally low pH values,[77] allowing for the potential to selectively target afflicted tissues for drug release based on rationally-designed pH-

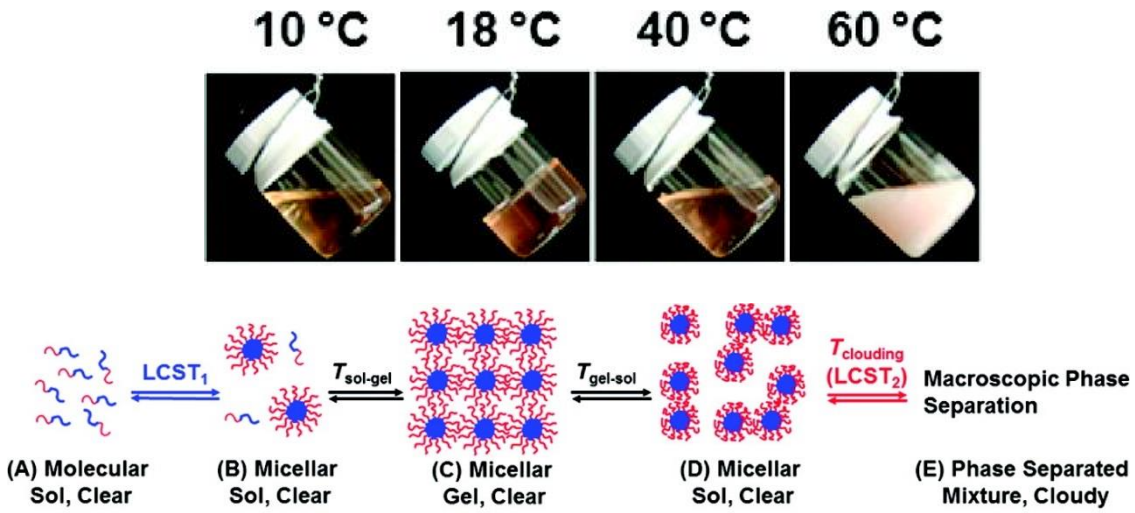

Figure 1.3. (Top) Optical photographs showing sol-gel-sol-cloudy transitions 20 wt % aqueous solutions of a doubly thermo- and pH-responsive P(TEGMA-*co*-AA)-*b*-P(DEGEA-*co*-AA) diblock copolymer. (Bottom) Schematic illustration of the transitions from a clear molecular solution to a clear molecular sol, clear micellar close-pack gel, back to a clear micellar sol, and finally a cloudy phase-separated mixture upon increases in temperature. (Reprinted from Ref. 71 with permission from The American Chemical Society)

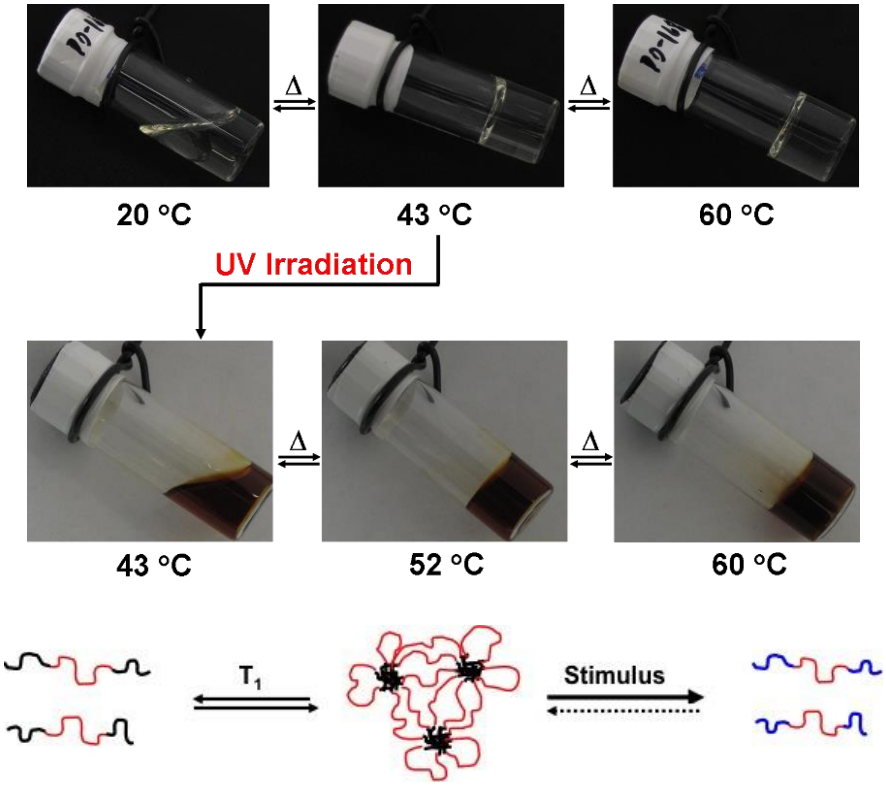

Figure 1.4. Sol-gel-sol transitions of ABA triblock copolymers with doubly thermo- and light-responsive outer blocks. (Reprinted from Ref. 74 with permission from The Royal Society of Chemistry)

responsive materials. In Chapter 5, we present a study of tertiary-amine containing thermosensitive ABA triblock copolymers that were designed to result in injectable hydrogels with increased solubility at lower pH values due to protonation of the tertiary amine, thus allowing for faster release of drugs. We investigated the effect of different alkyl substituents on the tertiary amine on the sol-gel properties.

1.2. Dissertation Overview

This main focus of this dissertation work is the synthesis and behavior of molecular brushes that are capable of undergoing morphological changes in response to a variety of stimuli. The first part deals with the development of an efficient method to prepare molecular brushes by a "grafting to" method using water-soluble PEO as model side chains. This modular synthetic approach is employed in the next sections to prepare homografted and binary heterografted molecular brushes exhibiting thermo-, light-, and pH-responsive properties. The investigation of stimuli-responsive molecular brushes culminates in a demonstration where binding interactions between biotin-containing thermosensitive heterografted molecular brushes and avidin, a tetrameric protein, can be regulated by temperature. The final chapter diverges somewhat from the previous sections as we study sol-gel transitions of aqueous solutions of tertiary amine-containing thermosensitive ABA triblock copolymers.

In order to prepare stimuli-responsive molecular brushes with a variety of different architectures, it is desirable to develop a robust "grafting to" method such that the backbone and side chains can be prepared separately. In this way, a library of brushes with different side chain compositions can be obtained readily depending on the type of side chains that are added to the reaction feed. Due to the inherent limitations of the grafting to approach, namely steric crowding between grafted chains and incoming chains, we employed highly efficient copper-catalyzed

azide-alkyne cycloaddition “click” reactions to couple the side chains to the backbone polymer. In Chapter 2, we developed a new azide containing backbone polymer that was prepared from ATRP of a silyl ether-protected methacrylate monomer containing a flexible triethylene glycol spacer followed by post-polymerization reactions to install azide moieties on the backbone. Two backbone polymers with DPs of 527 and 800 were prepared with high degrees of azide functionality (≥90 %). Using alkyne end-functionalized PEO with molecular weights of 2 and 5 kDa as model side chain polymers, we prepared well-defined homografted molecular brushes in DMF using CuCl as the catalyst with nearly quantitative grafting densities when a molar ratio of approximately 1 : 2 for the ratio of backbone monomer units to side chains was adopted. Grafting densities were determined by SEC analysis using the ratio of peak areas from the brushes and unreacted side chains, and we found that the grafting density could be readily tuned by adjusting the ratio of backbone monomer units to side chain polymers in the feed. The synthesis of densely grafted molecular brushes was directly confirmed using atomic force microscopy (AFM) of PEO brushes spin coated from aqueous solution onto mica.

We extended the methodology to stimuli-responsive side chains in Chapter 3. Homografted molecular brushes were prepared with side chains composed of either thermosensitive poly(di(ethylene glycol) ethyl ether acrylate) (PDEGEA), thermo- and light-responsive poly((di(ethylene glycol) methyl ether acrylate)-*co*-(*o*-nitrobenzyl acrylate)) (P(DEGMA-*co*-NBA)), or pH-responsive poly(*N*,*N*-diethylaminoethyl methacrylate) (PDEAEMA). We employed the same azide-functionalized backbone polymers with DPs of 527 and 800 whose synthesis is detailed in Chapter 2. The alkyne end-functionalized side chain polymers were prepared by either atom transfer radical polymerization (ATRP) or reversible addition-fragmentation chain transfer (RAFT) polymerization from an alkyne-functionalized initiator or chain transfer agent. We found

that high grafting densities could be achieved even for these more sterically-hindered stimuli-responsive polymers using the grafting to "click" strategy developed in Chapter 2. Dynamic light scattering (DLS) was used to observe dramatic changes in size from an extended worm-like state to a collapsed state in response to applied stimuli.

In Chapter 4, we prepared binary heterografted molecular brushes with water-soluble PEO (2 kDa) and stimuli-responsive PDEGEA, PDEAEMA, or PNBA side chains randomly distributed along the backbone. We used the longer azide-functionalized backbone with a DP of 800 in order to narrow the scope to high aspect ratio brushes for which stimuli-induced shape transitions would likely be more easily observed. Compared to homografted brushes, the collapsed state was found to be stabilized by the incorporation of PEO side chains. Stimuli-induced size changes were studied by DLS, and we used AFM to directly observe shape transitions from the extended worm-like conformation to the collapsed, roughly spherical globular state. Additionally, we explored the possibility of exploiting these stimuli-induced morphological transitions to regulate interactions between heterografted molecular brushes and other macromolecules. We prepared PDEGEA side chains that were incorporated with small amounts of a biotin-containing monomer (BA) and a fluorescent monomer (NBDA) and prepared heterografted brushes containing PEO (5 kDa) and P(DEGEA-*co*-BA-*co*-NBDA) side chains. From an aqueous solution containing PEO/P(DEGEA-*co*-BA-*co*-NBDA) brushes and rhodamine-labelled avidin, which is known to strongly complex biotin, we used temperature as a trigger to "unfold" the brushes, resulting in an increase in binding between biotin-containing brushes and avidin, as observed by fluorescence spectroscopy.

Finally, Chapter 5 shifts the focus to stimuli-responsive hydrogels based on ABA triblock copolymers. A series of tertiary amine-containing ABA triblock copolymers, composed of a PEO central block and thermo- and pH-sensitive outer blocks were prepared, and we studied the effect

of different tertiary amines on thermally induced sol-gel transitions of moderately concentrated aqueous solutions. The doubly responsive ABA triblock copolymers were prepared from a difunctional PEO macroinitiator by ATRP of methoxydi(ethylene glycol) methacrylate (DEGMMA) and ethoxydi(ethylene glycol) methacrylate (DEGEMA) and a small amount of either DEAEMA, *N*,*N*-diisopropylaminoethyl methacrylate (DPAEMA), or *N*,*N*-di(*n*-butyl)aminoethyl methacrylate (DBAEMA). Using rheological measurements, we determined the pH dependences of $T_{\text{sol-gel}}$ of 10 wt % aqueous solutions of these copolymers in a phosphate buffer. In addition, we studied the effect of different tertiary amines on the release behavior of FITC-dextran from micellar gels of these copolymers in acidic medium.

A summary of this dissertation work and future prospects are provided in Chapter 6.

References

1. Milner, S. T. *Science* **1991**, *251*, 905-914.
2. Halperin, A.; Tirrell, M.; Lodge, T. P. *Adv. Polym. Sci.* **1992**, *100*, 31-71.
3. Szleifer, I.; Carignano, M. A. *Adv. Chem. Phys.* **1996**, *94*, 165-260.
4. Zhao, B.; Brittian, W. J. Prog. Polym. Sci. 2000, 25, 677-710.
5. Sheiko, S. S.; Sumerlin, B. S.; Matyjaszewski, K. *Prog. Polym. Sci.* **2008**, *33*, 759-785.
6. Lee, H.; Pietrasik, J.; Sheiko, S. S.; Matyjaszewski, K. *Prog. Polym. Sci.* **2010**, *35*, 24-44.
7. Rzayev, J. *ACS Macro Lett.* **2012**, *1*, 1146-1149.
8. Xiaosong, Y. S.; Gao, H. *Nanoscale* **2016**, *8*, 4864-4881.
9. Gao, H.; Matyjaszewski, K. *J. Am. Chem. Soc.* **2007**, *129*, 6633-6639.
10. Tsarevsky, N. V.; Bencherif, S. A.; Matyjaszewski, K. *Macromolecules* **2007**, *40*, 4439-4445.
11. Yan, Y.; Shi, Y.; Zhu, W.; Chen, Y. *Polymer* **2013**, *54*, 5634-5642.
12. Shi, Y.; Wang, X.; Graff, R. W.; Phillip, W. A.; Gao, H. J. *Polym. Sci., Part A: Polym. Chem.* **2015**, *53*, 239-248.
13. Beers, K. L.; Gaynor, S. G.; Matyjaszewski, K. *Macromolecules* **1998**, *31*, 9413-9415.
14. Cheng, G.; Boker, A.; Zhuang, M.; Krausch, G.; Muller, A. H. E. *Macromolecules* **2001**, *34*, 6883-6888.
15. Matyjaszewski, K.; Qin, S.; Boyce, J. R.; Shirvanyants, D.; Sheiko, S. S. *Macromolecules* **2003**, *36*, 1843-1849.
16. Xia, Y.; Olsen, B. D.; Kornfield, J. A.; Grubbs, R. H. *J. Am. Chem. Soc.* **2009**, *131*, 18525-18532.
17. Xia, Y.; Kornfield, J. A.; Grubbs, R. H. *Macromolecules* **2009**, *42*, 3761-3766.

18. Cheng, C.; Khoshdel, E.; Wooley, K. L. *Macromolecules* **2007**, *40*, 2289-2292.

19. Li, Z.; Zhang, K.; Ma, J.; Cheng, C.; Wooley, K. L. *J. Polym. Sci. Part A: Polym. Chem.* **2009**, *47*, 5557-5563.

20. Li, A.; Ma, J.; Sun, G.; Li, Z.; Cho, S.; Clark, C.; Wooley, K. L. *J. Polym. Sci. Part A: Polym. Chem.* **2012**, *50*, 1681-1688.

21. Li. Z.; Ma, J.; Cheng, C.; Zhang, K.; Wooley, K. L. *Macromolecules* **2010**, *43*, 1182-1184.

22. Miyake, G. M.; Weitekamp, R. A.; Piunova, V. A.; Grubbs, R. H. *J. Am. Chem. Soc.* **2012**, *134*, 14249-14254.

23. Miyake, G. M.; Piunova, V. A.; Weitekamp, R. A.; Grubbs, R. H. *Angew. Chem. Int. Ed.* **2012**, *51*, 11246-11248.

24. Gil, E. S.; Hudson, S. M. *Prog. Polym. Sci.* **2004**, *29*, 1173-1222.

25. Seuring, J.; Agarwal, S. *Macromol. Rapid Commun.* **2012**, *33*, 1898-1920.

26. Jeong, B. M.; Bae, Y. M.; Lee, D. S.; Kim, S. W. *Nature* **1997**, *388*, 860-862

27. Lutz, J-F. J. Polym. Sci. Part A: Polym. Chem. 2008, 46, 3459-3470.

28. Schild, H. G. *Prog. Polym. Sci.* **1992**, 17, 163-249.

29. Dimitrov, I.; Trzebicka, B.; Muller, A. H. E.; Dworak, A.; Tsvetanov, C. B. *Prog. Polym. Sci.* **2007**, *32*, 1275-1343.

30. Li, C.; Ge, Z.; Fang, J.; Liu, S. *Macromolecules* **2009**, *42*, 2916-2924.

31. Yin, J.; Ge, Z.; Liu, H.; Liu, S. *J. Polym. Sci. Part A: Polym. Chem.* **2009**, *47*, 2608-2619.

32. Lian, X.; Wu, D.; Song, X.; Zhao, H. *Macromolecules* **2010**, *43*, 7434-7445.

33. Zehm, D.; Laschewsky, A.; Liang, H.; Rabe, J. P. *Macromolecules* **2011**, *44*, 9635-9641.

34. Li, C.; Gunari, N.; Fischer, K.; Janshoff, A.; Schmidt, M. *Angew. Chem. Int. Ed.* **2004**, *43*, 1101-1104.

35. Balamurugan, S. S.; Grigor, B. B.; Yang, Y.; McCarley, R. L. *Angew. Chem. Int. Ed.* **2005**, *44*, 4872-4876.

36. Pietrasik, J.; Sumerlin, B. S.; Lee, B. Y.; Matyjaszewski, K. *Macromol. Chem. Phys.* **2007**, *208*, 30-36.

37. Yamamoto, S.; Pietrasik, J.; Matyjaszewski, K. *Macromolecules* **2007**, *40*, 9348-9353.

38. Yamamoto, S.; Pietrasik, J.; Matyjaszewski, K. *Macromolecules* **2008**, *41*, 7013-7020.

39. Zhang, N.; Huber, S.; Schulz, A.; Luxenhofer, R.; Jordan, R. *Macromolecules* **2009**, *42*, 2215-2221.

40. Zhang, N.; Luxenhofer, R.; Jordan, R. *Macromol. Chem. Phys.* **2012**, *213*, 973-981.

41. Zhang, N.; Luxenhofer, R.; Jordan, R. *Macromol. Chem. Phys.* **2012**, *213*, 1963-1969.

42. Lee, H.; Boyce, J. R.; Nese, A.; Sheiko, S. S.; Matyjaszewski, K. *Polymer* **2008**, *49*, 5490-5496.

43. Xu, Y.; Bolisetty, S.; Drechsler, M.; Fang, B.; Yuan, J.; Ballauff, M.; Muller, A. X. E. *Polymer* **2008**, *49*, 3957–64.

44. Xu, Y.; Bolisetty, S.; Drechsler, M.; Fang, B.; Yuan, J.; Harnau, L.; Ballauff, M.; Muller, A. X. E. *Soft Matter* **2009**, *5*, 379–84.

45. Xu, Y.; Bolisetty, S.; Ballauff, M.; Mueller, A. H. E. *J. Am. Chem. Soc.* **2009**, *131*, 1640–1641.

46. Lee, H. L.; Pietrasik, J.; Matyjaszewski, K. *Macromolecules* **2006**, *39*, 3914-3920.

47. Yao, J.; Chen, Y.; Zhang, J.; Bunyard, C.; Tang, C. *Macromol. Rapid Commun.* **2013**, *34*, 645-651.

48. Alexander-Katz, A. *Macromolecules* **2014**, *47*, 1503−1513.

49. Savage, B.; Sixma, J. J.; Ruggeri, Z. M. *Proc. Natl. Acad. Sci. U. S. A.* **2002**, *99*, 425−430.

50. Sadler, J. E. *Annu. Rev. Biochem.* **1998**, *67*, 395-424.

51. Joo, M. K.; Park, M. H.; Choi, B. G.; Jeong, B. *J. Mater. Chem*. **2009**, *19*, 5891–5905.

52. He, C. L.; Kim, S. W.; Lee, D. S. *J. Controlled Release* **2008**, *127*, 189–207.

53. Jeong, B.; Kim, S.W; Bae, Y. H. *Adv. Drug Delivery Rev*. **2002**, *54*, 37–51.

54. Yu, L.; Ding, J. *Chem. Soc. Rev*. **2008**, *37*, 1473–1481.

55. Ahn, S. -K.; Kasi, R. M.; Kim, S. -C.; Sharma, N.; Zhou, Y. *Soft Matter* **2008**, *4*, 1151–1 157.

56. Hamley, I. W.; Pople, J. A.; Fairclough, J. P. A.; Ryan, A. J.; Booth, C.; Yang, Y. W. *Macromolecules* **1998**, *31*, 3906-3911.

57. Mortensen, K.; Brown, W.; Nordén, B., *Phys. Rev. Lett.* **1992,** *68*, 2340-2343.

58. Pozzo, D. C.; Walker, L. M., *Macromolecules* **2007,** *40*, 5801-5811.

59. Hamley, I., Block Copolymers in Solution: Fundamentals and Applications. John Wiley & Sons, Ltd: 2005.

60. Kirkland, S. E.; Hensarling, R. M.; McConaughy, S. D.; Guo, Y.; Jarrett, W. L.; McCormick, C. L., *Biomacromolecules* **2008,** *9*, 481-486.

61. Madsen, J.; Armes, S. P.; Lewis, A. L., *Macromolecules* **2006,** *39*, 7455-7457.

62. Mortensen, K.; Brown, W.; Joergensen, E., *Macromolecules* **1994,** *27*, 5654-5666.

63. Zhou, C.; Hillmyer, M. A.; Lodge, T. P., *J. Am. Chem. Soc.* **2012,** *134*, 10365-10368.

64. Butun, V.; Billingham, N. C.; Armes, S. P., *J. Am. Chem. Soc.* **1998,** *120*, 11818- 11819.

65. Liu, S.; Armes, S. P., *Angew. Chem. Int. Ed.* **2002,** *41*, 1413-1416.

66. Lokitz, B. S.; York, A. W.; Stempka, J. E.; Treat, N. D.; Li, Y.; Jarrett, W. L.; McCormick, C. L., *Macromolecules* **2007,** *40*, 6473-6480.

67. Yin, X.; Hoffman, A. S.; Stayton, P. S., *Biomacromolecules* **2006,** *7*, 1381-1385.

68. Jiang, X.; Zhao, B., *Macromolecules* **2008,** *41*, 9366-9375.

69. Jiang, X.; Lavender, C. A.; Woodcock, J. W.; Zhao, B., *Macromolecules* **2008,** *41*, 2632-2643.

70. Jin, N.; Woodcock, J. W.; Xue, C.; O'Lenick, T. G.; Jiang, X.; Jin, S.; Dadmun, M. D.; Zhao, B., *Macromolecules* **2011,** *44*, 3556-3566.

71. Jin, N.; Zhang, H.; Jin, S.; Dadmun, M. D.; Zhao, B., *Macromolecules* **2012,** *45*, 4790-4800.

72. Jin, N.; Zhang, H.; Jin, S.; Dadmun, M. D.; Zhao, B., *J. Phys. Chem. B* **2012,** *116*, 3125-3137.

73. Woodcock, J. W.; Jiang, X.; Wright, R. A. E.; Zhao, B., *Macromolecules* **2011,** *44* (14), 5764-5775.

74. Woodcock, J. W.; Wright, R. A. E.; Jiang, X.; O'Lenick, T. G.; Zhao, B., *Soft Matter* **2010,** *6*, 3325-3336.

75. O'Lenick, T. G.; Jin, N.; Woodcock, J. W.; Zhao, B., *J. Phys. Chem. B* **2011,** *115*, 2870-2881.

76. O'Lenick, T. G.; Jiang X. G.; Zhao, B. *Langmuir* **2010**, *26*, 8787–8796.

77. Zhou, K. J.; Wang, Y. G.; Huang, X. N.; Luby-Phelps, K..; Sumer, B. D.; Gao, J. M. *Angew.Chem., Int. Ed.* **2011**, *50*, 6109–6114.

Chapter 2: Water-Soluble Poly(ethylene oxide) Homografted Linear Molecular Brushes with High and Tunable Grafting Densities Synthesized by a "Grafting to" Method

Abstract

This chapter presents the development of a robust method to synthesize well-defined molecular bottlebrushes by a "grafting to" technique using water soluble poly(ethylene oxide) (PEO) as model side chains. We employed highly efficient copper-catalyzed azide-alkyne cycloaddition (CuAAC) "click" reactions to couple alkyne end-functionalized PEO side chains to azide functionalized backbone polymers. Two backbone polymers with degrees of polymerization (DPs) of 527 and 800 were synthesized by atom transfer radical polymerization (ATRP) and post-polymerization reactions to install azide moieties with high degrees of functionality (≥90 %). Alkyne end-functionalized PEO side chain polymers with DPs of 45 and 114 (PEO-45 and PEO-114, respectively) were prepared from commercially available PEO monomethyl ether with molecular weights of 2 kDa and 5 kDa via the reaction of the hydroxyl end group with 4-pentynoic acid. "Grafting to" click reactions were performed in DMF at ambient temperature with CuCl as catalyst, and the grafting densities, defined as the percentage of backbone monomer units that are grafted with a side chain polymer, were determined by size exclusion chromatography using the relative peak areas from the brushes and unreacted side chains. Using this method, we were able to prepare PEO brushes with a backbone DP of 527 and a side chain DP of 45 with a nearly quantitative grafting density (98.0 %) when a molar ratio of backbone monomer units to side chains of 1 : 1.48 was used. When the longer PEO-114 side chains were used with a molar ratio of approximately 1 : 2 for the backbone monomer units to side chains, a grafting density of 92.6% was achieved. The grafting density could be readily tuned by adjusting this ratio. Under similar conditions, slightly lower grafting densities were observed when the backbone with a DP of 800 was employed with either PEO-45 or PEO-114. Pure PEO brush molecules were obtained by

centrifugal filtration to remove unreacted side chains, and their synthesis was directly confirmed by atomic force microscopy.

2.1. Introduction

Molecular bottlebrushes, a type of graft copolymer composed of side chains that are densely tethered at one end to a polymer backbone, have received considerable attention in recent years due to their unique molecular structures.[1-3] Recent advances in polymer synthesis offers excellent opportunities for rationally designed architectures and functionalities that can be applied to a wide range of disciplines, including biomedicine, lubrication, and nanotechnology.

In Chapter 1, we discussed three general strategies for the synthesis of molecular brushes: "grafting from," "grafting through," and "grafting to."[1,2] Each strategy has its own inherent strengths and weaknesses, and the desired brush architecture is often the determining factor for which method is the most suitable. The "grafting from" approach is probably the most commonly used route because the complication due to steric crowding of side chains is alleviated by the gradual growth of side chains from the backbone.[4-20] Although this technique is well suited for the synthesis of homografted molecular brushes, it's utility is limited when more complex brush architectures are desired, such as heterografted brushes in which different side chains are randomly distributed along the backbone. The "grafting through" technique would be well suited for the synthesis of such brush compositions, except that polymerizations of macromonomers often cannot reach high conversions due to the low concentration of polymerizable end groups and the high steric hindrance at the propagating chain end. These drawbacks can oftentimes be alleviated by ring opening metathesis polymerization of norbornene-bearing macromonomers using highly active Grubbs catalysts,[21-28] although it can still be difficult to obtain high backbone DPs and narrow molecular weight distributions for more sterically hindered side chains. The "grafting to" approach is unique in that the backbone and side chain polymers can be synthesized and characterized separately, and different brush compositions can be readily prepared based on the

types of side chains that are added to the reaction feed. This makes grafting to an ideal strategy for the synthesis of heterografted brushes. Although low grafting densities are traditionally obtained with this method due to steric crowding between grafted chains and incoming chains, recent advances in the combination of highly efficient "click" reactions, the most popular being copper-catalyzed azide-alkyne cycloaddtion (CuAAC), with macromolecular synthetic techniques have allowed for high grafting densities to be achieved using the "grafting to" route.[29-41] This technique combined with the highly robust nature of the CuAAC reaction, exhibiting very high functional group tolerance, can be a powerful method for the synthesis of molecular brushes with a wide range of architectures and functionalities.

There have been several reports where molecular brushes were synthesized by a grafting to approach using CuAAC "click" reactions, although with varying degrees of success in terms of high grafting densities being achieved. Gao and Matyjaszewski prepared alkyne-functionalized backbone polymers by atom transfer radical polymerization (ATRP) of 2-hydroxyethyl methacrylate followed by esterification of the monomer units with pentynoic acid.[34] Homografted molecular brushes with different side chain compositions were synthesize by CuAAC reactions at ambient temperature with azide end-functionalized poly(ethylene glycol) (PEO), polystyrene (PS), poly(*n*-butyl acrylate) (P*n*BA), and P*n*BA-*b*-PS. The azide moiety on the side chains was installed by end group transformation using sodium azide to substitute either a mesylate group (for PEO) or the halogen chain end from ATRP (for PS, P*n*BA, and P*n*BA-*b*-PS). They found that the grafting density was affected by the molecular weight and chemical structure (steric hindrance) of the side chains as well as the initial molar ratio of backbone monomer units to side chains. A maximum grafting density of 88.4 % was achieved when 775 Da PEO side chains were used with a molar ratio of 1 : 8.50 for backbone alkyne units to side chains in the feed. Significantly lower grafting

densities were achieved when a lower molar ratio of 1 : 1.80 was employed for brushes prepared using 775 Da PEO (62.5 %) as well as more sterically hindered 2025 Da PEO (47.7 %), 1380 Da PS (37.1 %), 2060 Da P*n*BA (40.1 %), and 3810 Da P*n*BA-*b*-PS (20.3 %). These results suggest that a large excess of side chains are required to obtain high grafting densities even when highly linear and relatively low molecular weight 775 Da PEO side chains are used. However, Chen et al. synthesized PS, P*n*BA and P*t*BA molecular brushes with high grafting densities (>85 %) using a 1 : 1 molar ratio of backbone monomer units to side chains, although much lower grafting densities (~50 %) were observed for polymethacrylate side chains.[36] In the work by Chen et al., the click reactions between azide-functionalized backbone polymers and alkyne end-functionalized side chains were performed in DMF at 50 ^{o}C using a $CuSO_4$/ascorbic acid catalyst system. The backbone polymer was prepared by radical addition-fragmentation chain transfer (RAFT) polymerization of glycidyl methacrylate followed by opening of the epoxide repeat units with sodium azide. The side chains were prepared by RAFT polymerization using an alkyne-containing chain transfer agent. Gao et al. achieved similarly high grafting densities (>90 %) under similar conditions (1 : 1 molar ratio, 50 ^{o}C, $CuSO_4$/ascorbic acid catalyst) using alkyne end-functionalized poly(methyl acrylate), PS, PEO, and P*t*BA-*b*-PS side chains and a degradable polycarbonate backbone containing two azide moieties on each repeat unit.[39]

We are interested in the synthesis of homografted as well as heterografted molecular bottlebrushes that undergo dramatic changes in both size and shape in response to a variety of stimuli. With this in mind, we set out to develop a robust grafting to "click" method that could be extended to a wide variety of side chain compositions. In the present work, we developed a new azide containing backbone polymer that was prepared from ATRP of a silyl ether-protected methacrylate monomer containing a flexible triethylene glycol spacer followed by post-

polymerization reactions to functionalize the backbone monomer units with azide moieties. Two backbone polymers with DPs of 527 and 800 were prepared with high degrees of azide functionality. Using alkyne end-functionalized PEO with molecular weights of 2 and 5 kDa as model side chain polymers, we prepared well-defined homografted molecular brushes in DMF using CuCl as the catalyst with nearly quantitative grafting densities when a molar ratio of approximately 1 : 2 for the ratio of backbone monomer units to side chains was adopted (Scheme 2.1). Additionally, we found that the grafting density could be readily tuned by adjusting this ratio. The synthesis of densely grafted "worm-like" PEO molecular brushes was directly confirmed using atomic force microscopy (AFM).

2.2. Experimental Section

2.2.1. Materials

Ethyl 2-bromoisobutyrate (EBiB, 98%, Aldrich) and *N,N,N',N'',N''*-pentamethyldiethylenetriamine (PMDETA, 99%, Acros) were purified by vacuum distillation over calcium hydride. Triethylene glycol (99 %), imidazole (99 %), *tert*-butylchlorodimethylsilane (98 %), methacryloyl chloride (95 %), *p*-toluenesulfonyl chloride (99 %), and sodium azide (99 %) were purchased from Acros and used as received. Triethylamine (99 %) was purchased from Alfa Aesar and used as received. CuBr (98%, Aldrich) was stirred in glacial acetic acid overnight, filtered, and washed with absolute ethanol and diethyl ether. The solid was then collected, dried under vacuum, and stored in a desiccator. Poly(ethylene glycol) monomethyl ether (CH_3O-PEO-OH) with molecular weights of 2000 and 5000 g/mol were purchased from Aldrich. All other chemicals were purchased from either Aldrich or Fisher and used as received.

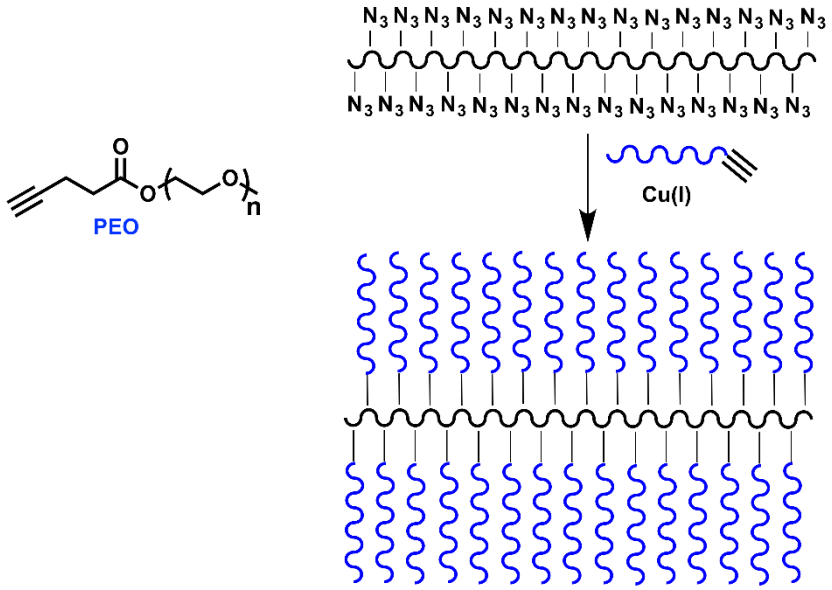

Scheme 2.1. Synthesis of Water-Soluble PEO Molecular Brushes by "Grafting To" CuAAC "Click" Reaction.

2.2.2. General Characterization

Size exclusion chromatography (SEC) of PEO molecular brush samples was carried out at ambient temperature using a PL-GPC 50 Plus (an integrated GPC/SEC system from Polymer Laboratories, Inc.) with a differential refractive index detector, one PLgel 10 µm guard column (50 × 7.5 mm, Agilent Technologies), and three PLgel 10 µm Mixed-B columns (each 300 × 7.5 mm, linear range of molecular weight from 500 to 10,000,000 Da according to Agilent Technologies). The data were processed using Cirrus™ GPC/SEC software (Polymer Laboratories, Inc.). *N*,*N*-Dimethylformamide (DMF) with 50 mM LiBr was used as the carrier solvent at a flow rate of 1.0 mL/min. SEC of PEO side chain polymers was carried out using a PL-GPC 20 integrated GPC/SEC system from Polymer Laboratories, Inc. with a refractive index detector, one PLgel 5 µm guard column (50 × 7.5 mm, Agilent Technologies), and two PLgel 5 µm Mixed-C columns (each 300 × 7.5 mm, linear range of molecular weight from 200 to 2,000,000 Da according to Agilent Technologies). THF was used as the eluent at a flow rate of 1.0 mL/min. Each system was calibrated with a set of near-monodisperse linear polystyrene standards (Polymer Laboratories, Inc.). ^{1}H and ^{13}C NMR (300 or 500 MHz) spectra were recorded on a Varian Mercury 300 NMR spectrometer or a Varian VNMRS 500 NMR spectrometer, respectively, and the residual solvent proton signal was used as the internal standard. High resolution mass spectroscopy (HRMS) experiments were performed using a JEOL Model JMS-T100LC (AccuTOF) orthogonal time-of-flight (TOF) mass spectrometer (Peabody, MA) with an IonSense (Danvers, MA) DART source.

2.2.3. Synthesis of Tri(ethylene glycol) Mono(*t*-butyldimethylsilyl) Ether (TEGSi)

Triethylene glycol (16.049 g, 0.107 mol), imidazole (8.202 g, 0.120 mol), and DMF (20 mL, dried over molecular sieves) were added to a 100 mL three-necked round bottom flask with a stir

bar. With stirring, *t*-butylchlorodimethylsilane (8.118 g, 53.9 mmol) was added in 4 portions over 1 h. The mixture was stirred under nitrogen overnight. DMF was then distilled off under high vacuum. The mixture was diluted with methylene chloride (150 mL), washed 4 times with water (5 mL) and saturated sodium chloride solution (1 mL), and dried over anhydrous sodium sulfate. The crude product was then purified by column chromatography with ethyl acetate eluent and dried under high vacuum to obtain a clear, colorless liquid (7.547 g, 52.9 %). ^{1}H NMR δ (ppm, $CDCl_3$): 3.77 (t, HOC*H*$_2$CH$_2$O-, 2H), 3.72 (m, HOCH$_2$C*H*$_2$O-, 2H), 3.66 (s, HOCH$_2$CH$_2$OC*H*$_2$C*H*$_2$O-, 4H), 3.61 (m, -OC*H*$_2$CH$_2$OSi-, 2H), 3.56 (t, -OCH$_2$C*H*$_2$OSi-, 2H), 2.44 (br s, -O*H*, 1H), 0.89 (s, -SiC(C*H*$_3$)$_3$, 9H), 0.04 (s, -Si(C*H*$_3$)$_2$, 6H). ^{13}C NMR δ (ppm, $CDCl_3$): 72.66 (-*C*H$_2$-), 72.49 (-*C*H$_2$-), 70.73 (-*C*H$_2$-), 70.43 (-*C*H$_2$-), 62.67 (-*C*H$_2$-), 61.75 (-*C*H$_2$-), 25.89 (-SiC(*C*H$_3$)$_3$), 18.34 (-Si*C*(CH$_3$)$_3$), -5.32 (-Si(*C*H$_3$)$_2$).

2.2.4. Synthesis of Tri(ethylene glycol) Mono(*t*-butyldimethylsilyl) Ether Methacrylate (TEGSiMA)

TEGSi (7.547 g, 28.5 mmol), triethylamine (4.209 g, 41.6 mmol), and methylene chloride (25 mL) were added into a 100 mL three-necked round bottom flask with a stir bar, and the mixture was stirred under nitrogen in an ice/water bath for 20 min. A solution of methacryloyl chloride (3.607 g, 34.5 mmol) in methylene chloride (10 mL) was added dropwise over a period of 45 min. The solution turned light orange-pink, and a white precipitate was observed. The mixture was stirred at room temperature under nitrogen overnight. The precipitate was filtered off; the mixture was diluted to 120 mL with methylene chloride, washed 4 times with aqueous sodium bicarbonate (water : saturated sodium bicarbonate solution, v/v = 1:1) and saturated sodium chloride solution (1.5 mL), and dried over anhydrous sodium sulfate. The crude product was purified by column chromatography using a mixture of ethyl acetate and hexanes (v/v = 1:4) as eluent. The product

was dried under high vacuum and obtained as a clear, colorless liquid (8.274 g, 87.4 %). The product was further purified by vacuum distillation in the presence of a small amount of hydroquinone, dissolved in methylene chloride, and washed with 1.0 M aqueous NaOH to remove any remaining inhibitor. The product was then dried over anhydrous sodium sulfate, filtered, and dried under high vacuum to obtain a clear, colorless liquid (5.411 g, 65.4 % yield). ^{1}H NMR δ (ppm, $CDCl_3$): 6.13 and 5.57 (2s, C*H*$_2$=CH-, 2H), 4.30 (t, -COOC*H*$_2$-, 2H), 3.75 (m, -COOCH$_2$C*H*$_2$OCH$_2$CH$_2$OC*H*$_2$CH$_2$O-, 4H), 3.66 (s, -COOCH$_2$CH$_2$OC*H*$_2$C*H*$_2$O-, 4H), 3.56 (t, -OCH$_2$C*H*$_2$OSi-, 2H), 1.92 (s, α-C*H*$_3$, 3H), 0.87 (s, -SiC(C*H*$_3$)$_3$, 9H), 0.04 (s, -Si(CH$_3$)$_2$, 6H). ^{13}C NMR δ (ppm, $CDCl_3$): 167.34 (-*C*OO-), 136.14 (CH$_2$=*C*H-), 125.66 (*C*H$_2$=CH-), 72.70 (-O*C*H$_2$-), 70.73 (-O*C*H$_2$-), 70.69 (-O*C*H$_2$-), 69.14 (-O*C*H$_2$-), 63.89 (-COO*C*H$_2$-), 62.71 (-*C*H$_2$OSi-), 25.90 (-SiC(*C*H$_3$)$_3$), 18.34 (-Si*C*(CH$_3$)$_3$), 18.28 (α-*C*H$_3$), -5.30 (-Si(*C*H$_3$)$_2$). HRMS (DART-TOF): m/z calc $C_{16}H_{32}O_5Si$ $[M+H]^+$: 333.20918; found: 333.20902; mass error: 0.48 ppm.

2.2.5. Synthesis of Silyl Ether-Protected Backbone Polymers: Poly(tri(ethylene glycol) mono(*t*-butyldimethylsilyl) ether methacrylate) (PTEGSiMA)

Described below is the procedure for the synthesis of silyl ether-protected backbone polymer PTEGSiMA with a DP of 527 (PTEGSiMA-527). A similar procedure was used for the preparation of PTEGSiMA with a DP of 800 (PTEGSiMA-800). Ethyl 2-bromoisobutyrate (EBiB, 0.894 mg, 0.00458 mmol, from a stock solution in anisole), TEGSiMA (1.514 g, 4.55 mmol), CuBr (1.9 mg, 0.013 mmol), $CuBr_2$ (0.7 mg, 0.003 mmol), PMDETA (5.0 µL, 0.024 mmol), and anisole (2.054 g) were weighed into a 25 mL two-neck round bottom flask equipped with a magnetic stir bar. The mixture was degassed by three freeze-pump-thaw cycles and then stirred in a 60 °C oil bath. The polymerization was monitored by ^{1}H NMR spectroscopy and SEC. After 8 h 35 min, the flask was removed from the oil bath and opened to air. A sample was taken immediately for ^{1}H NMR

analysis to determine the monomer conversion. The mixture was passed through neutral alumina to remove the catalyst. The polymer was then purified by precipitation three times in methanol and dried under high vacuum to yield a colorless, viscous polymer (0.612 g). The DP was 527, calculated using the monomer conversion and the molar ratio of monomer to initiator. The monomer conversion was determined by ^{1}H NMR spectroscopy using the integrals of the peaks at 4.30 ppm (-COOCH_2- of monomer) and 3.98-4.14 ppm (-COOCH_2- of polymer). The results of SEC analysis with THF as carrier solvent: $M_{n,SEC}$ = 67,100 Da; PDI = 1.07.

2.2.6. Synthesis of Azide-Functionalized Backbone Polymers: PTEGN$_3$MA

Described below is the procedure for the synthesis of azide-functionalized backbone polymer with a DP of 527 (PTEGN$_3$MA-527). A similar procedure was used for the preparation of azide-functionalized backbone polymer with a DP of 800 (PTEGN$_3$MA-800). PTEGSiMA-527 (0.591 g, 1.78 mmol repeat units) was added into a 100 mL 3-necked round bottom flask equipped with a stir bar and dissolved in ethanol (30.047 g). HCl (1.0 M, 3.6 mL) was added dropwise, and the mixture was stirred under nitrogen at room temperature. After 3 h, volatile compounds were distilled off under high vacuum to yield a colorless, viscous polymer. The polymer was then dissolved in chloroform (50 mL) and placed in an ice/water bath. Triethylamine (1.940 g, 19.2 mmol) was added, followed by the addition of *p*-toluenesulfonyl chloride (tosyl chloride, 1.740 g, 9.13 mmol) in chloroform (20 mL) dropwise over a period of 40 min under nitrogen. The mixture was stirred overnight. The mixture was then concentrated, and the polymer was precipitated in diethyl ether (50 mL), washed with water (20 mL) twice, and dried under high vacuum. To ensure complete functionalization with tosylate, the reaction was repeated by dissolving the crude polymer in chloroform (12 mL), followed by the addition of triethylamine (1.401 g, 13.8 mmol) and tosyl chloride (1.404 g, 7.36 mmol). After being stirred under nitrogen at room temperature

overnight, the mixture was then concentrated. The polymer was precipitated in diethyl ether (40 mL) three times, rinsed with water (25 mL) five times, dissolved in methylene chloride, and dried over anhydrous sodium sulfate. The polymer solution was concentrated and dried under high vacuum to yield a light yellow, viscous polymer (PTEGTsMA-527, 0.489 g, 73.6 % yield).

PTEGTsMA-527 (0.489 g, 1.31 mmol repeat units assuming 100% functionalization with tosylate) was placed in a 20 mL vial equipped with a magnetic stir bar and dissolved in DMF (7.526 g). NaN_3 (0.446 g, 6.86 mmol) was added, and the mixture was stirred at room temperature for 3 h and then 35 °C for 24 h. The mixture was diluted with acetone and gravity filtered to remove the precipitate. The mixture was then concentrated, passed through a small silica gel column, and filtered with a 0.4 µm syringe filter. The product was finally dried under high vacuum to yield a light yellow, viscous polymer (PTEGN_3MA-527, 0.258 g, 80.9 % yield). The results of SEC analysis with DMF containing 50 mM LiBr as carrier solvent: $M_{n,SEC}$ = 196,800 Da; PDI = 1.08.

2.2.7. Synthesis of Alkyne End-Functionalized Water-Soluble PEO Side Chain Polymers

Described below is the procedure for the synthesis alkyne end-functionalized PEO side chain polymer with a molecular weight of 2000 Da (DP = 45) (PEO-45). Alkyne-functionalized PEO side chain polymer with a molecular weight of 5000 Da (DP = 114) (PEO-114) was prepared using a similar procedure. CH_3O-PEO-OH (3.100 g, 1.55 mmol, 2000 g/mol) was weighed out into a 25 mL two-necked round bottom flask equipped with a magnetic stir bar and dried under high vacuum at 75 °C for 3.5 h to remove the absorbed water. The flask was cooled to room temperature and methylene chloride (10 mL) was added to dissolve the PEO. 4-(*N*,*N*-Dimethylamino)pyridine (19.7 mg, 0.161 mmol) and 4-pentynoic acid (0.188 g, 1.92 mmol) were added, and the mixture was stirred under nitrogen in an ice/water bath. A solution of *N*-(3-dimethylaminopropyl)-*N′*-ethylcarbodiimide hydrochloride (0.410 g, 2.14 mmol) in methylene chloride (10 mL) was added

dropwise under nitrogen, and the mixture was allowed to warm to room temperature and stirred overnight. The reaction mixture was then diluted with methylene chloride (100 mL) and washed with a mixture of pure water/saturated NaCl solution (5/1, v/v) twice, a mixture of 1.0 M NaOH/saturated NaCl solution (5/1, v/v) twice, and once again with a mixture of pure water/saturated NaCl solution (5/1, v/v). The organic layer was dried over anhydrous sodium sulfate, gravity filtered, and concentrated. The polymer was further purified by precipitation in diethyl ether twice and dried under high vacuum to yield a white, powdery polymer (2.944 g, 90.4 %). ^{1}H NMR δ (ppm, $CDCl_3$): 4.21 (t, HC≡CCH$_2$CH$_2$COOC*H*$_2$- of alkyne end group, 2H), 3.42-3.76 (s, -OC*H*$_2$C*H*$_2$- of PEO monomer units, 180H), 3.33 (s, -OC*H*$_3$ of methyl end group, 3H), 2.42-2.56 (m, HC≡CC*H*$_2$C*H*$_2$COOCH$_2$- of alkyne end group, 4H), 1.94 (t, *H*C≡CCH$_2$CH$_2$COOCH$_2$- of alkyne end group, 1H). The results of SEC analysis using PL GPC-20 system with THF as carrier solvent: $M_{n,SEC}$ = 2,800 Da; PDI = 1.08.

2.2.8. Synthesis of Water-Soluble PEO Homografted Molecular Brushes

Below is the procedure for the synthesis of PEO molecular brushes with a backbone DP of 527 and a side chain DP of 45 (PEO MB-1). Similar procedures were employed for the synthesis of other PEO molecular brushes with different backbone and side chain DPs. PTEGN$_3$MA-527 (5.1 mg, 0.0210 mmol monomer units, from a stock solution in THF) was added into a 3.7 mL vial equipped with a stir bar. THF was evaporated off with a stream of nitrogen, and DMF (0.5 mL) was added. PEO-45 (65.0 mg, 0.0310 mmol alkyne end groups) was weighed into a separate vial, dissolved in DMF (2.0 mL), and transferred to the vial containing PTEGN$_3$MA-527. CuCl (2.3 mg, 0.023 mmol) was added, and a rubber septum was used to seal the reaction vial. The mixture was flushed with nitrogen via needles for 15 min, and PMDETA (5.0 µL, 0.024 mmol) was injected using a microsyringe. The reaction progress was monitored by SEC. After 24 h, the

reaction mixture was opened to air, diluted with methylene chloride, and passed through a short neutral alumina/silica gel column to remove the catalyst. The grafting density, defined as the percentage of backbone monomer units that are grafted with a side chain polymer, was determined to be 98.0 % by comparison of the brush and the unreacted side chain polymer peak areas from SEC chromatogram of the reaction mixture at the end of the reaction. The results of SEC analysis of the purified brushes with DMF containing 50 mM LiBr as carrier solvent: $M_{n,SEC}$ = 713,900; PDI = 1.10.

2.2.9. Atomic Force Microscopy of PEO Molecular Brushes

Atomic force microscopy (AFM) was performed using a Digital Instruments Multimode IIIa Scanning Probe Microscope operated in tapping mode under ambient conditions. Reflective Al-coated Si probes (Budget Sensors) with a nominal resonant frequency of 300 kHz and force constant of 40 N/m were employed. Aqueous solutions of molecular brushes with a concentration of 0.1-0.01 mg/g for AFM imaging were prepared using Milli-Q water and spin coated at 3000 rpm onto freshly cleaved mica.

2.3. Results and Discussion

2.3.1. Synthesis of Azide-Functionalized Backbone Polymers (PTEGN_3MA)

Azide-functionalized backbone polymers (PTEGN_3MA) were synthesized by ATRP of TEGSiMA, a silyl ether protected methacrylate monomer, followed by first removal of the *t*-butyldimethylsilyl ether moiety, then reaction with tosyl chloride, and finally substitution with sodium azide to yield PTEGN_3MA (Scheme 2.2). TEGSiMA monomer was chosen based on three important features: (i) the polymerization of the silyl ether protected methacrylate monomer by ATRP can be well-controlled, producing well-defined backbone polymer precursors with

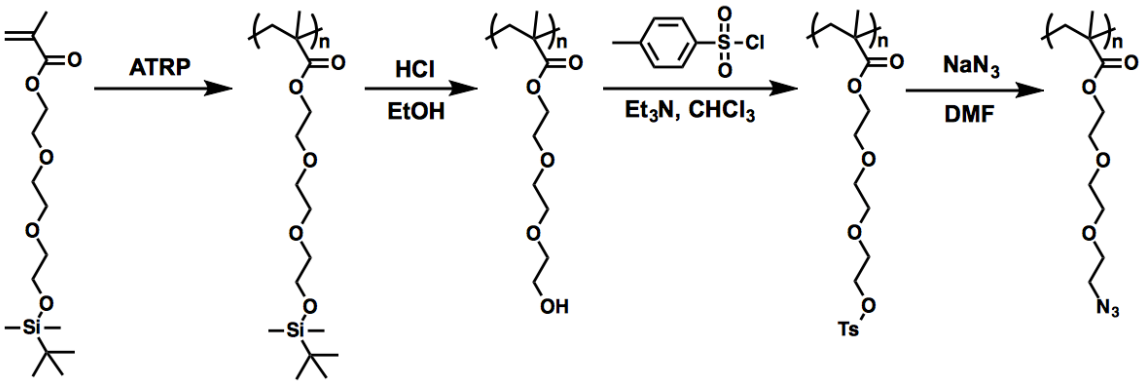

Scheme 2.2. Synthesis of Azide-Functionalized Backbone Polymer $PTEGN_3MA$ by Atom Transfer Radical Polymerization and Subsequent Post-Polymerization Reactions Including Removal of Protective Silyl Ether, Reaction with Tosyl Chloride, and Substitution with Azide.

sufficiently high DPs and small polydispersity indices; (ii) the desired azide functionality can be introduced through a series of (nearly) quantitative post-polymerization reactions as reported in the literature; (iii) the incorporation of a tri(ethylene glycol) spacer between the backbone and the azide moiety should alleviate steric hindrance during the "grafting to" reaction and result in higher grafting densities for more sterically hindered stimuli responsive polymers. We used this synthetic route instead of direct polymerization of a halogen-, or tosylate-, or azide-containing (meth)acrylate monomer by ATRP because it is known to be problematic to synthesize high molecular weight well-defined polymers by ATRP or other "living"/controlled radical polymerization of these monomers due to the chain transfer or other side reactions with alkyl bromide, tosylate, and azide groups, making it difficult to achieve narrow polydispersities. As a matter of fact, we attempted to synthesize backbone polymer precursors from alkyl bromide- and chloride-containing (meth)acrylates but could not obtain polymers with sufficiently large DPs and low PDIs at the same time.

The silyl ether protected methacrylate monomer TEGSiMA was prepared via a two-step process (Scheme 2.3). Triethylene glycol was first reacted with *t*-butylchlorodimethylsilane in the presence of imidazole in DMF to protect one hydroxyl group with *t*-butyldimethylsilyl ether. The mono(*t*-butyldimethylsilyl) ether of triethylene glycol (TEGSi) was isolated by column chromatography and then reacted with methacryloyl chloride in the presence of triethylamine in methylene chloride to yield TEGSiMA monomer, which was purified by column chromatography and vacuum distillation. The molecular structure was verified by ^{1}H and ^{13}C NMR spectroscopy (Figure 2.1); all characteristic peaks were observed and the integrals in the ^{1}H NMR spectrum were in agreement with the molecular structure of TEGSiMA. High resolution mass spectrometry

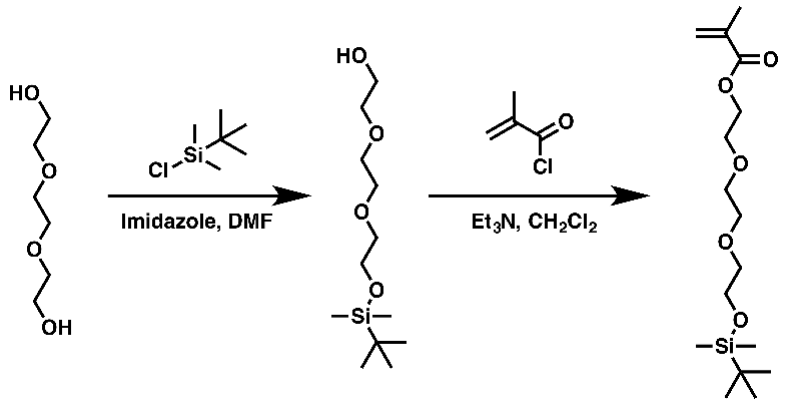

Scheme 2.3. Synthesis of Monomer TEGSiMA via a Two-Step Process.

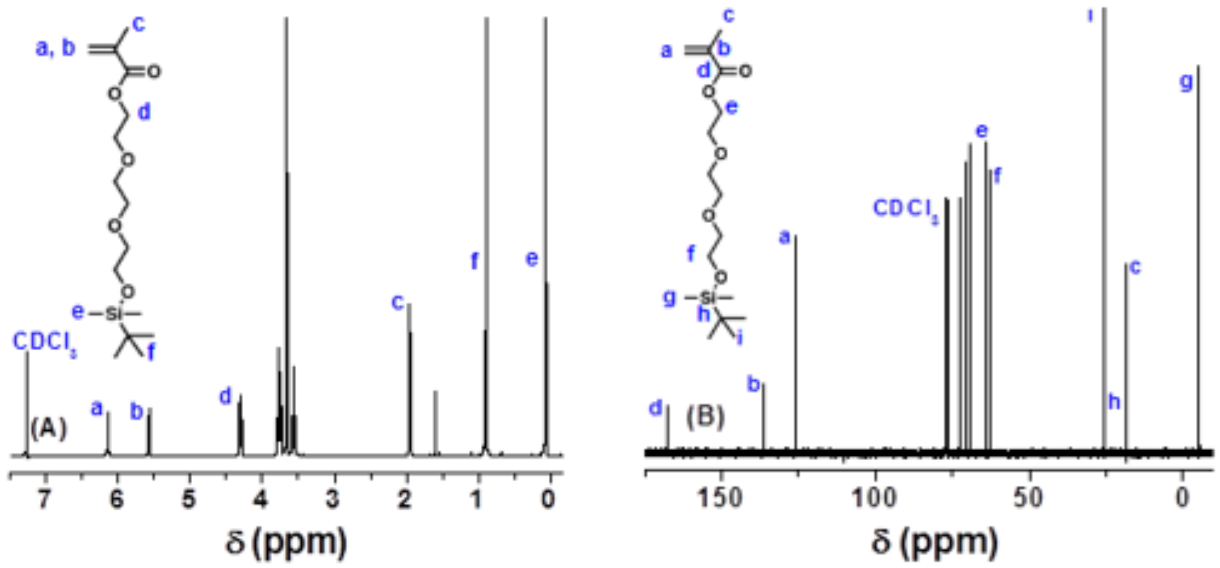

Figure 2.1. (A) ^{1}H NMR and (B) ^{13}C NMR spectra of TEGSiMA monomer in $CDCl_3$.

analysis showed that the $[M + H]^+$ ion was observed at *m/z* 333.20902, which is very close to the calculated value of 333.20918.

To achieve stimuli-induced shape changing of molecular brushes from an extended worm-like state to a collapsed spherical state or vice versa (discussed later in Chapters 3 and 4), the backbone polymer must be sufficiently long and the aspect ratio should be large. Therefore, we prepared PTEGSiMA backbone polymer precursors with DPs of 527 and 800, referred to as PTEGSiMA-527 and PTEGSiMA-800, respectively, by ATRP. The polymerizations were carried out in anisole at 60 °C using ethyl 2-bromoisobutyrate as initiator and $CuBr/CuBr_2$/PMDETA as catalyst and were monitored by SEC and ^{1}H NMR spectroscopy analysis. The final monomer conversions were calculated from the ^{1}H NMR spectra of the reaction mixtures using the integrals of the peaks at 4.30 ppm (-COOCH_2- of monomer) and 3.98-4.14 ppm (-COOCH_2- of polymer). The polymers were purified by repetitive precipitation in methanol, dried under high vacuum, and analyzed by size exclusion chromatography (SEC) and ^{1}H NMR spectroscopy. The SEC traces and ^{1}H NMR spectra of PTEGSiMA-527 and PTEGSiMA-800 are shown in Figure 2.2. From SEC, it can be seen that the ATRP polymerizations of TEGSiMA were well-controlled, yielding backbone polymer precursors with PDIs of 1.07 and 1.11 for PTEGSiMA-527 and PTEGSiMA-800, respectively. ^{1}H NMR spectroscopy analysis showed that the integral ratios of the peaks located at 3.98-4.14 ppm (-COOCH_2-), 3.48-3.79 ppm (--COOCH_2CH_2OCH_2CH_2OCH_2CH_2O-, 0.77-1.15 ppm (-CCH_3 of backbone and –SiC(CH_3)$_3$), and 0.01-0.08 ppm (-Si(CH_3)$_2$) were 2 : 10 : 12 : 6, consistent with the molecular structure of PTEGSiMA, indicating that the silyl ether remained intact after the polymerization and purification.

Azide-functionalized backbone PTEGN_3MA polymers were prepared from PTEGSiMA precursors through a series of post-polymerization reactions laid out in Scheme 2.2. The *t*-

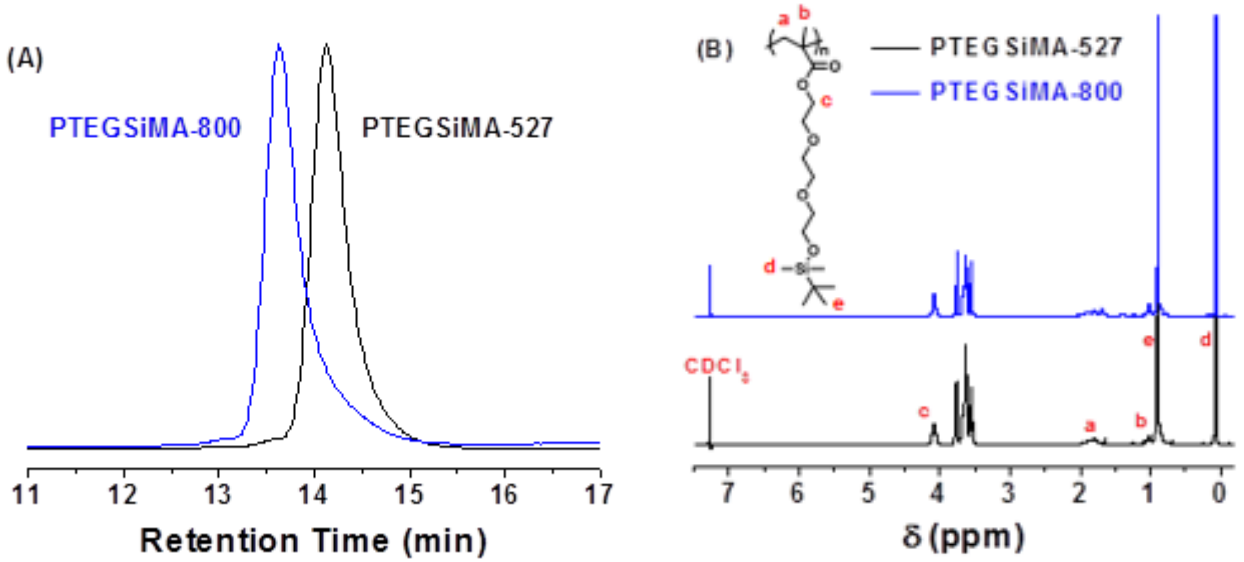

Figure 2.2. (A) SEC traces and (B) ^{1}H NMR spectra ($CDCl_3$ solvent) of PTEGSiMA-527 and PTEGSiMA-800 backbone polymer precursors. SEC analysis was carried out using a PL GPC-20 system with THF as the mobile phase.

butyldimethylsilyl ether protecting group was first removed using HCl in ethanol, followed by tosylation and substitution with sodium azide to yield backbone polymers that contained an azide moiety theoretically on each repeat unit. Figure 2.3A shows the SEC traces of PTEGN_3MA backbone polymers with DPs of 527 and 800, referred to as PTEGN_3MA-527 and PTEGN_3MA-800, which were prepared from PTEGSiMA-527 and PTEGSiMA-800 precursors, respectively. PTEGN_3MA-527 and PTEGN_3MA-800 remained narrow with the PDIs of 1.08 and 1.09, respectively, indicating that the post-polymerization reactions essentially did not cause any change in the molecular weight distribution and no crosslinking reactions between backbone polymer molecules occurred. Figure 2.3B shows the ^{1}H NMR spectra of PTEGN_3MA-527 and precursor PTEGSiMA-527 as well as the tosylated backbone polymer intermediate (PTEGTsMA-527) for comparison. The ^{1}H NMR spectra of PTEGN_3MA-800 and the tosylated backbone intermediate PTEGTsMA-800 can be found in Appendix A (Figure A1). From the ^{1}H NMR spectroscopy analysis, the excellent efficiency of the deprotection and tosylation reactions can be clearly seen from the nearly complete disappearance of the silyl ether peak at 0.05 ppm (-OSi(C(CH_3)$_3$)(CH_3)$_2$) and the appearance of tosylate peaks at 7.67-7.81 ppm (aromatic, 2*H*), 7.27-7.38 ppm (aromatic, 2*H*), 4.11 ppm (-CH_2OTs), and 2.41 ppm (-C_6H_4CH_3) in the ^{1}H NMR spectrum of PTEGTsMA-527. After the reaction of PTEGTsMA-527 with sodium azide, the tosylate peaks essentially disappeared, accompanied by the appearance of a peak at 3.34-3.47 ppm (–OCH_2C$H_2$$N_3$). Quantitative analysis showed that the degree of azide functionalization, calculated by using the integral ratio of the peaks at 3.98-4.14 ppm (ester –COOC$H_2$$CH_2$-) and 3.34-3.47 ppm (azide –OCH_2C$H_2$$N_3$), was 98% for PTEG$N_3$MA-527 and 90% for PTEG$N_3$MA-800. Table 2.1 summarizes the characterization data for both PTEGN_3MA-527 and PTEGN_3MA-800 backbone polymers and their precursors PTEGSiMA-527 and -800.

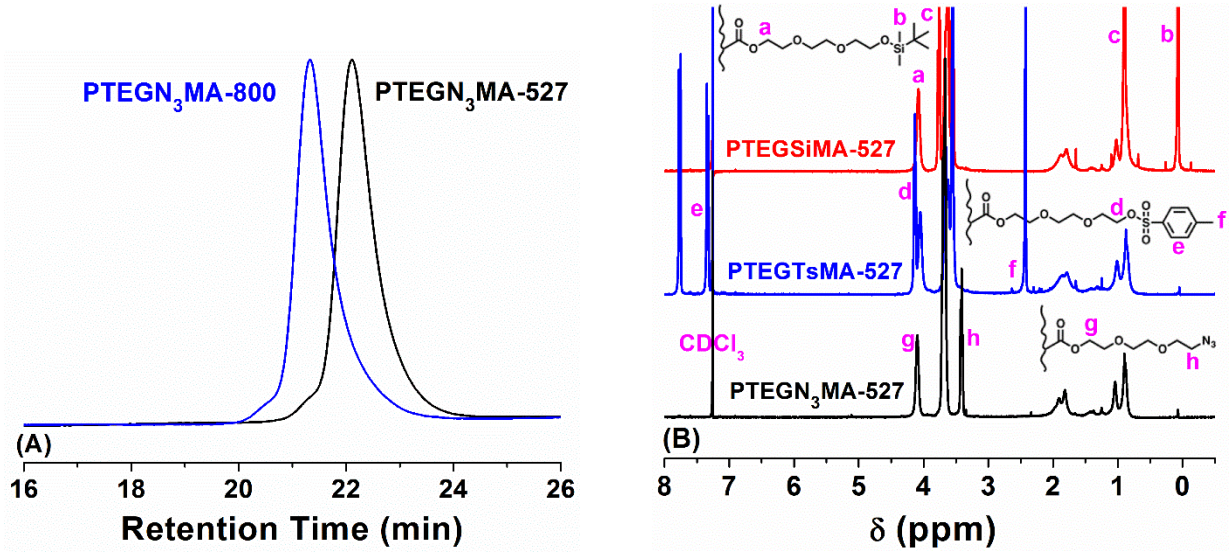

Figure 2.3. (A) SEC traces of azide-functionalized backbone polymers $PTEGN_3MA$-527 and $PTEGN_3MA$-800. SEC analysis was performed using PL GPC-50 Plus system with Agilent Mixed-B columns and DMF containing 50 mM LiBr as solvent. (B) ^1H NMR spectra in $CDCl_3$ of $PTEGN_3MA$-527, PTESiGMA-527, and the tosylated backbone intermediate PTEGTsMA-527.

Table 2.1. Characterization Data for Azide-Functionalized Backbone PTEGN_3MA Polymers and Their PTEGSiMA Precursors

Backbone Polymer Sample	$M_{n,SEC}$ (kDa)	PDI	DP [c]	Degree of Azide Functionalization (%) [d]
PTEGSiMA-527	67.1 [a]	1.07 [a]	527	--
PTEGN_3MA-527	196.8 [b]	1.08 [b]	527	98
PTEGSiMA-800	112.6 [a]	1.11 [a]	800	--
PTEGN_3MA-800	313.4 [b]	1.09 [b]	800	90

[a] The values of number average molecular weight ($M_{n,SEC}$) and polydispersity index (PDI) were measured by SEC in THF using polystyrene standards for calibraion. [b] SEC was performed using Agilent Mixed-B columns with DMF containing 50 mM LiBr as mobile phase. Note that no polymer peak in SEC was observed when THF was used as carrier solvent for PTEGN_3MA. [c] DP of the PTEGSiMA precursor polymer was calculated from the monomer conversion, determined by ^{1}H NMR spectroscopy analysis, and the monomer-to-initiator molar ratio. [d] The degree of azide functionalization was calculated by ^{1}H NMR spectroscopy analysis using the integral ratio of the peaks at 3.98-4.14 ppm (–COOCH_2CH$_2$-) and 3.34-3.47 ppm (–OCH$_2$CH_2N$_3$).

2.3.2. Synthesis of Alkyne End-Functionalized Water-Soluble PEO Side Chain Polymers

Alkyne end-functionalized water-soluble PEO side chains with DPs of 45 and 114 (PEO-45 and PEO-114, respectively) were synthesized from commercially available PEO-monomethyl ether with molecular weights of 2 kDa and 5 kDa. The PEO polymers were end-functionalized with an alkyne moiety by reacting the alcohol end group of PEO with EDC-activated 4-pentynoic acid in the presence of DMAP catalyst in methylene chloride (Scheme 2.4).[42]

Both PEO side chain polymers were purified by washing the methylene chloride reaction mixture with water and 1.0 M aqueous NaOH, followed by precipitation in diethyl ether and drying under high vacuum. Figure 2.4 shows the SEC traces of purified PEO-45 and PEO-114 as well as the ^{1}H NMR spectrum of purified alkyne end-functionalized PEO-45. From SEC analysis, the end group modification did not affect the molecular weight distribution for either PEO side chain polymer, as reflected by the narrow, monomodal peak for each. The degree of alkyne functionalization was determined to be essentially quantitative for both PEO-45 and PEO-114 by ^{1}H NMR spectroscopy using the integral values of the peaks at 4.21 ppm ($HC{\equiv}CCH_2CH_2COOCH_2$- of alkyne end group) and 3.33 ppm (s, -OCH_3 of methyl end group) of the purified polymer. The ^{1}H NMR spectrum of purified PEO-114 can be found in Appendix A (Figure A2), and the characterization data for both PEO side chain polymers is shown in Table 2.2.

2.3.3. Synthesis of Water-Soluble PEO Homografted Molecular Brushes from PEO-45

Water-soluble PEO homografted molecular brushes were prepared by a “grafting to” method using copper-catalyzed azide-alkyne cycloaddition “click” reactions between azide-containing repeat units of the backbone polymer $PTEGN_3MA$ and alkyne end-functionalized water-soluble side chain polymer PEO. The reactions were performed in DMF using

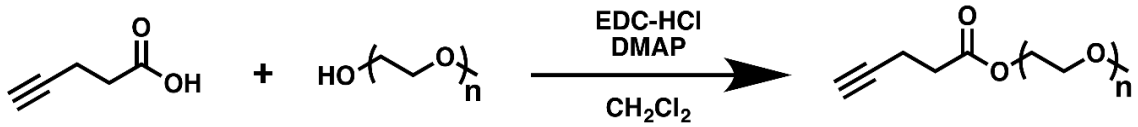

Scheme 2.4. Synthesis of Alkyne End-Functionalized Water-Soluble Side Chain Polymer PEO by End-Group Modification of Commercially Available PEO with 4-Pentynoic acid.

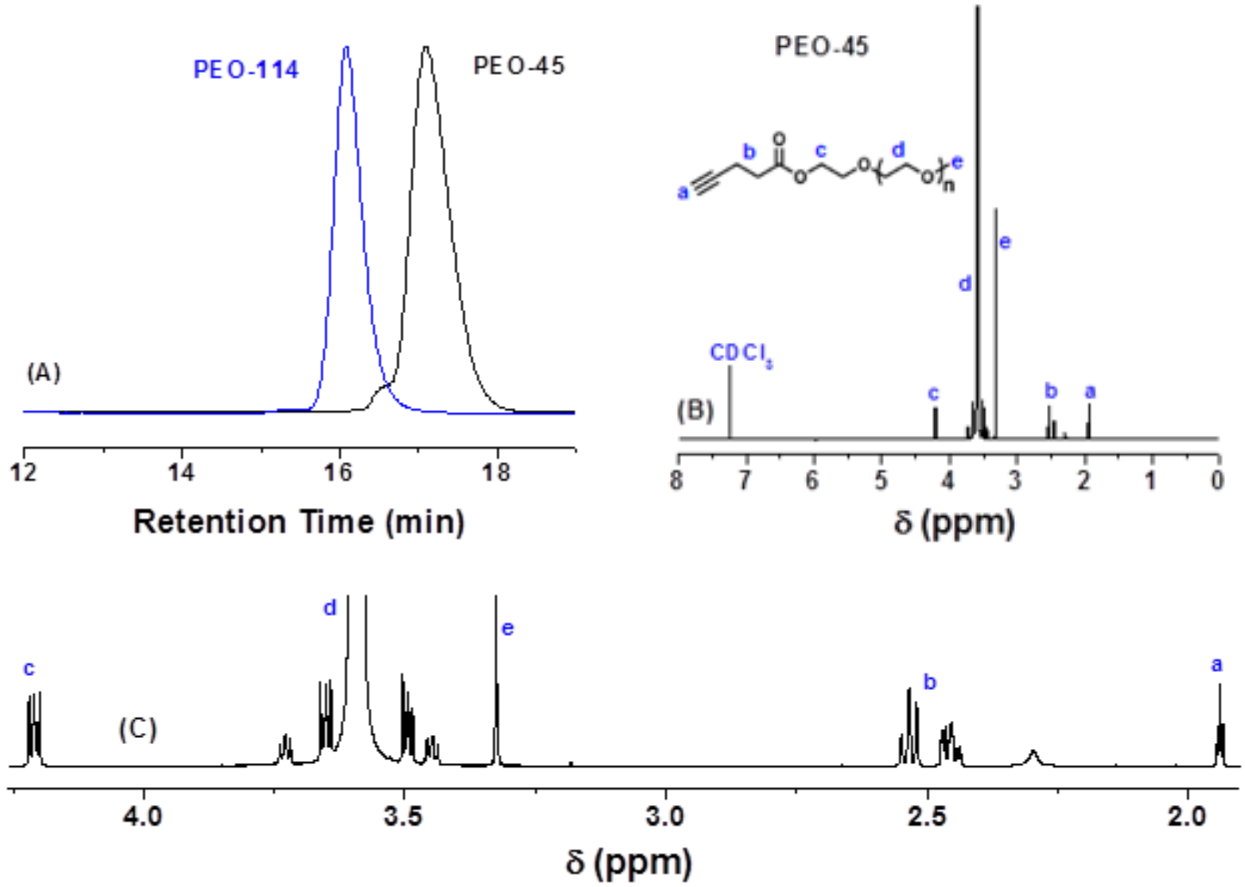

Figure 2.4. (A) SEC trace of alkyne-end-functionalized PEO side chain polymers with a DP's of 45 (PEO-45) and 114 (PEO-114). (B) ^{1}H NMR spectrum of PEO-45 in $CDCl_3$. (C) Zoomed in portion of the ^{1}H NMR spectrum of PEO-45 showing peaks from end groups. SEC analysis was carried out on PL GPC-20 system using THF as carrier solvent.

Table 2.2. Characterization Data for Alkyne End-Functionalized Water-Soluble PEO Side Chain Polymers

Side Chain Polymer Sample	$M_{n,SEC}$ (kDa) [a]	PDI [a]	DP [b]
PEO-45	2.8	1.08	45
PEO-114	8.7	1.04	114

[a] The values of number average molecular weight ($M_{n,SEC}$) and polydispersity index (PDI) were measured by SEC using PL GPC-20 system with THF as solvent. [b] DP was calculated from the nominal molecular weight (2 kDa or 5 kDa) divided by the molecular weight of each monomer unit (44 Da).

CuCl/PMDETA as catalyst at ambient temperature. The grafting density, defined as the percentage of backbone repeat units that are grafted with a side chain polymer, was calculated from the SEC chromatogram using the ratio of peak areas from the molecular brushes and the unreacted side chain polymer and the molar ratio of backbone monomer units to the side chain polymer in the feed. Using a series of mixtures of two polystyrene homopolymers with very different molecular weights, 8 kDa and 152 kDa, we have confirmed that the peak area ratio of the two different molecular weight polymers is essentially the same as the mass ratio (see Appendix A, Figure A3).

We first prepared PEO molecular brushes using PTEGN_3MA-527 backbone polymer and PEO-45 side chains. A molar ratio of 1 : 1.48 for the backbone monomer units in PTEGN_3MA-527 to side chain polymer PEO-45 was used (PEO MB-1 in Table 2.3 and Figure 2.5). The reaction progress was monitored by SEC analysis; Figure 2.6A shows the SEC traces of the reaction mixture after 2 h and 6 h of reaction time. For comparison, the SEC curve of backbone polymer PTEGN_3MA-527 is also shown. After the reaction had proceeded for 2 h, a high molecular weight peak was observed in the SEC chromatogram with a $M_{n,SEC}$ of 715,200 Da and a PDI of 1.09, indicating the formation of brush molecules. From the relative peak areas, the mixture contained 68.34 % of brushes and 31.66 % of unreacted PEO-45. Since the molar ratio of monomer units of PDEGN_3MA-527 to the side chain polymer in the feed was 1 : 1.48, this gives a grafting density of 97.6 % after two hours of reaction. SEC analysis of the reaction mixture after 6 h of reaction time showed only a marginal increase in the amount of brushes relative to unreacted side chain polymer, indicating that the reaction was essentially complete after only 2 h. The relative amount of brushes in the reaction mixture after 6 h was 68.70 %, giving a grafting density of 98.0 % ($M_{n,SEC}$ = 713,900; PDI = 1.10). This indicates that almost every available azide group on the backbone

Table 2.3. PEO Molecular Brushes from PEO-45 with Different Grafting Densities and Backbone Lengths Synthesized by "Grafting to" Using CuAAC "Click" Reactions

Molecular Brush Sample	$DP_{Backbone}$-$DP_{Sidechain}$	Feed Molar Ratio of Backbone Monomer Units to PEO	$M_{n,SEC}$ (kDa) [a]	PDI [a]	Grafting Density (%)[b]	Reaction Time (h)
PEO MB-1	527-45	1 : 1.48	713.9	1.10	98.0	6
PEO MB-2	800-45	1 : 2.01	990.5	1.12	85.9	22
PEO MB-3	800-45	1 : 1.51	1000.9	1.12	85.0	4
PEO MB-4	800-45	1 : 1.10	993.9	1.13	81.8	24
PEO MB-5	800-45	1 : 0.52	841.7	1.13	50.9	2

[a] The values of number average molecular weight ($M_{n,SEC}$) and polydispersity index (PDI) were measured by size exclusion chromatography (SEC) of the final reaction mixture against linear polystyrene standards using PL GPC-50 Plus system with Agilent Mixed-B columns and DMF containing 50 mM LiBr as carrier solvent. [b] Grafting density was calculated from the molar ratio of backbone monomer units to side chain polymer in the feed and the ratio of peak areas in SEC from molecular brushes and unreacted side chain polymer.

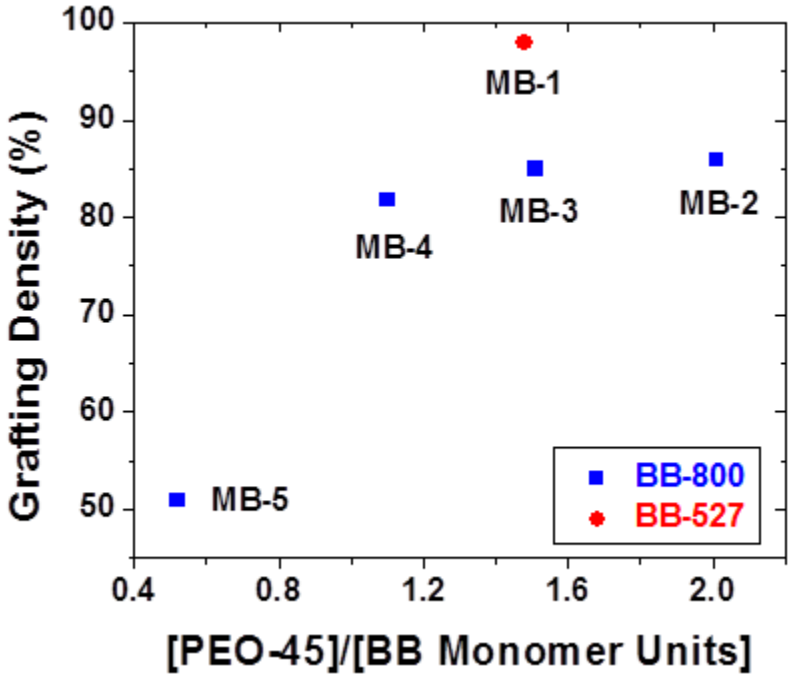

Figure 2.5. Plot of grafting density versus the molar ratio of PEO-45 side chains to backbone monomer units in the feed for PEO molecular brushes prepared from PEO-45.

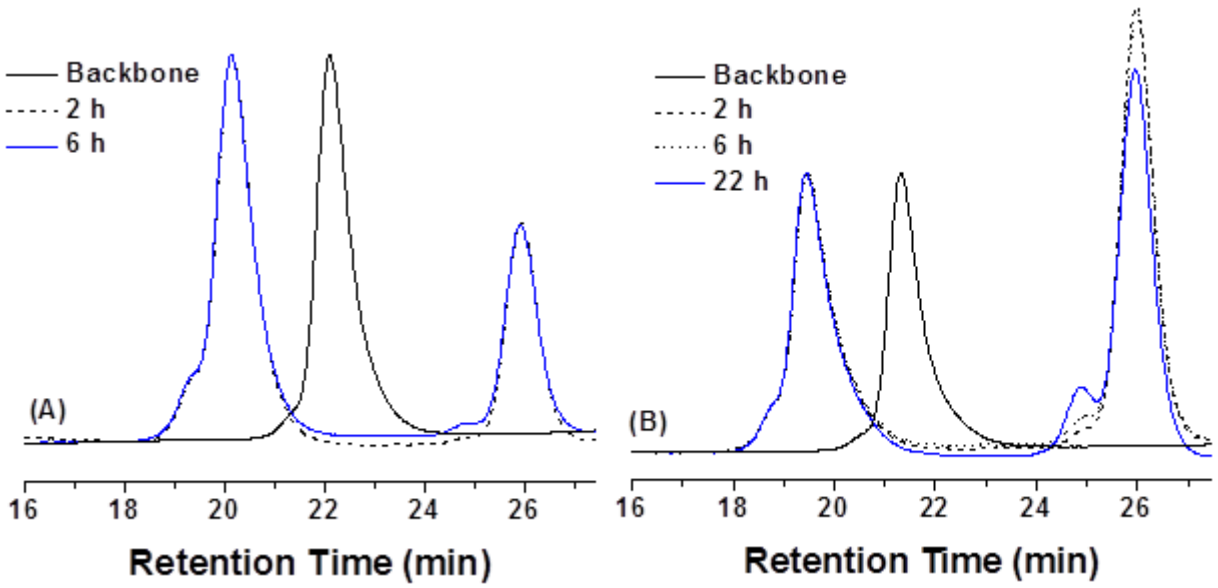

Figure 2.6. SEC traces of the reaction mixture at different reaction times from the synthesis of (A) PEO MB-1 as well as PTEGN_3MA-527 backbone polymer and (B) PEO MB-2 as well as PTEGN_3MA-800 backbone polymer. SEC analysis was performed using PL GPC-50 Plus system with Agilent Mixed-B columns in DMF with 50 mM LiBr.

PTEGN$_3$MA-527 had reacted with a side chain polymer molecule. A more detailed description of the calculation of grafting density can be found in Appendix A.1.

Encouraged by the high grafting density achieved for PEO MB-1 using PTEGN$_3$MA-527 backbone and PEO-45 side chains, we prepared PEO brushes using the longer PTEGN$_3$MA-800 backbone and the same PEO-45 side chains, with a molar ratio of 1 : 2.01 for the backbone monomer units to side chain polymer. Figure 2.6B shows the SEC traces of the reaction mixture at different reaction times, as well as the SEC curve of backbone polymer PTEGN$_3$MA-800 for comparison. After the reaction had proceeded for 2 h, a high molecular weight peak was observed in the SEC chromatogram with a $M_{n,SEC}$ of 986,600 Da and a PDI of 1.12, indicating the formation of brush molecules. The relative amount of brushes in the reaction mixture was 44.65 %, based on peak areas. This gives a grafting density of 85.0 %, since the molar ratio of monomer units of PDEGN$_3$MA-800 to the side chain polymer in the feed was 1 : 2.01. SEC analysis of the reaction mixture after 6 h and 22 h of reaction time showed only small increases in the amount of brushes relative to unreacted side chain polymer, with the mixture containing 44.83 % brushes after 6 h (grafting density = 85.4 %) and 45.09 % brushes after 22 h (grafting density = 85.9 %). This indicates that the reaction was nearly complete after 2 h, similar to what was observed for PEO MB-1. The lower grafting density observed for MB-2 compared to MB-1 (85.9 % versus 98.0 %, respectively) is likely due to the lower degree of azide functionalization for PTEGN$_3$MA-800 (90 %) compared to PTEGN$_3$MA-527 (98 %). It is interesting to note that although there was not much change in the molecular weight distribution of the brushes after 22 h ($M_{n,SEC}$ = 990,500; PDI = 1.12), we did observe the formation of a high molecular weight shoulder for the side chain peak in the SEC chromatogram after long reaction times (Figure 2.6B). This is likely due to the occurrence

of alkyne-alkyne coupling between PEO-45 free side chains, which is catalyzed by copper (I) in the presence of oxygen.[43,44]

To study how the feed molar ratio of backbone monomer units to PEO-45 side chain polymer affected the grafting density, we carried out a series of click reactions to synthesize PEO molecular brushes by using different molar ratios of backbone monomer units of PTEGN_3MA-800 to PEO-45, ranging from 1 : 2.01 to 1 : 1.51, 1 : 1.10, and 1 : 0.52. The grafting density of each sample was determined by SEC at different reaction times (Figures A4-A6), and the results are summarized in Table 2.3. As discussed previously, for PEO MB-2, the grafting density reached a maximum of 85.9 % after 22 h, although the reaction was nearly complete after 2 h with a grafting density of 85.0 % when a molar ratio of backbone monomer units to side chain polymer of 1 : 2.01 was used. Decreasing the molar ratio of backbone monomer units to PEO-45 to 1:1.51 (MB-3) resulted in a slight reduction of grafting density after 2 h reaction time (81.3 %), but the maximum value was nearly achieved (85.0 %) after 2 additional hours of reaction time. With further decreasing the ratio to 1 : 1.10, we observed only a small decrease in grafting density to 81.8 % after the reaction was allowed to proceed for 24 h. In order to achieve a lower grafting density, we used an excess of backbone monomer units, employing a molar ratio of 1 : 0.52 for the backbone monomer units to PEO-45 side chains. Under these conditions, the side chains had almost completely reacted after 2 h, indicating the highly efficient nature of the grafting to "click" reaction. The relative amount of brushes determined by SEC was 97.81 %, giving a grafting density of 50.9 %. There was essentially no further change after 2 additional hours of reaction time.

2.3.4. Synthesis of Water-Soluble PEO Homografted Molecular Brushes from PEO-114

Having successfully synthesized PEO molecular brushes with high and tunable grafting densities using PEO-45, we decided to investigate how increasing the PEO side chain length would

affect the grafting density. We prepared PEO molecular brushes from the longer PEO-114 side chain polymer using the same grafting to "click" method and under similar reaction conditions as was described for the synthesis of PEO brushes using PEO-45 side chains. We first used a molar ratio of 1 : 1.90 for the backbone monomer units in PTEGN_3MA-527 to side chain polymer PEO-114 to synthesize PEO molecular brushes (PEO MB-6 in Table 2.4 and Figure 2.7). Like the previous experiments, the reaction progress was followed by SEC analysis; Figure 2.8A shows the SEC traces of the reaction mixture after 24 h reaction time and PEO MB-6 after the removal unreacted side chain polymer by centrifugal filtration. Anticipating the larger steric hindrance for longer PEO-114 side chains, we allowed the reaction to proceed overnight before taking a sample for SEC analysis. After the reaction proceeded for 24 h, a high molecular weight peak in the SEC chromatogram indicated the formation of brush molecules with a $M_{n,SEC}$ of 863,300 Da and a PDI of 1.10. From the relative peak areas, the mixture contained 49.83 % brushes and 50.17 % unreacted PEO-114. Since the molar ratio of monomer units of PDEGN_3MA-527 to the side chain polymer in the feed was 1:1.90, this gives a grafting density of 92.5 % after 24 h of reaction. After 47 h reaction time, propargyl alcohol (50 µL) was injected under nitrogen to cap any unreacted azide units in the backbone to prevent side reactions during purification. (The importance of capping unreacted azide units will be discussed later.) SEC analysis after 48 h reaction time showed almost no change in relative peak areas, indicating the reaction essentially reached the limit after 24 h. After 48 h, the $M_{n,SEC}$ was 865,900 Da and the PDI was 1.10, and the relative amount of brushes was 49.87%, giving a final grafting density of 92.6 %. This is slightly lower that the grafting density (98.0 %) that was achieved using PEO-45 and molar ratio of 1 : 1.48 for the backbone monomer units to side chain polymer, which is apparently a result of the larger steric hindrance for the longer PEO-114 side chains.

Table 2.4. PEO Molecular Brushes from PEO-114 with Different Grafting Densities and Backbone Lengths Synthesized by "Grafting to" Using CuAAC "Click" Reactions

Molecular Brush Sample	$DP_{Backbone}$-$DP_{Sidechain}$	Feed Molar Ratio of Backbone Monomer Units to PEO	$M_{n,SEC}$ (kDa) [a]	PDI [a]	Grafting Density (%)[b]	Reaction Time (h)
PEO MB-6	527-114	1 : 1.90	865.9	1.10	92.6	48
PEO MB-7	527-114	1 : 1.00	839.7	1.13	89.7	24
PEO MB-8	527-114	1 : 0.75	833.5	1.13	74.4	19
PEO MB-9	527-114	1 : 0.50	733.2	1.13	49.5	19
PEO MB-10	800-114	1 : 1.81	1199.3	1.15	78.6	17
PEO MB-11	800-114	1 : 0.59	1131.4	1.15	58.5	17
PEO MB-12	800-114	1 : 0.51	1034.6	1.13	49.9	17
PEO MB-13	800-114	1 : 0.30	939.8	1.19	29.5	17

[a] The values of number average molecular weight ($M_{n,SEC}$) and polydispersity index (PDI) were measured by size exclusion chromatography (SEC) of the final reaction mixture against linear polystyrene standards using PL GPC-50 Plus system with Agilent Mixed-B columns and DMF containing 50 mM LiBr as carrier solvent. [b] Grafting density was calculated from the molar ratio of backbone monomer units to side chain polymer in the feed and the ratio of peak areas in SEC from molecular brushes and unreacted side chain polymer.

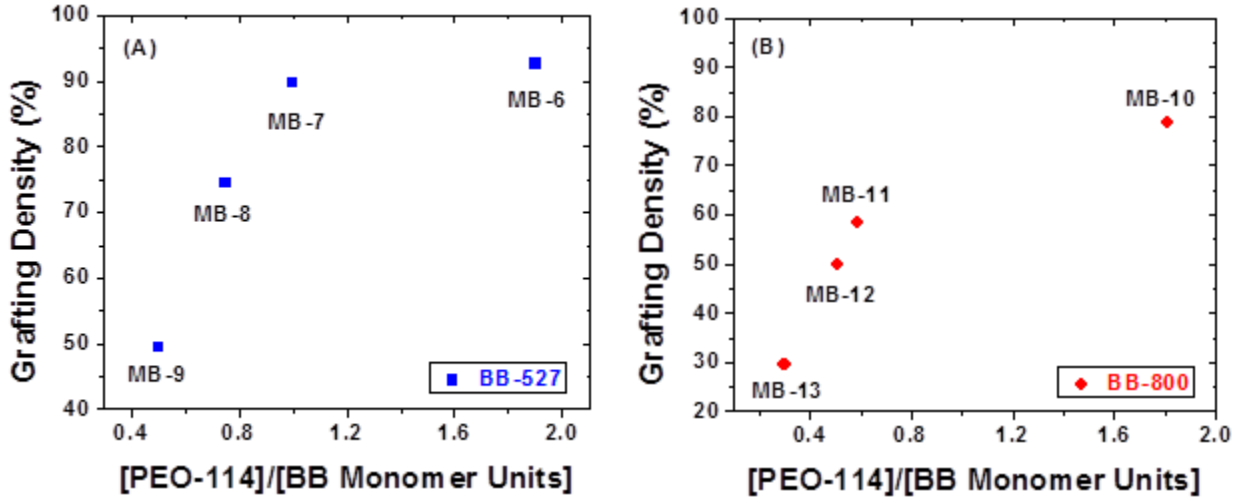

Figure 2.7. Plot of grafting density versus the molar ratio of PEO-114 side chains to backbone monomer units in the feed for PEO molecular brushes prepared from PEO-114 and (A) $PTEGN_3MA$-527 and (B) $PTEGN_3MA$-800.

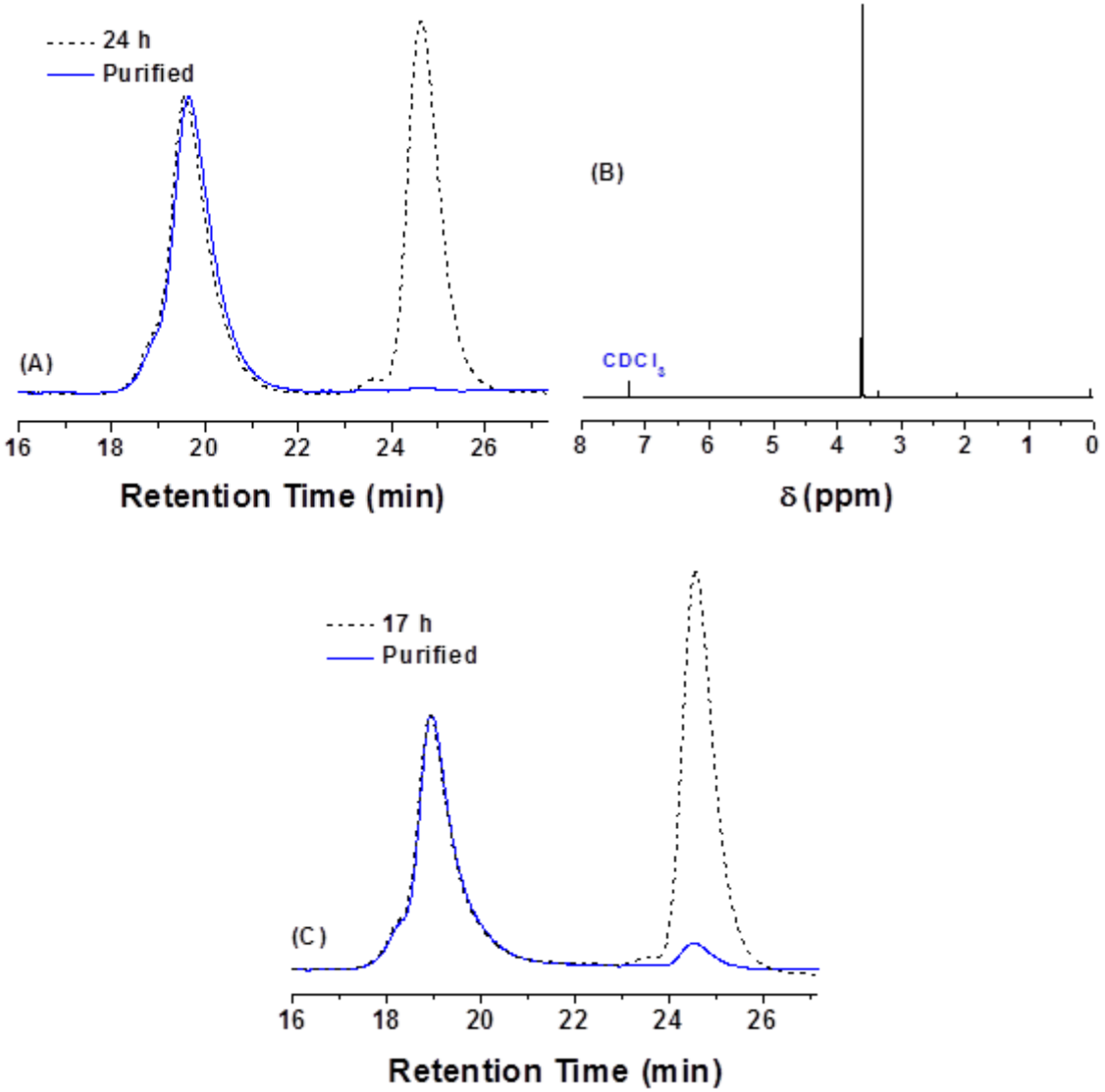

Figure 2.8. (A) SEC traces of PEO MB-6 before and after purification by centrifugal filtration. (B) ^{1}H NMR spectrum of purified PEO MB-6 (in $CDCl_3$). (C) SEC traces of PEO MB-10 before and after purification by centrifugal filtration. SEC analysis was performed using PL GPC-50 Plus system with Agilent Mixed-B columns in DMF with 50 mM LiBr.

After 48 h, the reaction was stopped by opening the vial to air and passing the mixture through a small neutral alumina column to remove the copper catalyst. The PEO brush molecules were then concentrated, and the excess side chains were removed by repeated centrifugal filtration in water using 50 kDa MWCO dialysis membranes. SEC analysis of the purified PEO MB-6 showed that the excess side chain polymer PEO-114 was almost completely removed (less than 1 % side chains remained by SEC peak areas) and the molecular weight distribution remained the same ($M_{n,\ SEC}$ = 831,100; PDI = 1.10) (Figure 2.8A). The ^{1}H NMR spectrum of the purified PEO MB-6 brushes is shown in Figure 2.8B.

Similar to previous experiments using PEO-45 side chains, we carried out a series of grafting to reactions to synthesize PEO molecular brushes using different molar ratios of backbone monomer units of PTEGN_3MA-527 to PEO-114, ranging from 1 : 1.90 to 1 : 1.00, 1 : 0.75, and 1 : 0.50 in order to study how the feed molar ratio affects the grafting density. The reactions were allowed to proceed for between 19 and 24 h, and SEC was used to determine the grafting density for each molecular brush sample (Figures A7-A9). The results are summarized in Table 2.4. As discussed earlier, for PEO MB-6, the grafting density was 92.6 % when a molar ratio of backbone monomer units to side chain polymer of 1 : 1.90 was used. Decreasing the molar ratio of backbone monomer units to PEO-114 to 1 : 1.00 resulted in only a slight reduction of grafting efficiency to 89.7 % (PEO MB-7). When we further decreased the ratio to 1 : 0.75 (MB-8) and 1 : 0.50 (MB-9), the side chain polymers had almost completely reacted after 19 h, similar to what was observed for PEO MB-5, using a molar ratio of 1 : 0.52 for backbone monomer units to PEO-45. The relative amount of brushes determined by SEC were 98.95 % and 98.90 %, giving grafting densities of 74.4 % and 49.5 % for PEO MB-8 and MB-9, respectively. These experiments demonstrated that

the synthesis of PEO homografted molecular brushes with tunable grafting densities is highly efficient even when using the longer PEO-114 side chains.

We then prepared PEO molecular brushes using the longer backbone polymer PTEGN$_3$MA-800 and PEO-114 under similar reaction conditions. Initially, we used a molar ratio of 1 : 1.81 for the backbone monomer units in PTEGN$_3$MA-800 to side chain polymer PEO-114 to synthesize PEO MB-10 (Table 2.4). Figure 2.8C shows the SEC traces of the reaction mixture after 17 h reaction time and PEO MB-10 after the removal of unreacted side chain polymer by centrifugal filtration. After 17 h, we observed a high molecular weight peak by SEC with a $M_{n,SEC}$ of 1,199,300 Da and a PDI of 1.15. Based on relative peak areas, the mixture contained 44.25 % brushes, giving a grafting density of 78.6 %. Based on previous experiments, the reaction had likely reached the limit by this time, so propargyl alcohol (50 µL) was injected under nitrogen to cap any unreacted azide units in the backbone. The slightly lower grafting density of 78.6 % observed for PEO MB-10 compared with MB-6 (92.6 % using PTEGN$_3$MA-527 backbone) is likely caused by the lower degree of azide functionalization for PTEGN$_3$MA-800 (90%) and the increased steric hindrance in the longer backbone polymer. This is consistent with the trend observed for PEO MB-1 (98.0 % using PTEGN$_3$MA-527 backbone) and MB-2 (85.9 % using PTEGN$_3$MA-800 backbone) with PEO-45 side chains under similar conditions.

After 48 h, the MB-10 reaction was stopped and purified by repeated centrifugal filtration in a similar fashion as PEO MB-6. SEC analysis of the purified PEO MB-10 showed that the excess side chain polymer PEO-114 was mostly removed (approximately 5 % side chains remained by SEC peak areas) and the molecular weight distribution was not changed much ($M_{n,\,SEC}$ = 1,224,200; PDI = 1.11) (Figure 2.8C). We found that continued centrifugal filtration did not further reduce the amount unreacted side chains.

Similarly, we carried out a series of grafting to reactions using different molar ratios of backbone monomer units of PTEGN$_3$MA-800 to PEO-114, ranging from 1 : 1.81 to 1 : 0.59, 1 : 0.51, and 1 : 0.30. Each reaction was allowed to proceed for 17 h, and SEC was used to determine the grafting density for each molecular brush sample (Figures A10-A12). The results are summarized in Table 2.4. As discussed earlier, for PEO MB-10, the grafting density was 78.6 % when a molar ratio of backbone monomer units to side chain polymer of 1 : 1.81 was used. When we decreased the molar ratio to 1 : 0.59 (MB-11), 1 : 0.51 (MB-12), and 1 : 0.30 (MB-13), the side chain polymers had almost completely reacted after 17 h. The relative amounts of brushes determined by SEC were, 98.78 %, 98.54 %, and 98.74 %, giving grafting densities of 58.5 %, 49.9 %, and 29.5 % for PEO MB-11, MB-12, and MB-13, respectively.

After 18 h, we injected propargyl alcohol (50 µL) into the PEO MB-12 reaction mixture under nitrogen to cap any unreacted azide units in the backbone. The reaction was allowed to continue for an additional 24 h before it was stopped by passing it through neutral alumina to remove the copper catalyst. We note that the PEO MB-11 and MB-13 reactions were stopped without the addition of propargyl alcohol. Each brush sample was concentrated, and purification was attempted using repeated centrifugal filtration in water as described previously. Surprisingly, for the low grafting density samples that were not capped with propargyl alcohol (PEO MB-11 and MB-13), we found that the amount of side chains actually increased during purification. Using PEO MB-11 as an example, the relative amount of side chains went from 1.22 % before purification to 8.37 % after six rounds of centrifugal filtration (Figure 2.9A, $M_{n,\,SEC}$ = 1,063,200; PDI = 1.14). PEO MB-13 exhibited similar behavior (Figure A10), with the relative amount of side chains increasing from 1.26 % to 5.56 % during purification. Apparently, some of the side chains had degrafted from the backbone through some unknown side reaction during purification.

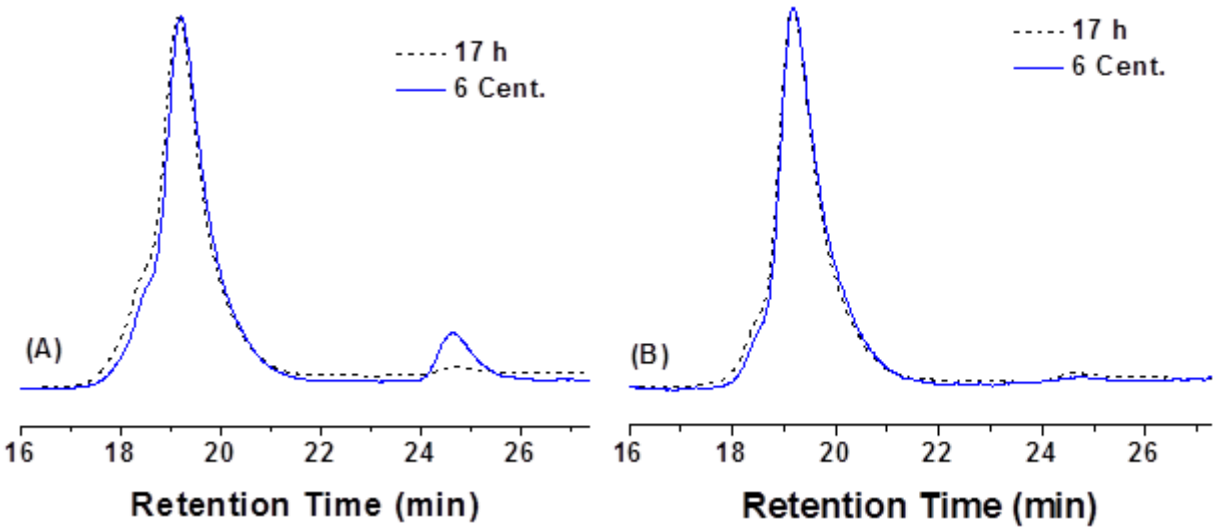

Figure 2.9. SEC traces before and after centrifugal filtration for (A) PEO MB-11, which was not capped with propargyl alcohol, and (B) PEO MB-12, which was capped with propargyl alcohol. SEC analysis was performed using PL GPC-50 Plus system with Agilent Mixed-B columns in DMF with 50 mM LiBr.

(We actually observed the same phenomenon with PEO MB-8 and MB-9 as well. See Figures A8 and A9.) In contrast to PEO MB-11 and MB-13, we mentioned earlier that propargyl alcohol had been injected into the reaction mixture for PEO MB-12, and it was allowed to react for an additional 24 h to cap the unreacted azide monomer units of the backbone. We found that the relative amount of side chains for MB-12 did not increase after six rounds of centrifugal filtration, actually decreasing to 0.57 % (Figure 2.9B, $M_{n,\,SEC}$ = 1,004,100; PDI = 1.12). This indicates that the use of propargyl alcohol as a capping agent did in fact prevent side reactions that had previously to led to degrafting of side chains in PEO MB-11 and MB-13. Although, similar to PEO MB-6 and MB-10 (for which propargyl alcohol was also injected), we found that the side chains could not be completely removed by centrifugal filtration for some unknown reason.

2.3.5. AFM of Water-Soluble PEO Homografted Molecular Brushes

The synthesis of PEO brush molecules was directly confirmed by atomic force microscopy (AFM). Figure 2.10 shows AFM images of PEO MB-6 brushes that were spin cast onto freshly cleaved mica from aqueous solution at concentrations of 0.1 mg/g and 0.01 mg/g. We observed a highly stretched cylindrical or worm-like morphology that would be expected for densely grafted molecular brushes in a good solvent. Interestingly, images of MB-6 spin cast from the relatively concentrated solution (0.1 mg/g) show that the brush molecules stacked into somewhat ordered rows, likely due to their rigid structure (Figure 2.10). Spin casting from a 10x diluted solution resulted in the brushes being better separated, and the side chains appeared to be more spread out on the mica substrate (Figure 2.11). Using images from brushes cast from the 0.01 mg/g solution, length analysis gave an average contour length of 127 nm and a typical height of approximately 0.5 nm. With a backbone DP of 527, the length of a fully extended worm, in an all-trans

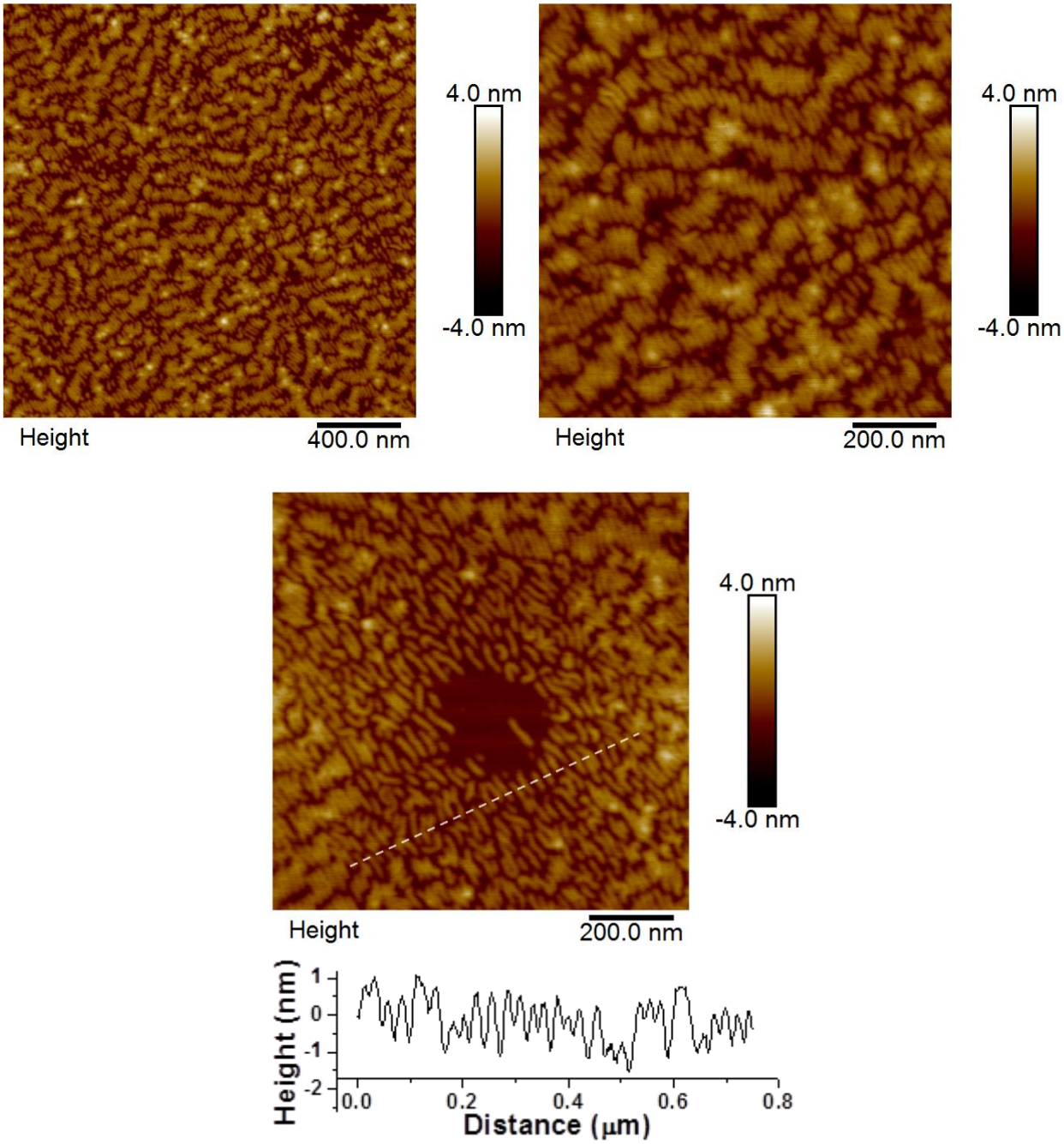

Figure 2.10. Representative AFM height images of PEO MB-6 spin cast onto freshly cleaved mica from a 0.1 mg/g solution in water.

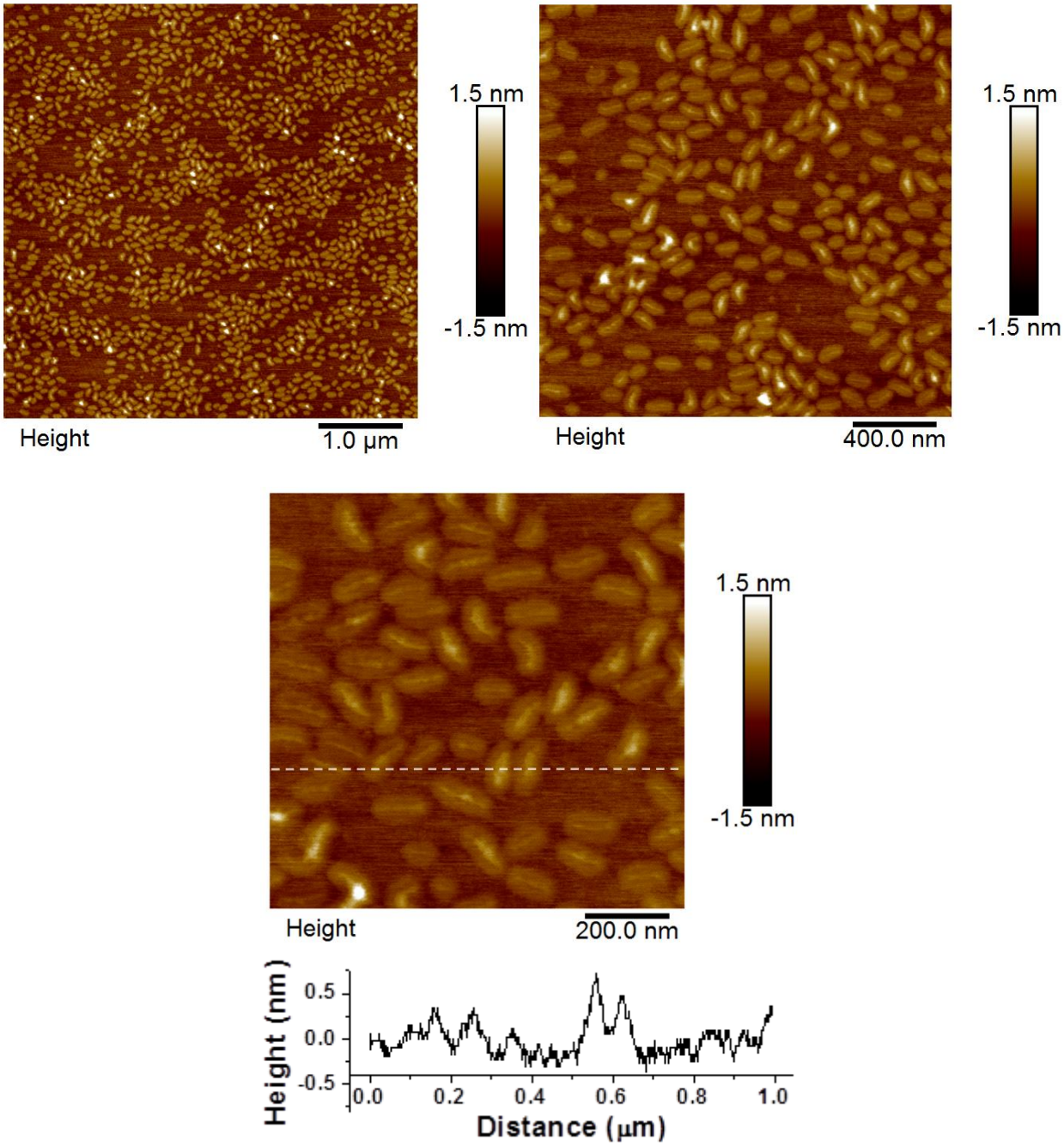

Figure 2.11. Representative AFM height images of PEO MB-6 spin cast onto freshly cleaved mica from a 0.01 mg/g solution in water.

conformation, would theoretically be 134 nm (found by 527*0.254 nm). The measured contour length of 127 nm indicates that the degree of stretching is approximately 95 %.

2.4. Conclusions

A highly efficient "grafing to" method using CuAAC "click" chemistry was developed to prepare well-defined molecular bottlebrushes with high and tunable grafting densities using water-soluble PEO as model side chain polymers. Azide-functionalized backbone polymers with DPs of 527 and 800 were prepared by ATRP and post-polymerization reactions. Alkyne end-functionalized PEO side chain polymers with DPs of 45 and 114 (PEO-45 and PEO-114, respectively) were prepared from commercially available PEO-monomethyl ether with molecular weights of 2 kDa and 5 kDa, and the alkyne moiety was installed by reacting the alcohol end group with 4-pentynoic acid. "Grafting to" click reactions were performed in DMF at ambient temperature with CuCl as catalyst, and the grafting densities were determined by size exclusion chromatography using the relative peak areas from the brushes and unreacted side chains. A nearly quantitative grafting density was achieved for brushes prepared from PEO-45 and the backbone polymer with a DP of 527 when a molar ratio 1 :1.48 for backbone monomer units to side chains was used. A small decrease in grafting density was observed when the longer PEO-114 (92.6 %) side chains were used. Under similar conditions, slightly lower grafting densities were observed when the longer backbone with a DP of 800 was employed with either PEO-45 (85.9 %) or PEO-114 (78.6 %) side chains and a molar ratio of backbone monomer units to side chains of approximately 1 : 2 was used. Additionally, we found that the grafting density could be readily tuned by adjusting this ratio. Interestingly, for lower grafting density samples, we found that it is important to cap unreacted azide units with an "inert" alkyne (we used propargyl alcohol) in order to avoid side reactions that resulted in degrafting of side chains during purification. Pure PEO

brushes were obtained by centrifugal filtration to remove unreacted side chains, and their synthesis was directly confirmed by atomic force microscopy. The “click” gratfting to technique developed here provides a good foundation for the synthesis of more complex molecular brushes, such as homografted and heterografted stimuli-responsive brushes described in Chapters 3 and 4, respectively.

References

1. Sheiko, S. S.; Sumerlin, B. S.; Matyjaszewski, K. *Prog. Polym. Sci.* **2008**, *33*, 759-785.
2. Lee, H.; Pietrasik, J.; Sheiko, S. S.; Matyjaszewski, K. *Prog. Polym. Sci.* **2010**, *35*, 24-44.
3. Rzayev, J. *ACS Macro Lett.* **2012**, *1*, 1146-1149.
4. Beers, K. L.; Gaynor, S. G.; Matyjaszewski, K. *Macromolecules* **1998**, *31*, 9413-9415.
5. Cheng, G.; Boker, A.; Zhuang, M.; Krausch, G.; Muller, A. H. E. *Macromolecules* **2001**, *34*, 6883-6888.
6. Matyjaszewski, K.; Qin, S.; Boyce, J. R.; Shirvanyants, D.; Sheiko, S. S. *Macromolecules* **2003**, *36*, 1843-1849.
7. Li, C.; Gunari, N.; Fischer, K.; Janshoff, A.; Schmidt, M. *Angew. Chem. Int. Ed.* **2004**, *43*, 1101-1104.
8. Balamurugan, S. S.; Grigor, B. B.; Yang, Y.; McCarley, R. L. *Angew. Chem. Int. Ed.* **2005**, *44*, 4872-4876.
9. Pietrasik, J.; Sumerlin, B. S.; Lee, B. Y.; Matyjaszewski, K. *Macromol. Chem. Phys.* **2007**, *208*, 30-36.
10. Yamamoto, S.; Pietrasik, J.; Matyjaszewski, K. *Macromolecules* **2007**, *40*, 9348-9353.
11. Yamamoto, S.; Pietrasik, J.; Matyjaszewski, K. *Macromolecules* **2008**, *41*, 7013-7020.
12. Zhang, N.; Huber, S.; Schulz, A.; Luxenhofer, R.; Jordan, R. *Macromolecules* **2009**, *42*, 2215-2221.
13. Zhang, N.; Luxenhofer, R.; Jordan, R. *Macromol. Chem. Phys.* **2012**, *213*, 973-981.
14. Zhang, N.; Luxenhofer, R.; Jordan, R. *Macromol. Chem. Phys.* **2012**, *213*, 1963-1969.
15. Lee, H.; Boyce, J. R.; Nese, A.; Sheiko, S. S.; Matyjaszewski, K. *Polymer* **2008**, *49*, 5490-5496.

16. Xu, Y.; Bolisetty, S.; Drechsler, M.; Fang, B.; Yuan, J.; Ballauff, M.; Muller, A. X. E. *Polymer* **2008**, *49*, 3957–64.

17. Xu, Y.; Bolisetty, S.; Drechsler, M.; Fang, B.; Yuan, J.; Harnau, L.; Ballauff, M.; Muller, A. X. E. *Soft Matter* **2009**, *5*, 379–84.

18. Xu, Y.; Bolisetty, S.; Ballauff, M.; Mueller, A. H. E. *J. Am. Chem. Soc.* **2009**, *131*, 1640–1641.

19. Lee, H. L.; Pietrasik, J.; Matyjaszewski, K. *Macromolecules* **2006**, *39*, 3914-3920.

20. Yao, J.; Chen, Y.; Zhang, J.; Bunyard, C.; Tang, C. *Macromol. Rapid Commun.* **2013**, *34*, 645-651.

21. Xia, Y.; Olsen, B. D.; Kornfield, J. A.; Grubbs, R. H. *J. Am. Chem. Soc.* **2009**, *131*, 18525-18532.

22. Xia, Y.; Kornfield, J. A.; Grubbs, R. H. *Macromolecules* **2009**, *42*, 3761-3766.

23. Cheng, C.; Khoshdel, E.; Wooley, K. L. *Macromolecules* **2007**, *40*, 2289-2292.

24. Li, Z.; Zhang, K.; Ma, J.; Cheng, C.; Wooley, K. L. *J. Polym. Sci. Part A: Polym. Chem.* **2009**, *47*, 5557-5563.

25. Li, A.; Ma, J.; Sun, G.; Li, Z.; Cho, S.; Clark, C.; Wooley, K. L. *J. Polym. Sci. Part A: Polym. Chem.* **2012**, *50*, 1681-1688.

26. Li. Z.; Ma, J.; Cheng, C.; Zhang, K.; Wooley, K. L. *Macromolecules* **2010**, *43*, 1182-1184.

27. Miyake, G. M.; Weitekamp, R. A.; Piunova, V. A.; Grubbs, R. H. *J. Am. Chem. Soc.* **2012**, *134*, 14249-14254.

28. Miyake, G. M.; Piunova, V. A.; Weitekamp, R. A.; Grubbs, R. H. *Angew. Chem. Int. Ed.* **2012**, *51*, 11246-11248.

29. Rostovtsev, V. V.; Green, L. G.; Fokin, V. V.; Sharpless, K. B. *Angew. Chem. Int. Ed.* **2002**, *41*, 2596-2599.

30. Kolb, H. C.; Sharpless, K. B. *Drug Delivery Today* **2003**, *8*, 1128-1137.

31. Binder, W. H.; Sachsenhofer, R. *Macromol. Rapid Commun.* **2007**, *28*, 15-54.

32. Binder, W. H.; Sachsenhofer, R. *Macromol. Rapid Commun.* **2008**, *29*, 952-981.

33. Xiaosong, Y. S.; Gao, H. *Nanoscale* **2016**, *8*, 4864-4881.

34. Gao, H.; Matyjaszewski, K. *J. Am. Chem. Soc.* **2007**, *129*, 6633-6639.

35. Tsarevsky, N. V.; Bencherif, S. A.; Matyjaszewski, K. *Macromolecules* **2007**, *40*, 4439-4445.

36. Yan, Y.; Shi, Y.; Zhu, W.; Chen, Y. *Polymer* **2013**, *54*, 5634-5642.

37. Zhao, P.; Yan, Y. C.; Feng, X. Q.; Liu, L. X.; Wang, C.; Chen, Y. M. *Polymer* **2012**, *53*, 1992-2000.

38. Zhao, P.; Liu, L.; Feng, X.; Wang, C.; Shuai, X.; Chen, Y. *Macromol. Rapid Commun.* **2012**, *33*, 1351-1355.

39. Shi, Y.; Wang, X.; Graff, R. W.; Phillip, W. A.; Gao, H. J. *Polym. Sci., Part A: Polym. Chem.* **2015**, *53*, 239-248.

40. Sun, J.; Hu, J.; Liu, G.; Xiao, D.; He, G.; Lu, R. *J. Polym. Sci. Part A: Polym. Chem.* **2011**, *49*, 1282-1288.

41. Tang, H.; Li, Y.; Lahasky, S. H.; Sheiko, S. S.; Zhang, D. *Macromolecules* **2011**, *44*, 1491-1499.

42. Opsteen, J. A.; van Hest, J. C. M. *Chem. Commun.* **2005**, *48*, 57-59.

43. Hay, A. S. *J. Org. Chem.* **1962**, *27*, 3320-3321.

44. Sindhu, K. S.; Anilkumar, G. *RSC Adv.* **2014**, *4*, 27867-27887.

Appendix A

for

Chapter 2: Water-Soluble Poly(ethylene oxide) Homografted Molecular Brushes with High and Tunable Grafting Densities Synthesized by a "Grafting To" Method

Appendix A.1. Example Calculation of Grafting Density of PEO Homografted Molecular Brushes

The following is an example calculation of grafting density for PEO MB-1 after 6 h reaction time using the molar ratio of backbone monomer units to the side chain polymer in the feed and the ratio of peak areas for the brushes and the unreacted side chains from SEC. The feed contained 5.1 mg of PTEGN_3MA-527 backbone, with a monomer unit molar mass of 243.27 g/mol, assuming 100 % azide functionalization. The feed contained 65.0 mg of PEO-45 side chain polymer with an absolute molecular weight of 2,100 g/mol (found by 2,000 + 80.08). For 100 % grafting density, 5.1 mg PTEGN_3MA-527 can react with 44.0 mg PEO-45 side chains to give 49.1 mg brushes. So the reaction mixture would contain (49.1 mg)/(70.1 mg) = 70.04 % brushes by mass. From SEC after 6 h reaction time, we found that the reaction mixture contained 68.70 % brushes by mass using peak areas. This gives a grafting density of (68.70 %)/(70.04 %) = 98.0 %. (We have confirmed that the peak areas in SEC are proportional to the masses of polymers, see Appendix A Figure A3).

Appendix A.2. Supplemental Figures

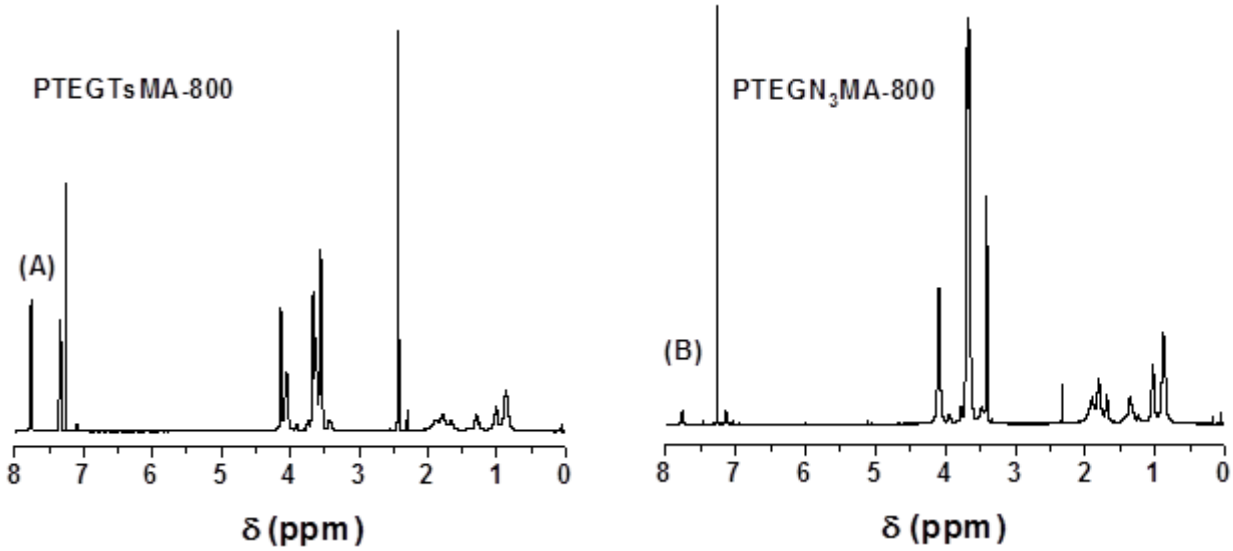

Figure A1. ^{1}H NMR spectra of (A) PTEGTsMA-800 and (B) PTEGN_3MA-800 ($CDCl_3$ solvent).

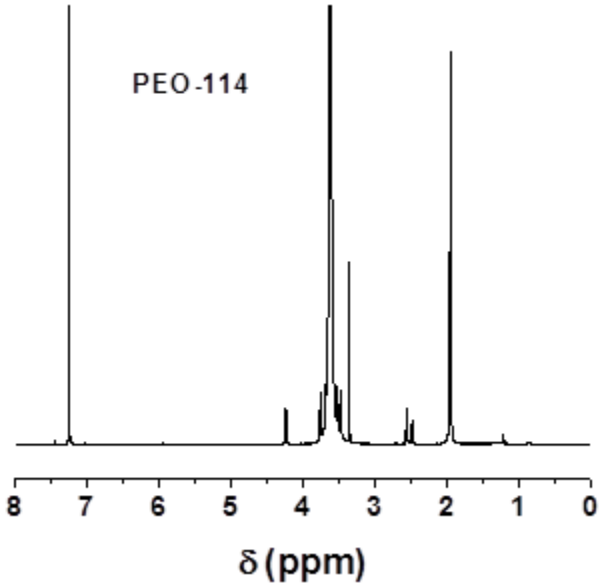

Figure A2. ^{1}H NMR spectrum of PEO-114 in $CDCl_3$.

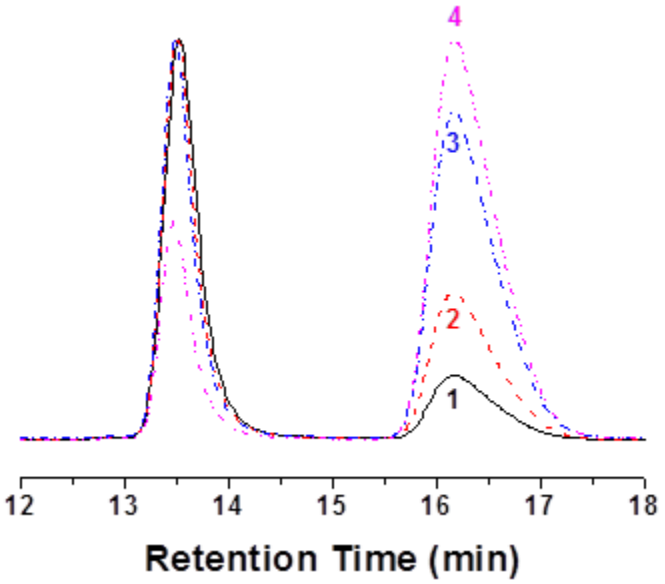

Sample	Composition (% by mass, 152k and 8k)	Peak Area Ratio (% by area, 152k and 8k)
1	77.90, 22.10	78.10, 21.90
2	59.77, 40.23	59.32, 40.68
3	38.82, 61.18	38.65, 61.35
4	22.03, 77.97	21.67, 78.33

Figure A3. SEC traces of mixtures of 152 kDa and 8 kDa polystyrene polymers with different compositions (top) and summary of composition by mass and peak area ratio, determined by SEC, for each sample. SEC analysis was carried out on PL GPC-20 system using THF as carrier solvent.

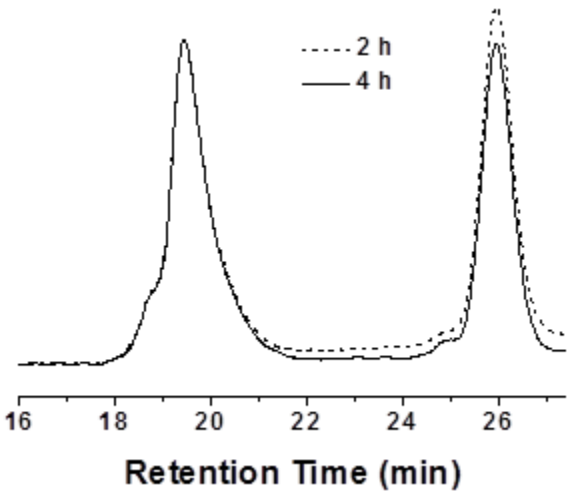

Figure A4. SEC traces of the reaction mixture for the synthesis of PEO MB-3 after 2 h and 4 h reaction time. SEC analysis was carried out on PL GPC-50 Plus system with Agilent Mixed-B columns using DMF containing 50 mM LiBr as carrier solvent.

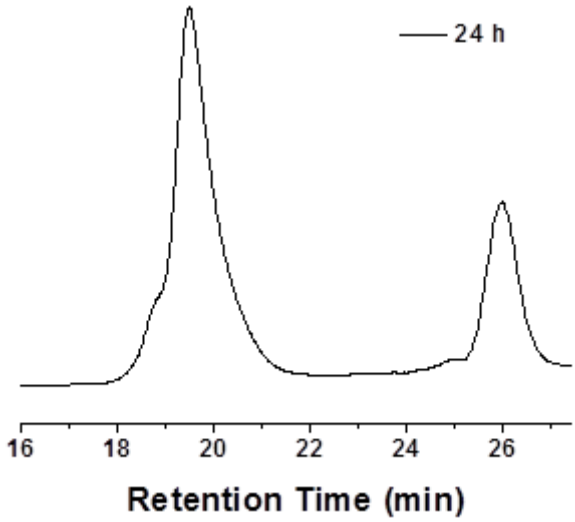

Figure A5. SEC trace of the reaction mixture for the synthesis of PEO MB-4 after 24 h reaction time. SEC analysis was carried out on PL GPC-50 Plus system with Agilent Mixed-B columns using DMF containing 50 mM LiBr as carrier solvent.

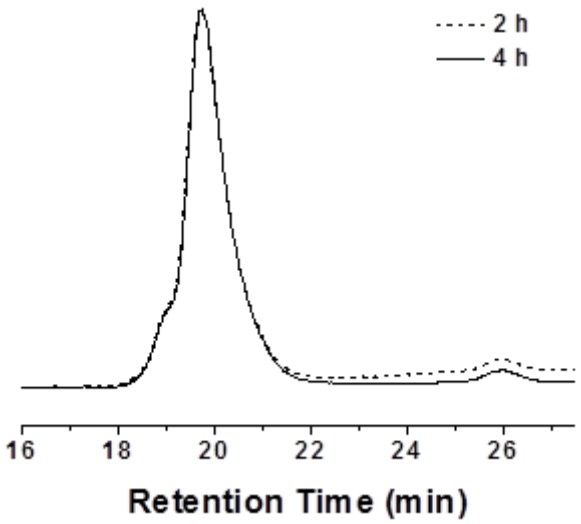

Figure A6. SEC traces of the reaction mixture for the synthesis of PEO MB-5 after 2 h and 4 h reaction time. SEC analysis was carried out on PL GPC-50 Plus system with Agilent Mixed-B columns using DMF containing 50 mM LiBr as carrier solvent.

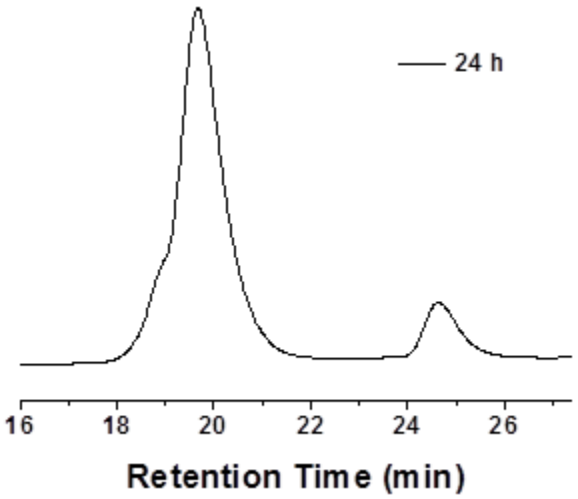

Figure A7. SEC trace of the reaction mixture for the synthesis of PEO MB-7 after 24 h reaction time. SEC analysis was carried out on PL GPC-50 Plus system with Agilent Mixed-B columns using DMF containing 50 mM LiBr as carrier solvent.

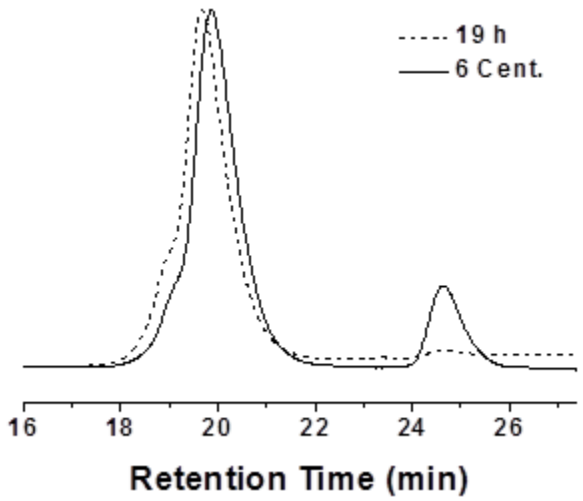

Figure A8. SEC traces of the reaction mixture for the synthesis of PEO MB-8 (not capped with propargyl alcohol) before and after six rounds of centrifugal filtration. SEC analysis was carried out on PL GPC-50 Plus system with Agilent Mixed-B columns using DMF containing 50 mM LiBr as carrier solvent.

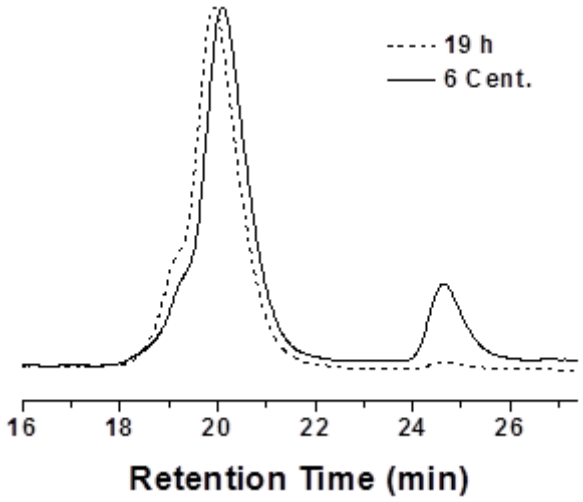

Figure A9. SEC traces of the reaction mixture for the synthesis of PEO MB-9 (not capped with propargyl alcohol) before and after six rounds of centrifugal filtration. SEC analysis was carried out on PL GPC-50 Plus system with Agilent Mixed-B columns using DMF containing 50 mM LiBr as carrier solvent.

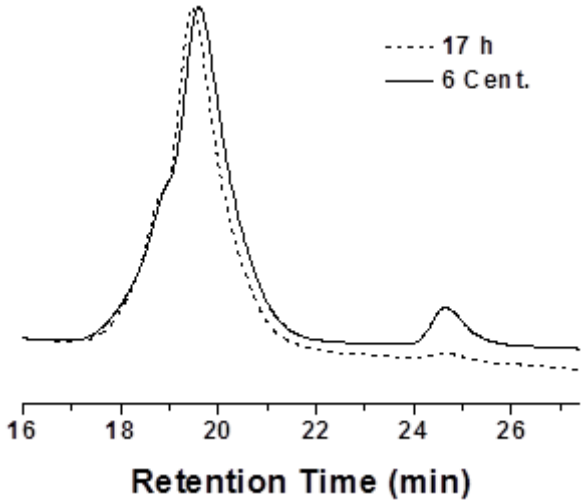

Figure A10. SEC traces of the reaction mixture for the synthesis of PEO MB-13 (not capped with propargyl alcohol) before and after six rounds of centrifugal filtration. SEC analysis was carried out on PL GPC-50 Plus system with Agilent Mixed-B columns using DMF containing 50 mM LiBr as carrier solvent.

Chapter 3: Synthesis and Characterization of Stimuli-Responsive Homografted Linear Molecular Brushes with High and Tunable Grafting Densities

Abstract

This chapter presents the synthesis and characterization of stimuli-responsive homografted linear molecular brushes with side chains composed of either thermosensitive poly(di(ethylene glycol) ethyl ether acrylate) (PDEGEA), thermo- and light-responsive poly((di(ethylene glycol) methyl ether acrylate)-*co*-(*o*-nitrobenzyl acrylate)) (P(DEGMA-*co*-NBA)), or pH-responsive poly(*N*,*N*-diethylaminoethyl methacrylate) (PDEAEMA). The brushes were made by a "grafting to" method using copper-catalyzed azide-alkyne cycloaddition "click" reactions between azide-functionalized backbone polymers and alkyne end-functionalized side chain polymers. The two backbone polymers with degrees of polymerization (DPs) of 527 and 800 employed here were synthesized by atom transfer radical polymerization (ATRP) and post-polymerization reactions discussed previously in Chapter 2. Alkyne end-functionalized side chain polymers were prepared by either ATRP or reversible addition-fragmentation chain transfer polymerization (RAFT) from an alkyne-functionalized initiator or chain transfer agent. The "grafting to" click reactions were performed at ambient temperature, and the grafting densities were determined by either size exclusion chromatography or ^{1}H NMR spectroscopy analysis. Using this method, we were able to prepare PDEGEA brushes with a backbone DP of 527 and a side chain DP of 36 with a nearly quantitative grafting density (97.8 %) when a molar ratio of backbone monomer units to side chains of 1 : 1.86 was used, and the grafting density could be tuned by adjusting this ratio. Under similar conditions, similar grafting densities were achieved for P(DEGMA-*co*-NBA) brushes. PDEAEMA brushes, however, exhibited lower grafting densities, likely due the increased chain rigidity of PDEAEMA, a polymethacrylate. Pure brush molecules were obtained by fractionation, and their stimuli responsive properties in aqueous solution were investigated. Dynamic light scattering (DLS) study of PDEGEA brushes in water at a concentration of 0.2 mg/g showed a sharp decrease

in size near the reported lower critical solution temperature (LCST) of 9 °C for PDEGEA linear polymer. This suggested a unimolecular collapse of brush molecules from an extended cylindrical state to a collapsed globular state. Dual thermo- and light-responsive P(DEGMA-*co*-NBA) brushes exhibited similar behavior, with a sharp decrease in size occurring at 20 °C for a 0.2 mg/g aqueous solution. After irradiation with 365 nm UV for 1 h, the LCST transition was shifted to a higher temperature (~36 °C), due to the cleavage of hydrophobic *o*-nitrobenzyl groups. The pH-responsive property of PDEAEMA brushes were studied in 5 mM KH_2PO_2 buffer, and from DLS at a concentration of 0.2 mg/g, we observed a sharp decrease in size around the reported pK_a of 7.4 for PDEAEMA linear polymer. At pH > ~ 8, aggregation and precipitation occurred even at a concentration of 0.002 mg/g.

3.1. Introduction

Molecular bottlebrushes consist of side chain polymers densely grafted a polymeric backbone.[1-3] Using "living"/controlled polymerization techniques, it is possible to synthesize molecular brushes with precisely controlled structures that are unique to this class of soft materials and can be useful for applications in a diverse range of disciplines from biomedicine to nanofabrication. In Chapter 2, we discussed the benefits and drawbacks of the different strategies available for the synthesis of molecular brushes, namely grafting from, grafting through, and grafting to.[1,2] The grafting to approach in particular, when combined with copper-catalyzed azide-alkyne cycloaddition (CuAAC) "click" reactions, can be a powerful technique for the synthesis of functional molecular brushes because of the inherent flexibility towards different side chain compositions and arrangements.[4-18] Gao and Matyjaszewski prepared molecular brushes by grafting to using CuAAC reactions between an alkyne-functionalized backbone and azide end-functionlized side chains.[9] A maximum grafting density of 88.4 % was achieved using relatively low molecular weight (775 Da) poly(ethylene oxide) (PEO) side chains with a large excess of side chains relative to backbone alkyne units. Significantly lower grafting densities were observed when a smaller excess of side chains was used or when more sterically hindered or higher molecular weight side chains were employed. More recently, reports by Chen et al.[11] and Gao et al.[14] have shown that high grafting densities (>85 %) can be achieved by CuAAC using an equimolar ratio of backbone azide units and alkyne-functionalized side chain polymers composed of PEO, polystyrene (PS), poly(*n*-butyl acrylate) (P*n*BA), poly(*t*-butyl acrylate) (P*t*BA), P*t*BA-*b*-PS, poly(methyl acrylate), or poly(*N*-alkyl acrylamide)s. The side chain molecular weights ranged from 2.0 to 11.2 kDa and the backbone lengths could be quite high (up to 1740 carbon-carbon bonds in the backbone polymer main chain).

Stimuli-responsive molecular brushes are particularly interesting because they can undergo dramatic changes in shape, size, and solubility in response to a variety of environmental triggers, most commonly temperature or pH.[17-50] Much of the research to date tends to focus on intermolecular assembly of molecular brushes into large micelle-like structures[24-34] or the tuning of cloud points of thermosensitive molecular brushes based on varying of the side chain composition.[35-43] In contrast, we are more interested in the stimuli-responsive behavior of single molecular bottlebrushes, particularly stimuli-induced shape-changing. As was discussed in Chapter 1, there are only a handful of such reports in the literature, with the vast majority of them being homografted molecular brushes that were synthesized by grafting from using "living"/controlled polymerization techniques, such as atom transfer radical polymerization (ATRP).[44-50] Additionally, it is important to note that as a result of the uniform composition of side chains in homografted molecular brushes, there is no built-in structural mechanism to stabilize the collapsed state. As a result, such brushes are prone to aggregation and precipitation upon application of the stimulus; thus the collapsed state is generally not stable except under specific conditions, such as very low polymer concentration.

The first report of such behavior was by Schmidt et al. in 2004 with thermosensitive PNIPAM brushes that were synthesized from a grafting from technique using ATRP.[44] They observed a unimolecular shape transition upon increasing temperature above the LCST of PNIPAM from an extended worm-like conformation to a collapsed, roughly spherical globular state by atomic force microscopy. However, the collapsed brushes were unstable at higher temperatures, which resulted in aggregation and eventually precipitation. McCarley et al. observed similar behavior from PNIPAM brushes that contained a conducting poly(thiophene) backbone.[45] Matyjaszewski and coworkers prepared loosely grafted pH-responsive poly(acrylic acid) (PAA)

brushes by grafting from that underwent a globule-to-wormlike transition upon increasing pH.[46] Mueller et al prepared dual thermo- and pH-responsive PDMAEMA brushes that exhibited a gradual conformation change from worm-like to curved to highly contracted as the pH was increased from 2 to 14 by cryogenic transmission electron microscopy of solutions that were vitrified from room temperature.[47] Additionally, they found that PDMAEMA brushes that were quarternized with methyl iodide underwent a worm-to-sphere transition in the presence of salts or anionic surfactant sodium dodecyl sulfate (SDS).[48,49] The worm-like state could be reformed upon addition of α- or β-cyclodextrin, which form inclusion complexes with SDS. β-Cyclodextrin could subsequently be removed by addition of a more competitive inclusion agent, inducing a transition back to the spherical state. Tang and coworkers synthesized salt-responsive, cationic poly(caprolactone) (PCL) brushes using a grafting through technique from norbornene end-functionalized macromonomers that were polymerized by ring opening metathesis polymerization.[50] At low concentration in aqueous solution, a transition from worms to spheres was observed when the ionic strength was gradually increased by the addition of NaCl, although the solutions eventually became turbid.

We emphasize that the overwhelming majority of molecular brushes for which stimuli-responsive shape-changing behavior has been demonstrated were synthesized by the grafting from approach which, although highly successful for the preparation of densely grafted homopolymer brushes, does not allow for the facile tuning of grafting density or synthesis of more complex architectures such as heterografted brushes, which are of particular interest to us. For this reason, we set out to extend the grafting to "click" methodology developed in Chapter 2 to the synthesis of a wide variety of stimuli-responsive molecular brushes with different side chain compositions.

Here, we show that stimuli-responsive molecular brushes with high and tunable grafting densities can be readily prepared using a grafting to CuAAC "click" method and that these brushes display intriguing responsive behavior upon application of stimuli. Three types of stimuli-responsive polymers were employed as side chains for responsive homografted molecular brushes, including thermosensitive poly(di(ethylene glycol) ethyl ether acrylate) (PDEGEA), thermo- and light-responsive poly((di(ethylene glycol) methyl ether acrylate)-*co*-(*o*-nitrobenzyl acrylate)) (P(DEGMA-*co*-NBA)), and pH-responsive poly(*N*,*N*-diethylaminoethyl methacrylate) (PDEAEMA) (Scheme 3.1). The two azide-containing backbone polymers whose synthesis is described in Chapter 2, with degrees of polymerization (DPs) of 527 and 800, were used to react with alkyne end-functionalized side chain polymers, which were prepared by either ATRP or reversible addition-fragmentation chain transfer polymerization (RAFT) from an alkyne-containing initiator or chain transfer agent. The "grafting to" click reactions were performed at ambient temperature in DMF or THF using CuCl as catalyst, and the grafting densities were determined by either size exclusion chromatography or ^{1}H NMR spectroscopy analysis. Using this method, we were able to prepare PDEGEA and P(DEGMA-*co*-NBA) brushes with high grafting densities when a molar ratio of backbone monomer units to side chains of approximately 1 : 2 was used, and we found that the grafting density could be tuned by adjusting this ratio. PDEAEMA brushes, however, exhibited slightly lower grafting densities, likely due the increased chain rigidity of PDEAEMA, a polymethacrylate. Pure brush molecules were obtained by fractionation, and their stimuli responsive properties in aqueous solution were investigated by visual inspection and dynamic light scattering (DLS). For thermoresponsive PDEGEA and P(DEGMA-*co*-NBA) brushes, we observed clouding at higher concentration (1 mg/g) and unimolecular collapse at lower concentration (0.2 mg/g) when the temperature was increased above the LCST of the side

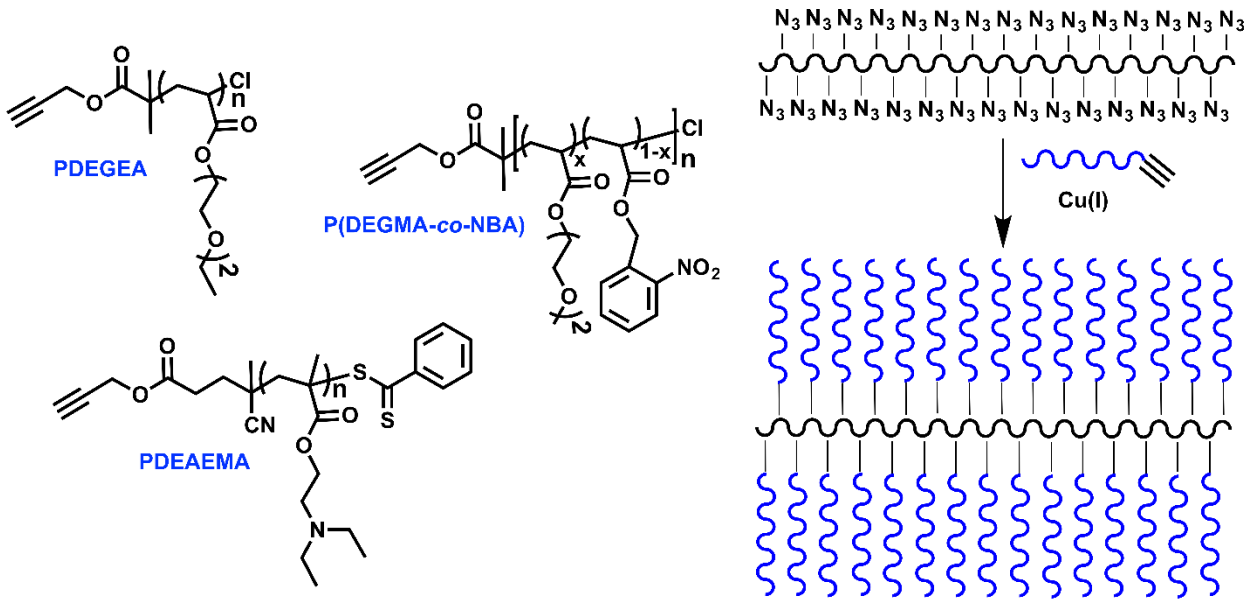

Scheme 3.1. Synthesis of Stimuli-Responsive Molecular Brushes by "Grafting To" CuAAC "Click" Reactions.

chains. For P(DEGMA-*co*-NBA) brushes the transition temperature was increased by 16 °C upon photocleavage of hydrophobic NBA groups using long-wave UV light. The pH-responsive PDEAEMA brushes in 5 mM KH_2PO_2 buffer underwent a decrease in size with an increase in pH, but aggregation and precipitation occurred at pH > ~8 even at very low polymer concentration.

3.2. Experimental Section

3.2.1. Materials

Di(ethylene glycol) ethyl ether acrylate (DEGEA, 90%, Aldrich) and *N,N,N',N'',N''*-pentamethyldiethylenetriamine (PMDETA, 99%, Acros) were purified by vacuum distillation over calcium hydride. *N,N*-Diethylaminoethyl methacrylate (DEAEMA, 99%, Aldrich) was passed through a basic alumina/silica gel column to remove the inhibitor prior to use. Di(ethylene glycol) methyl ether acrylate (DEGMA) was synthesized by the reaction of acryloyl chloride (97%, Aldrich) and di(ethylene glycol) monomethyl ether (99%, Aldrich) in the presence of triethylamine (99%, Acros). The product was purified by column chromatography and vacuum distillation, and the molecular structure was verified by ^{1}H NMR spectroscopy. *o*-Nitrobenzyl acrylate (NBA) was synthesized according to a literature procedure by the reaction of acryloyl chloride and *o*-nitrobenzyl alcohol (97%, Acros) in the presence of triethylamine.[51] The product was purified by column chromatography, and its molecular structure was confirmed by ^{1}H NMR spectroscopy analysis. 4-Cyano-4-(phenylcarbonothioylthio)pentanoic acid was synthesized according to a literature procedure.[52] The preparation of azide-functionalized backbone polymers with a DPs of 527 (PTEGN_3MA-527) and 800 (PTEGN_3MA-800) is described in Chapter 2. All other chemicals were purchased from either Aldrich or Fisher and used as received.

3.2.2. General Characterization

Size exclusion chromatography (SEC) of PDEGEA and P(DEGMA-*co*-NBA) molecular brush samples was carried out at ambient temperature using a PL-GPC 50 Plus (an integrated GPC/SEC system from Polymer Laboratories, Inc.) with a differential refractive index detector, one PLgel 10 µm guard column (50 × 7.5 mm, Agilent Technologies), and three PLgel 10 µm Mixed-B columns (each 300 × 7.5 mm, linear range of molecular weight from 500 to 10,000,000 Da according to Agilent Technologies). The data were processed using Cirrus™ GPC/SEC software (Polymer Laboratories, Inc.). *N,N*-Dimethylformamide (DMF) with 50 mM LiBr was used as the carrier solvent at a flow rate of 1.0 mL/min. Poly(*N,N*-diethylaminoethyl methacrylate) (PDEAEMA) side chain polymers were also analyzed with the same PL-GPC 50 Plus system, except with the use of one PSS GRAL guard column (50 × 8 mm, Polymer Standards Service-USA, Inc.) and two PSS GRAL linear columns (each 300 × 8 mm, linear range of molecular weight from 500 to 1,000,000 according to Polymer Standards Service USA, Inc.). SEC of PDEGEA and P(DEGMA-*co*-NBA) side chain polymers was carried out using a PL-GPC 20 integrated GPC/SEC system from Polymer Laboratories, Inc. with a refractive index detector, one PLgel 5 µm guard column (50 × 7.5 mm, Agilent Technologies), and two PLgel 5 µm Mixed-C columns (each 300 × 7.5 mm, linear range of molecular weight from 200 to 2,000,000 Da according to Agilent Technologies). THF was used as the eluent at a flow rate of 1.0 mL/min. Each system was calibrated with a set of near-monodisperse linear polystyrene standards (Polymer Laboratories, Inc.). ^{1}H and ^{13}C NMR (300 or 500 MHz) spectra were recorded on a Varian Mercury 300 NMR spectrometer or a Varian VNMRS 500 NMR spectrometer, respectively, and the residual solvent proton signal was used as the internal standard. High resolution mass spectroscopy (HRMS)

experiments were performed using a JEOL Model JMS-T100LC (AccuTOF) orthogonal time-of-flight (TOF) mass spectrometer (Peabody, MA) with an IonSense (Danvers, MA) DART source.

3.2.3. Synthesis of Propargyl 2-Bromoisobutyrate (PBiB)

Propargyl alcohol (0.823 g, 14.7 mmol), triethylamine (1.226 g, 12.2 mmol), and dry methylene chloride (8 mL) were added to a 100 mL three-necked round bottom flask with a stir bar and stirred under nitrogen in an ice/water bath for 20 min. A solution of 2-bromo-2-methylpropionyl bromide (2.148 g, 9.34 mmol) in dry methylene chloride (10 mL) was added dropwise over a period of 45 min. A white precipitate was observed. After the mixture was stirred at room temperature under nitrogen overnight, the precipitate was filtered off. The filtrate was diluted to 100 mL with methylene chloride, washed three times with saturated sodium bicarbonate (15 mL) and saturated sodium chloride (1 mL) solution, and finally dried over anhydrous sodium sulfate. The crude product was purified by column chromatography using a mixture of ethyl acetate and hexanes (v/v = 1:3) as eluent. The solvents were removed under high vacuum, yielding a clear, colorless liquid (1.528 g, 79.8 %). ^{1}H NMR δ (ppm, $CDCl_3$): 4.73 (d, -COOCH_2-, 2H), 2.49 (t, -CH_2C≡CH, 1H), 1.92 (s, -C(CH_3)$_2$Br, 6H). ^{13}C NMR δ (ppm, $CDCl_3$): 170.86 (-COO-), 76.86 (-CH_2C≡CH), 75.43 (-CH_2C≡CH), 54.89 (-$C$$H_2$C≡CH), 53.41 (-$C$($CH_3$)$_2$Br), 30.62 (-C($C$$H_3$)$_2$Br).

3.2.4. Synthesis of Propargyl 4-Cyano-4-(phenylcarbonothioylthio)pentanoate (PCPP)

4-Cyano-4-(phenylcarbonothioylthio)pentanoic acid (0.297 g, 1.06 mmol), propargyl alcohol (0.111 g, 1.98 mmol), and 4-(*N*,*N*-dimethylamino)pyridine (0.015 g, 0.12 mmol) were placed in a 25 mL two-necked round bottom flask with a stir bar and dissolved in methylene chloride (5 mL). A solution of *N,N'*-dicyclohexylcarbodiimide (0.461 g, 2.23 mmol) in methylene chloride (5 mL) was added dropwise under nitrogen with stirring. A white precipitate was observed, and the mixture was stirred under nitrogen at room temperature for 1.5 h, and then stored

in a freezer overnight. The white precipitate was filtered off from the cold solution, and the crude product was purified by column chromatography using a mixture of ethyl acetate and hexanes (v/v = 4:1). The product was dried under high vacuum to obtain a red, viscous liquid (0.305 g, 90.7 %). ^{1}H NMR δ (ppm, $CDCl_3$): 7.89 (d, -Ar*H*, 2H), 7.55 (t, -Ar*H*, 1H), 7.38 (t, -Ar*H*, 2H), 4.70 (d, -COOCH_2-, 2H), 2.39-2.81 (m, -CH_2CH_2-, CH_2C≡C*H*, 5H), 1.92 (s, -CH_3, 3H). ^{13}C NMR δ (ppm, $CDCl_3$): 222.14 (-*C*(S)S-), 170.72 (-*C*OO-), 144.50 (C_{Ar}), 133.03(C_{Ar}), 128.57(C_{Ar}), 126.67(C_{Ar}), 118.38 (-*C*N),77.19 (-CH_2*C*≡CH), 75.25 (-CH_2C≡*C*H), 52.47(-*C*H_2C≡CH), 45.65 (-*C*(CN)(CH_3)), 33.22 (-C*C*$H_2$$CH_2$-), 29.59 (-CC$H_2$*C*$H_2$-), 24.17 (-*C*$H_3$).

3.2.5. Synthesis of Thermosensitive Side Chain Polymers by ATRP

Described below is a typical procedure for the synthesis of an alkyne end-functionalized PDEGEA side chain polymer with a DP of 36 (PDEGEA-36) by ATRP. Similar procedures were employed for the synthesis of other PDEGEA homopolymers with different DPs. PBiB (75.0 mg, 0.366 mmol), DEGEA (8.297 g, 44.1 mmol), CuCl (41.0 mg, 0.414 mmol), anisole (8.396 g), and PMDETA (0.101 g, 0.583 mmol) were weighed into a 50 mL two-neck round bottom flask equipped with a magnetic stir bar. The mixture was degassed by three freeze-pump-thaw cycles and placed in an 80 °C oil bath. After 10 h and 15 min, the flask was removed from the oil bath and opened to air. The polymerization mixture was passed through neutral alumina/silica gel column to remove the catalyst. The polymer was purified by precipitation in hexanes three times and dried under high vacuum to obtain a light green, viscous polymer (1.519 g). The DP was calculated to be 36 by end group analysis from the ^{1}H NMR spectrum, using the integrals of the peaks at 4.62 ppm (HC≡CCH_2OOC- of the alkyne end group) and 4.07-4.24 ppm (-COOCH_2- of DEGEA monomer units). The results of SEC analysis with THF as carrier solvent: $M_{n,SEC}$ = 6,500 Da; PDI = 1.16.

3.2.6. Synthesis of Dual Thermo- and Light-Responsive Side Chain Polymer by ATRP

Described below is the procedure for the synthesis of a P(DEGMA-*co*-NBA) side chain copolymer with a DP of 47 (P(DEGMA-*co*-NBA)-47) by ATRP. PBiB (59.0 mg, 0.288 mmol), DEGMA (5.015 g, 28.8 mmol), NBA (0.681 g, 3.29 mmol), CuCl (28.6 mg, 0.289 mmol), anisole (5.693 g), and PMDETA (0.121 g, 0.698 mmol) were added into a 25 mL two-neck round bottom flask equipped with a magnetic stir bar. The mixture was degassed by three freeze-pump-thaw cycles and placed in an 80 °C oil bath. After 21 h and 30 min, the reaction mixture was removed from the oil bath, opened to air, and passed through a neutral alumina/silica gel column to remove the copper catalyst. The polymer was purified by precipitation in hexanes three times and dried under high vacuum to obtain a light yellow, viscous polymer (1.569 g). The numbers of DEGMA and NBA monomer units in the copolymer were 42 and 5, respectively, giving a total DP of 47, determined by end group analysis from ^{1}H NMR spectroscopy, using the integrals of the peaks at 4.62 ppm (HC≡CCH_2OOC- of the alkyne end group), 4.02-4.26 ppm (-COOCH_2- of DEGMA monomer units), and 5.33-5.56 ppm (-COOCH_2- of NBA monomer units). The results of SEC analysis with THF as carrier solvent: $M_{n,SEC}$ = 8,800 Da; PDI = 1.17.

3.2.7. Synthesis of pH-Responsive Side Chain Polymer by RAFT Polymerization

Described below is the procedure for the synthesis of a PDEAEMA side chain polymer with a DP of 43 (PDEAEMA-43) by RAFT. PCPP (71.6 mg, 0.226 mmol), DEAEMA (5.012 g, 27.1 mmol), AIBN (3.8 mg, 0.023 mmol, from 0.478 g of a stock solution in anisole with a concentration of 7.89 mg/g), and anisole (7.448 g) were added into a 25 mL two-neck round bottom flask equipped with a magnetic stir bar. The polymerization mixture was degassed by three freeze-pump-thaw cycles, and the flask was placed in a 70 °C oil bath. After 5 h and 25 min, the flask was removed from the oil bath and opened to air. The polymer was purified by precipitation four

times in hexanes cooled in a dry ice/acetone bath and dried under high vacuum, yielding a red, viscous polymer (1.035 g). The DP was found to be 43 by end group analysis from ^{1}H NMR spectroscopy, using the integrals of the peaks at 4.66 ppm (HC≡CCH_2OOC- of the alkyne end group) and 3.90-4.11 ppm (-COOCH_2- of DEAEMA monomer units). The results of SEC analysis with DMF containing 50 mM LiBr as carrier solvent: $M_{n,SEC}$ = 5,700 Da; PDI = 1.16.

3.2.8. Synthesis of Stimuli-Responsive Homografted Molecular Brushes

Below is the procedure for the synthesis of thermosensitive PDEGEA molecular brushes with a backbone DP of 527 and a side chain DP of 36 (PDEGEA MB-1). Similar procedures were employed for the synthesis of other PDEGEA molecular brushes with different backbone and side chain DPs as well as dual thermo- and light-responsive P(DEGMA-*co*-NBA) homografted molecular brushes. PTEGN_3MA-527 (5.0 mg, 0.021 mmol monomer units, from a stock solution in THF) was added into a 3.7 mL vial equipped with a stir bar. THF was evaporated off with a stream of nitrogen, and DMF (0.5 mL) was added. PDEGEA-36 (263.3 mg, 0.0382 mmol alkyne end groups) was weighed into a vial, dissolved in DMF (2.0 mL), and transferred to the vial containing PTEGN_3MA-527. CuCl (2.2 mg, 0.022 mmol) was added, and a rubber septum was used to seal the reaction vial. The mixture was flushed with nitrogen via needles for 15 min, and PMDETA (5.0 µL, 0.024 mmol) was injected using a microsyringe. The reaction progress was monitored by SEC. After 48 h, the mixture was opened to air, diluted with methylene chloride, and passed through a short neutral alumina/silica gel column to remove the catalyst. Excess side chains were removed by fractionation in a mixture of THF and hexanes twice to yield a light yellow, viscous polymer (96.0 mg, 65 % yield). The grafting density, defined as the percentage of backbone monomer units that are grafted with a side chain polymer, was determined to be 97.8 % by comparison of the brush and the unreacted side chain polymer peak areas from SEC

chromatogram of the reaction mixture at the end of the reaction. The results of SEC analysis of the purified brushes with DMF containing 50 mM LiBr as carrier solvent: $M_{n,SEC}$ = 880,300; PDI = 1.09.

PDEAEMA homografted molecular brushes were synthesized according to a slightly altered procedure due to their poor solubility in DMF. THF was used as the reaction medium, and the grafting density was determined from the conversion of the alkyne end group of the side chain polymer using ^{1}H NMR spectroscopy analysis of the reaction mixture. SEC analysis of PDEAEMA homografted molecular brushes could not be performed due to their poor solubility in DMF containing 50 mM LiBr.

3.2.9. Atomic Force Microscopy of PDEGEA Molecular Brushes

Atomic force microscopy (AFM) was performed using a Digital Instruments Multimode IIIa Scanning Probe Microscope operated in tapping mode under ambient conditions. Reflective Al-coated Si probes (Budget Sensors) with a nominal resonant frequency of 300 kHz and force constant of 40 N/m were employed. Aqueous solutions of molecular brushes with a concentration of 0.1 mg/g for AFM imaging were prepared using Milli-Q water and spin coated at 3000 rpm onto Si wafers that were freshly cleaned with piranha solution (concentrated H_2SO_4 : 30 wt % H_2O_2, v/v, 3:1).

3.2.10. Dynamic Light Scattering Study of Stimuli-Responsive Molecular Brushes in Water

Dynamic light scattering (DLS) measurements were performed using a Malvern Zetasizer Nano ZS system equipped with a He-Ne 633 nm laser and a temperature controller at a scattering angle of 173°. Aqueous solutions of molecular brushes for DLS measurements with a concentration of 0.2 mg/g were prepared by dissolving the brush molecules in either Milli-Q water or 5 mM KH_2PO_4 buffer and passed through a 0.2 μm PTFE filter prior to analysis. The reported sizes in this work were the intensity mean diameters. Photocleavage of thermo- and light-

responsive P(DEGMA-*co*-NBA) molecular brushes was performed using 2 mL of brush solution (0.2 mg/g solution in Milli-Q water) in a 3.7 mL vial by irradiating the sample with long wavelength (365 nm) UV light from a Spectroline ENF-240C hand-held UV lamp equipped with a 4 watt long wavelength tube filtered at 365 nm. For PDEAEMA molecular brushes, the pH of the aqueous solution was measured with a pH meter (Accumet AB15 pH meter from Fisher Scientific, calibrated with pH = 4.01, 7.00, and 10.01 standard buffer solutions), and the pH of the solution was adjusted using 0.1 M HCl and 0.1 M NaOH solutions.

3.3. Results and Discussion

3.3.1. Synthesis of Azide-Functionalized Backbone Polymers (PTEGN_3MA)

In Chapter 2, we described the synthesis of azide-functionalized backbone polymers (PTEGN_3MA) that were prepared by ATRP of TEGSiMA, a silyl ether protected methacrylate monomer, followed by first removal of the *t*-butyldimethylsilyl ether moiety, then reaction with tosyl chloride, and finally substitution with sodium azide (Scheme 2.2). We prepared backbone polymers with DPs of 527 and 800 (PTEGN_3MA-527 and PTEGN_3MA-800, respectively), and used them for the synthesis of water-soluble poly(ethylene oxide) (PEO) molecular brushes by a grafting to method using copper-catalyzed azide-alkyne cycloaddtion (CuAAC) “click” reactions. Here, we extend the methodology developed in Chapter 2 for the synthesis of thermo-, dual thermo- and light-, and pH-responsive homografted molecular brushes. SEC traces of both azide-functionalized backbone polymers and ^{1}H NMR spectra of PTEGN_3MA-527 along with its silyl ether and tosylate polymer precursors can be found in Chapter 2 (Figure 2.3). Characterization data for both backbone polymers can be found in Table 2.1. SEC analysis showed that the backbone polymers were well-defined, and the degrees of azide functionalization were high for each: 98 % for PTEGN_3MA-527 and 90 % for PTEGN_3MA-800, calculated from their ^{1}H NMR

spectra using the integral values of the peaks at 3.98-4.14 ppm (-COOCH_2CH$_2$-) and 3.34-3.47 ppm (-OCH$_2$CH_2N$_3$). A more detailed discussion of the synthesis can be found in Chapter 2.

3.3.2. Synthesis of Alkyne End-Functionalized Stimuli-Responsive Side Chain Polymers

Alkyne end-functionalized stimuli-responsive side chain polymers were prepared either by ATRP using an alkyne-functionalized ATRP initiator (PBiB) or by RAFT using an alkyne-containing chain transfer agent (PCPP) (Scheme 3.2). Thermosensitive PDEGEA and dual thermo- and light-responsive P(DEGMA-*co*-NBA) side chain polymers were synthesized by ATRP. CuCl/PMDETA was used as the catalyst for ATRP so that the chain would be terminated by chlorine, which is much less reactive than a bromine chain end in the presence of Cu(I)Br during the synthesis of molecular brushes by copper-catalyzed azide-alkyne cycloaddition "click" reaction. The ATRPs were carried out in anisole at 80 °C and stopped when desired molecular weights were achieved. Differently, the pH-responsive PDEAEMA side chain polymer was prepared by RAFT polymerization using alkyne-functionalized chain transfer agent PCPP, which was also performed in anisole at 70 °C using AIBN as initiator. In each case, the monomer conversion was kept below 50 % in order to avoid or minimize any possible side reactions involving the alkyne end group during the polymerization.

All of the side chain polymers were purified by repetitive precipitation in hexane (for PDEAEMA, hexane was cooled in a dry ice/acetone bath), dried under high vacuum, and characterized by SEC and ^{1}H NMR spectroscopy. As an example, Figure 3.1 shows the SEC trace and ^{1}H NMR spectrum of an alkyne-terminated PDEGEA with a DP of 36 (PDEGEA-36). SEC analysis showed that the polymerization was well controlled and side reactions involving the alkyne chain end were kept to a minimum, as reflected by the narrow, monomodal molecular weight distribution with a PDI of 1.16. The SEC traces and ^{1}H NMR spectra of other stimuli-

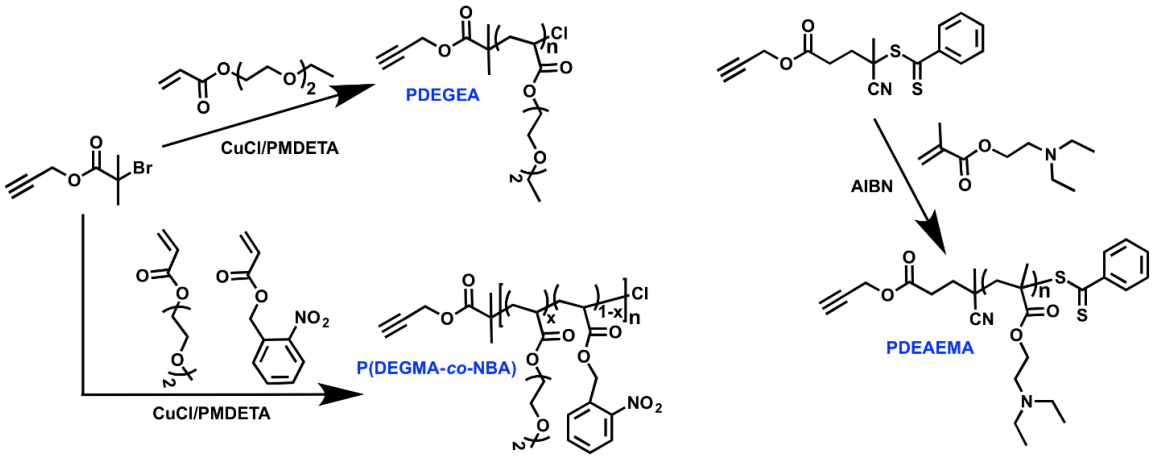

Scheme 3.2. Synthesis of Alkyne End-Functionalized Stimuli-Responsive Side Chain Polymers by Atom Transfer Radical Polymerization (ATRP) and Reversible Addition-Fragmentation Chain Transfer (RAFT) Polymerization.

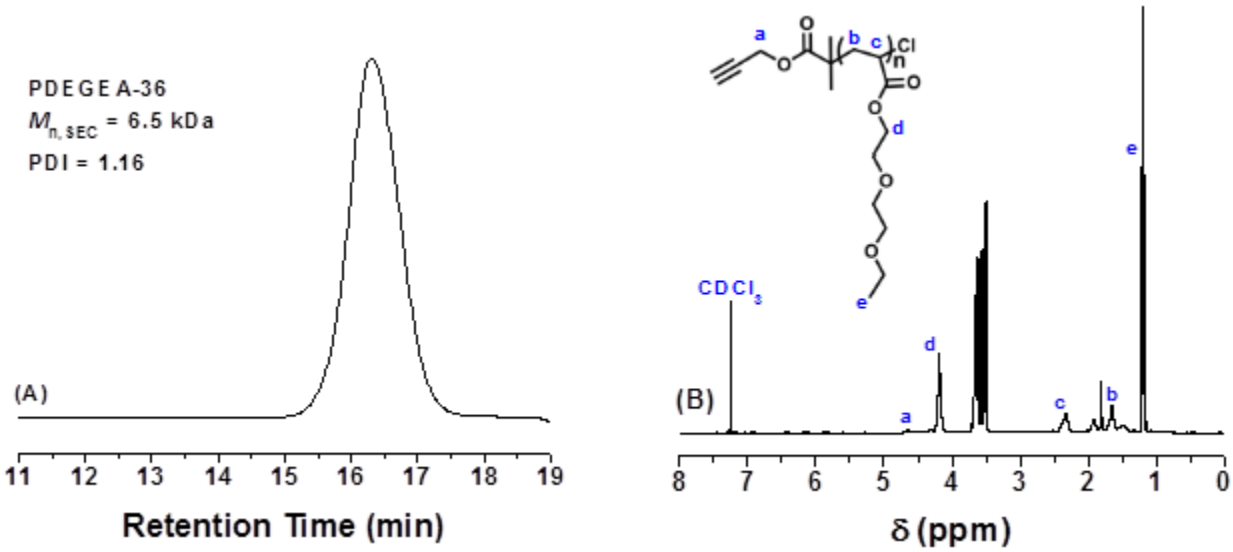

Figure 3.1. (A) SEC trace of side chain polymer PDEGEA-36 from SEC analysis using PL GPC-20 system with THF as mobile phase and (B) ^{1}H NMR spectrum of PDEGEA-36 in $CDCl_3$.

responsive side polymers can be found in Appendix B (Figure B1-B4). The DP of each side chain polymer was calculated from the ^{1}H NMR spectrum of the purified polymer using the integrals of the peaks from the alkyne chain end and the characteristic protons of monomer units. Specifically, for thermosensitive PDEGEA, the peaks at 4.62 ppm (HC≡CCH_2OOC- of the end group from PBiB) and 4.07-4.24 ppm (-COOCH_2CH$_2$- of DEGEA monomer units) were used for the calculation of DP. For PDEAEMA, the peaks at 4.66 ppm (HC≡CCH_2OOC- of the end group from PCPP) and 3.90-4.11 ppm (-COOCH_2CH$_2$- of DEAEMA monomer units) were used for the calculation of DP. For P(DEGMA-*co*-NBA), the peaks at 5.33-5.56 ppm (-COOCH_2($C_6H_4NO_2$), of NBA monomer units), 4.62 ppm (HC≡CCH_2OOC- of the end group from PBiB), and 4.02-4.26 ppm (-COOCH_2CH$_2$- of DEGMA monomer units) were used for the calculation of the numbers of DEGMA and NBA monomer units. The characterization data for all stimuli-responsive side chain polymers are summarized in Table 3.1.

3.3.3. Synthesis of Thermosensitive PDEGEA Homografted Molecular Brushes

Thermosensitive PDEGEA homografted molecular brushes were prepared by a "grafting to" method using copper-catalyzed azide-alkyne cycloaddition "click" reactions between azide-containing repeat units of the backbone polymer PTEGN_3MA and alkyne end-functionalized thermosensitive side chain polymer PDEGEA. Note that the reported cloud point of PDEGEA in water was 9 °C.[53] The reactions were performed in DMF using CuCl/PMDETA as catalyst at ambient temperature. The grafting density, defined as the percentage of backbone repeat units that are grafted with a side chain polymer, was calculated from the SEC chromatogram using the ratio of peak areas from the molecular brushes and the unreacted side chain polymer and the molar ratio of backbone monomer units to the side chain polymer in the feed. Using a series of mixtures of two polystyrene homopolymers with very different molecular weights, 8 kDa and 152 kDa, we

Table 3.1. Characterization Data for Alkyne End-Functionalized Stimuli-Responsive Side Chain Polymers Synthesized by ATRP and RAFT Polymerizations.

Side Chain Polymer Sample	$M_{n,SEC}$ (kDa)	PDI	DP [c]
PDEGEA-36	6.5 [a]	1.16 [a]	36
PDEGEA-59	11.3 [a]	1.20 [a]	59
PDEGEA-82	15.6 [a]	1.25 [a]	82
PDEAEMA-43	5.7 [b]	1.16 [b]	43
P(DEGMA-*co*-NBA)-47	8.8 [a]	1.17 [a]	47 (42, 5) [d]

[a] The values of number average molecular weight ($M_{n,SEC}$) and polydispersity index (PDI) were measured by SEC using PL GPC-20 system with THF as solvent. [b] SEC was performed using PL GPC-50 Plus system with PSS GRAL columns and DMF with 50 mM LiBr as mobile phase. [c] DP was calculated by ^{1}H NMR spectroscopy analysis using the integrals of the peaks from the monomer units and the end groups (from the alkyne containing initiator PBiB or RAFT chain transfer agent PCPP). [d] Number of DEGMA and NBA monomer units, respectively.

have confirmed that the peak area ratio of the two different molecular weight polymers is essentially the same as the mass ratio (see Appendix A, Figure A3).

We first used a molar ratio of 1 : 1.86 for the backbone monomer units in PTEGN_3MA-527 to side chain polymer PDEGEA-36 to synthesize PDEGEA molecular brushes (PDEGEA MB-1 in Table 3.2 and Figure 3.3). The reaction progress was followed by SEC analysis; Figure 3.2 shows the SEC traces of the reaction mixture at different reaction times. For comparison, the SEC curve of backbone polymer PTEGN_3MA-527 is shown as well as the PDEGEA MB-1 after the removal of excess side chain polymer by fractionation. After the reaction proceeded for two hours, a high molecular weight peak was observed in the SEC chromatogram with a $M_{n,SEC}$ of 810,700 and a PDI of 1.08, indicating the formation of brush molecules. From the relative peak areas, the mixture contained 44.68 % of brushes and 55.32 % of unreacted PDEGEA-36. Since the molar ratio of monomer units of PDEGN_3MA-527 to the side chain polymer in the feed was 1:1.86, this gives a grafting density of 81.7 % after two hours of reaction. SEC analysis of the reaction mixture at further time intervals showed a continued increase in the amount of brushes relative to unreacted side chain polymer, and the reaction essentially reached the limit after 24 h, as indicated by almost no change in relative peak areas between 24 and 48 h. After 48 h, the $M_{n,SEC}$ reached 862,000 Da and the PDI = 1.08; the relative amount of brushes was 53.53%, giving a final grafting density of 97.8 %. This means that almost every available azide group on the backbone PTEGN_3MA-527 had reacted with a side chain polymer molecule. A more detailed description of the calculation of grafting density from SEC can be found in Appendix B.1.

After 48 h, the reaction was stopped by opening the vial to air and passing the mixture through a small neutral alumina column to remove the copper catalyst. The PDEGEA brush molecules were then concentrated, and the excess side chains were removed by fractionation using

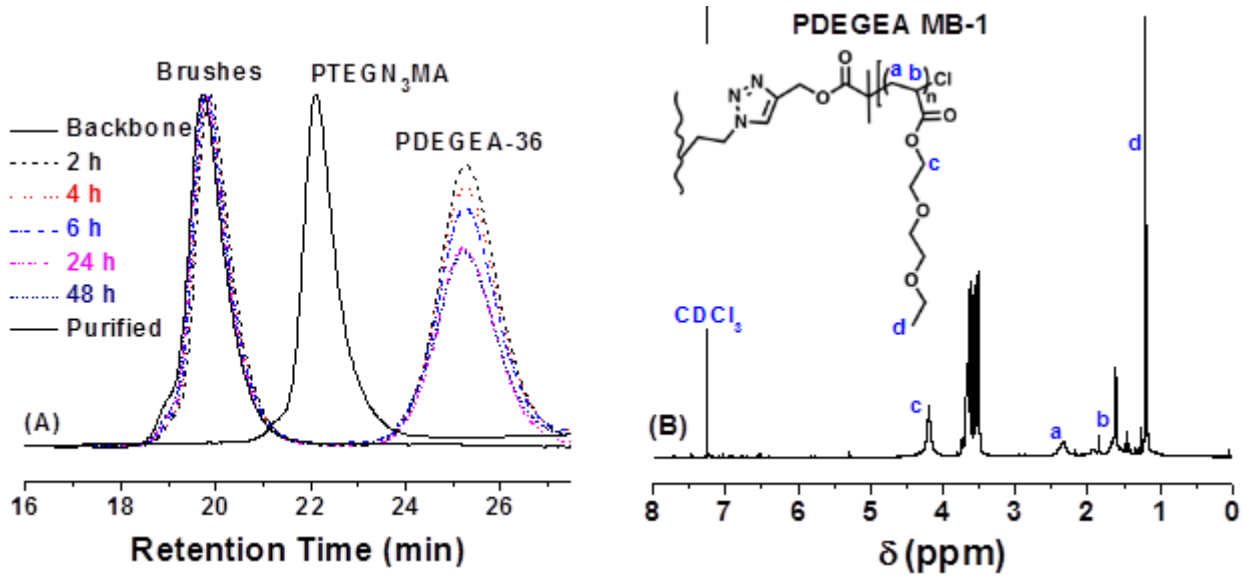

Figure 3.2. (A) SEC traces of the reaction mixture at different reaction times from the reaction for the synthesis of PDEGEA MB-1 molecular brushes and $PTEGN_3MA$-527 backbone polymer as well as the purified PDEGEA MB-1 after the removal of excess side chain polymer PDEGEA-36 by fractionation. SEC analysis was performed using PL GPC-50 Plus system with Agilent Mixed-B columns in DMF with 50 mM LiBr. (B) ^1H NMR spectrum of the purified PDEGEA MB-1 in $CDCl_3$.

Table 3.2. PDEGEA Molecular Brushes with Different Grafting Densities and Side Chain Lengths Synthesized by "Grafting to" Using CuAAC "Click" Reactions

Molecular Brush Sample	$DP_{Backbone}$-$DP_{Sidechain}$	Feed Molar Ratio of Backbone Monomer Units to PDEGEA	$M_{n,SEC}$ (kDa) [a]	PDI [a]	Grafting Density (%)[b]
PDEGEA MB-1	527-36	1:1.86	862.0	1.08	97.8
PDEGEA MB-2	527-36	1:1.40	830.0	1.10	92.1
PDEGEA MB-3	527-36	1:1.02	766.2	1.10	77.9
PDEGEA MB-4	527-36	1:0.74	709.1	1.10	62.5
PDEGEA MB-5	527-36	1:0.48	558.4	1.10	38.2
PDEGEA MB-6	527-59	1:1.96	1111.7	1.11	91.4
PDEGEA MB-7	527-82	1:2.01	1396.9	1.12	90.1
PDEGEA MB-8	800-36	1:1.83	1224.3	1.11	78.6

[a] The values of number average molecular weight ($M_{n,SEC}$) and polydispersity index (PDI) were measured by size exclusion chromatography (SEC) of the final reaction mixture against linear polystyrene standards using PL GPC-50 Plus system with Agilent Mixed-B columns and DMF containing 50 mM LiBr as carrier solvent. [b] Grafting density was calculated from the molar ratio of backbone monomer units to side chain polymer in the feed and the ratio of peak areas in SEC from molecular brushes and unreacted side chain polymer.

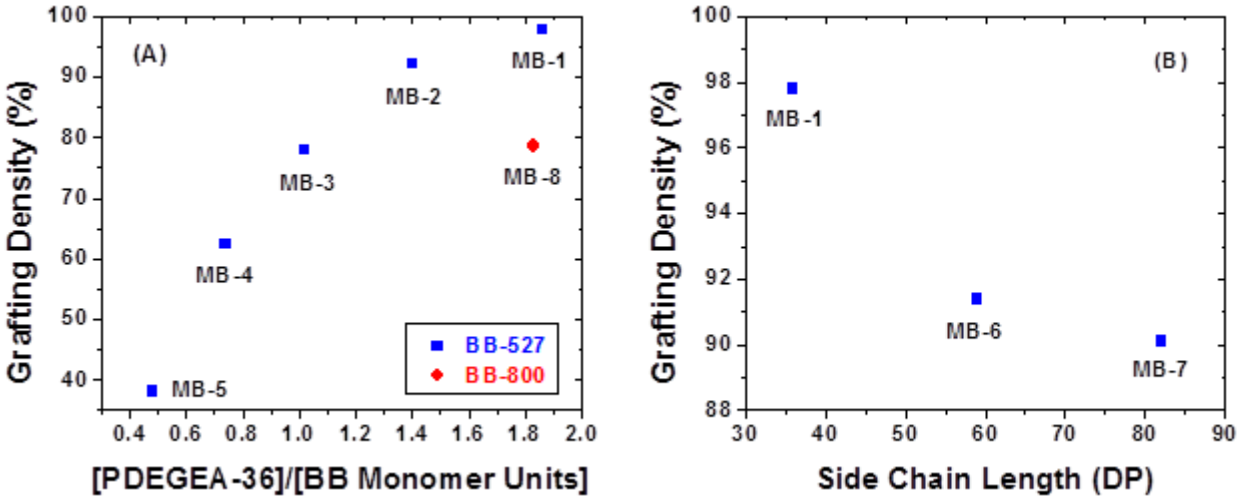

Figure 3.3. (A) Plot of grafting density versus the molar ratio of PDEGEA-36 to backbone monomer units for PDEGEA molecular brushes prepared from PDEGEA-36 side chains and $PTEGN_3MA$-527 or $PTEGN_3MA$-800 backbone. (B) Plot of grafting density versus PDEGEA side chain length for PDEGEA molecular brushes prepared from $PTEGN_3MA$-527 backbone and PDEGEA-36, PDEGEA-59, or PDEGEA-82 side chains.

THF and hexanes. SEC analysis of the final purified PDEGEA MB-1 showed that the excess side chain polymer PDEGEA-36 was completely removed and the molecular weight distribution was not changed ($M_{n,\ SEC}$ = 880,300; PDI = 1.09) (Figure 3.2A). The ^{1}H NMR spectrum of the purified PDEGEA MB-1 brushes is shown in Figure 3.2B, which is similar to that of PDEGEA-36 (Figure 3.1B).

To study how the feed molar ratio of backbone monomer units to PDEGEA-36 side chain polymer affected the grafting density, we carried out a series of click reactions to synthesize PDEGEA molecular brushes by using different molar ratios of backbone monomer units of PTEGN$_3$MA to PDEGEA-36, ranging from 1 : 1.86 to 1 : 1.40, 1 : 1.02, 1 : 0.74, and 1 : 0.48. The reactions were allowed to proceed for between 48 and 96 h, until there was no further change in grafting density. SEC was employed to determine the grafting density for each molecular brush sample (Figure B5-B8). The results are summarized in Table 3.2. Clearly, the grafting density of PDEGEA molecular brushes can be tuned by varying the backbone monomer units-to-PDEGEA-36 ratio in the feed. As discussed earlier, for PDEGEA MB-1, the grafting density was nearly quantitative (97.8 %) when a molar ratio of backbone monomer units to side chain polymer of 1:1.86 was used. Decreasing the molar ratio of backbone monomer units to PDEGEA-36 to 1:1.40 resulted in a slight reduction of grafting efficiency to 92.1% (PDEGEA MB-2). With further decreasing the ratio to 1 : 1.02, 1 : 0.74, and 1 : 0.48, the grafting density steadily decreased to 77.9% (PDEGEA MB-3), 62.5% (MB-4), and 38.2 % (MB-5), respectively, while the molecular weight distribution remained narrow (Table 3.2). These experiments demonstrated the highly efficient synthesis of thermosensitive PDEGEA homografted molecular brushes with tunable grafting densities. We also investigated the effect of side chain length on the grafting density of PDEGEA molecular brushes with PTEGN$_3$MA-527 as backbone polymer. Using a ~ 1 : 2 molar

ratio of backbone monomer units to alkyne end-functionalized side chain polymer PDEGEA in the feed as for PDEGEA MB-1, two additional PDEGEA molecular brush samples were prepared using PDEGEA side chain polymers with DPs of 59 (PDEGEA-59) and 82 (PDEGEA-82). The SEC traces are in Appendix B (Figure B9 and B10). The grafting density decreased only slightly due to the increased steric hindrance in the click reactions, with 91.4% for PDEGEA MB-6 made from PDEGEA-59 and 90.1% for PDEGEA MB-7 from PDEGEA-82. This indicated that for PDEGEA molecular brushes, the side chain length had a relatively small effect, at least in the studied DP range, on the resulting grafting density, while the molar ratio of backbone monomer units to side chain polymer in the feed had a much larger effect on grafting density.

PDEGEA molecular brushes were also prepared from the longer backbone polymer ($PTEGN_3MA$-800) using PDEGEA-36 as side chain polymer with a molar ratio of backbone repeat units to PDEGEA-36 of 1 : 1.83 under similar conditions (PDEGEA MB-8). A slightly lower grafting density of 78.6 % was achieved (Figure B11), probably due to the lower degree of azide functionalization for $PTEGN_3MA$-800 (90%) as well as the increased steric hindrance in the longer backbone polymer. The excess side chain polymer for PDEGEA MB-8 was removed by fractionation via a similar method as for PDEGEA MB-1, yielding well-defined PDEGEA molecular brushes with a backbone DP of 800 and a side chain PDEGEA DP of 36 ($M_{n,SEC}$ = 1 295 600; PDI = 1.11).

The formation of PDEGEA brush molecules was directly confirmed by atomic force microscopy (AFM). Figure 3.4 shows AFM images of PDEGEA MB-8 brushes that were spin cast onto freshly cleaned Si wafer from a 0.1 mg/g aqueous solution at 0 °C. We observed a worm-like morphology that would be expected for densely grafted molecular brushes in a good solvent.

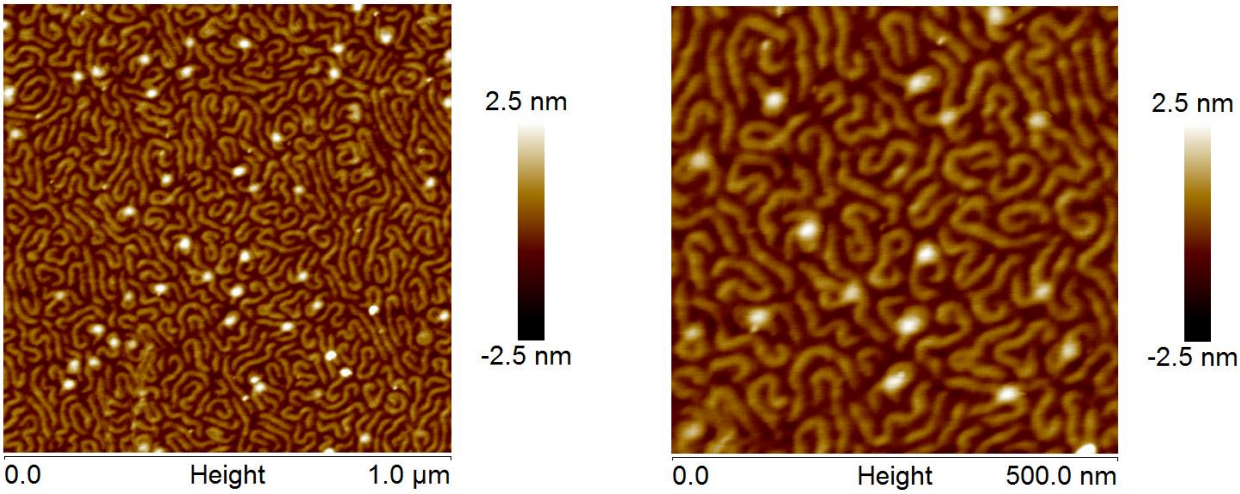

Figure 3.4. AFM height images of PDEGEA MB-8 spin cast onto a silicon wafer from a 0.1 mg/g aqueous solution at 0 °C.

3.3.4. Thermosensitive Properties of PDEGEA Homografted Molecular Brushes

The thermoresponsive properties of PDEGEA molecular brushes in water were studied by visual inspection and dynamic light scattering. We found that more concentrated aqueous solutions of PDEGEA molecular bottlebrushes (> 1 mg/g) underwent a clear to cloudy transition upon increasing temperature through the reported LCST of 9 °C for PDEGEA linear homopolymer. The transition was reversible; the samples turned clear upon cooling in an ice/water bath. Interestingly, for lower concentrations (< 0.5 mg/g), the solutions remained clear even at temperatures higher than the LCST of PDEGEA, suggesting a unimolecular collapse of thermosensitive PDEGEA brush molecules and the absence of intermolecular aggregation. To further investigate the thermoresponsive properties of PDEGEA molecular brushes, we performed dynamic light scattering measurements at different temperatures on 0.2 mg/g aqueous solutions of PDEGEA MB-1 and PDEGEA MB-8, with backbone DPs of 527 and 800, respectively, and a side chain DP of 36 for both. At 1 °C, MB-1 had an apparent hydrodynamic diameter (D_h) of 46 nm, and the size showed a relatively sharp decrease at approximately 6 °C, and leveled off to 32 nm as the temperature was increased to 13 °C (Figure 3.5A). The transition zone was about 5 °C. There was essentially no further change in size even when the temperature was raised to 25 °C, indicating that the collapsed state was stable at this concentration. PDEGEA MB-8 exhibited a similar behavior, with a larger size of 66 nm at 1 °C and decreasing to 36 nm upon heating to 15 °C (Figure 3.5B); little change in size was observed in the temperature range of 15 to 25 °C. The LCST transition of MB-8 occurred around 9 °C, which was slightly higher than the transition temperature observed for PDEGEA MB-1. This could be due to the lower grafting density for PDEGEA MB-8; the grafting densities of PDEGEA MB-1 and -8 were 97.8% and 78.6%, respectively. A higher grafting density means a higher segment density, which would result in the LCST transition

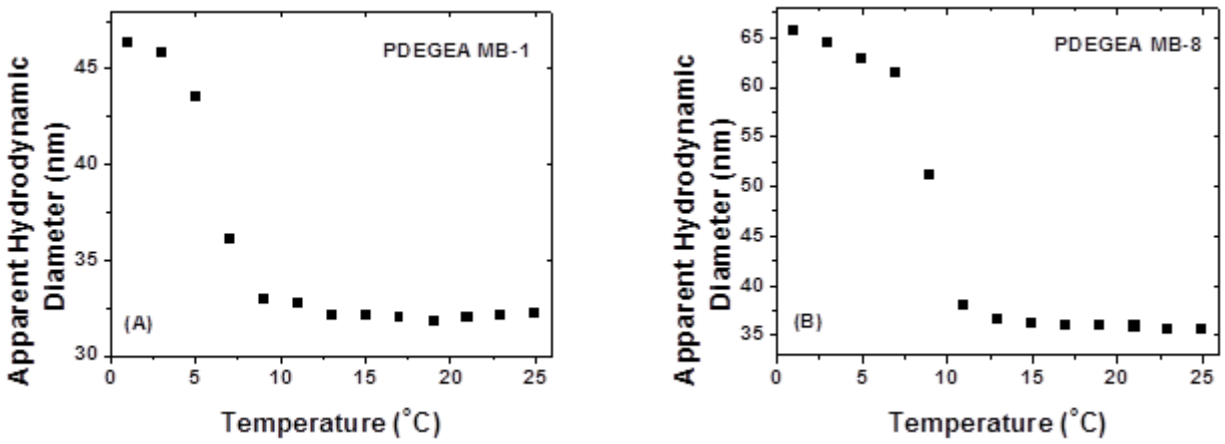

Figure 3.5. Apparent hydrodynamic diameter (D_h) of PDEGEA MB-1 (A) and PDEGEA MB-8 (B) in a 0.2 mg/g aqueous solution at different temperatures obtained from dynamic light scattering experiments.

occurring at a lower temperature. This is consistent with our group's previous observation of thermosensitive polymer brushes grafted on ~ 150 nm silica particles, where the LCST transition began at a lower temperature and continued over a broader temperature range (4 – 10 °C).

3.3.5. Synthesis of Dual Thermo- and Light-Responsive P(DEGMA-*co*-NBA) Homografted Molecular Brushes

The "click" grafting to method for the synthesis of thermosensitive PDEGEA molecular brushes can be used to synthesize other stimuli-responsive molecular bottlebrushes with high and tunable grafting densities. To demonstrate the versatility of this method, we synthesized and studied dual temperature- and light-responsive P(DEGMA-*co*-NBA) homografted molecular brushes as well as pH-responsive PDEAEMA brushes using a similar procedure for PDEGEA brushes. Our group previously reported that the LCST of a thermosensitive water-soluble polymer can be easily modified by incorporating a small amount of stimuli (e.g., light or pH)-responsive moieties via random copolymerization and applying corresponding stimuli, which allows for tuning of micellization and dissociation as well as sol-gel transition temperatures. Here we synthesized an alkyne end-functionalized, dually temperature- and light-responsive side chain polymer by ATRP of *o*-nitrobenzyl acrylate (NBA) and methoxydi(ethylene glycol) acrylate with a molar ratio of 11.4 : 100. PDEGMA is a thermosensitive water-soluble polymer with a cloud point of 38 °C and *o*-nitrobenzyl group can be cleaved by irradiation with a long wavelength, e.g., 365 nm UV light. The dually thermo- and light-responsive random copolymer P(DEGMA-*co*-NBA) had a total DP 47 (P(DEGMA-*co*-NBA)-47), and the numbers of DEGMA and NBA monomer units were 42 and 5, respectively. The molar ratio of two monomers (100 : 11.9) in the copolymer was similar to that in the feed (100 : 11.4). The $M_{n,SEC}$ and PDI from SEC analysis were 8.8 kDa and 1.17, respectively. The P(DEGMA-*co*-NBA) homografted molecular bottlebrushes

were prepared by the click reaction performed in DMF using CuCl/PMDETA as catalyst at ambient temperature. An approximately 1 : 2 molar ratio of backbone monomer units of PTEGN_3MA-527 to side chain polymer was employed, similar to that for the synthesis of PDEGEA MB-1. The reaction was followed by SEC, and was stopped after 45 h. The reaction mixture was passed through neutral alumina to remove the catalyst, and the unreacted side chains were removed by repeated fractionation using THF and hexanes, yielding purified brushes with $M_{n,SEC}$ of 909,000 and PDI of 1.13 (P(DEGMA-*co*-NBA) MB-9). Figure 3.6 shows the SEC traces of P(DEGMA-*co*-NBA) MB-9 molecular brushes with a backbone DP of 527 and a side chain DP of 47 before and after the removal of unreacted excess P(DEGMA-*co*-NBA) side chains as well as the ^{1}H NMR spectrum of the purified molecular brushes. The grafting density for P(DEGMA-*co*-NBA) MB-9 was 98.0 %, calculated from the SEC trace of the reaction mixture at 45 h using the ratio of peak areas from the brushes and the unreacted side chain polymer (50.74 : 49.26) and the molar ratio of backbone monomer units to side chains in the feed (1 : 1.96).

Another (PDEGMA-*co*-NBA) molecular brush sample (MB-10) was prepared using backbone polymer PTEGN_3MA-800 and purified via the same procedure. The SEC traces of P(DEGMA-*co*-NBA) MB-10 before and after purification can be found Appendix B (Figure B12). From the SEC of the final reaction mixture at 44 h, the grafting density for P(DEGMA-*co*-NBA) MB-10 was determined to be 80.2 %, which is lower than the grafting density of 98.0% for P(DEGMA-*co*-NBA) MB-9 with a shorter backbone DP of 527. This is likely due to the lower degree of azide functionalization for PTEGN_3MA-800 (90 %) as well as the increased steric hindrance with the longer backbone polymer. Nevertheless, the grafting densities of MB-9 and -10 were similar to those of PDEGEA molecular brushes MB-1 (97.8 %) and MB-8 (78.6 %) with backbone DPs of 527 and 800 (Table 3.2), respectively, obtained using similar molar ratios of

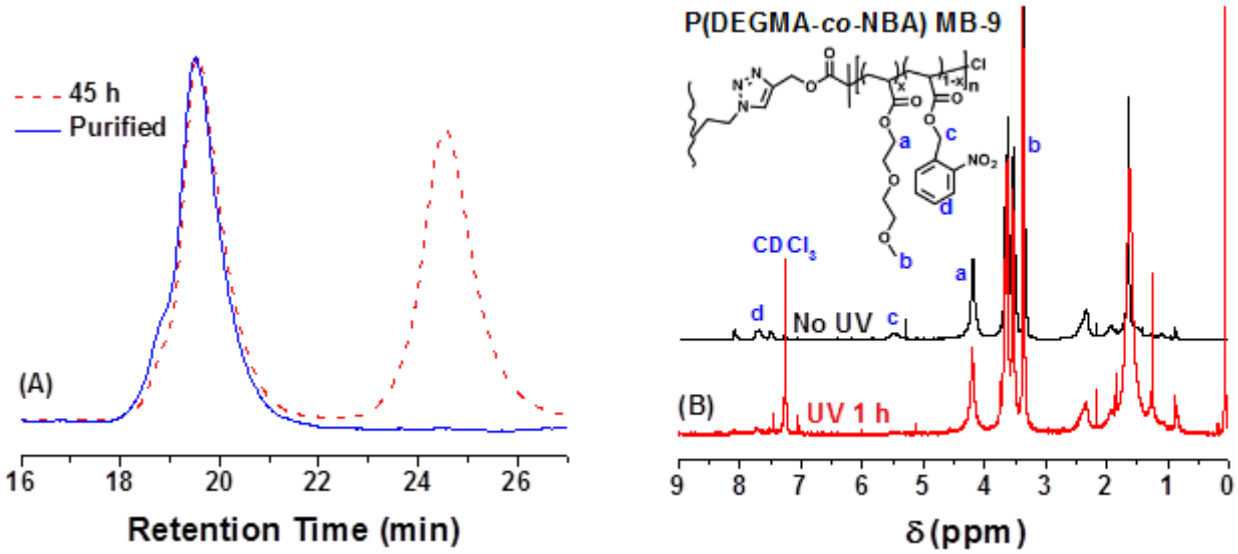

Figure 3.6. (A) SEC traces of P(DEGMA-*co*-NBA) MB-9 before and after the removal of excess P(DEGMA-*co*-NBA)-47 side chains by fractionation. (B) ^{1}H NMR spectrum of purified P(DEGMA-*co*-NBA) MB-9 in $CDCl_3$. SEC analysis was performed using PL GPC-50 Plus system with Agilent Mixed-B columns and DMF with 50 mM LiBr as carrier solvent.

backbone monomer units to side chain polymer (~1 : 2). Considering the similar molecular structures of DEGEA and DEGMA, these results demonstrated the robustness of the method. The characterization data for these two samples are summarized in Table 3.3.

3.3.6. Thermo- and Light-Responsive Properties of P(DEGMA-*co*-NBA) Homografted Molecular Brushes

The thermo- and light-responsive properties of P(DEGMA-*co*-NBA) homografted molecular brushes in aqueous solution were investigated. Similar to PDEGEA brushes, we found that aqueous solutions of P(DEGMA-*co*-NBA) molecular brushes with a concentration of > 1 mg/g underwent a clear to cloudy transition upon increasing the temperature from 0 °C to room temperature (~ 22 °C). At concentrations of 0.2 mg/g and below, however, aqueous solutions of P(DEGMA-*co*-NBA) brushes, both MB-9 and -10, remained clear at room temperature, indicating a unimolecular collapse. Note that the LCST for PDEGMA homopolymer was reported to be 38 °C, and the incorporation of ~ 10 mol % of hydrophobic NBA units decreased the LCST of the polymer significantly as reported in the literature.[51] DLS was employed to investigate the thermoresponsive properties of MB-9 and MB-10 at the concentration of 0.2 mg/g before and after UV irradiation (Figure 3.7). Like PDEGEA brushes shown in Figure 3.5, both MB-9 and MB-10 exhibited a clear decrease in apparent hydrodynamic size upon increasing temperature, although over a slightly greater temperature range. MB-9, with a backbone DP of 527 and a side chain DP of 47, had an apparent hydrodynamic diameter of 58 nm at 1 °C, which is noticeably larger than the hydrodynamic diameter of 46 nm observed for PDEGEA MB-1 with a backbone DP of 527 and a side chain DP of 36, consistent with its larger side chain DP (47 versus 36 for PDEGEA MB-1). Upon heating, MB-9 showed a relatively sharp decrease in size at approximately 20 °C and leveled off at a diameter of 38 nm as the temperature was raised to above 35 °C. There was

Table 3.3. Characterization Data for P(DEGMA-*co*-NBA) and PDEAEMA Molecular Brushes.

Molecular Brush Sample	$DP_{Backbone}$ - $DP_{Sidechain}$	Molar Ratio of Backbone Monomer Units to Side Chains	$M_{n,\ SEC}$ (kDa) [a]	PDI [a]	Grafting Density (%)
P(DEGMA-*co*-NBA) MB-9	527-47	1 : 1.96	870.3	1.10	98.0 [b]
P(DEGMA-*co*-NBA) MB-10	800-47	1 : 1.90	1204.1	1.12	80.2 [b]
PDEAEMA MB-11	527-43	1 : 1.91	--[c]	--[c]	83.7 [d]
PDEAEMA MB-12	800-43	1 : 1.88	--[c]	--[c]	70.5 [d]

[a] The values of $M_{n,SEC}$ and polydispersity index (PDI) were measured by size exclusion chromatography (SEC) of the final reaction mixture using PL GPC-50 Plus system with Agilent Mixed-B columns in DMF containing 50 mM LiBr and using linear polystyrene standards for calibration. [b] Grafting density was calculated from the ratio of peak areas in SEC from molecular brushes and unreacted side chain polymer in the final reaction mixture and the molar ratio of backbone monomer units to side chains in the feed. [c] SEC analysis could not be performed due to the poor solubility in DMF with 50 mM LiBr. [d] Grafting density was calculated from the molar ratio of backbone monomer units to side chains and the conversion of alkyne end groups of the side chain polymer as determined by ^{1}H NMR spectroscopy analysis.

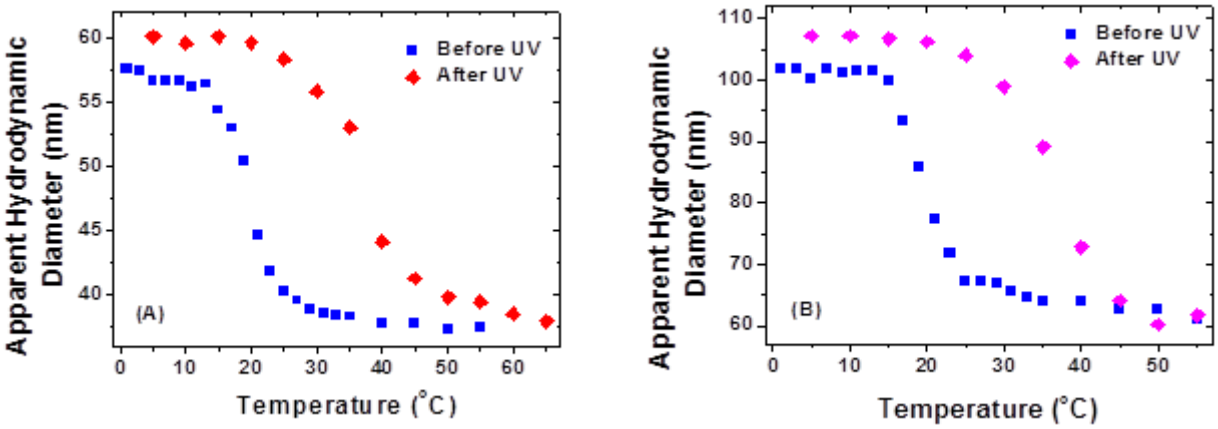

Figure 3.7. Apparent hydrodynamic diameter of (A) P(DEGMA-*co*-NBA) MB-9 and (B) MB-10, obtained from DLS studies of 0.2 mg/g aqueous solutions, as a function of temperatures before and after irradiation with 365 nm UV light at ambient temperature for 1 h.

little change in size from 35 °C up to 55 °C, indicating that the collapsed state was stable at the concentration of 0.2 mg/g. P(DEGMA-*co*-NBA) MB-10, with a backbone DP of 800 and a side chain DP of 47, exhibited a similar behavior. The apparent hydrodynamic size was 102 nm at 1 °C, which was larger than that of MB-9 at the same temperature as expected. The apparent size decreased to 64 nm upon increasing the temperature to 35 °C, and little change in size was observed beyond that. The transition occurred at ~ 20 °C, similar to P(DEGMA-*co*-NBA) MB-9.

The hydrophobic *o*-nitrobenzyl group can be cleaved with long wavelength UV light, yielding hydrophilic carboxylic acid group and thus increasing the LCST transition temperature.[51] The 0.2 mg/g aqueous solutions of MB-9 and -10 were then irradiated with 365 nm UV for 1 h at ambient temperature (~ 22 °C) to cleave off the *o*-nitrobenzyl group, producing molecular brushes containing (PDEGMA-*co*-acrylic acid) side chains, which were referred to as P(DEGMA-*co*-AA) MB-9′ and MB-10′, respectively. After UV irradiation, the apparent size for MB-9′ at 5 °C was 60 nm, which was slightly larger than that before UV irradiation (57 nm) and was attributed to the more hydrophilic side chains and the electrostatic repulsion between the ionized carboxylic acid groups in the side chains after the cleavage of *o*-nitrobenzyl group.

With increasing temperature, we again saw a significant decrease in size but at higher temperatures with a middle point at ~37 °C, indicating that the conversion of the hydrophobic *o*-nitrobenzyl to hydrophilic carboxylic acid group shifted the LCST transition to a higher temperature, consistent with what we expected (Figure 3.7A). Interestingly, at 65 °C, the D_h decreased to 38 nm, approaching the size of the fully collapsed P(DEGMA-*co*-NBA) MB-9 before UV irradiation. P(DEGMA-*co*-NBA) MB-10 exhibited similar behavior after irradiation for 1 h, with the size at 5 °C increasing slightly to 107 nm and a fast decrease in size occurring at approximately 36 °C. At 55 °C, the size decreased to 62 nm, which is essentially the same as the

fully collapsed size before UV irradiation. To determine the extent to which the photocleavage of *o*-nitrobenzyl had occurred after 1 h, we irradiated 10 g of a 0.2 mg/g aqueous solution of P(DEGMA-*co*-NBA) MB-9 for 1 h under conditions that were identical to those used for the DLS samples (The 10 g of solution was divided into four vials (3.7 mL capacity) which were the same type of vial used for the irradiation of DLS samples). The water was the then removed under high vacuum, and the dried brushes were dissolved in $CDCl_3$ for ^{1}H NMR spectroscopy analysis. As can be seen from the ^{1}H NMR spectra of P(DEGMA-*co*-NBA) MB-9 before and after UV irradiation included in Figure 3.6b, the peak at 5.35-5.60 ppm (-COOCH_2($C_6H_4NO_2$) of NBA monomer units) almost disappeared. Using the peak at 4.05-4.25 ppm (-COOCH_2CH$_2$- of DEGMA monomer units) as an internal standard, we found that the integral value for the peak at 5.35-5.60 ppm decreased by > 92 %, indicating that the percentage of photocleavage was > 92 % after UV irradiation for 1 h.

3.3.7. Synthesis of pH-Responsive PDEAEMA Homografted Molecular Brushes

PDEAEMA is a pH-responsive polymer with a pK_a value of 7.4 in water.[54] Two PDEAEMA homografted molecular brush samples, PDEAEMA MB-11 and MB-12, were prepared using PTEGN$_3$MA-527 and -800 backbone polymers, respectively, and side chain polymer PDEAEMA-43 by a similar but slightly altered procedure as for PDEGEA and P(DEGMA-*co*-NBA) molecular brushes. Due to the poor solubility of the resultant PDEAEMA brushes in DMF, THF was used as the reaction medium. Additionally, SEC analysis could not be performed for PDEAEMA brushes due to their poor solubility in the carrier solvent (DMF with 50 mM LiBr); the grafting density was calculated from the conversion of alkyne end groups of the side chain polymer as determined by ^{1}H NMR spectroscopy analysis. The alkyne end group conversion was calculated from the decrease in the integral value of the peak at 4.66 ppm (HC≡CCH_2OOC-) using the peaks at 3.90-

4.11 ppm (-COOCH_2-) from the repeat units of PDEAEMA as an internal standard. The grafting density was then calculated from the molar ratio of monomer units of the backbone to the side chain polymer in the feed and the alkyne end group conversion. As an example, Figure 3.8A shows a portion of the ^{1}H NMR spectra of side chain polymer PDEAMA-43 and the reaction mixture for the synthesis of PDEAEMA molecular brushes with a backbone DP of 527 and a side chain DP of 43 (PDEAEMA MB-11) taken after reaction for 23 h at which the reaction was stopped. With the integral value of the peaks at 3.90-4.11 ppm set to 200.00 as an internal standard, the integral value of the alkyne end group peak at 4.66 ppm decreased from 4.64 to 2.61. This indicates that 43.8 % of the alkyne end groups of the side chains had reacted with the backbone. Since the molar ratio of backbone monomer units to side chain polymer in the feed was calculated to be 1:1.91, this gave a grafting density of 83.7 % for PDEAEMA MB-11. The PDEAEMA brushes were purified by passing the reaction mixture through neutral alumina to remove the catalyst and repeated precipitation from THF into cold hexane to remove the unreacted side chains. Figure 3.8B shows the ^{1}H NMR spectrum of the purified PDEAEMA MB-11 molecular brushes. The complete removal of unreacted side chains was verified by the disappearance of the peak at 4.66 ppm from the alkyne end group of PDEAEMA-43. The grafting density for PDEAEMA molecular brushes with a backbone DP of 800 and a side chain DP of 43 (PDEAEMA MB-12) was calculated to be 70.5 % using the same method. In comparison to PDEGEA and P(DEGMA-*co*-NBA) molecular brushes with side chain DPs of 36 and 47, respectively, we observed substantially lower grafting densities for PDEAEMA brushes even though both the side chain DP and the molar ratios of backbone monomer units to side chain polymer in the feed were similar (Tables 3.2 and 3.3). Since the monomer unit molecular weights are similar for PDEGEA (188.22 Da), PDEGMA (174.19 Da), and PDEAEMA (185.26

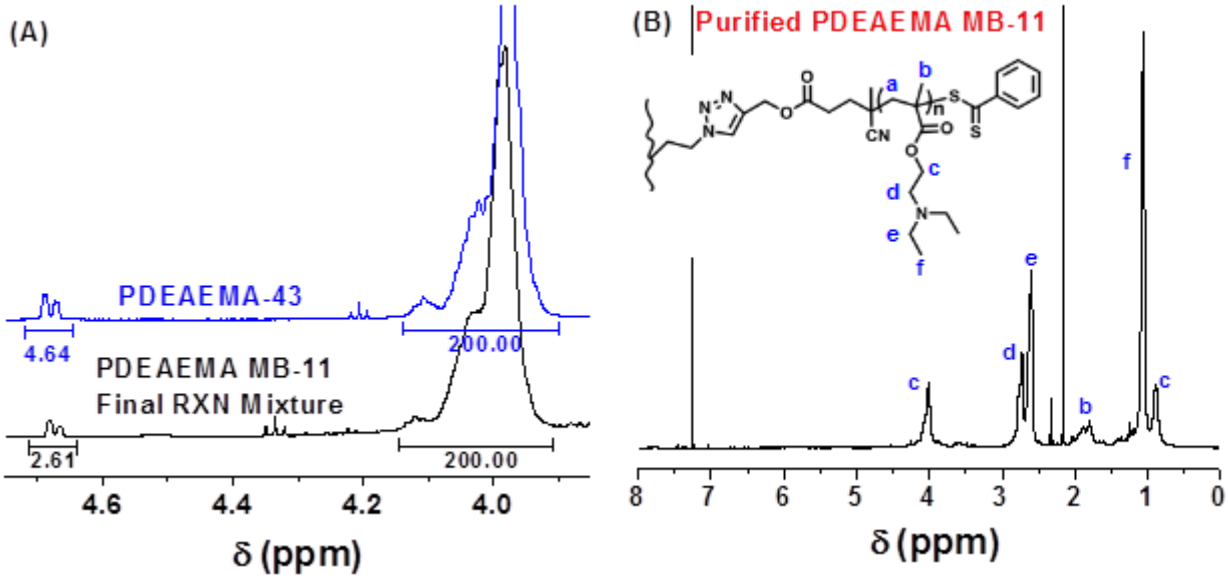

Figure 3.8. (A) ^{1}H NMR spectra of PDEAEMA-43 and the final reaction mixture for the synthesis of PDEAEMA MB-11 in $CDCl_3$. (B) ^{1}H NMR spectrum of PDEAEMA MB-11 in $CDCl_3$ after purification by fractionation.

Da), the steric hindrance of the pendant groups of the side chain polymers are unlikely responsible for this discrepancy in grafting density. Thus, the lower grafting densities of PDEAEMA brushes are likely caused by the increased chain rigidity of PDEAEMA, a polymethacrylate, compared with PDEGEA and P(DEGMA-co-NBA), which are polyacrylates, due to the methyl group in the backbone.

3.3.8. pH-Responsive Properties of PDEAEMA Homografted Molecular Brushes

The pH responsive properties of PDEAEMA molecular brushes in aqueous solution were investigated by visual inspection and DLS. Solutions of PDEAEMA brushes with a polymer concentration of 0.2 mg/g were prepared in 5 mM KH_2PO_4 buffer, and the pH was adjusted using either 0.1 M HCl or NaOH and measured using a pH meter. Similar to PDEAEMA linear polymer, which has a reported pK_a value of 7.4, we found that PDEAEMA brushes were readily soluble in acidic buffer solution, but aggregated and precipitated when the pH was increased to pH = ~ 8. In contrast to PDEGEA and P(DEGMA-*co*-NBA) molecular brushes, which showed no aggregation above the LCST of the side chains at a concentration of 0.2 mg/g, PDEAEMA brushes underwent aggregation at a pH value of ~ 8 even at a very low concentration of 0.002 mg/g, indicating the highly hydrophobic nature of PDEAEMA brushes at higher pH values.

Figure 3.9 shows the apparent hydrodynamic sizes of PDEAEMA MB-11 and MB-12 in 5 mM KH_2PO_4 aqueous buffer with a polymer concentration of 0.2 mg/g at different pH values, measured by DLS. For PDEAEMA MB-11, with a backbone DP of 527 and a side chain DP of 43, the D_h at pH = 4.18 was 67 nm, which is significantly larger than the DLS sizes of 46 nm and 58 nm observed for PDEGEA MB-1 and P(DEGMA-*co*-NBA) MB-9, respectively, at 1 °C, each with a backbone DP of 527 and a comparable side chain DP (36 for MB-1 and 47 for MB-9). The larger size of PDEAEMA MB-11 at pH = 4.18 was apparently the result of a higher degree of

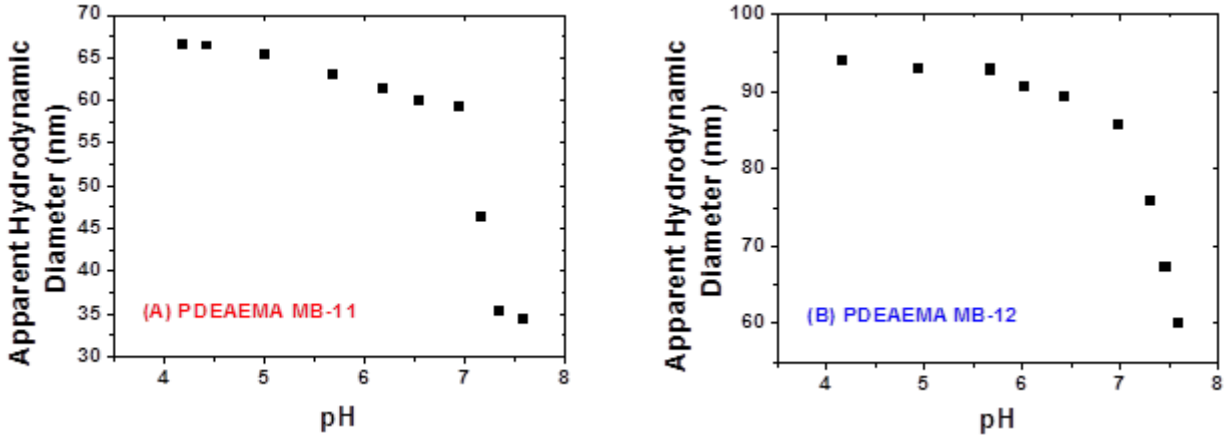

Figure 3.9. Apparent hydrodynamic size of (A) PDEAEMA MB-11 and (B) PDEAEMA MB-12 in 5 mM KH_2PO_4 aqueous buffer with a concentration of 0.2 mg/g at different pH values obtained from dynamic light scattering studies.

chain stretching due to electrostatic repulsions between positively charged monomer units in the side chains. With increasing pH, the size decreased slightly and steadily until there was a sharp decrease near the reported pK_a of 7.4 for PDEAEMA linear polymer, reaching a minimum size of 34 nm at pH = 7.58. This indicates the unimolecular collapse of PDEAEMA bottlebrushes as the degree of protonation of the side chains decreased with increasing the pH. Above pH = 7.58, the brushes underwent aggregation and precipitation, as indicated by a sharp increase in hydrodynamic size as well as visual cloudiness of the solution. For PDEAEMA MB-12, with a backbone DP of 800 and a side chain DP of 43, the hydrodynamic size at pH = 4.17 was 94 nm, which is again significantly larger than the DLS size of 66 nm at 1 °C observed for PDEGEA MB-8 with a backbone DP of 800 and side chain DP of 36, consistent with a highly stretched conformation due to the electrostatic repulsions between side chains. However, the hydrodynamic size of 94 nm for PDEAEMA MB-12 at pH = 4.17 was actually slightly smaller than the hydrodynamic size of 102 nm observed for P(DEGMA-*co*-NBA) MB-10 with a backbone DP of 800 and a side chain DP of 47. This is likely due to the lower grafting density combined with the slightly lower side chain DP of PDEAEMA MB-12. Similar to PDEAEMA MB-11, the apparent hydrodynamic diameter of PDEAEMA MB-12 decreased steadily as the pH was increased, with a sharp decrease near the pK_a of PDEAEMA linear polymer; the smallest apparent hydrodynamic size of 60 nm was observed at pH = 7.60. Above pH = 7.60, the PDEAEMA molecular brushes underwent aggregation similar to PDEAEMA MB-11.

3.4. Conclusions

The “grafting to” method developed in Chapter 2 was extend to the synthesis of stimuli-responsive homografted molecular brushes with high and tunable grafting densities using copper-

catalyzed azide-alkyne cycloaddition “click” reactions between azide-containing repeat units of backbone polymers and alkyne end-functionalized stimuli-responsive side chain polymers. Three types of molecular brushes, composed of either thermosensitive PDEGEA, or dually thermo- and light-responsive P(DEGMA-*co*-NBA), or pH-responsive PDEAEMA as side chain polymer, were prepared and studied. For PDEGEA and P(DEGMA-*co*-NBA) molecules brushes synthesized from the backbone polymer with a DP of 527, nearly quantitative grafting densities were achieved when a molar ratio of backbone monomer units to side chain polymer of ~ 1 : 2 was used, and the grafting density can be tuned by varying the feed molar ratio. For PDEAEMA brushes, lower grafting densities were obtained, likely due to the higher chain rigidity of PDEAEMA, a polymethacrylate. Pure brush molecules were obtained by fractionation to remove unreacted side chain polymers, and their stimuli responsive properties in aqueous solution were investigated. At concentrations > 1.0 mg/g, PDEGEA brushes underwent a clear-to-cloudy transition upon increasing the temperature to above the LCST of PDEGEA linear polymer. From DLS studies of 0.2 mg/g aqueous solutions, unimolecular collapse of brush molecules was observed upon heating. P(DEGMA-*co*-NBA) molecular brushes exhibited responses to both temperature and light. For 0.2 mg/g aqueous solutions, a fast decrease in size occurred at ~ 20 °C. After irradiation with 365 nm UV for 1 h, the LCST transition was shifted to a higher temperature (~ 36 °C), due to the cleavage of hydrophobic *o*-nitrobenzyl groups. The pH-responsive PDEAEMA brushes at a concentration of 0.2 mg/g in 5 mM aqueous KH_2PO_2 buffer showed a rapid reduction in size around the pK_a of 7.4 for PDEAEMA linear polymer. At pH values above ~ 8, aggregation and precipitation occurred. This work demonstrates that the “grafting to” method in combination with “click” chemistry is a robust synthetic strategy for the preparation of responsive molecular brushes with high and tunable grafting densities. This provides a good foundation for the synthesis of molecular

brushes with more complex compositions and architectures, such as brushes with heterografted side chains or star copolymer brushes.

References

1. Sheiko, S. S.; Sumerlin, B. S.; Matyjaszewski, K. *Prog. Polym. Sci.* **2008**, *33*, 759-785.
2. Lee, H.; Pietrasik, J.; Sheiko, S. S.; Matyjaszewski, K. *Prog. Polym. Sci.* **2010**, *35*, 24-44.
3. Rzayev, J. *ACS Macro Lett.* **2012**, *1*, 1146-1149.
4. Rostovtsev, V. V.; Green, L. G.; Fokin, V. V.; Sharpless, K. B. *Angew. Chem. Int. Ed.* **2002**, *41*, 2596-2599.
5. Kolb, H. C.; Sharpless, K. B. *Drug Delivery Today* **2003**, *8*, 1128-1137.
6. Binder, W. H.; Sachsenhofer, R. *Macromol. Rapid Commun.* **2007**, *28*, 15-54.
7. Binder, W. H.; Sachsenhofer, R. *Macromol. Rapid Commun.* **2008**, *29*, 952-981.
8. Xiaosong, Y. S.; Gao, H. *Nanoscale* **2016**, *8*, 4864-4881.
9. Gao, H.; Matyjaszewski, K. *J. Am. Chem. Soc.* **2007**, *129*, 6633-6639.
10. Tsarevsky, N. V.; Bencherif, S. A.; Matyjaszewski, K. *Macromolecules* **2007**, *40*, 4439-4445.
11. Yan, Y.; Shi, Y.; Zhu, W.; Chen, Y. *Polymer* **2013**, *54*, 5634-5642.
12. Zhao, P.; Yan, Y. C.; Feng, X. Q.; Liu, L. X.; Wang, C.; Chen, Y. M. *Polymer* **2012**, *53*, 1992-2000.
13. Zhao, P.; Liu, L.; Feng, X.; Wang, C.; Shuai, X.; Chen, Y. *Macromol. Rapid Commun.* **2012**, *33*, 1351-1355.
14. Shi, Y.; Wang, X.; Graff, R. W.; Phillip, W. A.; Gao, H. J. *Polym. Sci., Part A: Polym. Chem.* **2015**, *53*, 239-248.
15. Sun, J.; Hu, J.; Liu, G.; Xiao, D.; He, G.; Lu, R. *J. Polym. Sci. Part A: Polym. Chem.* **2011**, *49*, 1282-1288.

16. Tang, H.; Li, Y.; Lahasky, S. H.; Sheiko, S. S.; Zhang, D. *Macromolecules* **2011**, *44*, 1491-1499.

17. Kutnyanszky, E.; Hempenius, M. A.; Vancso, G. J. *Polym. Chem.* **2014**, *5*, 771-783.

18. Yuan, W.; Zhang, J.; Zuo, H.; Shen, T.; Ren, J. *Polymer* **2012**, *53*, 956-966.

19. Gil, E. S.; Hudson, S. M. *Prog. Polym. Sci.* **2004**, *29*, 1173-1222.

20. Seuring, J.; Agarwal, S. *Macromol. Rapid Commun.* **2012**, *33*, 1898-1920.

21. Jeong, B. M.; Bae, Y. M.; Lee, D. S.; Kim, S. W. *Nature* **1997**, *388*, 860-862

22. Lutz, J-F. *J. Polym. Sci. Part A: Polym. Chem*. 2008, 46, 3459-3470.

23. Schild, H. G. *Prog. Polym. Sci.* **1992**, 17, 163-249.

24. Li, C.; Ge, Z.; Fang, J.; Liu, S. *Macromolecules* **2009**, *42*, 2916-2924.

25. Yin, J.; Ge, Z.; Liu, H.; Liu, S. *J. Polym. Sci. Part A: Polym. Chem.* **2009**, *47*, 2608-2619.

26. Lian, X.; Wu, D.; Song, X.; Zhao, H. *Macromolecules* **2010**, *43*, 7434-7445.

27. Zehm, D.; Laschewsky, A.; Liang, H.; Rabe, J. P. *Macromolecules* **2011**, *44*, 9635-9641.

28. Song, X.; Zhang, Y.; Yang, D.; Yuan, L.; Hu, J.; Lu, G.; Huang, X. *J. Polym. Sci. Part A: Polym. Chem.* **2011**, *49*, 3328-3337.

29. Jiang, X.; Li, Y.; Lu, G.; Huang, X. *Polym. Chem.* **2013**, *4*, 1402-1411.

30. Jiang, X.; Lu, G.; Feng, C.; Li, Y.; Huang, X. *Polym. Chem.* **2013**, *4*, 3876-3884.

31. Luo, Y-L.; Yu, W.; Xu, F.; Zhang, L-L. *J. Polym. Chem. Part A: Polym. Chem.* **2012**, *50*, 2053-2067.

32. Ding, L.; Huang, Y.; Zhang, Y.; Deng, J.; Yang, W. *Macromolecules* **2011**, *44*, 736-743.

33. Ding, L.; Chen, C.; Deng, J.; Yang, W. *Polym. Bull.* **2012**, *69*, 1023-1040.

34. Yi, Y.; Zheng, S. *RSC Adv.* **2014**, *4*, 28439-38450.

35. Pietrasik, J.; Sumerlin, B. S.; Lee, B. Y.; Matyjaszewski, K. *Macromol. Chem. Phys.* **2007**, *208*, 30-36.

36. Yamamoto, S.; Pietrasik, J.; Matyjaszewski, K. *Macromolecules* **2007**, *40*, 9348-9353.

37. Yamamoto, S.; Pietrasik, J.; Matyjaszewski, K. *Macromolecules* **2008**, *41*, 7013-7020.

38. Zhang, N.; Huber, S.; Schulz, A.; Luxenhofer, R.; Jordan, R. *Macromolecules* **2009**, *42*, 2215-2221.

39. Zhang, N.; Luxenhofer, R.; Jordan, R. *Macromol. Chem. Phys.* **2012**, *213*, 973-981.

40. Zhang, N.; Luxenhofer, R.; Jordan, R. *Macromol. Chem. Phys.* **2012**, *213*, 1963-1969.

41. Lahasky, S. H.; Lu, L.; Huberty, W. A.; Cao, J.; Guo, L.; Garno, J. C.; Zhang, D. *Polym. Chem.* **2014**, *5*, 1418-1426.

42. Li, X.; ShamsiJazeyi, H.; Pesek, S. L.; Agrawal, A.; Hammouda, B.; Verduzco, R. *Soft Matter* **2014**, *10*, 2008-2015.

43. Lee, H. L.; Pietrasik, J.; Matyjaszewski, K. *Macromolecules* **2006**, *39*, 3914-3920.

44. Li, C.; Gunari, N.; Fischer, K.; Janshoff, A.; Schmidt, M. *Angew. Chem. Int. Ed.* **2004**, *43*, 1101-1104.

45. Balamurugan, S. S.; Grigor, B. B.; Yang, Y.; McCarley, R. L. *Angew. Chem. Int. Ed.* **2005**, *44*, 4872-4876.

46. Lee, H.; Boyce, J. R.; Nese, A.; Sheiko, S. S.; Matyjaszewski, K. *Polymer* **2008**, *49*, 5490-5496.

47. Xu, Y.; Bolisetty, S.; Drechsler, M.; Fang, B.; Yuan, J.; Ballauff, M.; Muller, A. X. E. *Polymer* **2008**, *49*, 3957–64.

48. Xu, Y.; Bolisetty, S.; Drechsler, M.; Fang, B.; Yuan, J.; Harnau, L.; Ballauff, M.; Muller, A. X. E. *Soft Matter* **2009**, *5*, 379–84.

49. Xu, Y.; Bolisetty, S.; Ballauff, M.; Mueller, A. H. E. *J. Am. Chem. Soc.* **2009**, *131*, 1640–1641.

50. Yao, J.; Chen, Y.; Zhang, J.; Bunyard, C.; Tang, C. *Macromol. Rapid Commun.* **2013**, *34*, 645-651.

51. Jiang, X. G.; Lavender, C. A.; Woodcock, J. W.; Zhao, B. *Macromolecules* **2008**, *41*, 2632-2643.

52. Rodriguez-Emmenegger, C.; Schmidt, B. V. K. J.; Sedlakova, Z.; Subr, V.; Alles, A. B.; Brynda, E.; Barner-Kowollik, C. *Macromol. Rapid Commun.* **2011**, *32*, 958-965.

53. Jin, N. X.; Woodcock, J. W.; Xue, C. M.; O'Lenick, T. G.; Jiang, X. G.; Jin, S.; Dadmun, M. D.; Zhao, B. *Macromolecules* **2011**, *44*, 3556-3566.

54. Zhou, K. J.; Wang, Y. G.; Huang, X. N.; Luby-Phelps, K..; Sumer, B. D.; Gao, J. M. *Angew. Chem., Int. Ed.* **2011**, ***50,*** 6109–6114**.**

Appendix B

for

Chapter 3: Synthesis and Characterization of Stimuli-Responsive Homografted Linear Molecular Brushes with High and Tunable Grafting Densities

Appendix B.1. Example Calculation of Grafting Density of Stimuli-Responsive Homografted Molecular Brushes

The following is an example calculation of grafting density for PDEGEA MB-1 after 48 h reaction time using the molar ratio of backbone monomer units to the side chain polymer in the feed and the ratio of peak areas for the brushes and the unreacted side chains from SEC. The feed contained 5.0 mg of PTEGN_3MA-527 backbone, with a monomer unit molar mass of 243.27 g/mol, assuming 100 % azide functionalization. The feed contained 263.3 mg of PDEGEA-36 side chain polymer with an absolute molecular weight of 6,900 g/mol (found by 36*188.22 + 160.60). For 100 % grafting density, 5.0 mg PTEGN_3MA-527 can react with 141.8 mg PDEGEA-36 side chains to give 146.8 mg brushes. So the reaction mixture would contain (146.8 mg)/(268.3 mg) = 54.71 % brushes by mass. From SEC after 48 h reaction time, we found that the reaction mixture contained 53.53 % brushes by mass using peak areas. This gives a grafting density of (53.53 %)/(54.71 %) = 97.8 %. (We have confirmed that the peak areas in SEC are proportional to the masses of polymers, see Appendix A Figure A3).

Appendix B.2. Supplemental Figures

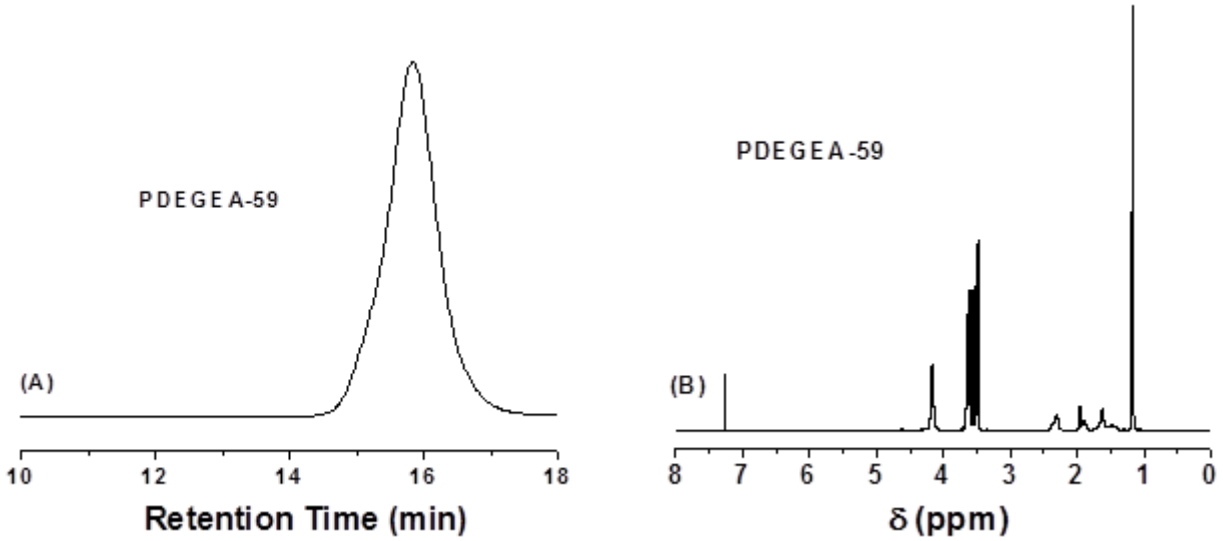

Figure B1. (A) SEC trace of PDEGEA side chain polymer with a DP of 59 (PDEGEA-59). (B) ^{1}H NMR spectrum of PDEGEA-59 in $CDCl_3$. SEC analysis was carried out on PL GPC-20 system using THF as carrier solvent.

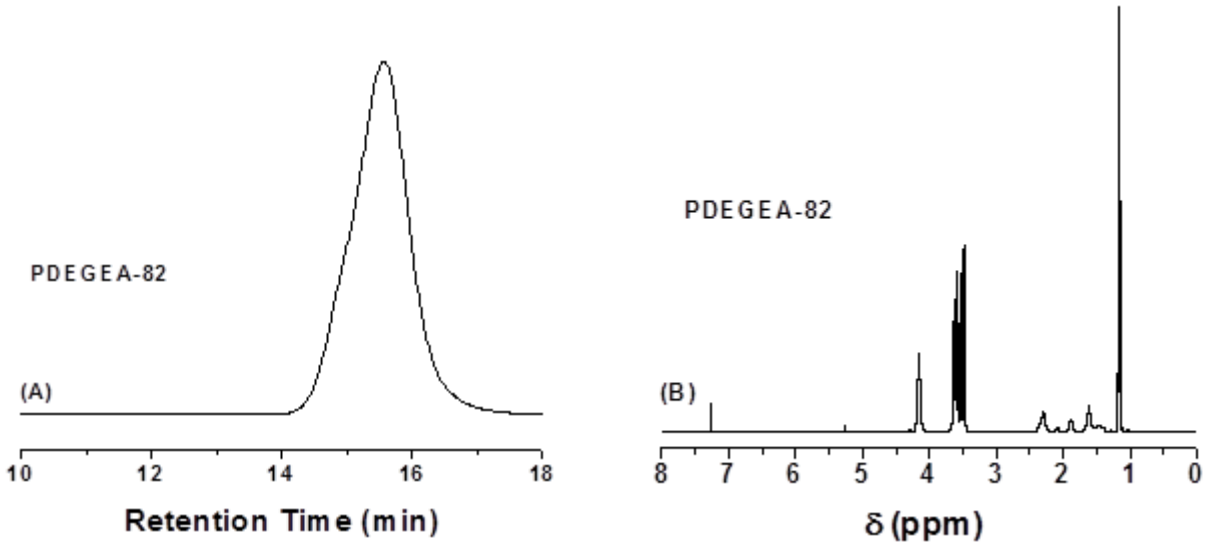

Figure B2. (A) SEC trace of PDEGEA-82 side chain polymer with a DP of 82. (B) ^{1}H NMR spectrum of PDEGEA-82 in $CDCl_3$. SEC analysis was carried out on PL GPC-20 system using THF as carrier solvent.

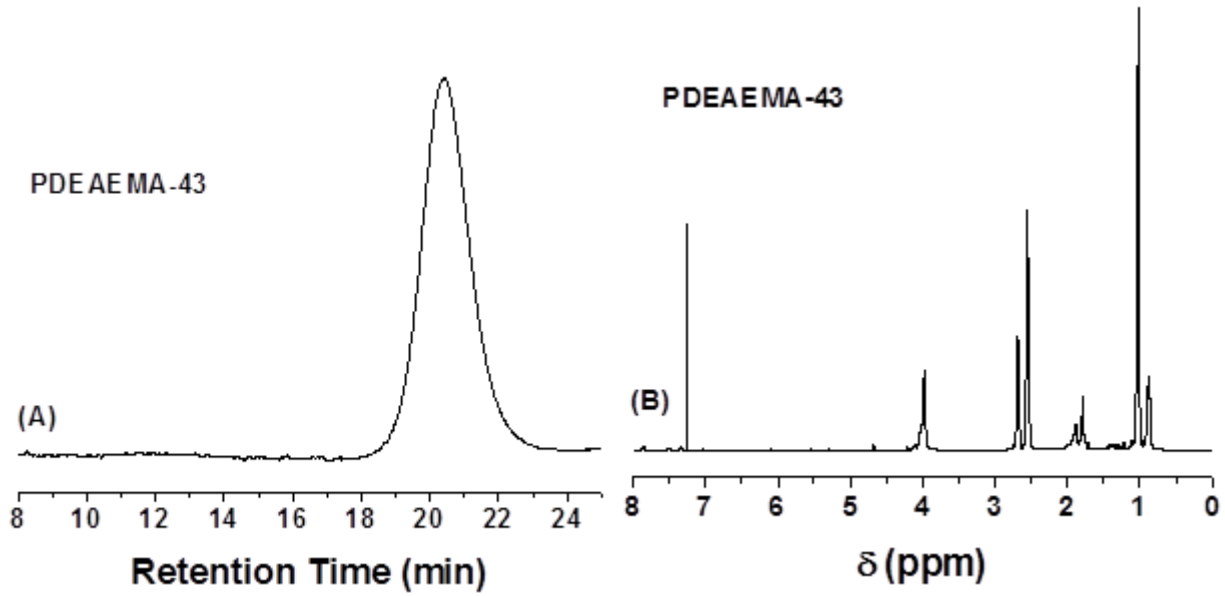

Figure B3. (A) SEC trace of PDEAEMA-43 side chain polymer and (B) ^{1}H NMR spectrum of PDEAEMA-43 in $CDCl_3$. SEC analysis was carried out on PL GPC-50 Plus system with PSS GRAL columns using DMF containing 50 mM LiBr as carrier solvent.

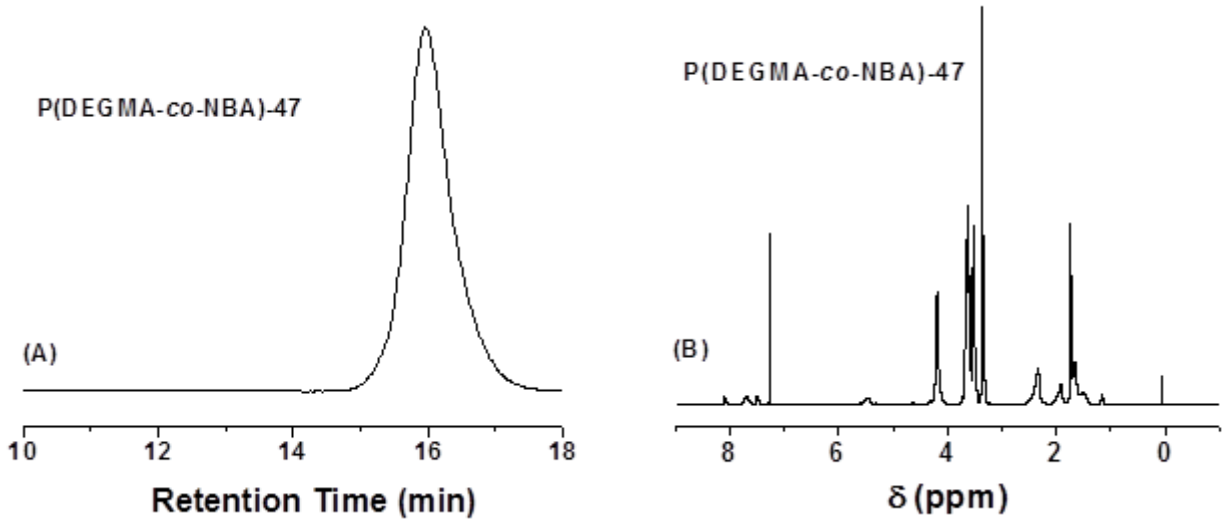

Figure B4. (A) SEC trace of P(DEGMA-*co*-NBA)-47 side chain polymer and (B) ^{1}H NMR spectrum of P(DEGMA-*co*-NBA)-47 in $CDCl_3$. SEC analysis was carried out on PL GPC-20 system using THF as carrier solvent.

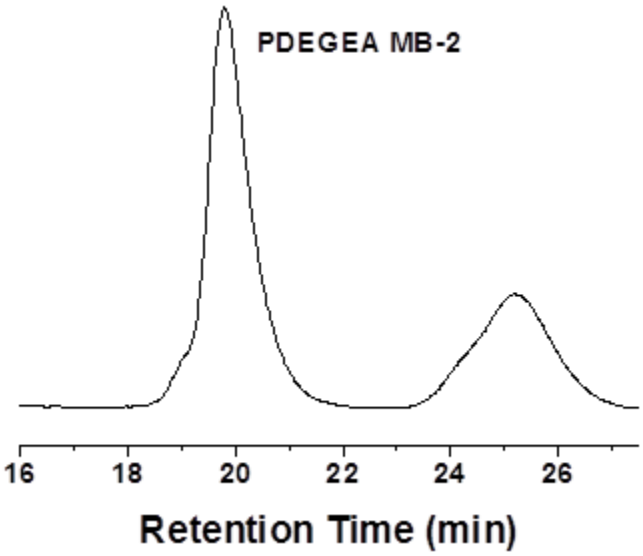

Figure B5. SEC trace of PDEGEA MB-2 after 96 h reaction time. SEC analysis was carried out on PL GPC-50 Plus system with Agilent Mixed-B columns using DMF containing 50 mM LiBr as carrier solvent.

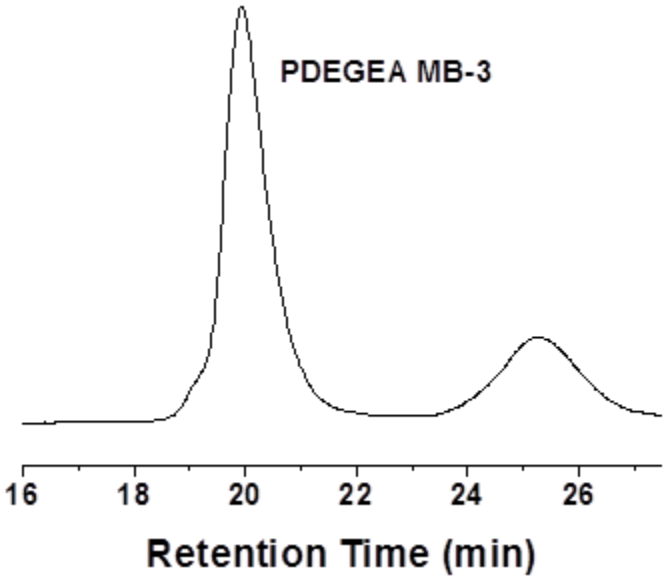

Figure B6. SEC trace of PDEGEA MB-3 after 48 h reaction time. SEC analysis was carried out on PL GPC-50 Plus system with Agilent Mixed-B columns using DMF containing 50 mM LiBr as carrier solvent.

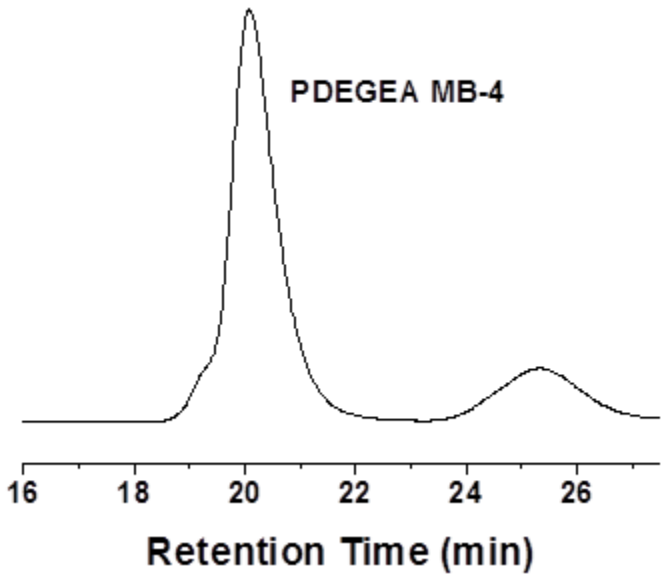

Figure B7. SEC trace of PDEGEA MB-4 after 72 h reaction time. SEC analysis was carried out on PL GPC-50 Plus system with Agilent Mixed-B columns using DMF containing 50 mM LiBr as carrier solvent.

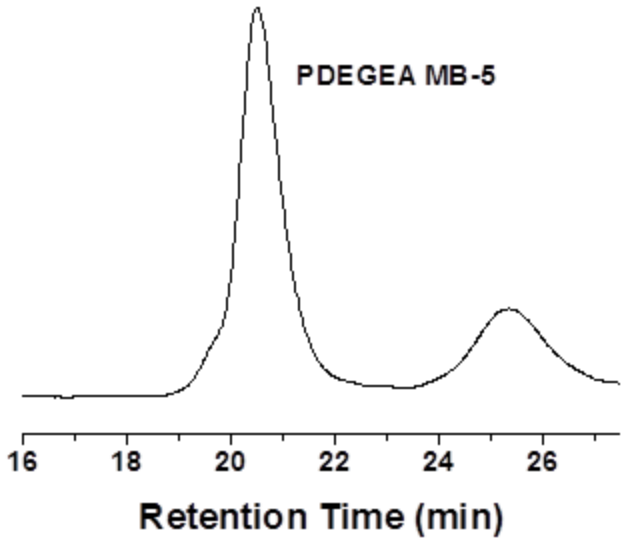

Figure B8. SEC trace of PDEGEA MB-5 after 78 h reaction time. SEC analysis was carried out on PL GPC-50 Plus system with Agilent Mixed-B columns using DMF containing 50 mM LiBr as carrier solvent.

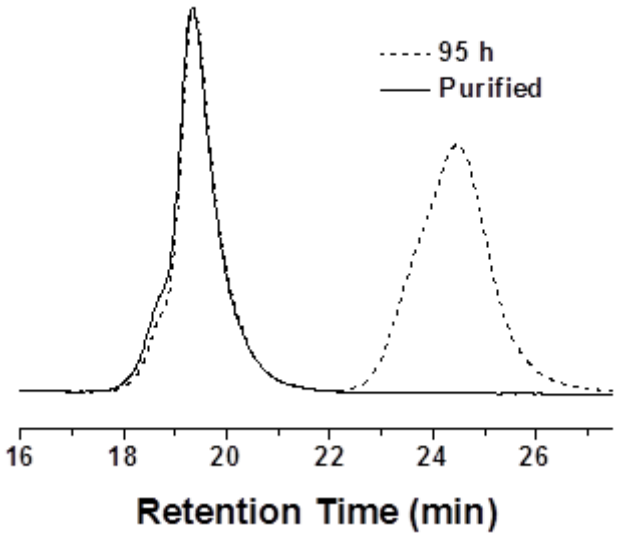

Figure B9. SEC traces of PDEGEA MB-6 before and after removal of the excess side chain polymer PDEGEA-59 by fractionation. After purification: $M_{n,\,SEC}$ = 1,147,500; PDI = 1.11. SEC analysis was carried out on PL GPC-50 Plus system with Agilent Mixed-B columns using DMF containing 50 mM LiBr as carrier solvent.

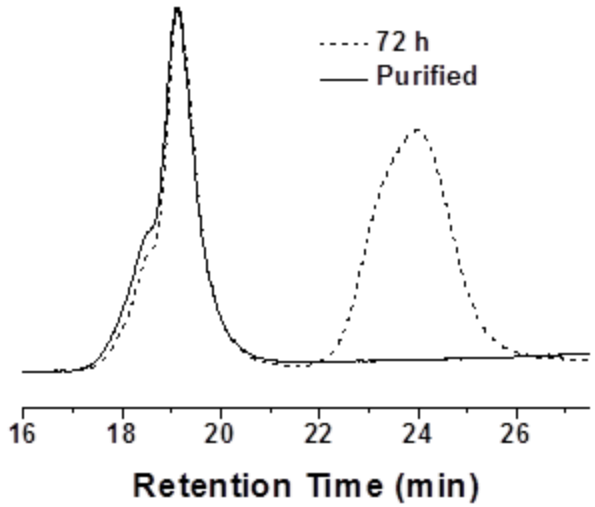

Figure B10. SEC traces of PDEGEA MB-7 before and after the removal of excess PDEGEA-82 side chains by fractionation. After purification: $M_{n,\,SEC}$ = 1,450,400; PDI = 1.13. SEC analysis was carried out on PL GPC-50 Plus system with Agilent Mixed-B columns using DMF containing 50 mM LiBr as carrier solvent.

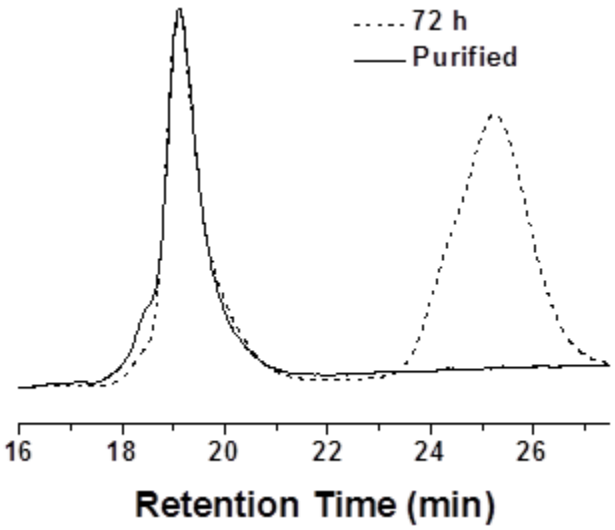

Figure B11. SEC traces of PDEGEA MB-8 before and after the removal of excess PDEGEA-36 side chains by fractionation. SEC analysis was carried out on PL GPC-50 Plus system with Agilent Mixed-B columns using DMF containing 50 mM LiBr as carrier solvent.

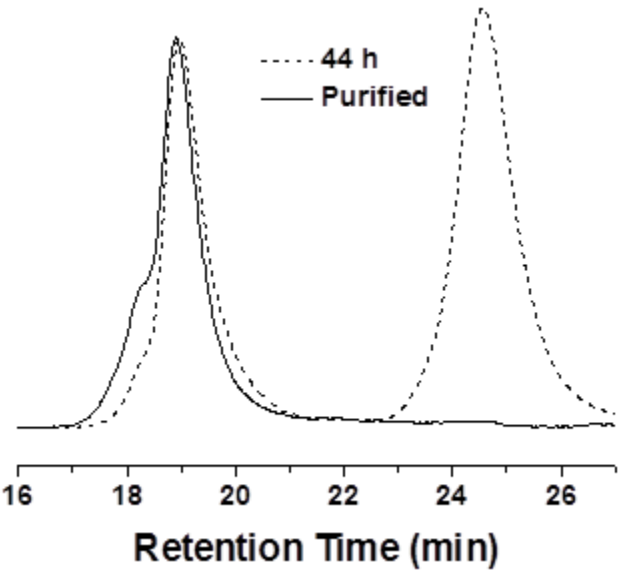

Figure B12. SEC traces of P(DEGMA-*co*-NBA) MB-10 before and after removal of excess P(DEGMA-*co*-NBA)-47 side chains by fractionation. After purification: $M_{n,SEC}$ = 1,380,800 Da; PDI = 1.14. SEC analysis was carried out on PL GPC-50 Plus system with Agilent Mixed-B columns using DMF containing 50 mM LiBr as carrier solvent.

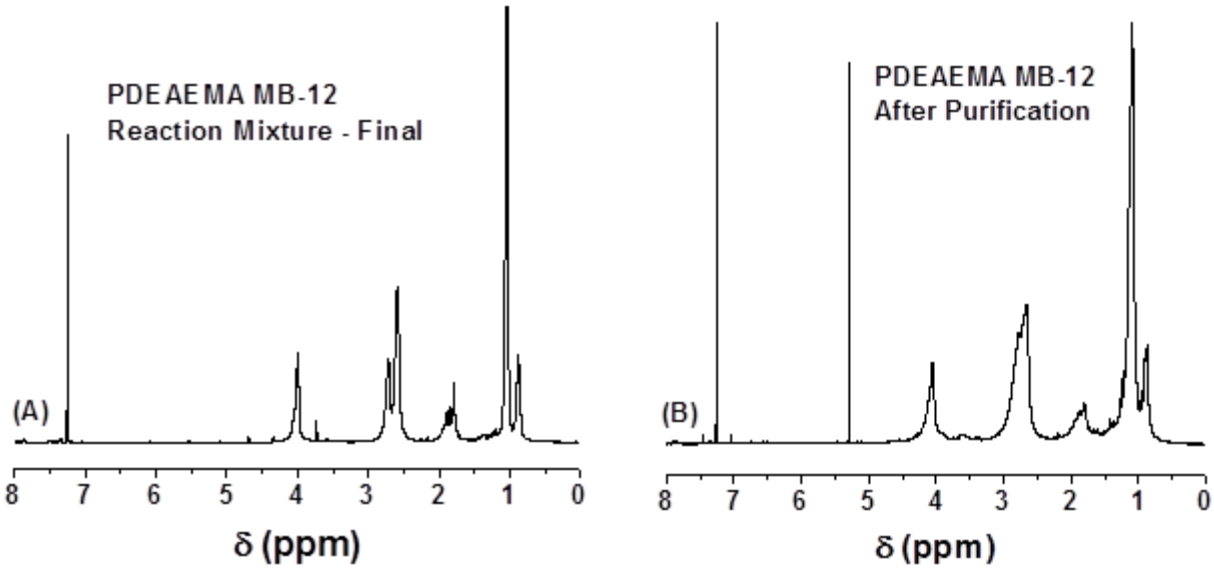

Figure B13. ^{1}H NMR spectra of PDEAEMA MB-12 (A) before purification and (B) after purification by fractionation in $CDCl_3$.

Chapter 4: Synthesis and Behavior of Stimuli-Responsive Shape-Changing Binary Heterografted Linear Molecular Brushes

Abstract

This chapter presents the synthesis and shape-changing behvior of stimuli-responsive binary heterografted linear molecular brushes containing both hydrophilic and stimuli-responsive side chains randomly distributed along the backbone. The side chains were composed of water-soluble poly(ethylene oxide) (PEO) and either thermosensitive poly(di(ethylene glycol) ethyl ether acrylate) (PDEGEA), pH-responsive poly(*N*,*N*-diethylaminoethyl methacrylate) (PDEAEMA), or light-responsive poly(*o*-nitrobenzyl acrylate) (PNBA). The brushes were made by a "grafting to" method using copper-catalyzed azide-alkyne cycloaddition "click" reactions between azide-functionalized backbone polymers and alkyne end-functionalized side chain polymers. The backbone polymer with a degree of polymerization (DP) of 800 employed here was synthesized by ATRP and post-polymerization reactions discussed previously in Chapter 2. Alkyne end-functionalized stimuli-responsive side chain polymers were prepared by either ATRP or reversible addition-fragmentation chain transfer polymerization (RAFT) from an alkyne-functionalized initiator or chain transfer agent. Alkyne end-functionalized PEO with DPs of 45 and 114 were prepared by esterification of the hydroxyl end group of PEO monomethyl ether with 4-pentynioc acid described in Chapter 2. The grafting to "click" reactions were performed at ambient temperature, and the grafting densities were determined by size exclusion chromatography. Binary heterografted brushes with high grafting densities were prepared using a molar ratio of backbone monomer units to total side chains of approximately 1 : 2. The molar ratio of PEO and the other (stimuli-responsive) side chain polymer in the purified brushes was found to be very close to that in feed, except for PEO/PDEAEMA heterografted brushes, which exhibited a higher molar content of PEO and a lower grafting density when compared to PEO/PDEGEA and PEO/PNBA brushes. Pure brush molecules were obtained by fractionation or centrifugal filtration to remove unreacted

side chains. The collapsed state of the binary heterografted molecular bottlebrushes in aqueous solution was more stable compared to their homografted counterparts by visual comparison. Stimuli-induced size changes in aqueous solution were studied by dynamic light scattering (DLS), and shape transitions from the extended worm-like conformation to the collapsed, roughly spherical globular state were directly observed by atomic force microscopy (AFM). As a demonstration to show that shape-changing of molecular brushes can be used to control the interaction of brush molecules with the environment, we prepared PDEGEA side chains that were incorporated with small amounts of a biotin-containing monomer (BA) and a fluorescent monomer (NBDA) and synthesized thermosensitive binary heterografted brushes containing PEO and P(DEGEA-*co*-BA-*co*-NBDA) side chains. An aqueous solution containing PEO/P(DEGEA-*co*-BA-*co*-NBDA) molecular brushes in the collapsed state and rhodamine-labelled avidin, which is known to strongly complex biotin, was prepared. Upon decreasing the temperature, the collapsed spherical brush molecules were unraveled, resulting in binding between biotin-containing brushes and avidin, as observed by fluorescence spectroscopy.

4.1. Introduction

Molecular bottlebrushes, also called molecular brushes, are composed of polymeric side chains that are densely grafted to a polymer backbone. "Living"/controlled polymerization techniques have been shown to allow for precise control over molecular structure, such as the composition and arrangement of side chains as well as the topology of the backbone (see Scheme 1.2 in Chapter 1).[1-3] Chapters 2 and 3 focused on the simplest type, homografted linear molecular brushes, in which the backbone is linear and all the side chains are identical. This chapter expands the scope to more complex architectures, namely binary heterografted brushes, where two types of side chains are randomly distributed along the backbone. Such brush structures provide opportunities for unique properties, such as single molecules that contain loadable compartments or brushes that are capable of self-assembly in solution or bulk, which may find applications in areas such as biomedicine (e.g., as drug carriers).

Stimuli-responsive molecular brushes exhibit particularly intriguing solution behavior, such as dramatic changes in shape, size, and solubility, which can be induced in situ using a variety of environmental triggers.[4-26] There have been several interesting studies of non-homografted (i.e., mixed or block heterografted) stimuli-responsive brushes, mainly focusing on intermolecular assembly into large micelle-like structures in aqueous solution.[27-40] Liu et al. prepared coil-brush diblock copoplymers containing a linear PEO block and a brush block composed of alternating thermosensitive poly(di(ethylene glycol) methyl ether methacrylate) (PDEGMMA, LCST = 26 °C) and pH-responsive poly(*N*,*N*-diethylaminoethyl methacrylate) (PDEAEMA, pK_a = 7.4) side chains.[28] The diblock copolymer backbone was prepared from ATRP of glycidyl methacrylate (GMA) from a 5 kDa PEO macroinitiator, followed by post-polymerization reactions to install an ATRP initiator moiety and an azide group on each GMA repeat unit. PDEGMMA side chains were

then grown by grafting from using ATRP, and alkyne end-functionalizaed PDEAEMA side chains were subsequently "clicked" by CuAAC onto the backbone via the azide moieties with a 71 % grafting efficiency. The brushes dissolved molecularly in pH = 4 water with a polymer concentration of 1 mg/g at room temperature exhibiting an average hydrodynamic radius (R_h) of ~7.6 nm, but upon increasing the temperature to 40 °C (above the LCST of PDEGMMA) they assembled into spherical micelles (R_h = ~107 nm) composed of a collapsed PDEGMMA core and corona containing PEO and protonated PDEAEMA. When the temperature was lowered to 15 °C and the pH was increased to 10, the brushes reassembled into inverted micelles (R_h = ~87 nm) composed of a collapsed PDEAEMA core and a hydrated PEO/PDEGMMA corona.

Huang et al. synthesized coil-brush diblock copolymers composed of a linear thermosensitive poly(*N*-isopropylacrylamide) (PNIPAM, LCST = 32 ^{o}C) block and a brush block with PDEAEMA side chains synthesized by grafting from using ATRP.[30] At room temperature, the brushes dissolved molecularly (D_h = ~30 nm) in acidic water at a concentration of 0.2 mg/g and assembled into vesicles (D_h = ~550 nm) upon increasing the pH above 7.2, where the vesicle wall is composed of the deprotonated PDEAEMA brush block and the corona is composed of linear PNIPAM. When the pH was decreased to 2, the brush molecules disassociated back into unimers.

Zhao and coworkers prepared asymmetric molecular brushes where each backbone repeat contained both PEO and poly(styrene)-*b*-PNIPAM (PS-*b*-PNIPAM) grafts.[34] They prepared a PGMA backbone by ATRP followed by post polymerization reactions to install a hydroxyl group and a chain transfer agent for RAFT polymerization on each repeat unit. Carboxyl-terminated PEO side chains (DP = 17) were grafted to the backbone via esterification with the -OH pendant groups, and PS-*b*-PNIPAM side chains were installed through grafting from by sequential RAFT

polymerization of styrene and then NIPAM. The brushes self-assembled in water by solvent switching at room temperature to form vesicles, as observed by transmission electron microscopy (TEM). They theorized that the vesicle wall was composed of hydrophobic PS segments and the short PEO chains were mainly partitioned into the hollow core (as evidenced by a suppressed ^{1}H NMR signal) while the longer PNIPAM segments mainly resided in the external corona. Additionally, the vesicles decreased in size in response to an increase in temperature above the LCST of the PNIPAM corona.

Lu et al. reported the synthesis of ternary heterografted molecular brushes in which hydrophobic PS, pH-responsive poly(*N*,*N*-dimethylaminoethyl methacrylate) (PDMAEMA), and thermosensitive poly(oligo(ethylene glycol)methyl ether methacrylate-*co*-DEGMMA) (P(OEGMA-*co*-DEGMMA)) side chains were randomly distributed along the backbone.[37] The brushes were prepared by grafting to CuAAC click reactions between an azide-functionalized PGMA backbone and alkyne end-functionalized side chains, and the total grafting density was relatively low (40 %). The brushes underwent self-assembly in water at room temperature and pH = 7 into spherical micelles (R_h = 168 nm) with PS chains residing in the core and protonated PDMAEMA and hydrated P(OEGMA-*co*-DEGMMA) chains in the corona. Thermo-induced collapse of the P(OEGMA-*co*-DEGMMA) side chains occurred upon increasing the temperature to 40 °C, causing a reduction in size to 76 nm. Increasing the pH to 9 caused a further decrease in size to 31 nm due to deprotonation and collapse of PDMAEMA chains. Holding the pH at 9 and bringing the temperature back to 25 °C caused the size of the aggregates to increase to 93 nm due to rehydration of P(OEGMA-*co*-DEGMMA) side chains.

In contrast to the above examples involving intermolecular assembly of molecular brushes, we are interested in the stimuli-responsive behavior of single bottlebrush molecules, such as

stimuli-triggered "unfolding" of heterografted brushes from a collapsed state, resembling a unimolecular micelle, to an extended worm-like conformation, or vice versa (Scheme 4.1.). This provides the potential to rationally design brush molecules that are capable of hiding moieties (e.g., binding sites) within the collapsed side chains in the micelle-like state that can be deliberately exposed to the environment by unraveling the brushes upon application of a chemical or physical stimulus. The design of such brush molecules would be a step toward mimicking the behavior of more complex biomacromolecules such as the von Willibrand Factor (VWF) discussed in Chapter 1, which unfolds to expose "sticky" binding sites for collagen in response to environmental changes that occur when a vessel wall is ruptured.[41-43]

In the present work, we demonstrate the synthesis of stimuli-responsive binary heterografted molecular brushes using a grafting to CuAAC "click" approach and that these brushes undergo dramatic changes in size and shape upon application of a variety of stimuli. The brushes were composed of PEO (DP = 45) and either thermosensitive poly(di(ethylene glycol) ethyl ether acrylate) (PDEGEA), pH-responsive poly(*N*,*N*-diethylaminoethyl methacrylate) (PDEAEMA), or light-responsive poly(*o*-nitrobenzyl acrylate) (PNBA) side chains randomly distributed along the backbone (Scheme 4.2). The backbone polymer with a degree of polymerization (DP) of 800 employed here was synthesized by ATRP and post-polymerization reactions discussed previously in Chapter 2. Alkyne end-functionalized stimuli-responsive side chain polymers were prepared by either ATRP or RAFT polymerization from an alkyne-functionalized initiator or chain transfer agent. Alkyne end-functionalized PEO with DPs of 45 and 114 were prepared by reaction of PEO monomethyl ether with 4-pentynioc acid described in Chapter 2. The grafting to "click" reactions were performed in DMF or THF using CuCl catalyst at ambient temperature, and the binary heterografted brushes achieved high grafting densities using a molar ratio of backbone monomer

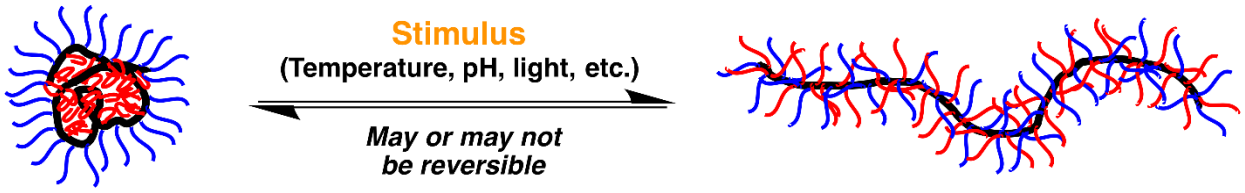

Scheme 4.1. Shape-Changing of Stimuli-Responsive Binary Heterografted Molecular Brushes.

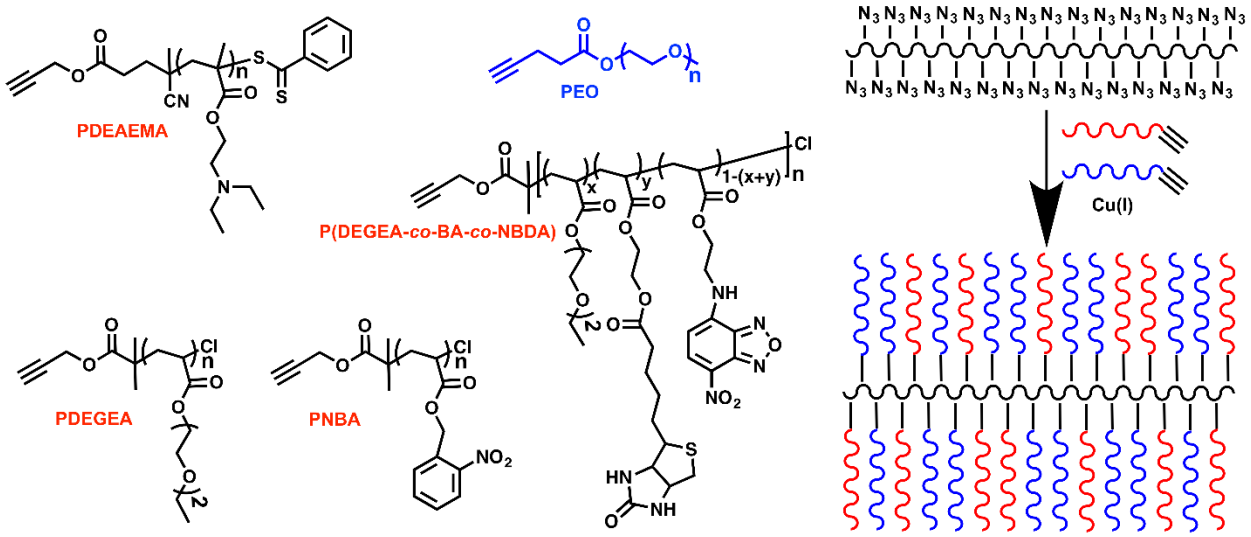

Scheme 4.2. Synthesis of Stimuli-Responsive Binary Heterografted Molecular Brushes by Grafting To CuAAC "Click" Reactions.

units to total side chains of approximately 1 : 2. The molar ratio of PEO and the other (stimuli-responsive) side chain in the feed was 0.6 : 0.4 and the composition of the purified brushes was usually very close to that in the feed. The brushes were purified by fractionation or centrifugal filtration, and their stimuli-responsive properties in aqueous solution were investigated by visual inspection and DLS. In general, the collapsed state of the heterografted brushes in aqueous solution were more stable compared to their homografted counterparts by visual comparison. The brushes underwent stimuli-induced unimolecular collapse or vice versa as observed by DLS, and shape transitions from the extended worm-like conformation to the collapsed, roughly spherical globular state were directly observed by AFM. As a demonstration, we used the well-known strong binding between biotin and avidin to show that the shape-changing behavior of molecular bottlebrushes can be used to control interactions between brush molecules and the environment.

4.2. Experimental Section

4.2.1. Materials

Di(ethylene glycol) ethyl ether acrylate (DEGEA, 90%, Aldrich) and *N,N,N',N'',N''*-pentamethyldiethylenetriamine (PMDETA, 99%, Acros) were purified by vacuum distillation over calcium hydride. *N,N*-Diethylaminoethyl methacrylate (DEAEMA, 99%, Aldrich) was passed through a basic alumina/silica gel column to remove the inhibitor prior to use. *o*-Nitrobenzyl acrylate (NBA) was synthesized according to a literature procedure by the reaction of acryloyl chloride (97 %, Aldrich) and *o*-nitrobenzyl alcohol (97%, Acros) in the presence of triethylamine (99%, Acros).[44] The product was purified by column chromatography, and its molecular structure was confirmed by ^{1}H NMR spectroscopy analysis. Propargyl 2-bromoisobutyrate (PBiB) and propargyl 4-cyano-4-(phenylcarbonothioylthio)pentanoate (PCPP) were synthesized by

procedures described in Chapter 3. The preparation of azide-functionalized backbone polymer with a DP of 800 (PTEGN_3MA-800) is described in Chapter 2. The syntheses of alkyne end-functionalized PEO polymers with DPs of 45 and 114 and alkyne end-functionalized poly(*N*,*N*-diethylaminoethyl methacrylate) (PDEAEMA) with a DP of 43 (PDEAEAM-43) are described in Chapters 2 and 3, respectively. Rhodamine (TMRITC) labelled avidin D (5 mg/g buffered aqueous solution) was purchased from Vector Laboratories and used as received. All other chemicals were purchased from either Aldrich or Fisher and used as received.

4.2.2. General Characterization

Size exclusion chromatography (SEC) of molecular brush samples, with the exception of PDEAEMA-containing brushes, was carried out at ambient temperature using a PL-GPC 50 Plus (an integrated GPC/SEC system from Polymer Laboratories, Inc.) with a differential refractive index detector, one PLgel 10 µm guard column (50 × 7.5 mm, Agilent Technologies), and three PLgel 10 µm Mixed-B columns (each 300 × 7.5 mm, linear range of molecular weight from 500 to 10,000,000 Da according to Agilent Technologies). The data were processed using Cirrus™ GPC/SEC software (Polymer Laboratories, Inc.). *N*,*N*-Dimethylformamide (DMF) with 50 mM LiBr was used as the carrier solvent at a flow rate of 1.0 mL/min. PDEAEMA-containing molecular brushes and PDEAEMA side chain polymers were also analyzed with the same PL-GPC 50 Plus system, except with the use of one PSS GRAL guard column (50 × 8 mm, Polymer Standards Service-USA, Inc.) and two PSS GRAL linear columns (each 300 × 8 mm, linear range of molecular weight from 500 to 1,000,000 according to Polymer Standards Service USA, Inc.). SEC of PDEGEA, P(DEGEA-*co*-BA-*co*-NBDA), and PNBA side chain polymers was carried out using a PL-GPC 20 integrated GPC/SEC system from Polymer Laboratories, Inc. with a refractive index detector, one PLgel 5 µm guard column (50 × 7.5 mm, Agilent Technologies), and two PLgel

5 μm Mixed-C columns (each 300 × 7.5 mm, linear range of molecular weight from 200 to 2,000,000 Da according to Agilent Technologies). THF was used as the eluent at a flow rate of 1.0 mL/min. Each system was calibrated with a set of near-monodisperse linear polystyrene standards (Polymer Laboratories, Inc.). ^{1}H and ^{13}C NMR (300 or 500 MHz) spectra were recorded on a Varian Mercury 300 NMR spectrometer or a Varian VNMRS 500 NMR spectrometer, respectively, and the residual solvent proton signal was used as the internal standard. High resolution mass spectroscopy (HRMS) experiments were performed using a JEOL Model JMS-T100LC (AccuTOF) orthogonal time-of-flight (TOF) mass spectrometer (Peabody, MA) with an IonSense (Danvers, MA) DART source.

4.2.3. Synthesis of 2-(Acryloyloxyethyl) 5-((3a*S*,4*S*,6a*R*)-2-oxohexahydro-1*H*-thieno[3,4-*d*]imidazole-4-yl)pentanoate (D-Biotin Oxyethyl Acrylate, BA)

2-Hydroxyethyl acrylate (0.254 g, 2.18 mmol), biotin (0.300 g, 1.23 mmol), N-(3-dimethylaminopropyl)-*N′*-ethylcarbodiimide hydrochloride (EDC) (0.424 g, 2.21 mmol), and DMAP (0.027 g, 0.22 mmol) were weighed out into a 25 mL round bottom flask equipped with a magnetic stir bar, dissolved in methylene chloride (15 mL), and stirred overnight. The reaction mixture was then concentrated and the crude product was purified by gradient column chromatography (DCM/methanol). The product was dried under high vacuum to yield 0.194 g (46.2 %) as a white powder. ^{1}H NMR δ (ppm, $CDCl_3$): 6.42 (dd, 1H), 6.13 (dd, 1H), 5.85 (dd, 1H), 5.69 (s, 1H), 5.17 (s, 1H), 4.49 (m, 1H), 4.31 (m, 5H), 3.13 (m, 1H), 2.89 (m, 1H), 2.71 (m, 1H), 2.34 (t, 2H), 1.67 (m, 4H), 5.69 (m, 2H). ^{13}C NMR δ (ppm, $CDCl_3$): 173.40, 165.87, 164.02, 131.44, 127.91, 62.23, 61.99, 61.94, 60.10, 55.55, 40.52, 33.69, 28.31, 28.18, 24.67. HRMS (DART-TOF): m/z calc $C_{15}H_{23}N_2O_5S$ $[M+H]^+$: 343.13222; found: 343.13265; mass error: 1.25 ppm.

4.2.4. Synthesis of 4-(2-Acryloyloxyethylamino)-7-nitro-2,1,3-benzoxodiazole (NBDA)

4-Chloro-7-nitro-2,1,3-benzoxadiazole (NBD-Cl, 0.768 g, 3.85 mmol) was added into a 25 mL round bottom two-necked flask equipped with a magnetic stir bar and dissolved in acetonitrile (10 mL). A solution of ethanolamine (0.592 g, 9.69 mmol) in acetonitrile (10 mL) was added, and an immediate color change from yellow to dark red-orange was observed. The mixture was stirred under nitrogen at room temperature overnight. The reaction mixture was concentrated under high vacuum and the crude product was purified by column chromatography using a mixture of methanol and methylene chloride (1:19, v/v) as eluent. The product was dried under high vacuum to yield 0.650 g (75.3 %) of 4-(2-Hydroxyethylamino)-7-nitro-2,1,3-benzoxadiazole (NBD-OH) as a red-orange solid. NBD-OH (0.220 g, 0.97 mmol) was dissolved in acetonitrile (60 mL), followed by the dropwise addition of acryloyl chloride (2.150 g, 23.9 mmol). The reaction mixture was refluxed for 4 h. The solvent was removed under reduced pressure, and the crude product was purified by column chromatography using CH_2Cl_2 as the eluent. The product was dried under high vacuum to yield 0.087 g (31.9 %) of 4-(2-acryloyloxyethylamino)-7-nitro-2,1,3-benzoxodiazole (NBDA) as an orange powder. ^{1}H NMR δ (ppm, $CDCl_3$): 8.49 (d, aromatic, 1H), 6.52 (b, -N*H*CH_2-, 1H), 6.47 (d, aromatic, 1H), 6.23 (dd, C*H*H=CH-, 1H), 6.14 (dd, CHH=C*H*-, 1H), 5.92 (dd, CH*H*=CH-, 1H), 4.53 (t, -COOCH_2-, 2H), 3.81 (m, -NHCH_2-, 2H). ^{13}C NMR δ (ppm, $CDCl_3$): 165.88 (-NHCH$_2$CH$_2$O*C*=O-), 145.59 (aromatic), 144.82 (aromatic), 144.47 (aromatic), 138.27 (aromatic), 132.46 (CH$_2$=*C*H-), 128.44 (*C*H$_2$=CH-), 121.65 (aromatic), 99.93 (aromatic), 62.34 (-NHCH$_2$*C*H$_2$OC=O-), 42.64 (-NH*C*H$_2$CH$_2$OC=O-). HRMS (DART-TOF): m/z calc $C_{11}H_{11}N_4O_5$ $[M+H]^+$: 279.07240; found: 279.07114; mass error: 4.51 ppm.

4.2.5. Synthesis of Thermosensitive PDEGEA Side Chain Polymer

Described below is the procedure for the synthesis of an alkyne end-functionalized PDEGEA side chain polymer with a DP of 46 (PDEGEA-46) by ATRP. PBiB (83.4 mg, 0.407 mmol), DEGEA (9.083 g, 48.3 mmol), CuCl (39.4 mg, 0.398 mmol), anisole (10.122 g), and PMDETA (79.2 mg, 0.457 mmol) were weighed into a 50 mL two-necked round bottom flask equipped with a magnetic stir bar. The mixture was degassed by three freeze-pump-thaw cycles and placed in an 80 °C oil bath. The polymerization was monitored by ^{1}H NMR spectroscopy and SEC. After 14 h, the flask was removed from the oil bath and opened to air. The polymerization mixture was passed through neutral alumina/silica gel column to remove the catalyst. The polymer was purified by precipitation in hexanes three times and dried under high vacuum to obtain a light green, viscous polymer (2.688 g). The DP was calculated to be 46 by end group analysis from the ^{1}H NMR spectrum, using the integrals of the peaks at 4.62 ppm (HC≡CCH_2OOC- of the alkyne end group) and 4.07-4.24 ppm (-COOCH_2- of DEGEA monomer units). The results of SEC analysis using PL GPC-20 system with THF as carrier solvent: $M_{n,SEC}$ = 8,800 Da; PDI = 1.17.

4.2.6. Synthesis of Light-Responsive PNBA Side Chain Polymer

Described below is the procedure for the synthesis of an alkyne end-functionalized NBA side chain polymer with a DP of 36 (PNBA-36) by ATRP. PBiB (49.9 mg, 0.243 mmol), NBA (5.846 g, 28.2 mmol), CuCl (25.1 mg, 0.254 mmol), anisole (5.927 g), and PMDETA (71.1 mg, 0.410 mmol) were weighed into a 25 mL two-neck round bottom flask equipped with a magnetic stir bar. The mixture was degassed by three freeze-pump-thaw cycles and placed in an 80 °C oil bath. The polymerization was monitored by ^{1}H NMR spectroscopy and SEC. After 9 h, the flask was removed from the oil bath and opened to air. The polymerization mixture was passed through neutral alumina/silica gel column to remove the catalyst. The polymer was purified by

precipitation in diethyl ether four times and dried under high vacuum to obtain a light yellow, powdery polymer (1.217 g). The DP was calculated to be 36 by end group analysis from the ^{1}H NMR spectrum, using the integrals of the peaks at 4.54 ppm (HC≡CCH_2OOC- of the alkyne end group) and 5.09-5.45 ppm (-COOCH_2- of NBA monomer units). The results of SEC analysis using PL GPC-20 system with THF as carrier solvent: $M_{n,SEC}$ = 4,800 Da; PDI = 1.29.

4.2.7. Synthesis of Thermosensitive P(DEGEA-*co*-BA-*co*-NBDA) Side Chain Copolymer

Described below is the procedure for the synthesis of an alkyne end-functionalized P(DEGEA-*co*-BA-*co*-NBDA) side chain polymer with a DP of 50 (P(DEGEA-*co*-BA-*co*-NBDA)-50) by ATRP. PBiB (50.1 mg, 0.244 mmol), DEGEA (5.196 g, 27.6 mmol), BA (0.107 g, 0.312 mmol), NBDA (12.5 mg, 0.0449 mmol, from 0.633 g of a stock solution in DMF with a concentration of 19.79 mg/g), CuCl (26.6 mg, 0.269 mmol), anisole (5.160 g), and PMDETA (0.126 g, 0.727 mmol) were weighed into a 25 mL two-necked round bottom flask equipped with a magnetic stir bar. The mixture was degassed by three freeze-pump-thaw cycles and placed in an 80 °C oil bath. The polymerization was monitored by ^{1}H NMR spectroscopy and SEC. After 21 h, the flask was removed from the oil bath and opened to air. The polymerization mixture was passed through neutral alumina/silica gel column to remove the catalyst. The polymer was purified by precipitation in hexanes three times and 75/25 hexanes/diethyl ether (v/v) twice and dried under high vacuum to obtain a red-orange, viscous polymer (1.568 g). The DP was calculated to be 50 by end group analysis from the ^{1}H NMR spectrum, using the integrals of the peaks at 4.62 ppm (HC≡CCH_2OOC- of the alkyne end group) and 4.07-4.24 ppm (-COOCH_2- of DEGEA monomer units). The average number of BA monomer units per chain was found to be 0.66 using the integrals of the peaks at 4.62 ppm (HC≡CCH_2OOC- of the alkyne end group) and 3.16 ppm (-

$OOCCH_2CH_2CH_2CH_2CH(S)(CH)$- of BA monomer units). The results of SEC analysis using PL GPC-20 system with THF as carrier solvent: $M_{n,SEC}$ = 10,600 Da; PDI = 1.16.

4.2.8. Synthesis of Stimuli-Responsive Binary Heterografted Molecular Brushes

Below is the procedure for the synthesis of thermosensitive PEO/PDEGEA binary heterografted molecular brushes with a backbone DP of 800 and side chain DPs of 45 and 46 for PEO and PDEGEA, respectively (PEO/PDEGEA MMB-1). Similar procedures were employed for the synthesis of other heterografted molecular brushes containing PEO and P(DEGEA-*co*-BA-*co*-NBDA), PDEAEMA, or PNBA side chain polymer. $PTEGN_3MA$-800 (6.25 mg, 0.0257 mmol monomer units, from a stock solution in THF) was added into a 3.7 mL vial equipped with a stir bar. THF was evaporated off with a stream of nitrogen, and DMF (0.5 mL) was added. PEO-45 (59.1 mg, 0.0281 mmol alkyne end groups) and PDEGEA-46 (163.4 mg, 0.0186 mmol alkyne end groups, from a stock solution in THF) were weighed into a separate vial. The THF was evaporated off with a stream of nitrogen, and DMF (2.0 mL) was added, and the side polymers were transferred to the vial containing $PTEGN_3MA$-800. CuCl (3.9 mg, 0.039 mmol) was added, and a rubber septum was used to seal the reaction vial. The mixture was flushed with nitrogen via needles for 15 min, and PMDETA (5.0 µL, 0.024 mmol) was injected using a microsyringe. The reaction progress was monitored by SEC. After 22 h, propargyl alcohol (50 µL, 0.86 mmol) was injected via a microsyringe under nitrogen to cap any unreacted backbone azide units. The mixture was stirred for another 1 h before the reaction mixture was opened to air, diluted with methylene chloride, and passed through a short neutral alumina/silica gel column to remove the catalyst. Excess side chains were removed by centrifugal filtration in 50/50 $MeOH/H_2O$ (v/v) using 50 kDa MWCO dialysis membrane followed by fractionation in a mixture of THF and hexanes to yield a light yellow, viscous polymer (48.2 mg, 37 % yield). The grafting density, defined as the

percentage of backbone monomer units that are grafted with a side chain polymer, was estimated to be 74.3 % by comparison of the brush and the unreacted side chain polymer peak areas from SEC chromatogram of the reaction mixture at the end of the reaction. The results of SEC analysis of the purified brushes using PL GPC-50 Plus system with Agilent Mixed-B columns in DMF containing 50 mM LiBr as carrier solvent: $M_{n,SEC}$ = 963,500; PDI = 1.14.

PEO/PDEAEMA heterografted molecular brushes were synthesized according to a slightly altered procedure due to the poor solubility observed for PDEAEMA homograft brushes in DMF. THF was used as the reaction medium, and the grafting density was determined by the comparison of the brush and the unreacted side chain polymer peak areas from SEC in a similar fashion as for other brush samples, except that PSS GRAL columns were employed for analysis using the PL GPC-50 Plus system with DMF containing 50 mM LiBr as carrier solvent. SEC analysis of PEO/PDEAEMA molecular brushes using Agilent Mixed-B columns could not be performed (no brush polymer peak was observed).

4.2.9. Dynamic Light Scattering Study of Stimuli Responsive Binary Hetergrafted Molecular Brushes in Water

Dynamic light scattering (DLS) measurements were performed using a Malvern Zetasizer Nano ZS instrument equipped with a He-Ne 633 nm laser and a temperature controller at a scattering angle of 173°. Aqueous solutions of thermosensitive and pH-responsive heterografted molecular brushes for DLS measurements with a concentration of 0.2 mg/g were prepared by dissolving the brush molecules in either Milli-Q water or 5 mM KH_2PO_4 buffer (for PDEAEMA-containing brushes) and passed through a 0.2 µm PTFE filter prior to analysis. Aqueous solutions of light-responsive PEO/PNBA heterografted molecular brushes for DLS measurements were prepared by dropwise addition of a 1.0 mg/mL solution of brushes in DMF (1.0 mL) into rapidly stirred Milli-Q water (10 mL). The brush solution was dialyzed against Milli-Q water using a 3500

Da MWCO dialysis membrane to remove DMF and passed through a 0.2 µm PTFE filter prior to analysis. The reported DLS sizes in this work were the intensity mean diameters. Photocleavage of light-responsive PEO/PNBA molecular brushes was performed using 2 mL of a 0.1 mg/g brush solution in Milli-Q water in a 3.7 mL vial by irradiating the sample with long wavelength (365 nm) UV light from a Spectroline ENF-240C hand-held UV lamp equipped with a 4 watt long wavelength tube filtered at 365 nm. For PEO/PDEAEMA molecular brushes, the pH of the aqueous solution was measured with a pH meter (Accumet AB15 pH meter from Fisher Scientific, calibrated with pH = 4.01, 7.00, and 10.01 standard buffer solutions), and the pH of the solution was adjusted using 0.1 M HCl and 0.1 M NaOH solutions.

4.2.10. Atomic Force Microscopy Study of Binary Heterografted Molecular Brushes

Atomic force microscopy (AFM) was performed using a Digital Instruments Multimode IIIa Scanning Probe Microscope operated in tapping mode under ambient conditions. Reflective Al-coated Si probes (Budget Sensors) with a nominal resonant frequency of 300 kHz and force constant of 40 N/m were employed. Aqueous solutions of molecular brushes with concentrations ranging from 0.01 to 0.1 mg/g for AFM imaging were prepared using Milli-Q water (or KH_2PO_4 buffer for PDEAEMA- or PAA-containing brushes) and either spin coated at 3000 rpm or drop cast onto freshly cleaved mica or PS-coated mica. For PDEAEMA-containing molecular brushes, the pH of the solution was measured with a pH meter and the pH of the solution was adjusted using 0.1 M HCl and 0.1 M NaOH solutions prior to spin coating onto mica.

4.2.11. FRET Study of PEO/P(DEGEA-*co*-BA-*co*-NBDA) Binary Heterografted Molecular Brushes and Rhodamine-Labelled Avidin D

An aqueous solution containing PEO/P(DEGEA-*co*-BA-*co*-NBDA) heterografted molecular brushes (MMB-4) with avidin and aqueous solutions of PEO/P(DEGEA-*co*-BA-*co*-NBDA) MMB-4 brushes alone and Avidin alone as controls were prepared from stock solutions of MMB-

4 brushes (0.010 mg/g brushes in Milli-Q water) and avidin (0.050 mg/g avidin in Milli-Q water). The MMB-4/avidin solution was prepared by mixing 0.598 g of the MMB-4 stock solution and 0.606 g of the avidin stock solution to give a brush concentration of 0.0050 mg/g and an avidin concentration of 0.025 mg/g. The MMB-4 control solution was prepared by mixing 0.507 g of the MMB-4 stock solution and 0.507 g of Milli-Q water to give a brush concentration of 0.0050 mg/g. The avidin control solution was prepared by mixing 0.526 g of the avidin stock solution and 0.526 g of Milli-Q water to give an avidin concentration of 0.025 mg/g. Each solution was prepared at maintained at 40 °C. Fluorescence emission spectra for each solution were recorded at various time intervals using a PerkinElmer LS 55 fluorescence spectrometer equipped with a 20 kW xenon discharge lamp. The excitation wavelength was 480 nm, and the fluorescence emission spectra were recorded from 500 to 700 nm. Both the excitation and emission slit widths were 10.0 nm. After 19 h of holding the solutions at 40 °C, the temperature was decreased and maintained at 0 ^{o}C. Fluorescence measurements were continued for each solution at various time intervals for an additional 29 h at 0 °C.

4.3. Results and Discussion

4.3.1. Synthesis of Azide-Functionalized Backbone Polymers PTEGN$_3$MA

In Chapter 2, we described the synthesis of azide-functionalized backbone polymers (PTEGN$_3$MA) that were prepared by ATRP of TEGSiMA, a silyl ether protected methacrylate monomer, followed by first removal of the *t*-butyldimethylsilyl ether moiety, then reaction with tosyl chloride, and finally substitution with sodium azide (Scheme 2.2). Backbone polymers with DPs of 527 and 800 (PTEGN$_3$MA-527 and PTEGN$_3$MA-800, respectively) were prepared, and we used them for the synthesis of PEO (Chapter 2) and stimuli-responsive (Chapter 3) homografted

molecular brushes using a "grafting to" method. In order to synthesize binary heterografted molecular brushes described in this chapter that are potentially capable of undergoing shape-changing from a stabilized collapsed state to an extended worm-like state, we chose to use only the longer PTEGN_3MA-800 backbone. Due to the backbone strain expected in the curved collapsed state, the larger aspect ratio and slightly lower grafting densities observed for the molecular brushes prepared using the PTEGN_3MA-800 backbone are likely to result in a more thermodynamically stable collapsed state. The SEC trace and ^{1}H NMR spectrum of PTEGN_3MA-800 can be found in Figures 2.3 and A1 in Chapter 2 and Appendix A, respectively. SEC analysis using Mixed-B columns from Agilent Inc. revealed an $M_{n,SEC}$ of 313.4 kDa and a narrow PDI of 1.09 (relative to polystyrene standards). The degree of azide functionalization was calculated to be 90 % from its ^{1}H NMR spectrum using the integral values of the peaks at 3.98-4.14 ppm (-COOCH_2CH$_2$-) and 3.34-3.47 ppm (-OCH$_2$CH_2N$_3$). A more detailed discussion of the synthesis can be found in Chapter 2.

4.3.2. Synthesis of Alkyne End-Functionalized Stimuli-Responsive and Water-Soluble Side Chain Polymers

Alkyne end-functionalized stimuli-responsive side chain polymers were prepared either by ATRP using an alkyne-functionalized ATRP initiator (PBiB) or by RAFT using an alkyne-containing chain transfer agent (PCPP) (Scheme 4.3), which is similar to the strategy for stimuli-responsive side chains laid out in Chapter 3. Thermosensitive PDEGEA and P(DEGEA-*co*-BA-*co*-NBDA) as well as light-responsive PNBA side chain polymers were synthesized by ATRP. The ATRP polymerizations were carried out in anisole at 80 °C and stopped when desired molecular weights were achieved. Differently, the pH-responsive PDEAEMA side chain polymer was prepared by RAFT polymerization using alkyne-functionalized chain transfer agent PCPP,

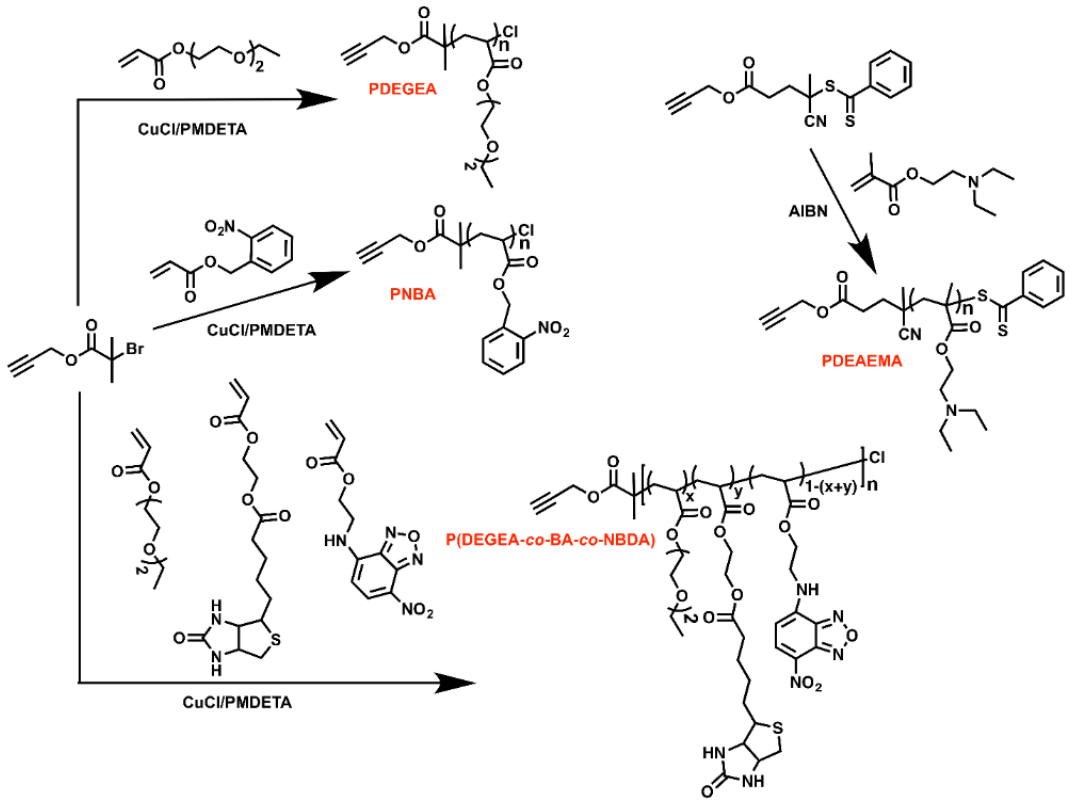

Scheme 4.3. Synthesis of Alkyne End-Functionalized Stimuli-Responsive Side Chain Polymers by ATRP and RAFT Polymerization.

which was performed in anisole at 70 °C using AIBN as initiator. In each case, the monomer conversion was kept below 50 % in order to avoid or minimize any possible side reactions involving the alkyne end group during the polymerization.

The side chain polymers were purified by repetitive precipitation in hexane, diethyl ether, or a mixture of the two (for PDEAEMA, hexane was cooled in a dry ice/acetone bath), dried under high vacuum, and characterized by SEC and ^{1}H NMR spectroscopy. As an example, Figure 4.1 shows the SEC trace and ^{1}H NMR spectrum of an alkyne-terminated PNBA with a DP of 36 (PNBA-36). SEC analysis showed that the polymerization was well controlled and side reactions were kept to a minimum, as reflected by the relatively narrow, monomodal molecular weight distribution with a PDI of 1.29. The SEC traces and ^{1}H NMR spectra of other stimuli-responsive side polymers can be found in Appendix C (Figure C1-C4). The DP of each side chain polymer was calculated from the ^{1}H NMR spectrum of the purified polymer using the integrals of the peaks from the alkyne chain end and the characteristic protons of monomer units. Specifically, for thermosensitive PDEGEA and P(DEGEA-*co*-BA-*co*-NBDA), the peaks at 4.62 ppm (HC≡CCH_2OOC- of the end group from PBiB) and 4.07-4.24 ppm (-COOCH_2CH$_2$- of DEGEA monomer units) were used for the calculation of DP. The molar contents of BA and NBDA were low (the molar ratios of DEGEA : BA : NBDA in the feed were 100 : 1.1 : 0.16) in P(DEGEA-*co*-BA-*co*-NBDA), so they were neglected in the calculation of DP. For PNBA, the DP was calculated using the peaks at 4.54 ppm (HC≡CCH_2OOC- of the end group from PBiB) and 5.09-5.45 ppm (-COOCH_2- of NBA monomer units). For PDEAEMA, the peaks at 4.66 ppm (HC≡CCH_2OOC- of the end group from PCPP) and 3.90-4.11 ppm (-COOCH_2CH$_2$- of DEAEMA monomer units) were used for the calculation of DP. The characterization data for four stimuli-responsive side chain polymers are summarized in Table 4.1.

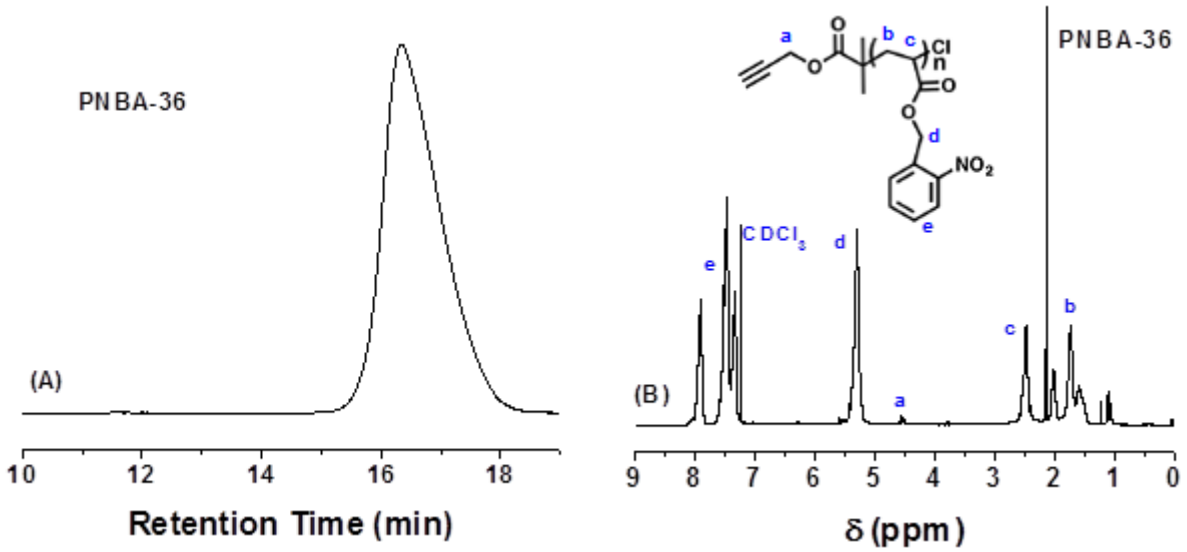

Figure 4.1. (A) SEC trace of side chain polymer PNBA with a DP of 36 (PNBA-36) and (B) ^{1}H NMR spectrum of PNBA-36 in $CDCl_3$. SEC analysis was carried out on PL GPC-20 system using THF as carrier solvent.

Table 4.1. Characterization Data for Alkyne End-Functionalized Stimuli-Responsive and Water-Soluble Side Chain Polymers

Side Chain Polymer Sample	$M_{n,SEC}$ (kDa)	PDI	DP
PDEGEA-46	8.8 [a]	1.17 [a]	46 [c]
PDEAEMA-43	5.7 [b]	1.16 [b]	43 [c]
PNBA-36	4.8 [a]	1.29 [a]	36 [c]
P(DEGEA-*co*-BA-*co*-NBDA)-50	10.6 [a]	1.16 [a]	50 [c]
PEO-45	2.8 [a]	1.08 [a]	45 [d]
PEO-114	8.7 [a]	1.04 [a]	114 [d]

[a] The values of number average molecular weight ($M_{n,SEC}$) and polydispersity index (PDI) were measured by SEC using PL GPC-20 system with THF as solvent. [b] SEC was performed using PL GPC-50 Plus system with PSS GRAL columns and DMF with 50 mM LiBr as mobile phase. [c] DP was calculated by ^{1}H NMR spectroscopy analysis using the integrals of the peaks from the monomer units and the end groups (from the alkyne containing initiator PBiB or RAFT chain transfer agent PCPP). [d] DP was calculated from the nominal molecular weight (2 kDa or 5 kDa) divided by the molecular weight of each monomer unit (44 Da).

Alkyne end-functionalized water-soluble PEO side chains with DPs of 45 and 114 (PEO-45 and PEO-114, respectively) were synthesized from commercially available PEO-monomethyl ether with molecular weights of 2 kDa and 5 kDa.. The PEO polymers were end-functionalized with an alkyne moiety by reacting the alcohol end group of PEO with EDC-activated 4-pentynoic acid in the presence of DMAP catalyst in methylene chloride (Scheme 2.4 in Chapter 2). The degree of alkyne functionalization was determined to be essentially quantitative for both PEO-45 and PEO-114 by ^{1}H NMR spectroscopy using the integral values of the peaks at 4.21 ppm ($HC{\equiv}CCH_2CH_2COOCH_2$- of alkyne end group) and 3.33 ppm (s, -OCH_3 of methyl end group) of the purified polymer. Their synthesis is discussed in detail in Chapter 2. The SEC traces and ^{1}H NMR spectra of PEO-45 and PEO-114 can be found in Figures 2.4 and A2 of Chapter 2 and Appendix A, respectively, and the characterization data for both PEO side chain polymers is shown in Table 4.1.

4.3.3. Synthesis of Thermosensitive PEO/PDEGEA Binary Heterografted Molecular Brushes

In Chapter 3, we prepared homografted molecular brushes with high and tunable grafting densities by a "grafting to" method and demonstrated the versatility of this strategy to prepare a variety of stimuli-responsive homografted molecular brushes. We found that high grafting densities could be achieved using a molar ratio of backbone monomer units to side chain polymer of approximately 1 : 2 and that the reaction is essentially complete after 24 h. In this chapter, we extend this method to synthesize a series of binary heterografted molecular brushes in which water-soluble and stimuli-responsive side chains are randomly distributed along the backbone. Thermosensitive PEO/PDEGEA binary heterografted molecular brushes were prepared by a "grafting to" method using copper-catalyzed azide-alkyne cycloaddition "click" reactions between azide-containing repeat units of the backbone polymer $PTEGN_3MA$ and alkyne end-functionalized

side chain polymer PDEGEA, a thermosensitive polymer with a reported cloud point in water of 9 ^{o}C, and PEO, a water-soluble polymer. The reactions were performed in DMF using CuCl/PMDETA as catalyst at ambient temperature. The grafting density, defined as the percentage of backbone repeat units that are grafted with a side chain polymer, was calculated from the SEC chromatogram using the ratio of peak areas from the molecular brushes and the unreacted side chain polymers and the molar ratio of backbone monomer units to the side chain polymers in the feed (see Appendix C.1 for a detailed calculation). We previously confirmed that the peak area ratio of the two different molecular weight polymers is essentially the same as the mass ratio using a series of mixtures of two polystyrene homopolymers with very different molecular weights (Appendix A, Figure A3). Here, for the calculation of grafting density for heterografted brushes, we assume that the molar ratio of side chains in the brushes is the same as in the feed.

We used a molar ratio of 1 : 1.82 for the backbone monomer units in PTEGN_3MA-800 to total side chain polymers PEO-45 and PDEGEA-46, with a molar ratio of 0.603 : 0.397 of PEO-45 to PDEGEA-46 in the feed to synthesize PEO/PDEGEA binary heterografted molecular brushes (PEO/PDEGEA MMB-1 in Table 4.2). The molar ratio of approximately 0.6 : 0.4 for PEO and PDEGEA side chains in the feed was designed to result in molecular brushes that are slightly rich in water-soluble PEO so as to provide increased stability to the collapsed state in water. The reaction progress was monitored by SEC analysis, and Figure 4.2 shows the SEC traces of the final reaction mixture after 22 h and PEO/PDEGEA MMB-1 after the removal of unreacted side chains by centrifugal filtration and fractionation. For comparison, the SEC trace of backbone polymer PTEGN_3MA-800 is shown as well. After the reaction had proceeded for 22 hours, a high molecular weight peak was observed in the SEC chromatogram with a $M_{n,SEC}$ of 927,200 and a PDI of 1.11, indicating the formation of brush molecules. From the relative peak areas, the mixture contained

Table 4.2. Characterization Data for Stimuli-Responsive Binary Heterografted Molecular Brushes

Binary Heterografted (Mixed) Molecular Brush Sample	$DP_{Backbone}$-DP_{PEO} / $DP_{Stimuli-responsive\ polymer}$	Feed Molar Ratio of Backbone Monomer Units to PEO and Stimuli-Responsive Polymer	$M_{n,SEC}$ (kDa); PDI	Grafting Density (%) [c]	Molar Ratio of PEO to Stimuli-Responsive Polymer in the Feed vs. the Purified Brushes [d]
PEO/PDEGEA **MMB-1**	800-45/46	1 : 1.10 : 0.723	927.2; 1.11 [a]	74.3	0.603 : 0.397; 0.624 : 0.376
PEO/PDEAEMA **MMB-2**	800-45/43	1 : 1.07 : 0.691	553.4; 1.18 [b]	65.6	0.607 : 0.393; 0.660 : 0.340
PEO/PNBA **MMB-3**	800-45/36	1 : 1.06 : 0.707	871.2; 1.15 [a]	78.4	0.600 : 0.400; 0.620 : 0.380
PEO/P(DEGEA-*co*-BA-*co*-NBDA) **MMB-4**	800-114/50	1 : 1.15 : 0.768	1226.2; 1.12 [a]	77.5	0.600 : 0.400; 0.611 : 0.389

[a] The values of $M_{n,SEC}$ and polydispersity index (PDI) were measured by size exclusion chromatography (SEC) of the final reaction mixture using PL GPC-50 Plus system with Agilent Mixed-B columns in DMF containing 50 mM LiBr and using linear polystyrene standards for calibration. [b] SEC was performed using PL GPC-50 Plus system with PSS GRAL columns in DMF containing 50 mM LiBr. [c] Grafting density was calculated from the ratio of peak areas in SEC from molecular brushes and unreacted side chain polymer in the final reaction mixture and the molar ratio of backbone monomer units to side chains in the feed. [d] The molar ratios of PEO and the other (stimuli-responsive) side chains were calculated from ^{1}H NMR spectroscopy of the purified brushes using the ratio of integrals from the monomer units of PEO and the other side chain.

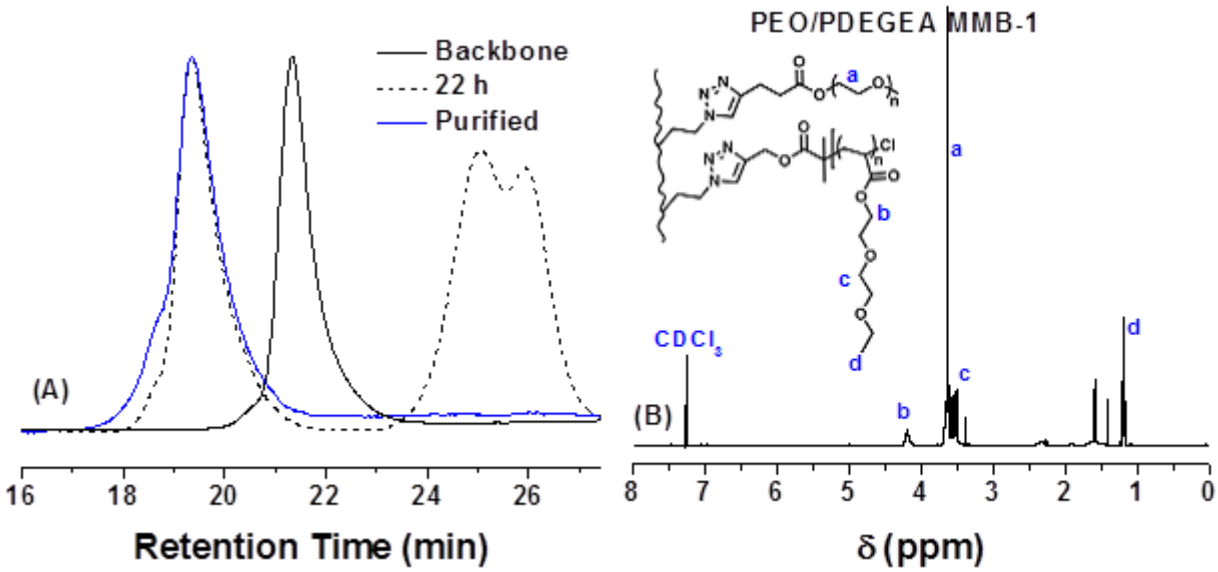

Figure 4.2. (A) SEC trace of PEO/PDEGEA MMB-1 before and after removal of excess side chains as well as PTEGN_3MA-800 backbone polymer for comparison. (B) ^{1}H NMR spectrum of PEO/PDEGEA MMB-1 in $CDCl_3$. SEC analysis was carried out on PL GPC-50 Plus system with Agilent Mixed-B columns using DMF containing 50 mM LiBr as carrier solvent.

41.94 % of brushes and 58.06 % of unreacted PEO-45 and PDEGEA-46 side chains. Since the molar ratio of monomer units of PTEGN_3MA-800 to the side chain polymer in the feed was 1:1.82, this gives a grafting density of 74.3 %. A more detailed description of the calculation of grafting density for heterografted molecular brushes from SEC can be found in Appendix C.

Previous syntheses of molecular brushes described in Chapter 3 using similar conditions showed that there is little change in grafting density after approximately 24 h, so the reaction was stopped by injecting an excess of propargyl alcohol (50 µL) to cap any unreacted azide units in order to prevent side reactions during purification. The mixture was allowed to stir for an additional 1 hour before it was opened to air and passed through neutral alumina column to remove the catalyst. The unreacted side chains were removed by repetitive centrifugal filtration in 50/50 v/v methanol/water using a 50 kDa MWCO dialysis membrane and one round of fractionation using THF as a good solvent and hexanes a poor solvent. SEC analysis of purified PEO/PDEGEA MMB-1 showed that the unreacted side chain polymers PEO-45 and PDEGEA-46 were completely removed and that the molecular weight distribution was not changed much ($M_{n,\,SEC}$ = 963,500; PDI = 1.14) (Figure 4.2A). The ^{1}H NMR spectrum of the purified PEO/PDEGEA MMB-1 brushes is shown in Figure 4.2B. The molar ratio of PEO to PDEGEA side chains in the purified brush was determined to be 0.624 : 0.376 by ^{1}H NMR spectroscopy using the integrals of the peaks at 4.08-4.31 ppm (-COOCH_2CH$_2$- of DEGEA monomer units) and 3.46-3.72 ppm (-OCH_2CH_2- of PEO and -COOCH$_2$CH_2OCH_2CH_2OCH_2CH$_3$ of DEGEA monomer units). This is very close to the feed ratio of 0.603 : 0.397, although slightly enriched with PEO, likely because of the linear molecular structure of PEO, and thus, decreased steric hindrance in the reaction.

4.3.4. Thermosensitive Properties of PEO/PDEGEA Binary Heterografted Molecular Brushes

The thermoresponsive properties of PEO/PDEGEA binary heterografted molecular brushes (PEO/PDEGEA MMB-1) in water were studied by visual inspection as well as dynamic light scattering (DLS) and atomic force microscopy (AFM). For direct comparison, we also prepared PDEGEA homografted molecular brushes using $PTEGN_3MA$-800 backbone and PDEGEA-46 side chains, referred to as PDEGEA MB-1, using a similar procedure as described in Chapter 3 for the synthesis of other homografted molecular brushes. The grafting density was determined to be 75.9 %, and the results of SEC analysis after purification by fractionation using PL GPC-50 Plus system with Agilent Mixed-B columns in DMF with 50 mM LiBr were $M_{n,\,SEC}$ = 1,190,100; PDI = 1.14. The SEC traces before and after purification as well as the ^{1}H NMR spectrum of purified PDEGEA MB-1 can be found in Appendix C (Figure C4). We prepared solutions of PEO/PDEGEA MMB-1 and PDEGEA MB-1 in water with a polymer concentration of 1.0 mg/g. Each solution was sonicated in an ice/water bath and then stored in a refrigerator (~4 ^{o}C) overnight in order to ensure complete dissolution. Both solutions were clear at low temperature. Upon increasing the temperature through the reported LCST of 9 °C for PDEGEA linear homopolymer, the PDEGEA MB-1 sample underwent an expected clear to cloudy transition due the aggregation of collapsed brush molecules. This is similar to what was observed in Chapter 3 for other PDEGEA homografted molecular brushes. In contrast, the PEO/PDEGEA MMB-1 solution remained clear at room temperature, suggesting that the collapsed state is stabilized by the water-soluble PEO side chains. An optical photograph of the 1.0 mg/g aqueous solutions at room temperature are shown in Figure 4.3.

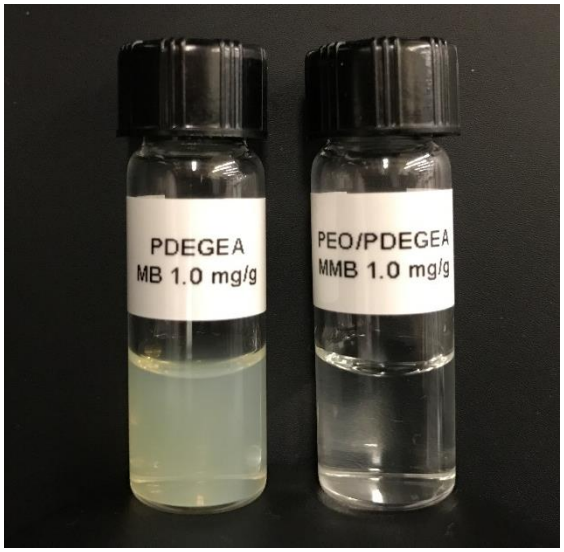

Figure 4.3. Digital optical photograph of solutions of PDEGEA MB-1 homografted bottlebrush (on left) and PEO/PDEGEA MMB-1 binary heterografted bottlebrush (on right) in water with a polymer concentration of 1.0 mg/g at room temperature.

To further investigate the thermoresponsive properties of PEO/PDEGEA binary heterografted molecular brushes, we performed dynamic light scattering measurements at different temperatures on an aqueous solution of PEO/PDEGEA MMB-1 at a concentration of 0.2 mg/g. At 1 ^{o}C, MMB-1 had an apparent hydrodynamic diameter (D_h) of 64 nm, and the size showed a relatively sharp decrease at approximately 10 °C, and leveled off to 43 nm as the temperature was increased to 17 ^{o}C (Figure 4.4A). The transition zone was about 10 °C. There was essentially no further change in size as the temperature was increased to 25 °C. This sharp decrease in size upon increasing the temperature through the LCST of the PDEGEA side chains without aggregation at higher temperatures suggests a unimolecular collapse of brush molecules. In order to investigate how polymer concentration affects the thermosensitive collapse of brush molecules, we preformed DLS studies of solutions of PEO/PDEGEA MMB-1 at higher concentrations of 1.0 and 2.0 mg/g in water at 25 °C. The size distribution by intensity for each concentration is shown in Figure 4.4B. MMB-1 solutions with concentrations of 0.2 and 1.0 mg/g both gave a single distribution with a size of 43 nm, indicating unimolecular collapse of brush molecules at 25 °C for both concentrations. In contrast, when the concentration was increased to 2.0 mg/g, we observed two distributions at 25 °C, one with a size of 42 nm and the other with a size of 359 nm. This indicates a mixture of unimolecularly collapsed brush molecules and aggregated brushes at this concentration, although we note that the solution remained visually clear.

DLS results of aqueous solutions of PEO/PDEGEA MMB-1 showed a relatively sharp decrease in size when the temperature was increased through the LCST of PDEGEA side chains, which we believed was accompanied by a shape transition from an extended worm-like conformation at low temperatures to a collapsed state that was roughly spherical at higher temperatures and stabilized by a corona of PEO side chains. To investigate the possible shape

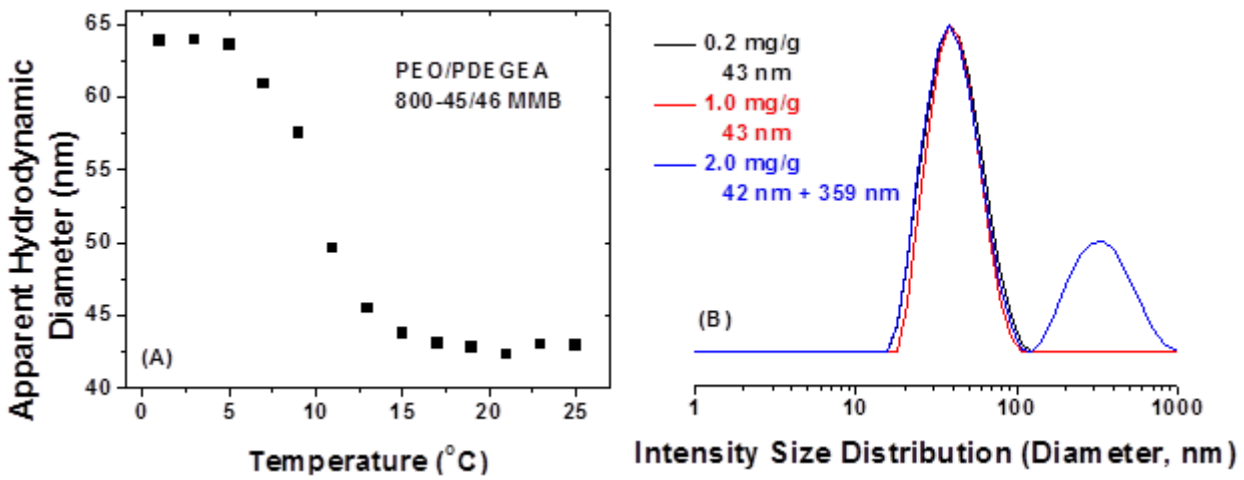

Figure 4.4. (A) Results of DLS at different temperatures for a 0.2 mg/g aqueous solution of PEO/PDEGEA MMB-1. (B) Size distribution by intensity from DLS of PEO/PDEGEA MMB-1 at 25 °C for different polymer concentrations.

change, we examined PEO/PDEGEA MMB-1 brush molecules that were spin coated onto freshly cleaved mica from 0.01 or 0.1 mg/g aqueous solutions at different temperatures using AFM. For the sample prepared at 0 °C, we observed a worm-like morphology that would be expected for densely grafted molecular brushes in a good solvent (Figure 4.5). Length analysis of typical worm-like brush molecules gave an average contour length of 160 nm and a typical height of approximately 1 nm. With a backbone DP of 800, the length of a fully extended worm, in an all-trans conformation, would theoretically be 203 nm (found by 800*0.254 nm). The measured contour length of 160 nm indicates that the degree of stretching is approximately 79 %. For the brushes spin coated at 40 ^{o}C, we observed a globular morphology for the collapsed state as anticipated (Figure 4.6). A cross-sectional analysis of representative collapsed brushes gave an average diameter of 51 nm and an average height of approximately 2.5 nm. It is interesting to note that we observed brush molecules with a worm-like morphology farther from the center of the sample that was spin coated at 40 ^{o}C. This is probably due to the increased shearing force during spinning at areas closer to the edge of the sample as well as favorable surface interactions between brush molecules and the hydrophilic mica substrate, which would promote stretching of the brush molecules as the water evaporated. A more detailed study of this phenomenon would be useful. Additional AFM images of PEO/PDEGEA MMB-1 spin coated onto mica at 0 ^{o}C and 40 ^{o}C can be found in Appendix C (Figures C5 and C6).

4.3.5. Synthesis of pH-Responsive PEO/PDEAEMA Binary Heterograft Molecular Brushes

To demonstrate the versatility of the “click” grafting to method that was used to synthesize thermosensitive PEO/PDEGEA MMB-1, we prepared binary heterografted molecular brushes containing PEO and pH-responsive PDEAEMA side chains using a similar but slightly altered procedure. PDEAEMA is a tertiary amine-containing polymer with a pK_a value of 7.4 in water.

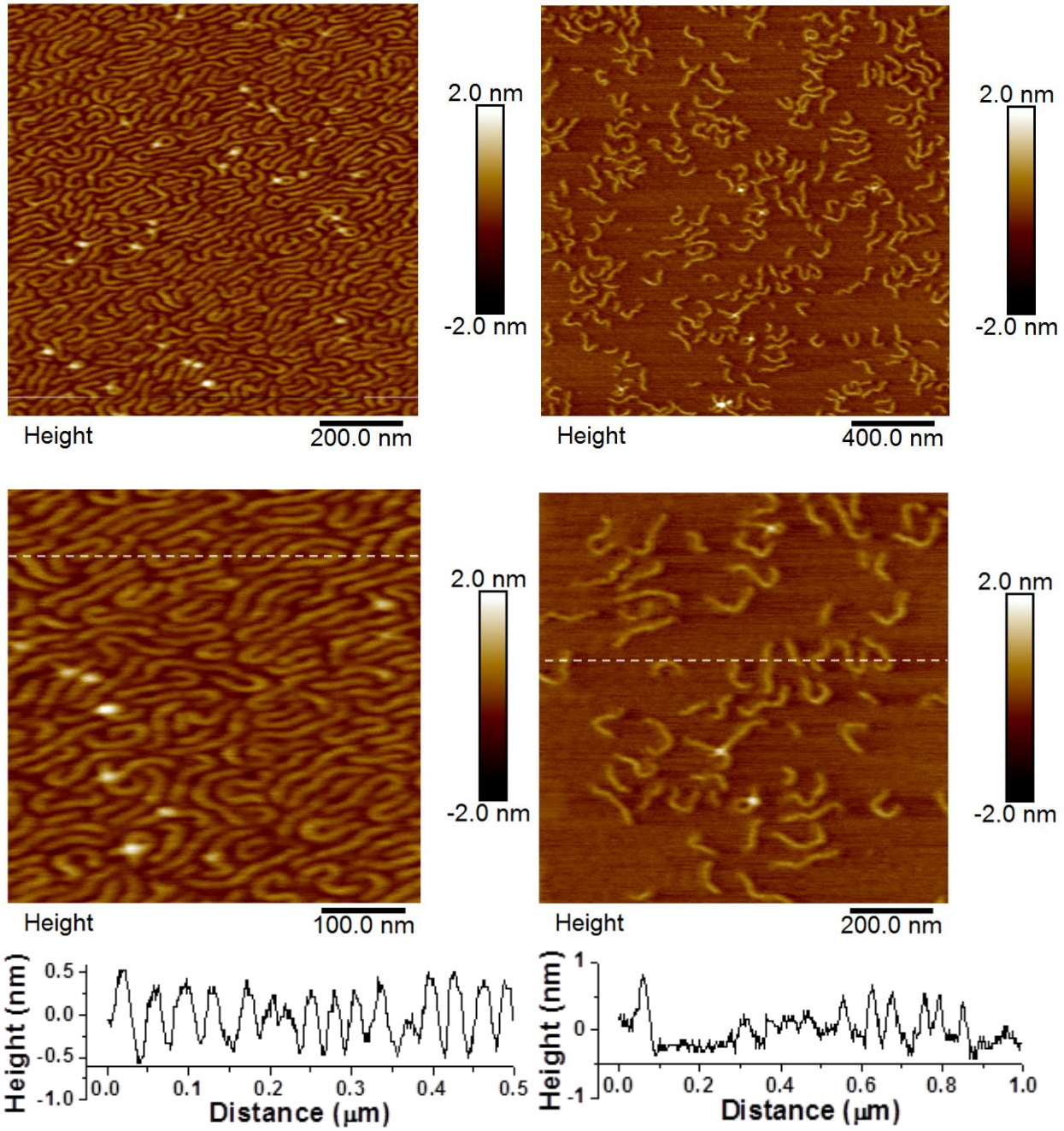

Figure 4.5. AFM height images of PEO/DEGEA MMB-1 brush molecules spin coated onto freshly cleaved mica at 0 °C from an aqueous solution with a polymer concentration of 0.1 mg/g.

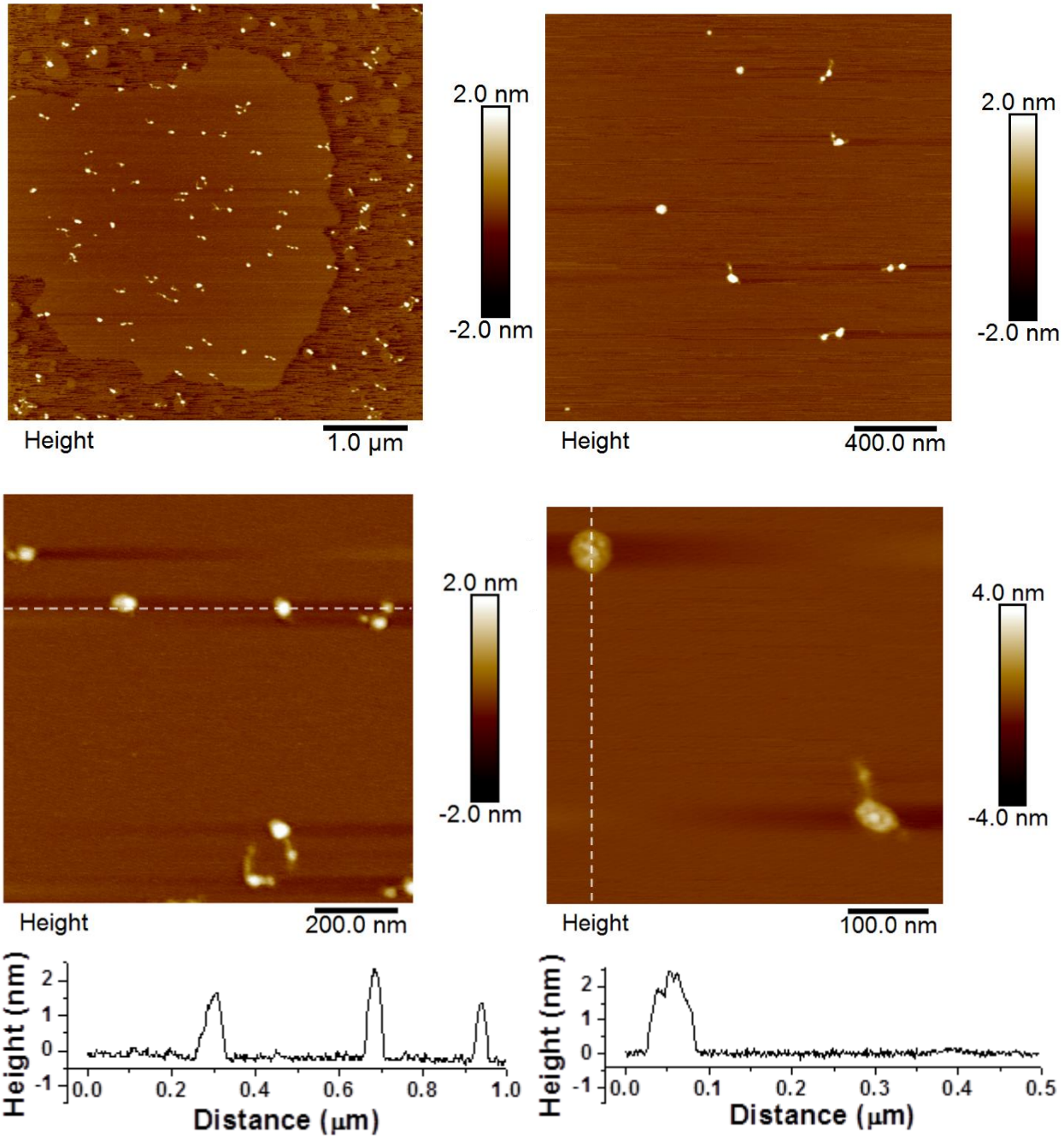

Figure 4.6. AFM height images of PEO/DEGEA MMB-1 brush molecules spin coated onto freshly cleaved mica at 40 °C from an aqueous solution with a polymer concentration of 0.01 mg/g.

Due to the poor solubility of PDEAEMA homografted brushes in DMF that was observed in Chapter 3, THF was used as the reaction medium. Additionally, SEC analysis was performed using PSS GRAL columns instead of Agilent Mixed-B columns, although the same PL GPC-50 Plus system and DMF with 50 mM LiBr mobile phase was employed. No brush polymer peak was observed using Agilent Mixed-B columns, probably due to interactions between the brush molecules and the packing material. The PSS GRAL columns, with a linear molecular weight range of 500 to 1,000,000 Da according to the manufacturer, are more suitable for analysis of lower molecular weight polymers than for high molecular weight brush polymers, for which it would be ideal to use the Agilent Mixed-B columns with a linear molecular weight range of 500 to 10,000,000. Indeed, we observed that PEO/PDEAEMA molecular brushes at least partially eluted outside the linear calibration range for PSS GRAL columns. At least some of the brush molecules have molecular weights that are above the working range of the column, meaning that some of the molecules are totally excluded from the pores of the stationary phase and elute at the exclusion limit. Although an accurate molecular weight distribution of the brushes (relative to linear polystyrene standards) cannot be obtained, they are still well-separated from the unreacted side chains, allowing for a measure of the grafting density based on the relative peak areas. Like for the calculation of grafting density for PEO/PDEGEA binary heterografted molecular brushes, we assume that the brush composition is the same as for the feed.

PEO/PDEAEMA binary heterografted molecular brushes, referred to as PEO/PDEAEMA MMB-2, were synthesized using PTEGN_3MA-800 backbone and PEO-45 and PDEAEMA-43 side chain polymers. Similar to PEO/PDEGEA brushes, we used a molar ratio of 1 : 1.76 for the backbone monomer units in PTEGN_3MA-800 to total side chains of PEO-45 and PDEAEMA-43. The molar ratio of PEO to PDEAEMA in the feed was 0.607 : 0.393. After the reaction proceeded

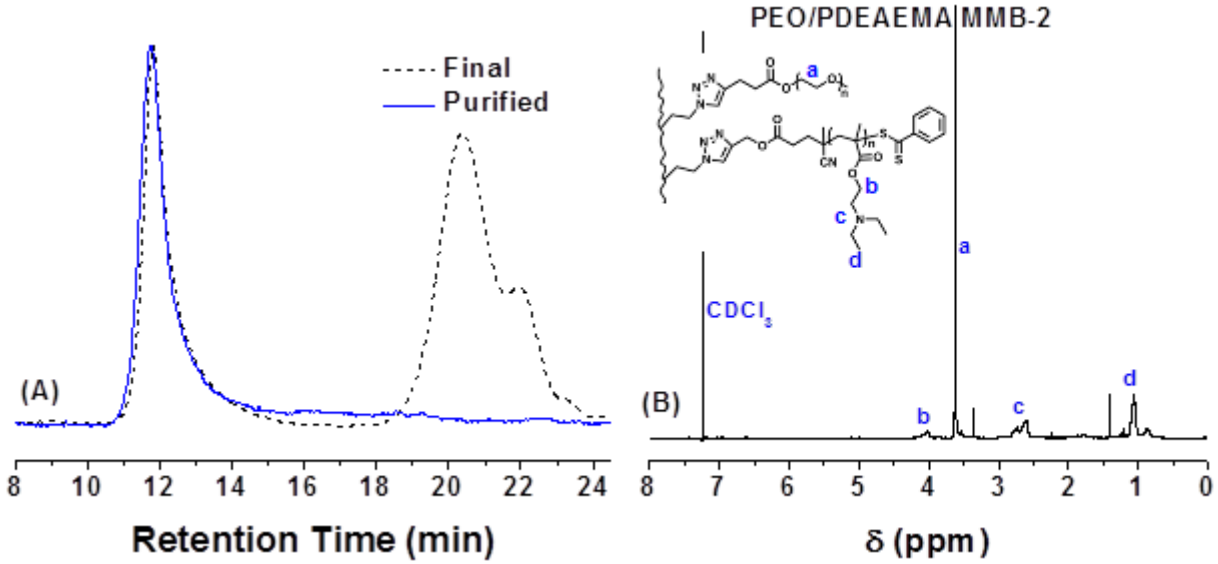

Figure 4.7. (A) SEC trace of PEO/PDEAEMA MMB-2 before and after removal of excess side chains. (B) ^{1}H NMR spectrum of PEO/PDEAEMA MMB-2 in $CDCl_3$. SEC analysis was carried out on PL GPC-50 Plus system with PSS GRAL columns using DMF containing 50 mM LiBr as carrier solvent.

at room temperature for 42 h, propargyl alcohol (100 µL) was injected in order to cap any unreacted backbone azide units to prevent any possible side reactions during purification. After an additional 6 h, the reaction was stopped. Figure 4.7A shows the SEC traces of the final reaction mixture as well as PEO/PDEAEMA MMB-2 after removal excess side chains by fractionation. A high molecular weight peak was observed in the SEC chromatogram at the exclusion limit with a $M_{n,\ SEC}$ of 553,400 and PDI of 1.18, indicating the formation of molecular brushes. From the relative peak areas, the mixture contained 38.49 % of brushes and 61.51 % of unreacted PEO-45 and PDEAEMA-43 side chains. Since the molar ratio of monomer units of PTEGN_3MA-800 to the total side chain polymer in the feed was 1 : 1.78, this gives a grafting density of 65.6 % if we assume that the molar ratio of PEO and PDEAEMA are the same in the brushes as in the feed. This is slightly lower than the grafting density observed for PEO/PDEGEA MMB-1 under similar conditions. This is likely due the increased chain rigidity for PDEAEMA (a polymethacrylate) because of the steric hindrance caused by the methyl group on the backbone of PDEAEMA. Similar behavior was observed in Chapter 3, where PDEAEMA homografted molecular brushes exhibited lower grafting densities than PDEGEA and P(DEGMA-*co*-NBA) homografted molecular brushes, which contain polyacrylate side chains.

PEO/PDEAEMA heterografted molecular brushes were purified by passing the reaction mixture through a neutral alumina column to remove the catalyst, and the unreacted side chains were removed by repeated fractionation in a mixture of THF and hexanes. SEC analysis of purified PEO/PDEAEMA MMB-2 (Figure 4.7A) showed that the excess side chains were completely removed. Results of SEC analysis after purification gave a $M_{n,\ SEC}$ of 626,100 and a PDI of 1.13, although the molecular weight distribution cannot be accurately determined with the PSS GRAL columns that were employed. The ^{1}H NMR spectrum of purified PEO/PDEAEMA MMB-2 is

shown in Figure 4.7B. The molar ratio of PEO to PDEAEMA side chains in the purified brushes was determined to be 0.660 : 0.340 by ^{1}H NMR spectroscopy using the integrals of the peaks at 3.92-4.22 ppm (-COOCH_2CH$_2$- of DEAEMA monomer units) and 3.55-3.68 ppm (-OCH_2CH_2- of PEO monomer units). This is fairly close to the feed ratio of 0.607 : 0.393, although richer in PEO, probably due to the larger size for PDEAEMA side chains. Interestingly, the discrepancy between the feed composition and the brush composition for PEO/PDEAEMA MMB-2 is larger than that for PEO/PDEGEA MMB-1 (5.3 % versus 2.1 %, respectively), which can also be explained by PDEAEMA exhibiting larger steric hindrance than both PDEGEA and PEO. We mentioned earlier that the calculation of grafting density for heterografted brushes using the relative peak areas in SEC requires the assumption that the molar ratio of each side chain is the same in the brush as in the feed. For PEO/PDEAEMA, because the molar fraction of PEO is higher in the brush than in the feed, the grafting density of 65.6 % obtained by SEC analysis is likely underestimated. Because the PEO side chains have a smaller molar mass than the PDEAEMA side chains (2.1 kDa versus 8.3 kDa, respectively), a brush with the same grafting density but a composition richer in PEO results in a smaller fraction of brushes by mass in the reaction mixture, and thus a smaller proportion by peak area in SEC, if we assume that the refractive indices for PEO and PDEAEMA are the same. (SEC was performed using a differential refractive index detector.) Adjusting the calculation of grafting density using the actual brush composition of 0.660 : 0.340 (PEO : PDEAEMA) gives an estimated grafting density of 71.1 %, which is closer to the value of 74.3 % observed for PEO/PDEGEA MMB-1.

The formation of PEO/PDEAEMA bottlebrush molecules was directly confirmed by AFM. Figure 4.8 shows AFM images of PEO/PDEAEMA MMB-2 brushes that were spin cast onto

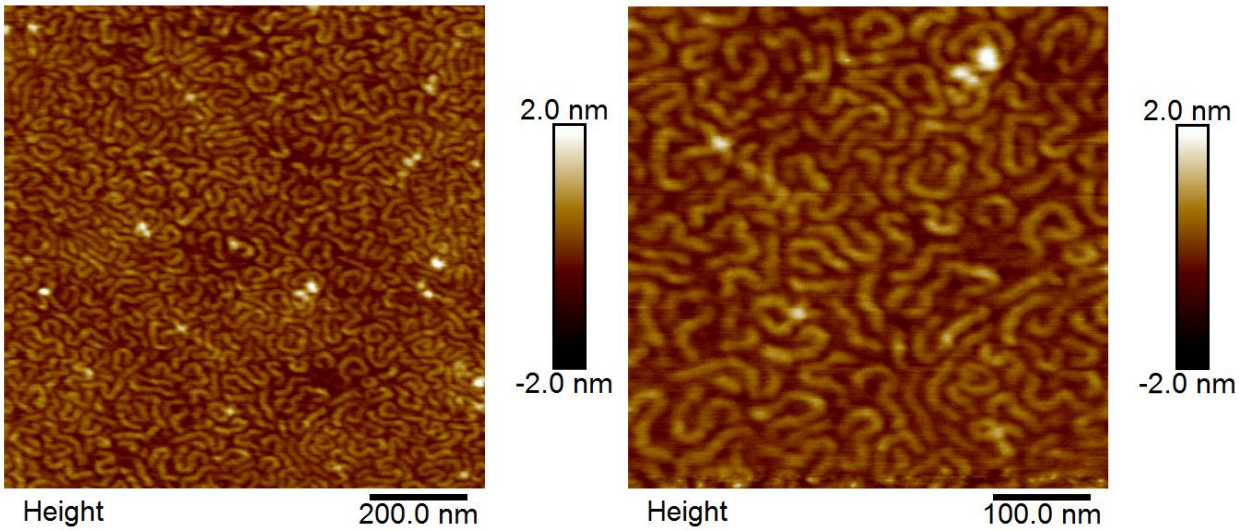

Figure 4.8. AFM height images of PEO/PDEAEMA MMB-2 spin coated onto freshly cleaved mica from a 0.1 mg/g solution in acetone.

freshly cleaved mica from a 0.1 mg/g solution in acetone. We observed a worm-like morphology that was expected for densely grafted molecular brushes in a good solvent for both side chains.

4.3.6. pH-Responsive Properties of PEO/PDEAEMA Binary Heterografted Molecular Brushes

The pH responsive properties of PEO/PDEAEMA MMB-2 in aqueous solution were investigated by visual inspection, DLS, and AFM. Solutions of PEO/PDEAEMA heterografted brushes with a polymer concentration of 0.2 mg/g were prepared in 5 mM KH_2PO_4 buffer, and the pH was adjusted using either 0.1 M HCl or NaOH and measured using a pH meter. Similar to PDEAEMA homografted molecular brushes (described Chapter 3) and PDEAEMA linear polymer, which has a reported pK_a value of 7.4, we found that PEO/PDEAEMA binary heterografted molecular brushes were readily soluble in acidic buffer solution. However, in contrast to PDEAEMA homografted brushes, which underwent aggregation and precipitation above pH = ~8 even at concentrations as low as 0.002 mg/g, the 0.2 mg/g solution of PEO/PDEAEMA heterografted brushes remained clear throughout the studied pH range, which was approximately 4 to 10 (Figure 4.9A). This suggests that the hydrophobic PDEAEMA side chain domains at high pH are stabilized by the water-soluble PEO side chains.

Figure 4.9B shows the apparent hydrodynamic diameter (D_h), measured by DLS, at different pH values for PEO/PDEAEMA MMB-2 in 5 mM KH_2PO_4 aqueous buffer with a polymer concentration of 0.2 mg/g. At pH = 4.92, MMB-2 had a diameter of 76 nm, which is significantly larger than the D_h of 64 nm that was observed for PEO/DEGEA MMB-1 at 1 ^oC, which has comparable side chain lengths to MMB-2. Apparently, the larger size for PEO/PDEAEMA MMB-2 at low pH is the result of a higher degree of chain stretching due to electrostatic repulsions between positively charged monomer units in the PDEAEMA side chains. With increasing the pH,

(A)

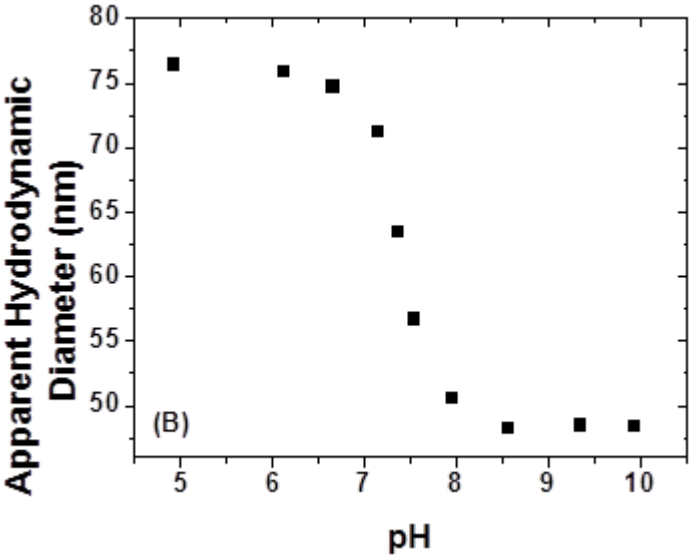

Figure 4.9. (A) Optical photograph of PEO/PDEAEMA MMB-2 in 5 mM KH_2PO_4 aqueous buffer at pH = 4.92 (left) and pH = 9.93 (right) with a polymer concentration of 0.2 mg/g. (B) DLS results at different pH values for PEO/PDEAEMA MMB-2 in 5 mM KH_2PO_4 aqueous buffer with a polymer concentration of 0.2 mg/g.

the size decreased slightly with a sharp drop near the reported pK_a of 7.4 for PDEAEMA linear polymer, reaching a minimum size of 48 nm at pH = 8.56. This is slightly larger than the size of 43 nm that was observed for the collapsed state of PEO/PDEGEA MMB-1 at 25 ^{o}C, which is possibly due to the larger molar fraction of water-soluble PEO side chains in MMB-2 (66 % PEO) than for MMB-1 (62 % PEO) as well as some degree of electrostatic repulsion between a very small number of remaining positively charged PDEAEMA monomer units inside the core. As the pH was increased further to 9.93, there was essentially no change in size. The transition zone was approximately two pH units.

Resembling the thermosensitive collapse observed for PEO/PDEGEA MMB-1, the sharp decrease in size observed for PEO/PDEAEMA MMB-2 upon increasing the pH suggests a unimolecular collapse of MMB-2 brush molecules, where the hydrophobic, largely non-protonated, PDEAEMA core is stabilized by a corona of PEO side chains at high pH. Based on the temperature-induced morphological transition of PEO/DEGEA MMB-1 that was observed by AFM, it is likely that this size transition for PEO/PDEAEMA MMB-2 is also the result of a change in shape from an extended worm-like conformation at low pH to a roughly spherical collapsed state at high pH. As an investigation into the possible shape change, we examined PEO/PDEAEMA MMB-2 brushes that were spin coated onto mica from dilute buffer solutions at high and low pH using AFM. Figure 4.10 shows AFM height images of MMB-2 spin coated onto mica from an aqueous 1.25 mM KH_2PO_4 solution at pH = 4.99 with a polymer concentration of 0.05 mg/g. We observed a worm-like morphology as expected. Length analysis of representative worm-like brush molecules gave an average contour length of 168 nm and a typical height of approximately 1.5 nm. This indicates that the degree of stretching is approximately 83 %, considering a fully stretched brush with a backbone DP of 800 would have a length of 203 nm

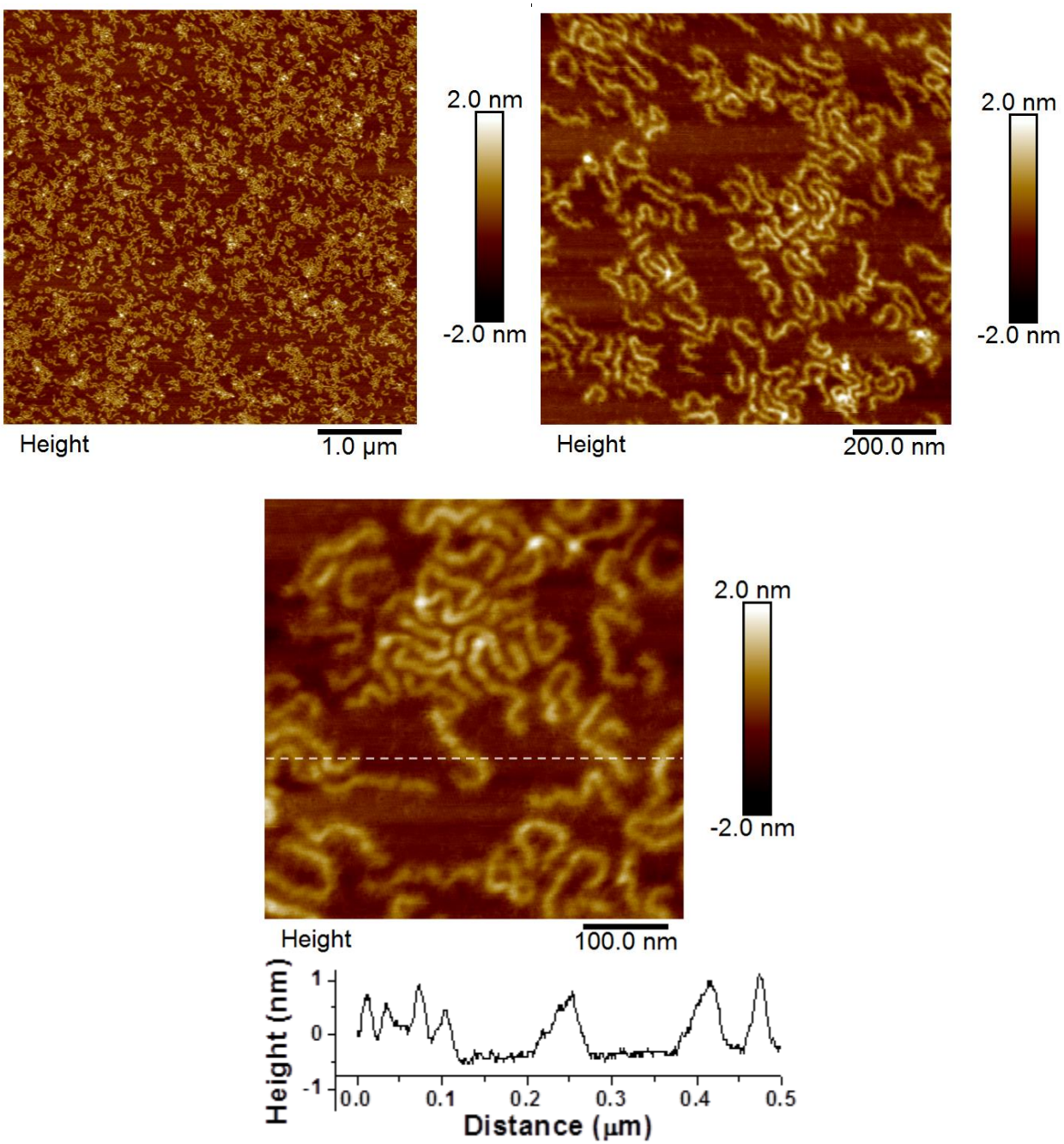

Figure 4.10. AFM height images of PEO/PDEAEMA MMB-2 spin coated onto mica from an aqueous 1.25 mM KH_2PO_4 solution at pH = 4.99 with a polymer concentration of 0.05 mg/g.

(800*0.254 nm). Compared with PEO/PDEGEA MMB-1, with an average contour length of 160 nm spin cast from water at 0 ^{o}C, PEO/DEAEMA MMB-2 worms spin cast at pH = 4.99 appeared to be more highly stretched, even though the side chain DP and grafting density are slightly lower than those for MMB-1. This is likely a result of electrostatic repulsions between positively charged PDEAEMA monomer units. In order to visualize the collapsed state by AFM, we spin coated MMB-2 from a 0.5 mM KH_2PO_4 solution at pH = 9.79 with a polymer concentration of 0.01 mg/g, shown in Figure 4.11. At high pH we observed a predominately spherical morphology, as expected. Many of the spherical nanoobjects seen in AFM images appear to be surrounded by a corona, which could be due to extended PEO side chains. Interestingly, in some cases the brush molecules are partially unwrapped, which could be casued either by the shear force applied during spin coating and/or by favorable brush-surface interactions. Cross-sectional analysis of typical collapsed MMB-2 molecules gave an average diameter of 54 nm and an average height of approximately 4 nm. As a control, we spin coated a blank 5 mM KH_2PO_4 buffer solution onto mica for AFM analysis (Figure 4.12). A clean, nearly featureless surface was observed, indicating that the presence of KH_2PO_4 salt does not affect imaging of spin coated brush molecules by AFM. Additional AFM images of PEO/PDEAEMA MMB-2 spin coated onto mica at pH = 4.99 and 9.79 can be found in Appendix C (Figures C7 and C8).

4.3.7. Synthesis of Light-Responsive PEO/PNBA Binary Heterografted Molecular Brushes

Having demonstrated the adaptability of this grafting to “click” strategy for the synthesis of thermosensitive and pH-responsive heterografted molecular brushes, we decided to extend the methodology to light-responsive binary heterografted brushes as well. We prepared molecular brushes composed of water-soluble PEO and light-responsive PNBA side chains using similar conditions as for PEO/PDEGEA heterografted brushes. PNBA is a hydrophobic polymer with a

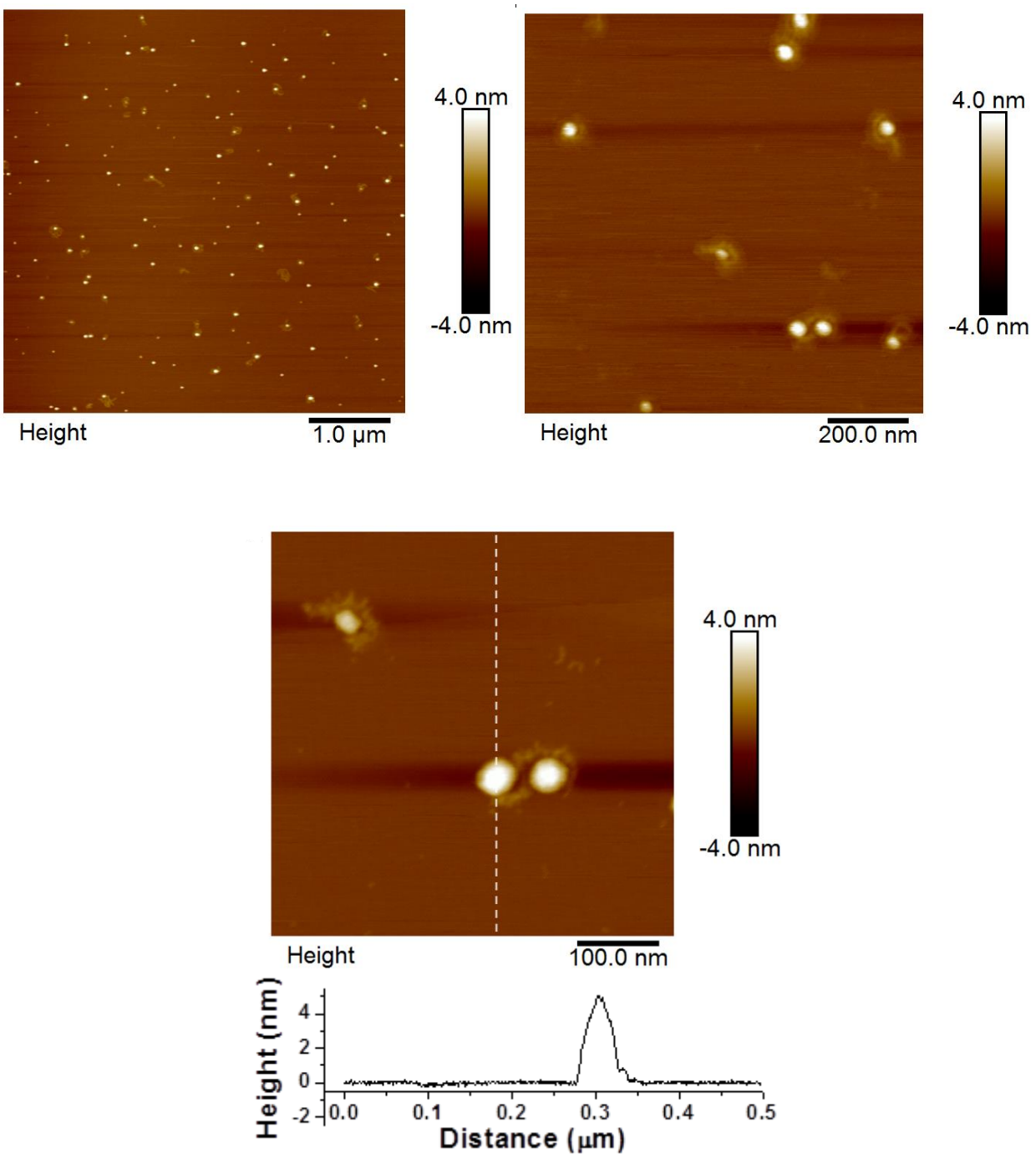

Figure 4.11. AFM height images of PEO/PDEAEMA MMB-2 spin coated onto mica from an aqueous 0.5 mM KH_2PO_4 solution at pH = 9.79 with a polymer concentration of 0.01 mg/g.

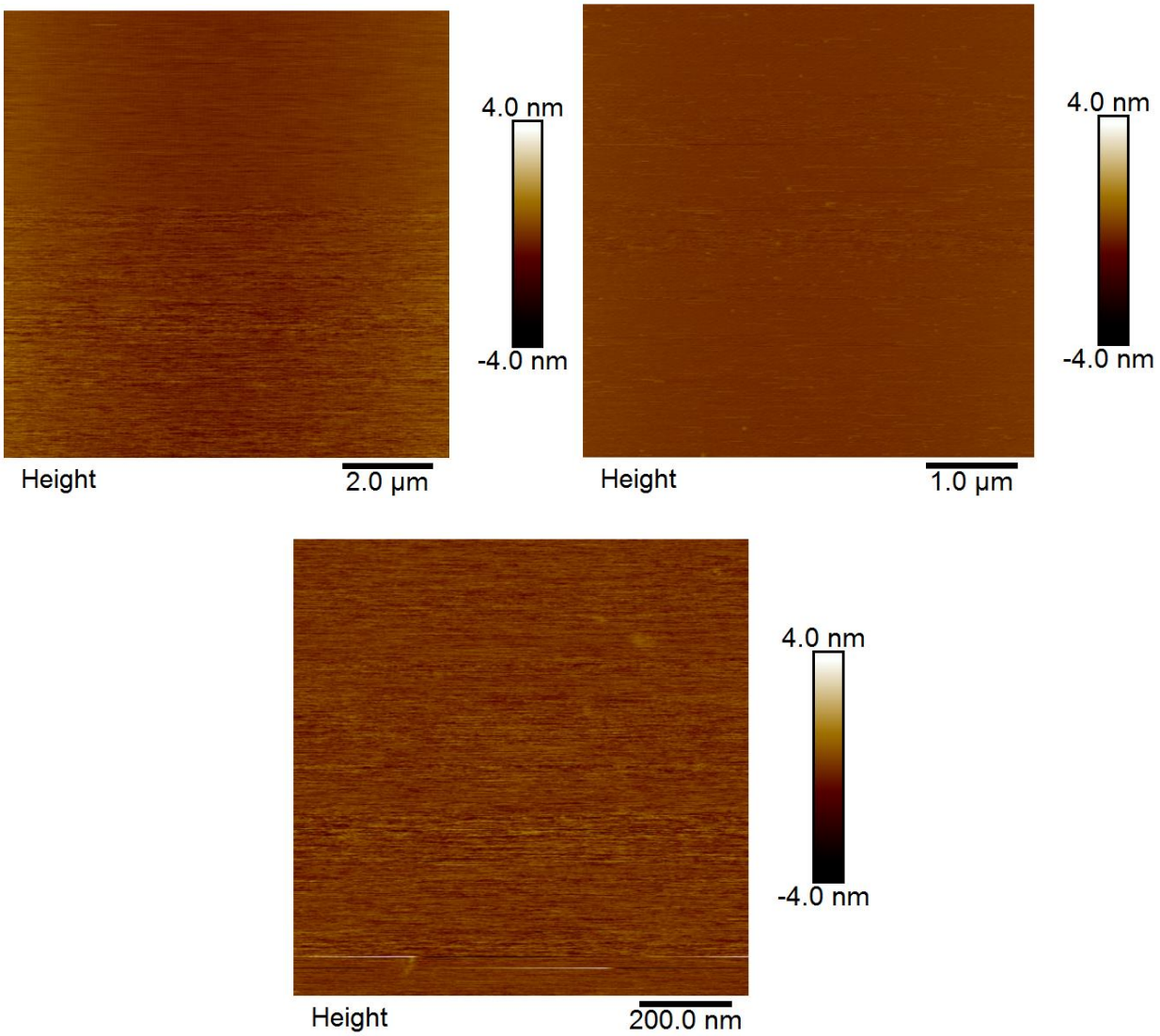

Figure 4.12. AFM height images of a 5 mM KH_2PO_4 buffer solution spin cast onto mica as a control.

glass transition temperature (T_g) that is above room temperature. It contains *o*-nitrobenzyl moieties on each repeat unit that can be efficiently cleaved with long wave (365 nm) UV light, resulting in water-soluble, ionizable poly(acrylic acid). Heterografted PEO/PNBA molecular brushes, referred to as PEO/PNBA MMB-3, were synthesized using PTEGN_3MA-800 backbone and PEO-45 and PNBA-36 side chain polymers. Similar to PEO/PDEGEA MMB-1 and PEO/PDEAEMA MMB-2, we used a molar ratio of 1 : 1.77 for the backbone monomer units in PTEGN_3MA-800 to total side chain polymer PEO-45 and PNBA-36. The molar ratio of PEO to PNBA in the feed was 0.600 : 0.400. Figure 4.13 shows the SEC traces of the final reaction mixture after 40 h as well as PEO/PNBA MMB-3 after removal of unreacted side chains by fractionation. Propargyl alcohol (50 µL) was injected 3 h earlier to cap any unreacted backbone azide units in order to prevent any side reactions during purification. After the click reaction proceeded for 40 h reaction time, brushes were observed by SEC with a $M_{n,\,SEC}$ = 871,200 and PDI of 1.15. From the relative peak areas in SEC, the mixture contained 45.44 % brushes and 54.56 % unreacted PEO-45 and PNBA-36 side chains. Since the molar ratio of monomer units of PTEGN_3MA-800 to the total side chain polymer in the feed was 1 : 1.77, this gives a grafting density of 78.4 %, assuming the molar ratio of PEO and PNBA are the same in the brushes as in the feed. This is similar the grafting density obtained for PEO/PDEGEA MMB-1 (74.3 %) under similar conditions, although slightly higher, probably due to the decreased steric hindrance for PNBA-36 (compared with the longer PDEGEA-46) as well as the longer reaction time (22 h for MMB-1 versus 37 h for MMB-3 before injection of propargyl alcohol).

The obtained PEO/PNBA heterografted molecular brushes were purified by passing the reaction mixture through a neutral alumina column to the remove the catalyst, and the unreacted side chains were removed by repeated fractionation in a mixture of THF and hexanes. SEC analysis

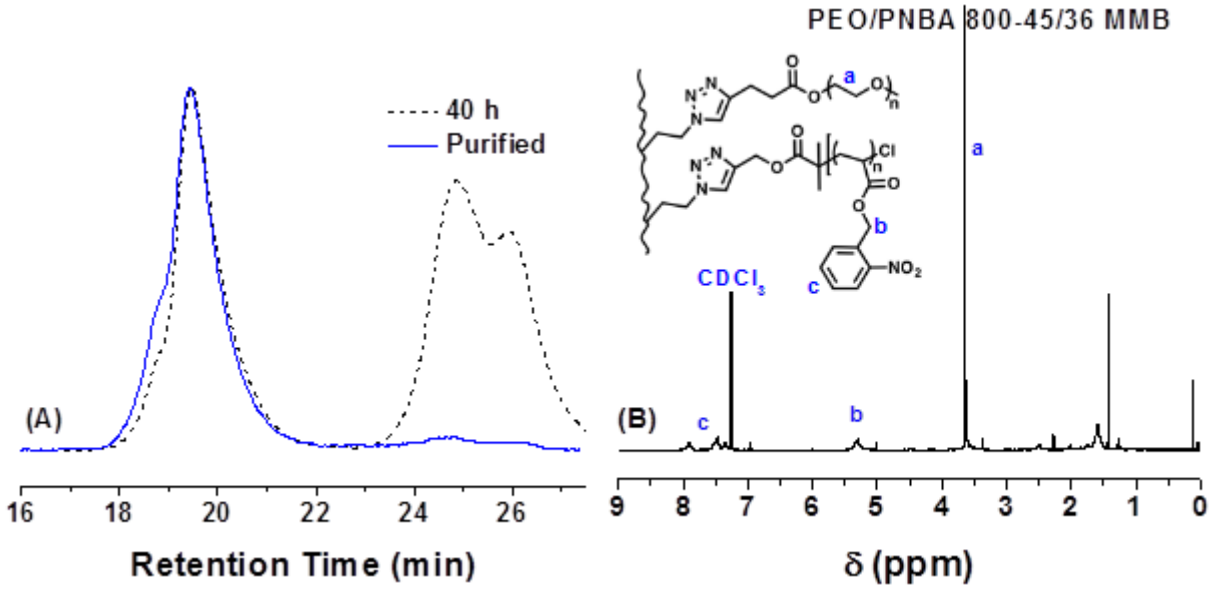

Figure 4.13. (A) SEC trace of PEO/PNBA MMB-3 before and after removal of unreacted side chains by fractionation (B) ^{1}H NMR spectrum of purified PEO/PNBA MMB-3 in $CDCl_3$. SEC analysis was carried out on PL GPC-50 Plus system with Agilent Mixed-B columns using DMF containing 50 mM LiBr as carrier solvent.

of purified PEO/PNBA MMB-3 (Figure 4.13A) showed that the excess side chains were almost completely removed, and the $M_{n,\,SEC}$ was 933,300 with a PDI of 1.16. From the peak areas, purified MMB-3 contained 2 % unreacted side chain polymers. Based on our previous experiments, further fractionation tends to result in broadening of the molecular weight distribution and a low brush yield with a relatively small increase in purity. We think that this level of purity was acceptable, and that small amount of unreacted side chains was unlikely to affect later experiments. The ^{1}H NMR spectrum of purified PEO/PNBA MMB-3 is shown in Figure 4.13B. The molar ratio of PEO to PNBA side chains in the purified brush was determined to be 0.620 : 0.380 by ^{1}H NMR spectroscopy using the integrals of the peaks at 5.18-5.45 ppm (-COOCH_2- of NBA monomer units) and 3.55-3.68 ppm (-OCH_2CH_2- of PEO monomer units). This is very close to the feed ratio of 0.600 : 0.400, although slightly more rich in PEO, likely because of the decreased steric hindrance of PEO. The small discrepancy between the feed composition and the purified brush composition (2.0 %) is similar to what was observed for PEO/PDEGEA MMB-1 (2.1 %).

4.3.8. Light-Responsive Properties of PEO/PNBA Binary Heterografted Molecular Brushes

The light-responsive property of PEO/PNBA MMB-3 in water was investigated using DLS and AFM. A solution of PEO/PNBA brushes with a polymer concentration of 1.0 mg/mL was prepared in DMF, which is a good solvent for both side chains. An aqueous solution of MMB-3 was prepared by dropwise addition of the DMF solution (1 mL) into vigorously stirred water (10 mL). The DMF and removal of DMF via dialysis against pure water. The solution was diluted with water to give a polymer concentration of 0.1 mg/g. Figure 4.14A shows the size distributions by intensity obtained by DLS of PEO/PNBA MMB-3 in DMF (0.2 mg/g) and in water after dialysis (0.1 mg/g). In DMF, MMB-3 had an apparent hydrodynamic diameter (D_h) of 62 nm, which is similar to the D_h of 64 nm that was observed for PEO/PDEGEA MMB-1 at 1 ^oC in water. After a

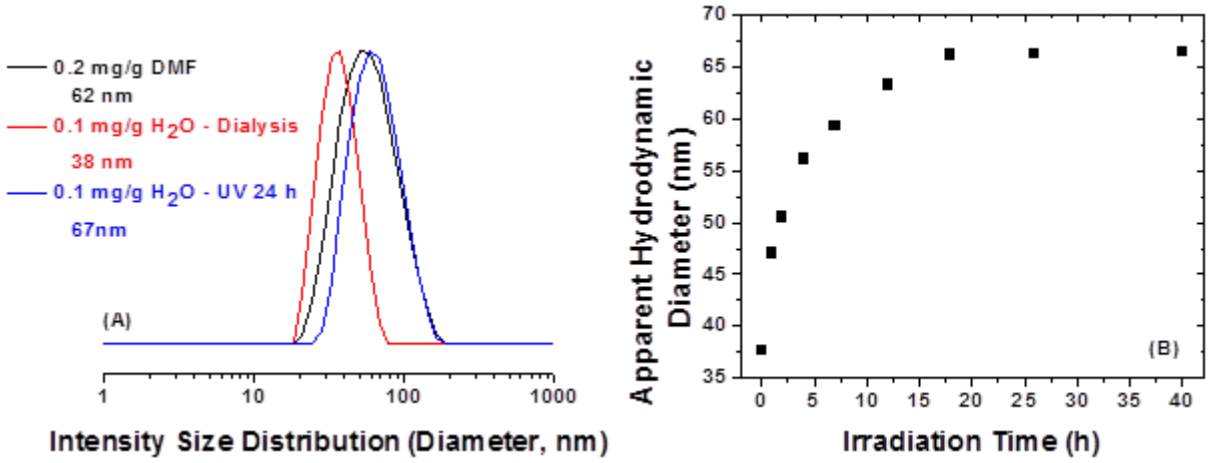

Figure 4.14. (A) Size distributions by intensity from DLS of PEO/PNBA MMB-3 in DMF (0.2 mg/g), water (0.1 mg/g) after dialysis, and in water (0.1 mg/g) after irradiation with 365 nm UV light for 24 h. (B) Apparent hydrodynamic diameter vs. irradiation time for a 0.1 mg/g aqueous solution of PEO/PNBA MMB-3.

1.0 mg/g solution of MMB-3 in DMF was diluted 10x with water by dropwise addition with rapid stirring, the solution remained clear, and a shift to a smaller size of 46 nm observed by DLS while maintaining a monomodal size distribution. We also Prepared an aqueous solution of MMB-3 by transferring a less concentrated DMF solution (0.2 mg/g) into a 10x amount (by volume) of vigorously stirred water and obtained a similar size of 45 nm from DLS before dialysis. This suggests that the collapse of hydrophobic PNBA side chains upon transferring to water results in unimolecular folding without aggregation at the concentrations used. Interestingly, after the removal of DMF by dialysis against pure water, the size decreased further to 38 nm, possibly due to the swelling of the PNBA core by DMF prior to dialysis. The size distribution remained monomodal (Figure 4.14A). The size of 38 nm for PEO/PNBA MMB-3 in water after dialysis is slightly smaller than the size of 43 nm that was observed for the collapsed state of PEO/PDEGEA MMB-1 in water at 25 ^{o}C. This is probably a result of the increased hydrophobicity of PNBA as well as the shorter DP of PNBA side chains. The hydrophobic *o*-nitrobenzyl groups of PNBA can be cleaved with long wavelength 365 nm UV light, yielding ionizable carboxylic acid groups, thus undergoing a hydrophobic-to-hydrophilic transition upon UV irradiation. A portion of the MMB-3 aqueous solution after dialysis with a polymer concentration of 0.1 mg/g was transferred to a 3.7 mL glass vial and irradiated with 365 nm light using a 4 watt UV lamp. After irradiation for 24 h, there was a clear increase in size to 67 nm (Figure 4.14A), which is slightly larger than the size of 62 nm that was observed in DMF before irradiation, suggesting a transition from the collapsed conformation to an extended worm-like conformation due to photocleavage of hydrophobic *o*-nitrobenzyl moieties of PNBA and solvation of the resulting poly(acrylic acid) (PAA) side chains. The larger size after photocleavage relative to the worm state in DMF is likely due to electrostatic repulsions between ionized carboxylic acid groups in PAA side chains. Figure 4.14B shows the

change in D_h for MMB-3 versus irradiation time. A gradual increase in size was observed in the first 18 h, and after that there was essentially no change in size, indicating that 24 h is sufficient to achieve complete photocleavage. In order to verify the extent of photocleavage, we irradiated 10 mL (split into four 3.7 vials) of an 0.1 mg/g MMB-3 solution after dialysis for 24 h under the same conditions as for the DLS samples. The water was then removed under high vacuum, and the dried brushes were dissolved in DMSO-d_6 for ^{1}H NMR spectroscopy analysis. As can be seen in the ^{1}H NMR spectrum after UV irradiation for 24 h (Appendix C, Figure C9), the peak at 5.18-5.45 ppm (-COOCH_2($C_6H_4NO_2$) of NBA monomer units had completely disappeared, indicating that photocleavage was complete.

The size changes for PEO/PNBA MMB-3 observed by DLS after switching the solvent from DMF to water and then UV irradiation suggest a change in shape in each step, where MMB-3 goes from an extended worm-like morphology in organic solvent (DMF in this case) to a collapsed, roughly spherical collapsed state in water, and then back to the extended worm-like conformation after photocleavage of the *o*-nitrobenzyl moieties with long-wave UV light. Similar to PEO/PDEAEMA and PEO/PDEGEA heterografted brushes before, we investigated the possible shape changing of PEO/PNBA MMB-3 by AFM. Figure 4.15 shows AFM height images of MMB-3 spin coated onto mica from a 0.01 mg/g solution in chloroform. A worm-like morphology was observed as expected for densely grafted molecular brushes in a good solvent for both side chains. Length analysis of representative worm-like brush molecules gave an average contour length of 153 nm and a typical height of approximately 1.5 nm, indicating that the degree of stretching is approximately 75 %. Figure 4.16 shows AFM height images of MMB-3 drop cast onto mica from the 0.1 mg/g solution in water after dialysis. We observed a collapsed globular morphology with a roughly spherical or elliptic shape for many of the collapsed brush molecules, although some

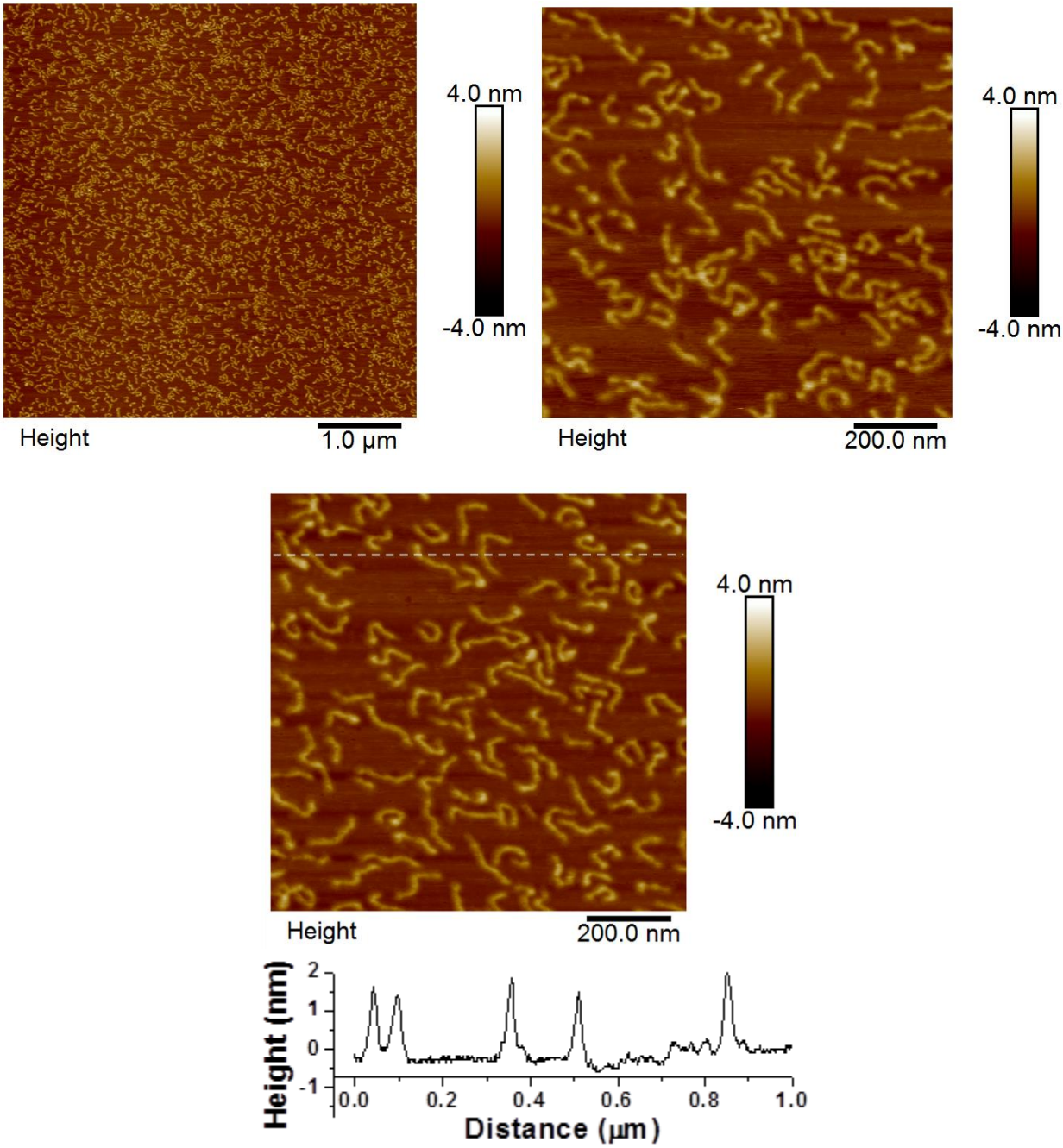

Figure 4.15. AFM height images of PEO/PNBA MMB-3 spin coated onto mica from a 0.01 mg/g solution in chloroform.

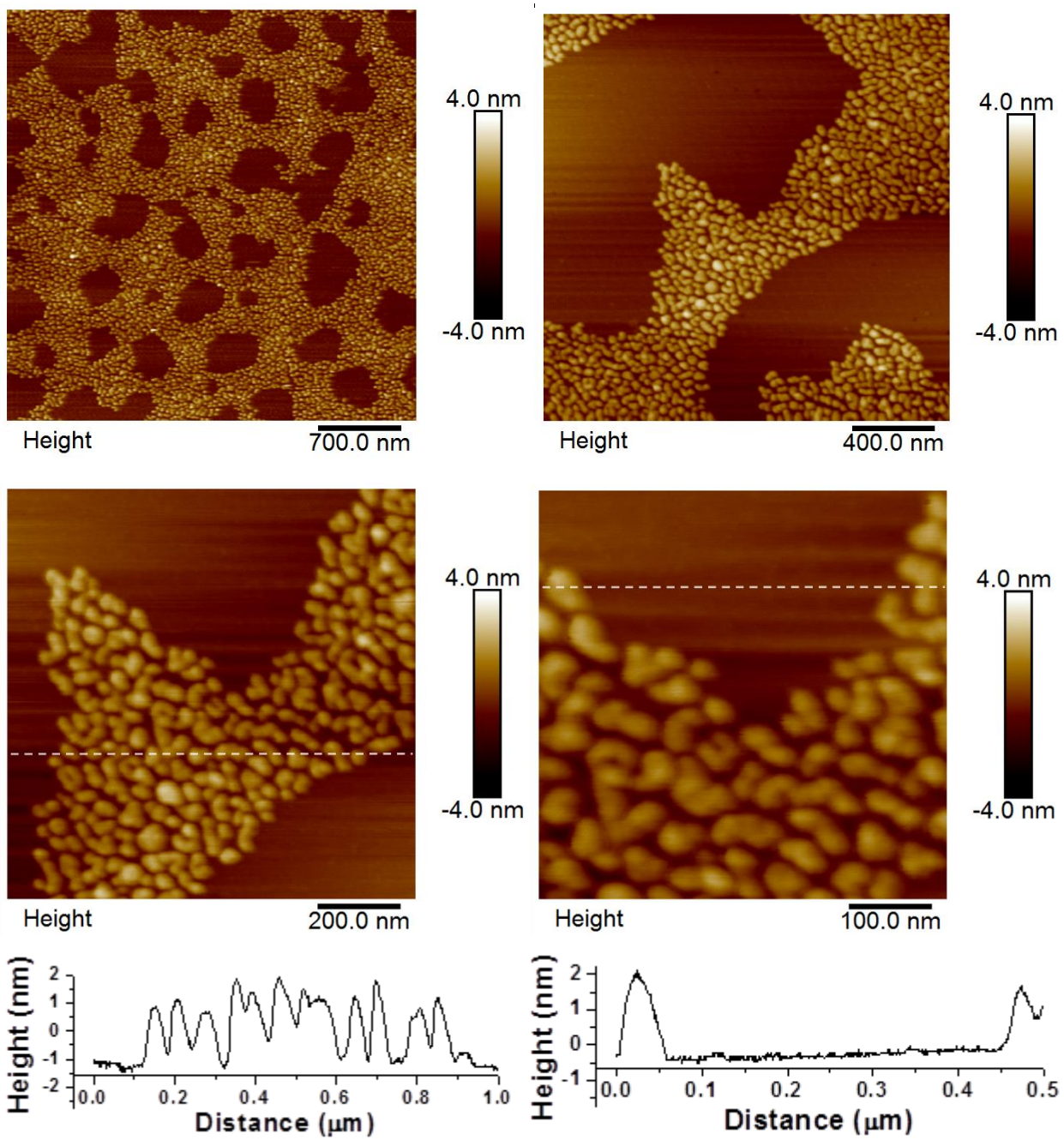

Figure 4.16. AFM height images of PEO/PNBA MMB-3 drop cast onto mica from a 0.1 mg/g solution in water obtained by dialysis against water.

brushes appear to be irregularly or not completely collapsed. This is possibly due the rapid folding of the very hydrophobic PNBA chains during solvent switching combined with the high T_g of PNBA, causing the brushes to become essentially "frozen" in a non-equilibrium collapsed state. Cross-sectional analysis of typical collapsed MMB-3 molecules gave an average diameter of 44 nm and an average height of approximately 2 nm. To visualize the brush molecules after UV irradiation by AFM, we prepared a solution of MMB-3 with a polymer concentration of 0.05 mg/g in 2 mM KH_2PO_4 buffered to a pH of 7.06. The solution was irradiated with 365 nm UV light for 22 h, after which an increase in size from 41 nm to 73 nm was observed by DLS, which is similar to what was observed in pure water shown in Figure 4.14A. Figure 4.17 shows AFM height images of MMB-3 that spin coated onto mica from the buffer solution after 22 h irradiation time. We observed a predominately worm-like morphology as expected, although the brush molecules appear to be clustered together, possibly due to complex electrostatic interactions of charged brush molecules with themselves and with the negatively charged mica surface. Additional AFM images of PEO/PNBA MMB-3 spin coated onto mica from chloroform before UV irradiation and from the buffer solution after UV irradiation can be found in Appendix C (Figures C10 and C11).

4.3.9. Synthesis of Thermosensitive Binary Heterografted Molecular Brushes Composed of PEO and Biotin- and Fluorescent Dye NBD-Containing P(DEGEA-*co*-BA-*co*-NBDA)

Having demonstrated the versatility of this grafting to "click" method to synthesize binary heterografted molecular brushes capable of undergoing changes in shape and size in response to a variety of stimuli, including temperature, pH, and light, we then explored the possibility of using this stimuli-induced shape-changing behavior to regulate interactions between molecular bottlebrushes and other molecules. Our hypothesis is that the functional groups incorporated into the core-forming side chain polymer will have little or no interactions with other molecules when

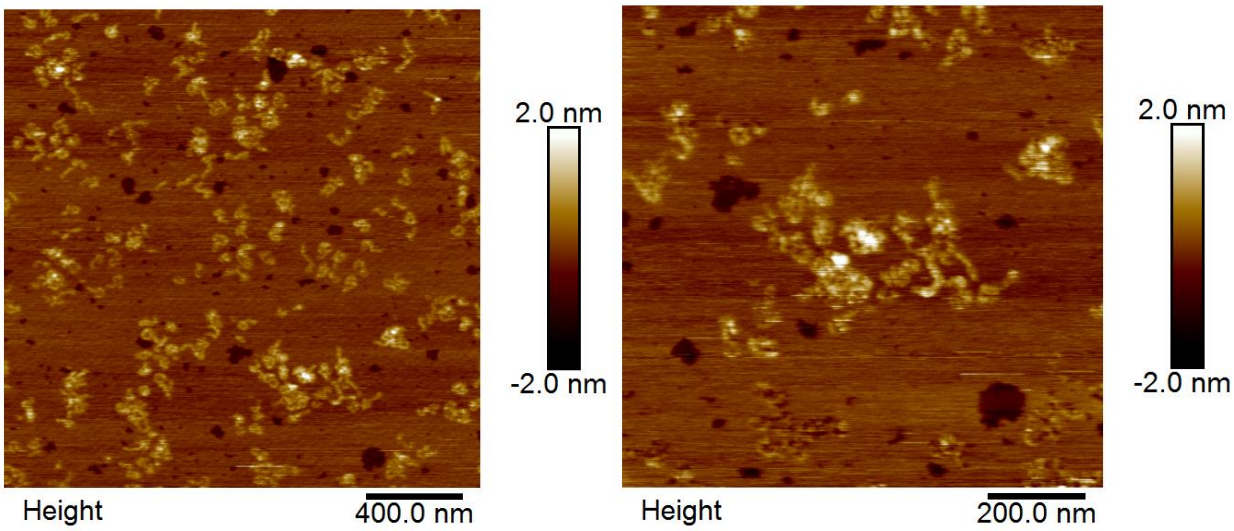

Figure 4.17. AFM height images of PEO/PNBA MMB-3 spin coated onto mica from an aqueous 2 mM KH_2PO_4 solution at pH = 7.06 with a polymer concentration of 0.05 mg/g that had been irradiated with 365 nm UV light for 22 h.

the bottlebrushes are in the collapsed globular state, but become accessible when the brushes are in the extended worm state. It is well known that biotin forms a very strong complex with avidin, a tetrameric protein (~66-69 kDa), that once formed, is essentially irreversible under normal conditions. With this in mind, we prepared a thermosensitive PDEGEA side chain polymer that were incorporated with a small amount of biotin-containing monomer (BA) as well as a fluorescent monomer (NBDA), referred to as P(DEGEA-*co*-BA-*co*-NBDA)-50. NBDA (a fluorescence resonance energy transfer (FRET) donor for rhodamine B) was incorporated as a probe to investigate the possibility of thermo-regulated binding between biotin-containing heterografted bottlebrushes and rhodamine B-labelled avidin using fluorescence spectroscopy. The copolymer was prepared from ATRP of a mixture of DEGEA, BA, and NBDA in anisole with a feed molar ratio of 100 : 1.1 : 0.16, respectively, using alkyne-containing PBiB as initiator. The polymer was purified by repetitive precipitation in hexanes and a mixture of hexanes and diethyl ether (75/25 v/v), and the DP was calculated to be 50 by end group analysis from the ^{1}H NMR spectrum of the purified polymer, using the integrals of the peaks at 4.62 ppm (HC≡CCH_2OOC- of the alkyne end group) and 4.07-4.24 ppm (-COOCH_2- of DEGEA monomer units). The molar contents of BA (0.66 monomer units on average per chain) and NBDA (not detectable by ^{1}H NMR although the polymer was brightly colored) were low, so they were neglected in the calculation of DP. SEC analysis using the PL GPC-20 system with THF showed that the polymerization was well controlled with an $M_{n,SEC}$ of 10,600 Da and a narrow PDI of 1.16. The SEC trace and ^{1}H NMR spectrum of the purified polymer can be found in Appendix C (Figure C3).

Thermosensitive PEO/P(DEGEA-*co*-BA-*co*-NBDA) binary heterografted molecular brushes, referred to as PEO/P(DEGEA-*co*-BA-*co*-NBDA) MMB-4 in Table 4.2, were synthesized using PTEGN$_3$MA-800 backbone and PEO-114 and P(DEGEA-*co*-BA-*co*-NBDA)-50 side chain

polymers under similar conditions as for PEO/PDEGEA MMB-1. Here, we used the longer PEO-114 (from 5 kDa PEO) instead of PEO-45 (from 2 kDa PEO) for the purpose of reducing the likelihood of interactions between the collapsed P(DEGEA-*co*-BA-*co*-NBDA) core at high temperature and avidin. Comparable to the other stimuli-responsive heterografted brushes discussed, we used a molar ratio of 1 : 1.92 for the backbone monomer units in PTEGN_3MA-800 backbone to total side chain polymers PEO-114 and P(DEGEA-*co*-BA-*co*-NBDA)-50. The molar ratio of PEO to P(DEGEA-*co*-BA-*co*-NBDA) in the feed was 0.600 : 0.400, similar to the other heterografted brushes. Figure 4.18 shows the SEC traces of the final reaction mixture after 44 h as well as PEO/P(DEGEA-*co*-BA-*co*-NBDA) MMB-4 after removal of unreacted side chains by centrifugal filtration. Propargyl alcohol was injected to cap any unreacted backbone azide units 2 h before the reaction was stopped. After 44 h, a high molecular weight peak was observed by SEC with a $M_{n,\,SEC}$ of 1,226,200 Da and a PDI of 1.12 which was attributed to the brushes molecules formed from the click reaction. From the relative peak areas in SEC, the mixture contained 41.01 % brushes and 58.99 % unreacted PEO and P(DEGEA-*co*-BA-*co*-NBDA) side chains. Once the basis of the molar ratio of monomer units of PTEGN_3MA-800 to the total side chain polymer in feed (1 : 1.92), the grafting density was calculated to be 77.5 %, assuming the molar ratio of PEO and P(DEGEA-*co*-BA-*co*-NBDA) are the same in the brushes as in the feed. This value is similar to the grafting density obtained for PEO/PDEGEA MMB-1 (74.3 %).

PEO/P(DEGEA-*co*-BA-*co*-NBDA) heterografted molecular bottlebrushes were purified by passing the reaction mixture through a neutral alumina column to remove the catalyst, and the unreacted side chains were removed by repeated centrifugal filtration in 50/50 v/v methanol/water using a 50 kDa MWCO dialysis membrane. SEC analysis of purified PEO/P(DEGEA-*co*-BA-*co*-NBDA) MMB-4 showed that the unreacted side chain polymers PEO-114 and P(DEGEA-*co*-BA-

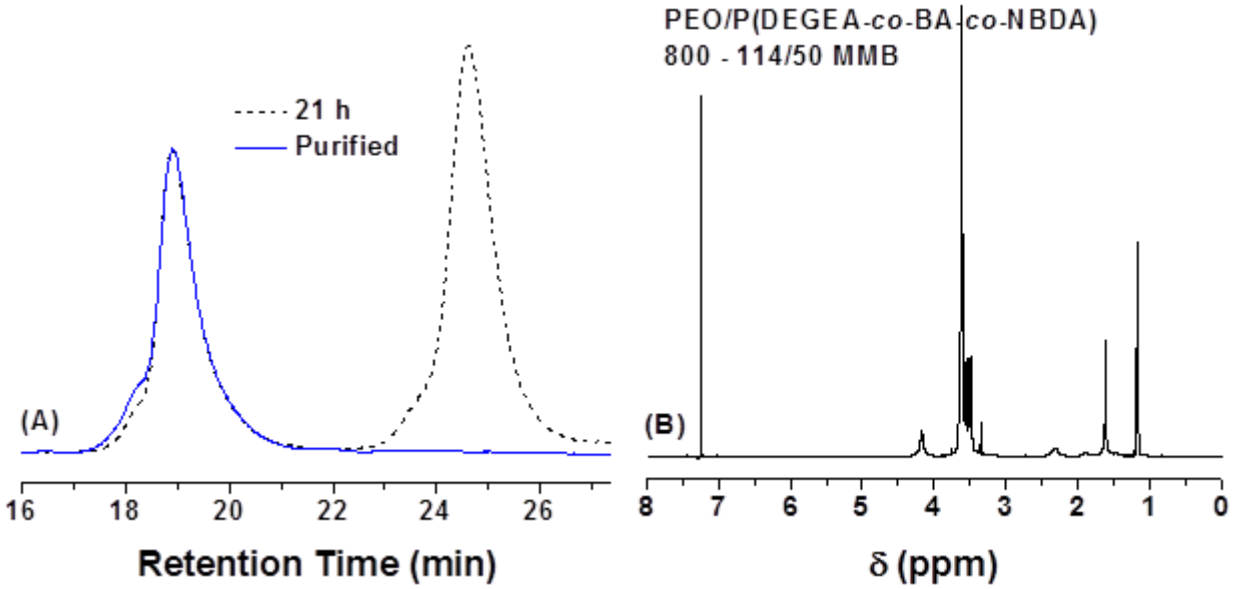

Figure 4.18. (A) SEC traces of PEO/P(DEGEA-*co*-BA-*co*-NBDA) MMB-4 before and after removal of unreacted side chains by centrifugal filtration. (B) ^{1}H NMR spectrum of PEO/P(DEGEA-*co*-BA-*co*-NBDA) MMB-4 in $CDCl_3$. SEC analysis was carried out on PL GPC-50 Plus system with Agilent Mixed-B columns using DMF containing 50 mM LiBr as carrier solvent.

co-NBDA)-50 were completely removed and that the molecular weight distribution was essentially the same ($M_{n,\ SEC}$ = 1,265,900; PDI = 1.13 after purification) (Figure 4.18A). The ^{1}H NMR spectrum of purified MMB-4 is shown in Figure 4.18B. Using the integrals of the peaks at 4.08-4.31 ppm (-COOCH_2CH$_2$- of DEGEA monomer units) and 3.46-3.72 ppm (-OCH_2CH_2- of PEO and -COOCH$_2$CH_2OCH_2CH_2OCH_2CH$_3$ of DEGEA monomer units) from the ^{1}H NMR spectrum, the molar ratio of PEO to P(DEGEA-*co*-BA-*co*-NBDA) side chains in the purified brush was found to be 0.611 : 0.389, which was very close to the feed ratio of 0.600 : 0.400, although slightly enriched in PEO, resembling the observations for MMB-1, MMB-2, and MMB-3. However, it is interesting to note that MMB-4 has the smallest discrepancy between the brush and feed compositions among all the heterografted molecular brushes described in this chapter: 1.1 % for MMB-4 compared to 2.1 %, 5.3 %, and 2.0 % for MMB-1, MMB-2, and MMB-3 respectively. This likely due to the smaller difference in molecular weight between the two side chains in MMB-4 (PEO-114 was used instead of PEO-45).

4.3.10. Thermosensitive Properties of PEO/P(DEGEA-*co*-BA-*co*-NBDA) Binary Heterografted Molecular Brushes

As for other binary heterografted molecular bottlebrushes, we studied the thermoresponsive properties of PEO/P(DEGEA-*co*-BA-*co*-NBDA) MMB-4 brushes in water by DLS and AFM. Figure 4.19 shows the apparent hydrodynamic diameter (D_h) at different temperatures for a solution of MMB-4 in water with a polymer concentration of 0.2 mg/g. At 1 ^{o}C, MMB-4 exhibited a D_h of 79 nm, which is significantly larger than the size of 64 nm observed for PEO/PDEGEA MMB-1 in water at 1 ^{o}C. This is most likely the result of the much longer PEO side chains in MMB-4. The size showed a significant decrease at approximately 11 ^{o}C and levelled off at ~19 ^{o}C with a size of 68 nm with little change in size up to 25 ^{o}C. The transition zone was 14 ^{o}C. Although

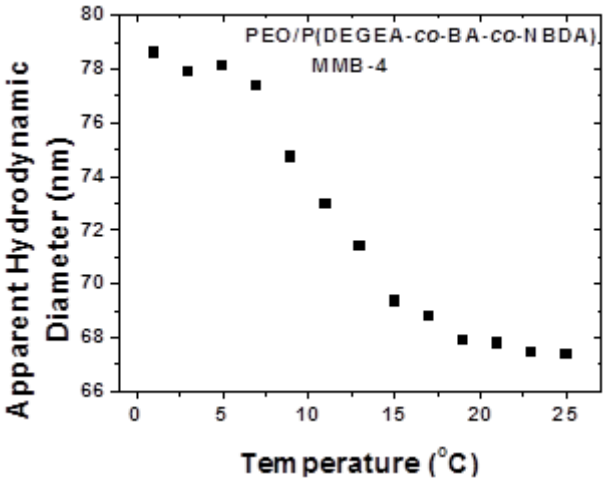

Figure 4.19. Results of DLS for a 0.2 mg/g aqueous solution of PEO/P(DEGEA-*co*-BA-*co*-NBDA) MMB-4 at different temperatures.

still centering around the same temperature, the transition is apparently broader for MMB-4 than MMB-1, and the relative size decrease is also less dramatic for MMB-4, which exhibits a 14 % reduction in size over 14 ^{o}C compared to a 33 % reduction in size over 10 ^{o}C for MMB-1. This is likely another result of the extended length of the PEO side chains in MMB-4, causing the P(DEGEA-*co*-BA-*co*-NBDA) side chains, whose collapse is responsible for the change in size, to occupy a relatively smaller proportion of volume per brush molecule in both the extended and collapsed states of MMB-4 (52.6 % P(DEGEA-*co*-BA-*co*-NBDA) by mass) compared to PDEGEA side chains in MMB-1 (68.0 % PDEGEA by mass).

Because PEO/P(DEGEA-*co*-BA-*co*-NBDA) MMB-4 exhibited similar thermosensitive responsive behavior as PEO/PDEGEA MMB-1, we used AFM to investigate whether the change in size observed by DLS was also accompanied by a change in shape from an extended worm-like state at low temperature to a collapsed globular state at temperatures above the LCST of P(DEGEA-*co*-BA-*co*-NBDA) side chains. We initially tried spin coating dilute aqueous solutions of MMB-4 onto freshly cleaved mica at 0 ^{o}C and 40 ^{o}C, similar to what was done for MMB-1 previously. For the sample prepared at 0 °C, we observed a worm-like morphology as expected (Figure 4.20). Compared to PEO/PDEGEA MMB-1 spin coated at 0 ^{o}C, MMB-4 appears to be more stretched and flatter on the mica substrate, probably due to the longer PEO side chains in MMB-4 and the favorable interactions with the hydrophilic mica surface. Length analysis of typical worm-like brush molecules gave an average contour length of 196 nm and a typical height of approximately 0.5 nm. Based on a maximum length of 203 nm for a fully extended backbone polymer chain with a DP of 800, this indicates that the degree of stretching is approximately 97 %. For MMB-4 spin coated onto mica at 40 ^{o}C, we observed a coexistence of brushes with worm-like as well as globular morphologies, with the majority of the brushes exhibiting an extended

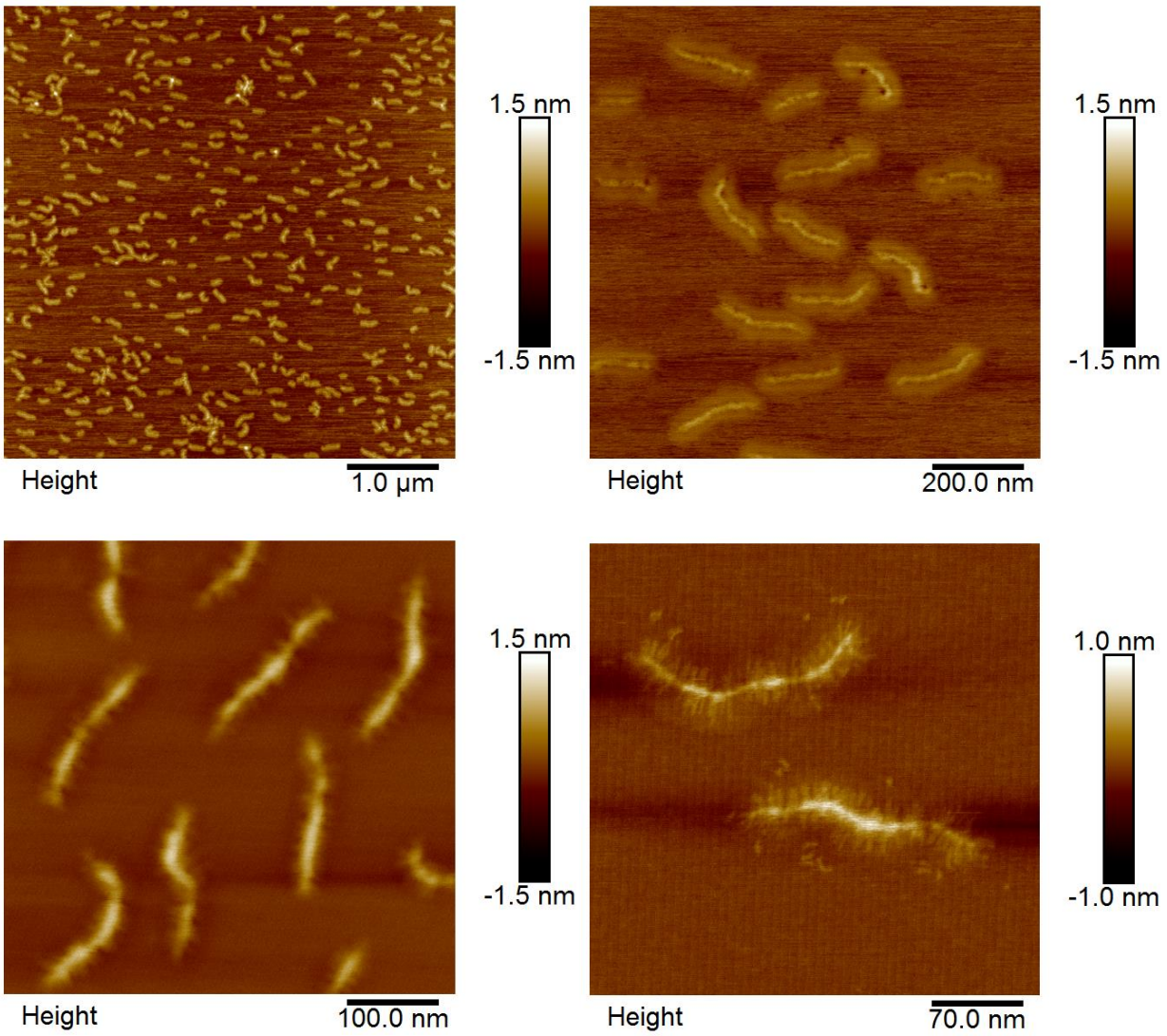

Figure 4.20. AFM height images of PEO/P(DEGEA-*co*-BA-*co*-NBDA) MMB-4 spin coated onto mica from an aqueous solution at 0 ºC with a polymer concentration of 0.05 mg/g.

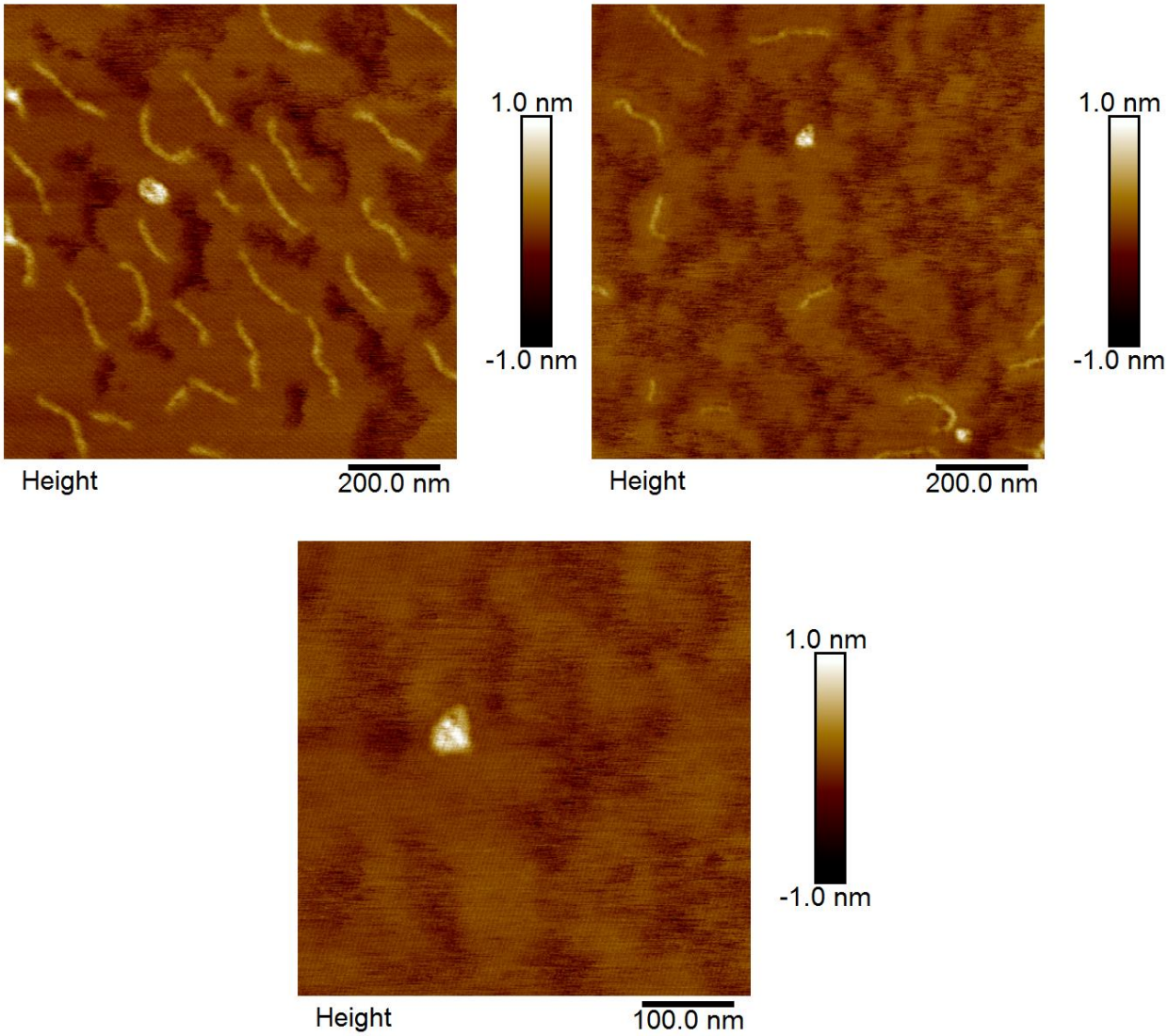

Figure 4.21. AFM height images of PEO/P(DEGEA-*co*-BA-*co*-NBDA) MMB-4 spin coated onto mica from an aqueous solution at 40 ^{o}C with a polymer concentration of 0.05 mg/g.

worm-like conformation (Figure 4.21). Cross-sectional analysis of one of the collapsed brushes with a globular morphology gave a diameter of 54 nm and a height of approximately 1 nm. The predominance of the worm-like morphology observed at 40 ^{o}C by AFM is contrary to what would be expected based on the size transition observed by DLS in Figure 4.19. We believe this is likely a result of unfolding of the brushes during sample preparation due to a combination of favorable surface interactions as well as the shear force exerted on the brushes by spin-coating, which is promoted by the high degree of conformational strain on the backbone by the longer PEO side chains. In fact, for MMB-1 spin cast onto mica at 40 ^{o}C, while collapsed brushes with a globular conformation were observed near the center of the substrate, we observed the worm-like morphology closer to the edge of the sample where the shearing force would be larger during spin coating.

In an effort to reduce surface interactions between the brushes and the hydrophilic mica substrate and thus observe a more accurate representation of the solution morphology for PEO/P(DEGEA-*co*-BA-*co*-NBDA) MMB-4 using AFM, we first hydrophobized the substrate by spin coating a thin layer of polystyrene (PS, 30 kDa, from a 1 wt % solution in chloroform) onto the freshly cleaved mica surface at 10,000 rpm. Subsequently, we deposited MMB-4 onto the polystyrene-coated mica (mica-PS) surface from dilute solutions in water at 0 ^{o}C and 45 ^{o}C by drop casting, instead of spin coating, in order to avoid any conformational changes due to the applied shear forces. For the sample drop cast onto mica-PS at 0 °C, we observed the worm-like morphology as expected (Figure 4.22). Length analysis of representative worm-like brush molecules gave an average contour length of 178 nm and a typical height of approximately 1 nm. This indicated a degree of stretching of approximately 88 %. For the brushes drop cast onto mica-PS at 45 ^{o}C, shown in Figure 4.23, we observed a globular morphology for the collapsed state,

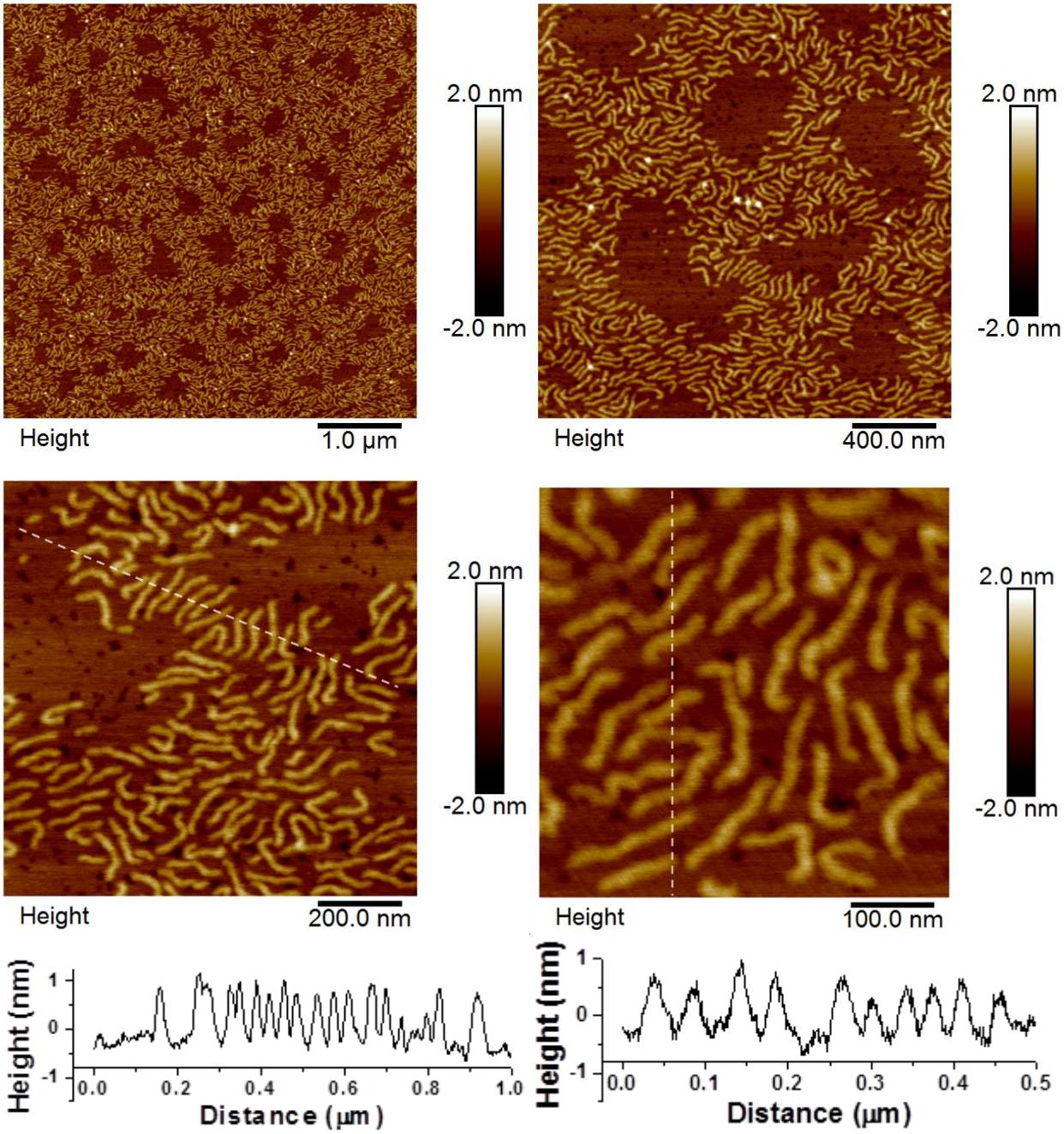

Figure 4.22. AFM height images of PEO/P(DEGEA-*co*-BA-*co*-NBDA) MMB-4 drop cast onto mica-PS from an aqueous solution at 0 ºC with a polymer concentration of 0.05 mg/g.

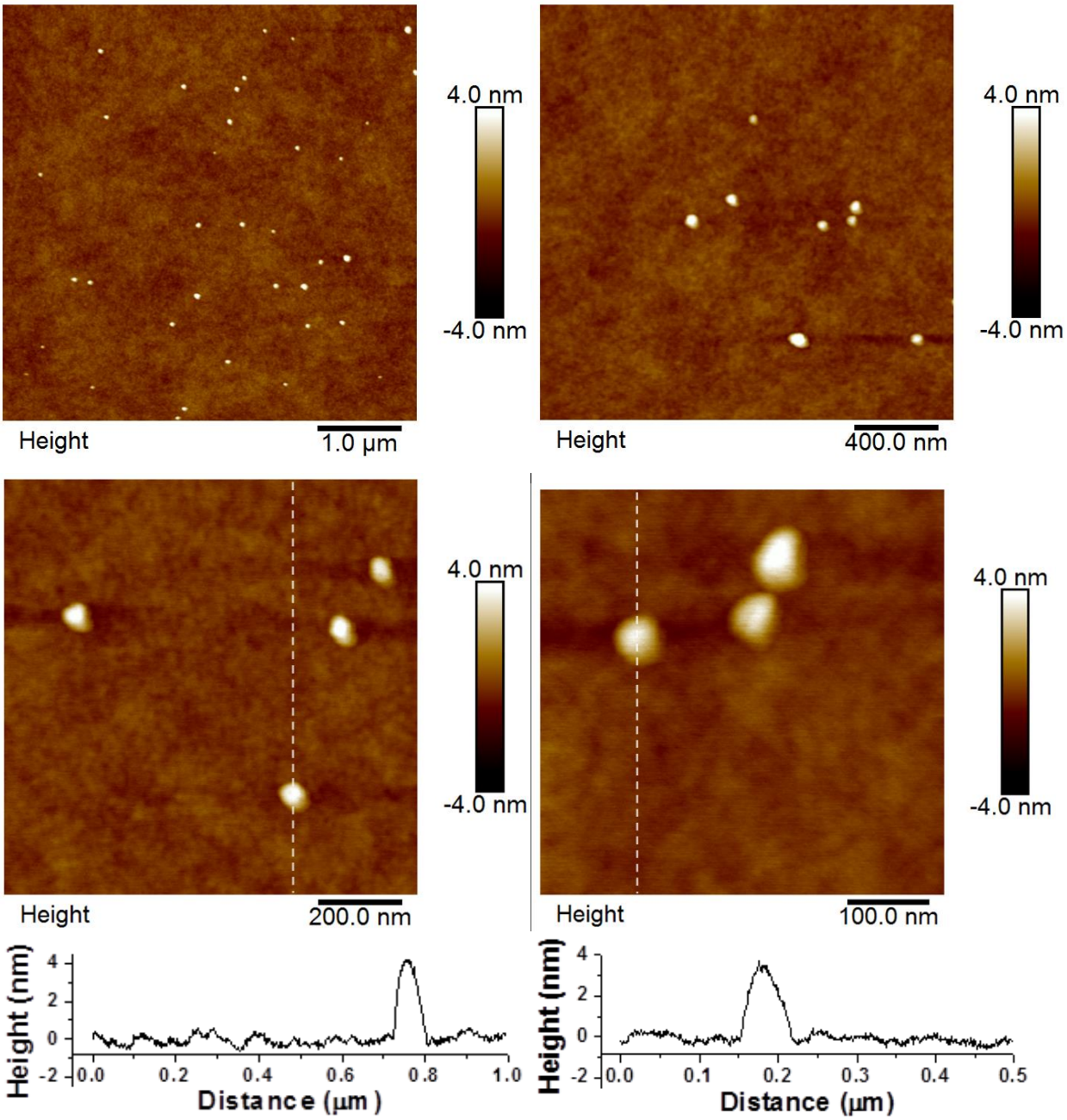

Figure 4.23. AFM height images of PEO/P(DEGEA-*co*-BA-*co*-NBDA) MMB-4 drop cast onto mica from an aqueous solution at 45 ºC with a polymer concentration of 0.01 mg/g.

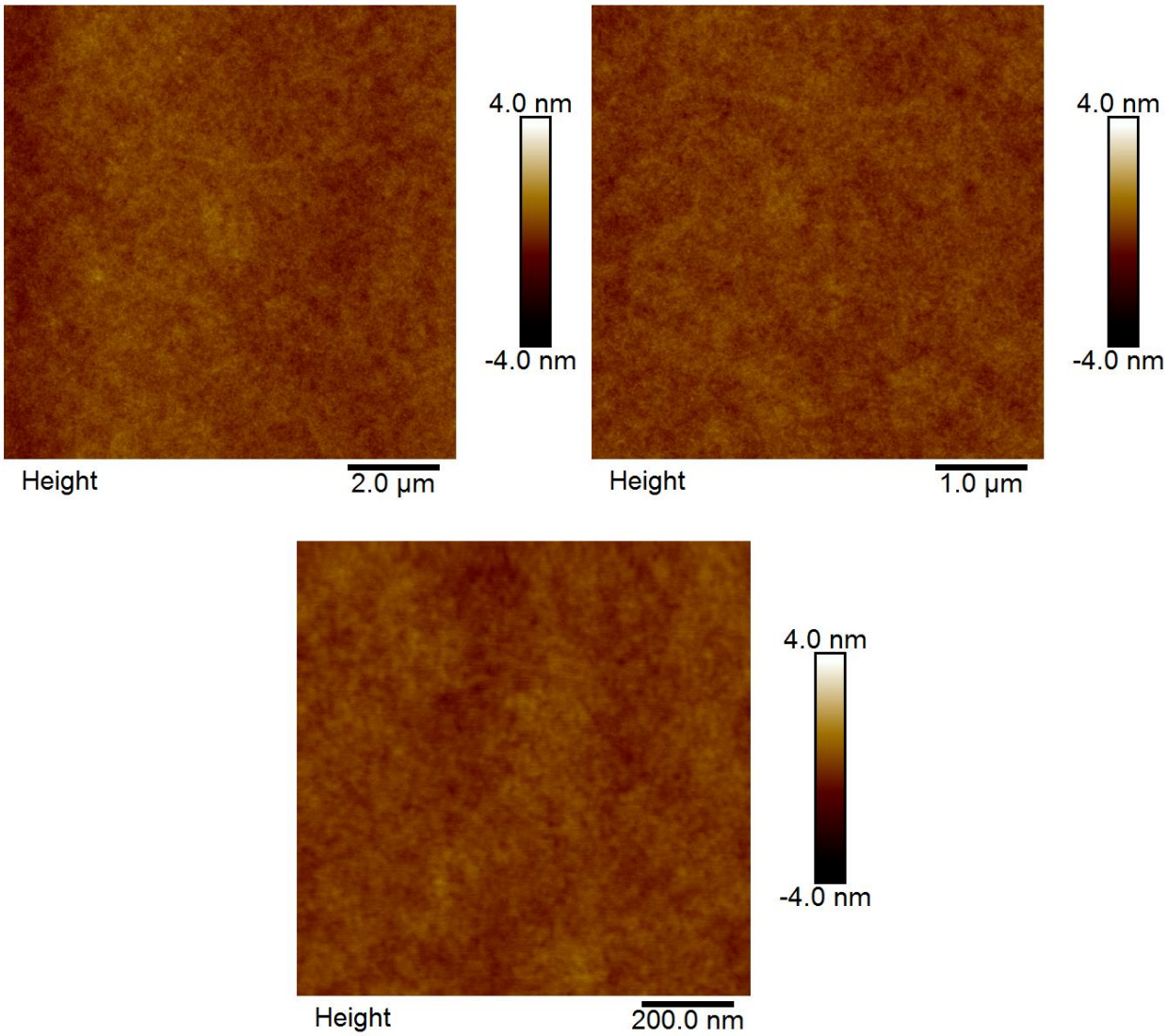

Figure 4.24. AFM height images of a mica-PS control sample that had been spin coated with Milli-Q water.

consistent with the DLS results of MMB-4 and the temperature-dependent morphological changes observed for MMB-1 previously. A cross-sectional analysis of typical collapsed brushes gave an average diameter of 65 nm and an average height of approximately 3.5 nm. As a control, we spin coated Milli-Q water onto a clean mica-PS substrate for AFM analysis (Figure 4.24). We observed a clean, flat surface, indicating that the polystyrene film is free of defects and did not interfere with AFM analysis. Additional AFM images of PEO/P(DEGEA-*co*-BA-*co*-NBDA) MMB-4 drop cast onto mica-PS at 0 ºC and 45 ºC can be found in Appendix C (Figures C13 and C14).

4.3.11. FRET Study of Thermo-Regulated Binding Between Biotin-Containing PEO/P(DEGEA-co-BA-co-NBDA) Binary Heterografted Molecular Brushes and Avidin

The stimuli-induced shape changing of binary heterografted molecular bottlebrushes offers an opportunity to control the interaction of brush molecules with their environment. As a demonstration, we studied the binding between biotin-containing PEO/P(DEGEA-*co*-BA-*co*-NBDA) MMB-4 and rhodamine-labelled avidin in aqueous solution at different temperatures using fluorescence spectroscopy. We prepared an aqueous solution containing a mixture of MMB-4 with a concentration of 0.005 mg/g and avidin with a concentration of 0.025 mg/g by mixing 0.598 g of a MMB-4 aqueous solution with a polymer concentration of 0.010 mg/g and 0.606 g of an avidin solution with an avidin concentration of 0.050 mg/g at 40 °C. Before mixing, both solutions were equilibrated at 40 °C for 2 h to ensure that the MMB-4 brush molecules were in the collapsed globular state. Two additional solutions containing 0.005 mg/g MMB-4 and 0.025 mg/g avidin alone were also prepared and used as controls for comparison. Each solution was prepared and maintained at 40 °C, and fluorescence emission spectra were recorded at various time intervals over a period of 19 h. The temperature of each solution was then lowered to 0 °C, and fluorescence measurements were continued for an additional 29 h at various time intervals. Fluorescence

resonance energy transfer (FRET), which occurs when the donor and acceptor molecules are within a distance of 1-10 nm of each other, between NBD (FRET donor) in the brushes and rhodamine (FRET acceptor) in avidin was used to probe the binding behavior between biotin-containing MMB-4 and avidin protein molecules.

Figure 4.25 shows the fluorescence emission spectra recorded at various time intervals at 40 °C and 0 °C for the 0.005 mg/g MMB-4 control sample (Figure 4.25A, Solution **1**), the 0.025 mg/g avidin control sample (Figure 4.25B, Solution **2**), and the mixture containing 0.005 mg/g MMB-4 and 0.025 mg/g avidin (Figure 4.25C, Solution **3**). After preparing and maintaining the samples at 40 °C for 19 h, we observed an overall decrease in fluorescence intensity for all three samples over time, although the intensity ratio of the NBD peak, with a maximum at approximately 520 nm, and the rhodamine peak, with a maximum at approximately 570 nm, did not appear to change much (see discussion later). After 19 h, we decreased the temperature of each of the three samples to 0 °C using an ice/water bath and continued monitoring the samples with fluorescence spectroscopy at various times intervals. After 5 min, the fluorescence intensity of MMB-4 at ~ 520 nm increased by ~ 13%, while the intensity of avidin at ~ 570 nm increased only very slightly (by ~ 1.7 %). Differently, for the sample containing both MMB-4 and avidin, the peak intensity at ~ 522 nm decreased by ~ 2.5% while the intensity of the peak at ~ 570 nm increased by ~ 7.4%. This suggested FRET occurred even after only 5 min. After that, we observed a continued gradual decrease in fluorescence intensity over time. However, the intensity ratio of the peaks at 570 nm and 520 nm increased gradually for the mixture of MMB-4 and avidin, while the intensity ratio from the two controls samples did not appear to change significantly, suggesting the occurrence of FRET between NBD and rhodamine due to binding between the biotin moieties in MMB-4 and avidin after the temperature was lowered to 0 °C.

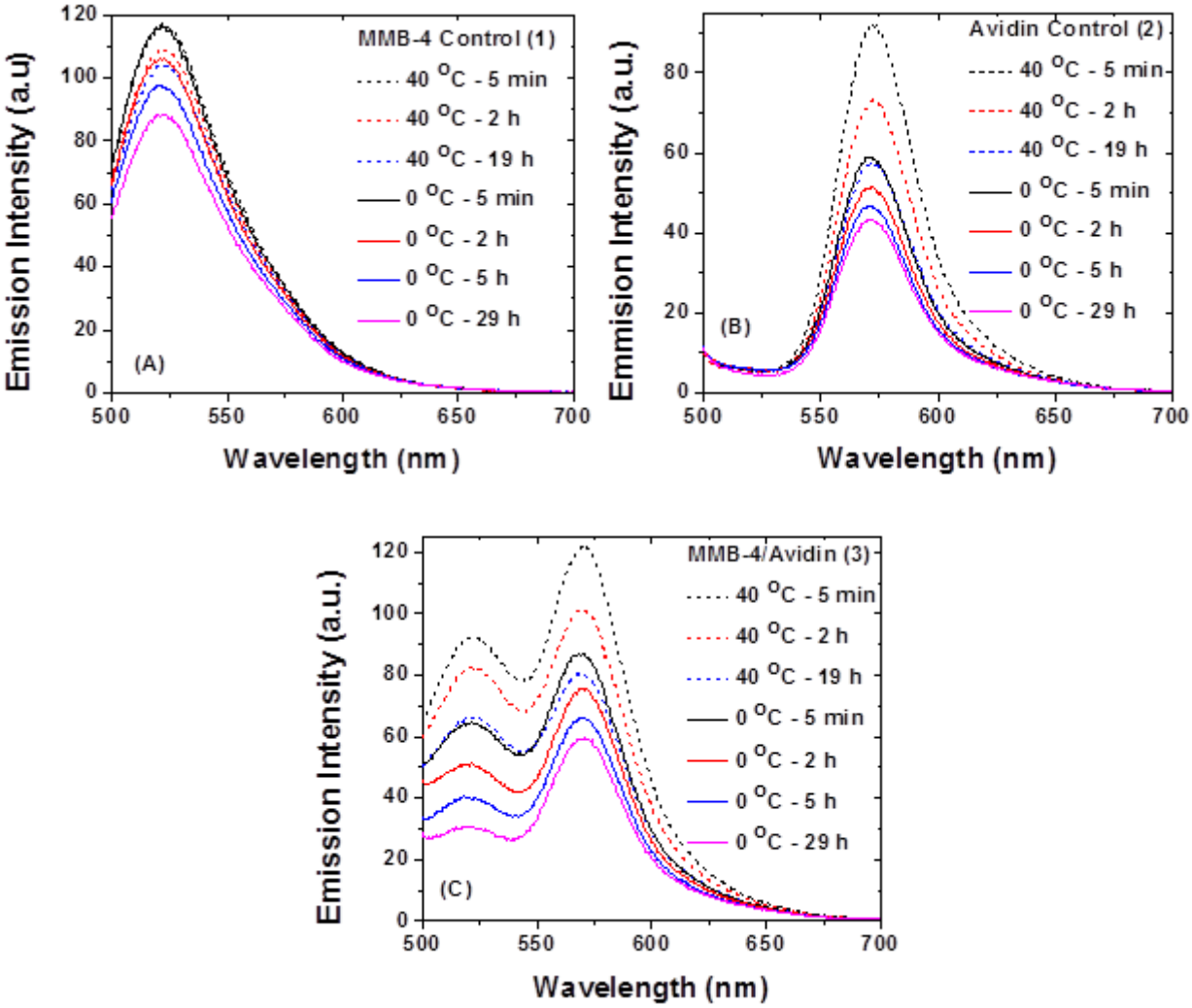

Figure 4.25. Fluorescence emission spectra recorded at various time intervals at 40 ºC and 0 ºC for aqueous solutions of (A) 0.005 mg/g MMB-4 as a control sample, (B) 0.025 mg/g avidin as a control sample, and (C) a mixture containing 0.005 mg/g MMB-4 and 0.025 mg/g avidin.

To get a better illustration of whether or not FRET occurred to an appreciable extent at each temperature, we plotted the ratio of the fluorescence emission intensity for the peaks at 570 nm (from rhodamine) and 520 nm (from NBD) for the MMB-4/avidin sample and the two control samples, shown in Figures 2.26 and 2.27. For the two control samples, we plotted both the I_{570}/I_{520} ratio from the two spectra summed together and the intensity ratio of the two curves alone. For the mixture of MMB-4 and avidin (Solution **3**), we found that there was an initial decrease in I_{570}/I_{520} over time at 40 °C, although it appeared to level off and reached a relatively steady state after approximately 2 h of incubation time. There was essentially no or very little change in the intensity ratio between 2 and 19 h (the ratios were 1.23 and 1.21, respectively), when the last spectrum at 40 °C was recorded. The intensity ratio obtained from the two control samples (**1** and **2**) showed a similar trend initially but continued to decrease gradually over time. After the temperature was lowered to 0 °C, below the LCST of the biotin-containing P(DEGEA-*co*-BA-*co*-NBDA) side chains of MMB-4, we observed an immediate increase in I_{570}/I_{520} after just 5 min of incubation time for the MMB-4/avidin mixture, while I_{570}/I_{520} decreased slightly for the control samples. This suggests the occurrence of FRET due to binding between biotin moieties in MMB-4 and avidin as a result of the P(DEGEA-*co*-BA-*co*-NBDA) side chains becoming exposed to the environment as the brushes unfolded from the collapsed globular state to the extended worm-like state. As the temperature was maintained at 0 ^{o}C over a period of 29 h, we continued to see a gradual increase in I_{570}/I_{520} for the MMB-4/avidin mixture, while the I_{570}/I_{520} decreased slightly for the control samples over the same time period. Although we cannot rule out the occurrence of FRET to some extent, and thus binding between biotin-containing brushes and avidin, during incubation at 40 °C, the clear increase in I_{570}/I_{520} for the MMB-4/avidin solution relative to the control samples

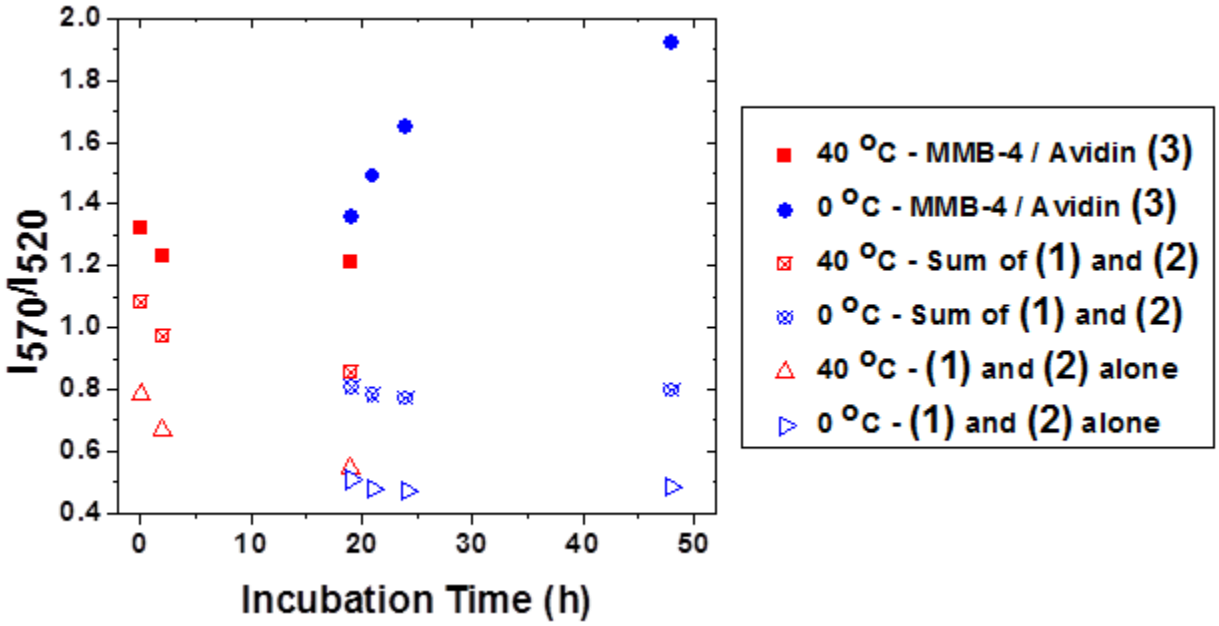

Figure 4.26. Plot of the ratio of fluorescence emission intensity for the peaks at 570 nm and 520 nm from the fluorescence emission spectra recorded at various time intervals at 40 ºC and 0 ºC for aqueous solutions containing a mixture of 0.005 mg/g MMB-4 and 0.025 mg/g avidin (Solution **3**) as well as solutions containing 0.005 mg/g MMB-4 alone (Solution **1**) and 0.025 mg/g avidin alone (Solution **2**) as control samples.

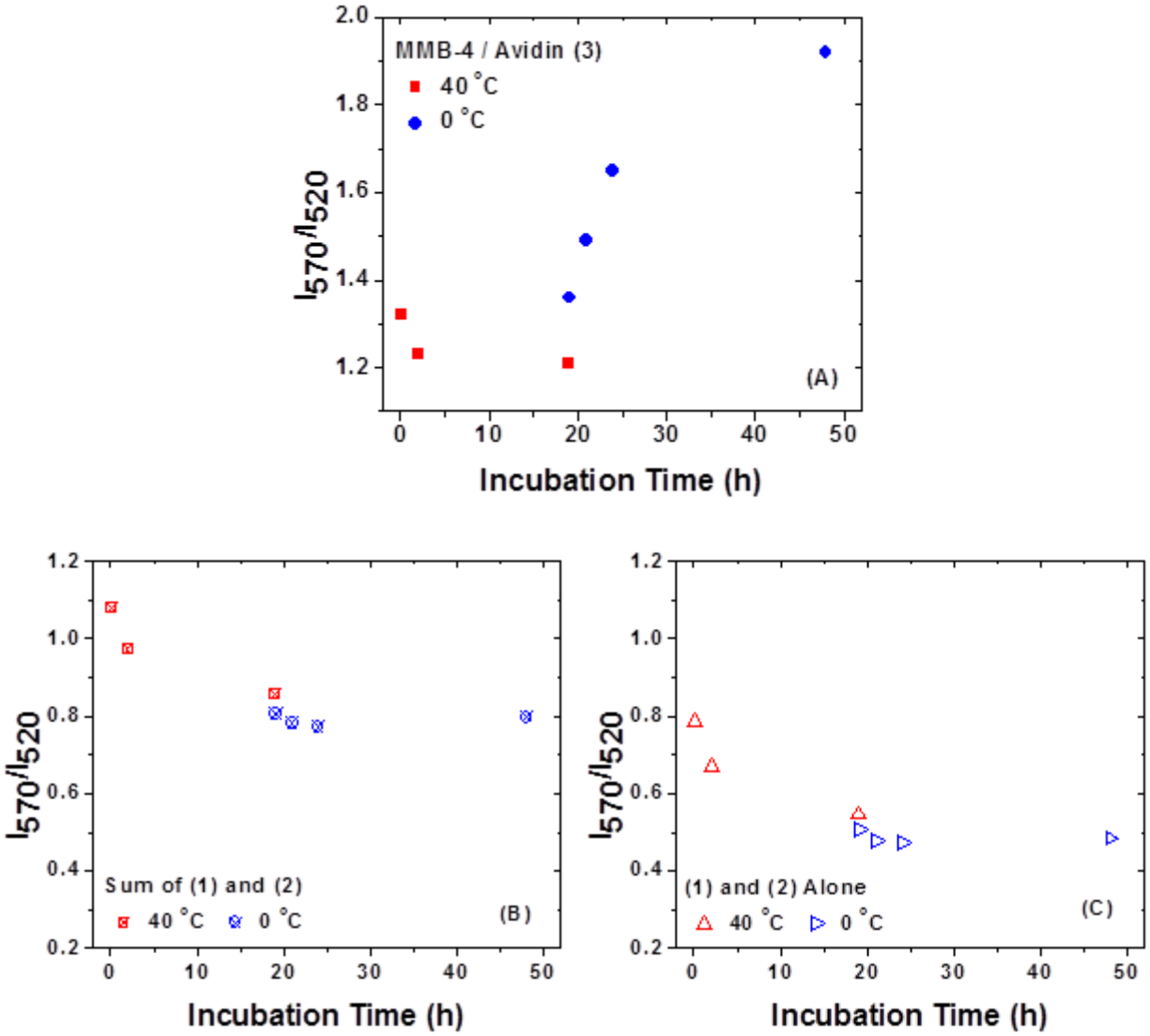

Figure 4.27. Graph from Figure 4.26 split into three separate plots. (A) Plot of the ratio of fluorescence emission intensity for the peaks at 570 nm and 520 nm (I_{570}/I_{520}) from the fluorescence emission spectra recorded at various time intervals at 40 ºC and 0 ºC for aqueous solutions containing a mixture of 0.005 mg/g MMB-4 and 0.025 mg/g avidin (Solution **3**). (B) Plot of (I_{570}/I_{520}) from the sum of the fluorescence emission spectra for the control samples containing 0.005 mg/g MMB-4 alone (Solution **1**) and 0.025 mg/g avidin alone (Solution **2**). (C) Plot of (I_{570}/I_{520}) from the separate fluorescence emission spectra for the control samples containing 0.005 mg/g MMB-4 alone (Solution **1**) and 0.025 mg/g avidin alone (Solution **2**).

observed upon lowering the temperature below the LCST of the P(DEGEA-*co*-BA-*co*-NBDA) side chains demonstrates a significant level of control over the binding interaction between brush molecules and avidin.

4.4. Conclusions

We demonstrated the synthesis and shape-changing behavior of stimuli-responsive binary heterografted molecular brushes composed of PEO (DP = 45) and either thermosensitive PDEGEA, pH-responsive PDEAEMA, or light-responsive PNBA side chains randomly distributed along the backbone. High aspect ratio brushes were made by a "grafting to" method using CuAAC "click" reactions between an azide-functionalized backbone polymer with a DP of 800 and alkyne end-functionalized side chain polymers. High grafting densities were achieved using a molar ratio of backbone monomer units to total side chains of approximately 1 : 2. For PEO/PDEGEA and PEO/PNBA heterografted brushes, the molar ratio of PEO and the other side chain in the purified brushes was found to be very close to that in feed. PEO/PDEAEMA brushes exhibited a larger discrepancy with the feed composition, being enriched in PEO and less densely grafted than the other two samples. Pure brushes were obtained by fractionation or centrifugal filtration. Stimuli-induced size changes in aqueous solution were studied by DLS, and shape transitions from the extended worm-like conformation to the collapsed, roughly spherical globular state and/or vice versa were directly observed AFM. Additionally, we synthesized thermosensitive binary heterografted brushes containing PEO (DP = 114) and biotin-containing, fluorescently-labelled P(DEGEA-*co*-BA-*co*-NBDA) side chains. We found that binding between rhodamine-labelled avidin and PEO/P(DEGEA-*co*-BA-*co*-NBDA) brushes was increased dramatically upon thermo-induced "unraveling" of the brushes from the collapsed state to the extended worm-like conformation, as observed by fluorescence spectroscopy. This work provides a step toward the

design of bio-inspired macromolecules that can exploit stimuli-induced changes in shape to regulate molecular interactions with the environment.

References

1. Sheiko, S. S.; Sumerlin, B. S.; Matyjaszewski, K. *Prog. Polym. Sci.* **2008**, *33*, 759-785.
2. Lee, H.; Pietrasik, J.; Sheiko, S. S.; Matyjaszewski, K. *Prog. Polym. Sci.* **2010**, *35*, 24-44.
3. Rzayev, J. *ACS Macro Lett.* **2012**, *1*, 1146-1149.
4. Yuan, W.; Zhang, J.; Zuo, H.; Shen, T.; Ren, J. *Polymer* **2012**, *53*, 956-966.
5. Gil, E. S.; Hudson, S. M. *Prog. Polym. Sci.* **2004**, *29*, 1173-1222.
6. Seuring, J.; Agarwal, S. *Macromol. Rapid Commun.* **2012**, *33*, 1898-1920.
7. Jeong, B. M.; Bae, Y. M.; Lee, D. S.; Kim, S. W. *Nature* **1997**, *388*, 860-862
8. Lutz, J-F. *J. Polym. Sci. Part A: Polym. Chem*. 2008, 46, 3459-3470.
9. Schild, H. G. *Prog. Polym. Sci.* **1992**, 17, 163-249.
10. Kutnyanszky, E.; Hempenius, M. A.; Vancso, G. J. *Polym. Chem.* **2014**, *5*, 771-783.
11. Pietrasik, J.; Sumerlin, B. S.; Lee, B. Y.; Matyjaszewski, K. *Macromol. Chem. Phys.* **2007**, *208*, 30-36.
12. Yamamoto, S.; Pietrasik, J.; Matyjaszewski, K. *Macromolecules* **2007**, *40*, 9348-9353.
13. Yamamoto, S.; Pietrasik, J.; Matyjaszewski, K. *Macromolecules* **2008**, *41*, 7013-7020.
14. Zhang, N.; Huber, S.; Schulz, A.; Luxenhofer, R.; Jordan, R. *Macromolecules* **2009**, *42*, 2215-2221.
15. Zhang, N.; Luxenhofer, R.; Jordan, R. *Macromol. Chem. Phys.* **2012**, *213*, 973-981.
16. Zhang, N.; Luxenhofer, R.; Jordan, R. *Macromol. Chem. Phys.* **2012**, *213*, 1963-1969.
17. Lahasky, S. H.; Lu, L.; Huberty, W. A.; Cao, J.; Guo, L.; Garno, J. C.; Zhang, D. *Polym. Chem.* **2014**, *5*, 1418-1426.
18. Li, X.; ShamsiJazeyi, H.; Pesek, S. L.; Agrawal, A.; Hammouda, B.; Verduzco, R. *Soft Matter* **2014**, *10*, 2008-2015.

19. Lee, H. L.; Pietrasik, J.; Matyjaszewski, K. *Macromolecules* **2006**, *39*, 3914-3920.

20. Li, C.; Gunari, N.; Fischer, K.; Janshoff, A.; Schmidt, M. *Angew. Chem. Int. Ed.* **2004**, *43*, 1101-1104.

21. Balamurugan, S. S.; Grigor, B. B.; Yang, Y.; McCarley, R. L. *Angew. Chem. Int. Ed.* **2005**, *44*, 4872-4876.

22. Lee, H.; Boyce, J. R.; Nese, A.; Sheiko, S. S.; Matyjaszewski, K. *Polymer* **2008**, *49*, 5490-5496.

23. Xu, Y.; Bolisetty, S.; Drechsler, M.; Fang, B.; Yuan, J.; Ballauff, M.; Muller, A. X. E. *Polymer* **2008**, *49*, 3957–64.

24. Xu, Y.; Bolisetty, S.; Drechsler, M.; Fang, B.; Yuan, J.; Harnau, L.; Ballauff, M.; Muller, A. X. E. *Soft Matter* **2009**, *5*, 379–84.

25. Xu, Y.; Bolisetty, S.; Ballauff, M.; Mueller, A. H. E. *J. Am. Chem. Soc.* **2009**, *131*, 1640–1641.

26. Yao, J.; Chen, Y.; Zhang, J.; Bunyard, C.; Tang, C. *Macromol. Rapid Commun.* **2013**, *34*, 645-651.

27. Yin, J. Ge, Z. Liu, H.; Liu, S. *J. Polym. Sci. Part A: Polym. Chem.* **2009**, *47*, 2608-2619.

28. Li, C.; Ge, Z.; Fang, J.; Liu, S. *Macromolecules* **2009**, *42*, 2916-2924.

29. Gu, L.; Shen, Z.; Feng, C.; Li, Y.; Lu, G.; Huang, X. *J. Polym. Sci. Part A: Polym. Chem.* **2008**, *46*, 4056-4069.

30. Feng, C.; Shen, Z.; Gu, L.; Zhang, S.; Li, L.; Lu, G.; Huang, X. *J. Polym. Sci. Part A: Polym. Chem.* **2008**, *46*, 5638-5651.

31. Song, X.; Zhang, Y.; Yang, D.; Yuan, L; Hu, J.; Huang, X. *J. Polym. Sci. Part A: Polym. Chem.* **2011**, *49*, 3328-3337.

32. Gu, L.; Feng, C.; Yang, D.; Li, Y.; Hu, J.; Lu, G.; Huang, X. *J. Polym. Sci. Part A: Polym. Chem.* **2009**, *47*, 3142-3153.

33. Jiang, X.; Lu, G.; Feng, C.; Li, Y.; Huang, X. *Polym. Chem.* **2013**, *4*, 3876-3884.

34. Lian, X.; Wu, D.; Song, X.; Zhao, H. *Macromolecules* **2010**, *43*, 7434-7445.

35. Luo, Y.-L.; Yu, W.; Xu, F.; Zhang, L.-L. *J. Polym. Sci. Part A: Polym. Chem.* **2012**, *50*, 2053-2067.

36. Yuan, W.; Zhang, J.; Zou, H.; Shen, T.; Ren, J. *Polymer* **2012**, *53*, 956-966.

37. Li, Y.; Zheng, X.; Wu, K.; Lu, M. *RSC Adv.* **2016**, *6*, 2571-2581.

38. Yi, Y.; Zheng, S. *RSC Adv.* **2014**, *4*, 28439-28450.

39. Li, J.-J.; Zhou, Y.-N.; Luo, Z.-H. *Soft Matter* **2012**, *8*, 11051-11061.

40. Tang, Y.; Liu, L.; Wu, J.; Duan, J. *J. of Colloid Interface Sci.* **2013**, *397*, 24-31.

41. Alexander-Katz, A. *Macromolecules* **2014**, *47*, 1503−1513.

42. Savage, B.; Sixma, J. J.; Ruggeri, Z. M. *Proc. Natl. Acad. Sci. U. S. A.* **2002**, *99*, 425−430.

43. Sadler, J. E. *Annu. Rev. Biochem.* **1998**, *67*, 395-424.

44. Jiang, X. G.; Lavender, C. A.; Woodcock, J. W.; Zhao, B. *Macromolecules* **2008**, *41*, 2632-2643.

Appendix C

for

Chapter 4: Synthesis and Behavior of Stimuli-Responsive Shape-Changing Binary Heterografted Linear Molecular Brushes

Appendix C.1. Example Calculation of Grafting Density of Binary Heterografted Molecular Brushes

The following is an example calculation of grafting density for PEO/PDEGEA MMB-1 after 22 h reaction time using the molar ratio of backbone monomer units to each side chain polymer in the feed and the ratio of peak areas for the brushes and the unreacted side chains from SEC. The feed contained 6.25 mg of PTEGN_3MA-800 backbone, with a monomer unit molar mass of 243.27 g/mol, assuming 100 % azide functionalization. The feed contained 59.1 mg of PEO-45 with an absolute molecular weight of 2,100 (found by 2,000 + 80.08) and 163.4 mg of PDEGEA-46 side chain polymers with an absolute molecular weight of 8,800 g/mol (found by 46*188.22 + 160.60). For 100 % grafting density, 6.25 mg PTEGN_3MA-800 can react with 32.4 mg PEO-45 and 90.4 mg PDEGEA-36 side chains to give 129.1 mg brushes, assuming that the molar ratio of PEO and PDEGEA in the brushes is the same as in the feed (0.60 : 0.40). So the reaction mixture would contain (129.1 mg)/(228.8 mg) = 56.42 % brushes by mass. From SEC after 22 h reaction time, we found that the reaction mixture contained 41.94 % brushes by mass using peak areas, again, assuming that the molar ratio of PEO and PDEGEA in the brushes is the same as in the feed. This gives a grafting density of (41.94 %)/ (56.42 %) = 74.3 %. (We have confirmed that the peak areas in SEC are proportional to the masses of polymers, see Appendix A Figure A3).

Appendix C.2. Supplemental Figures

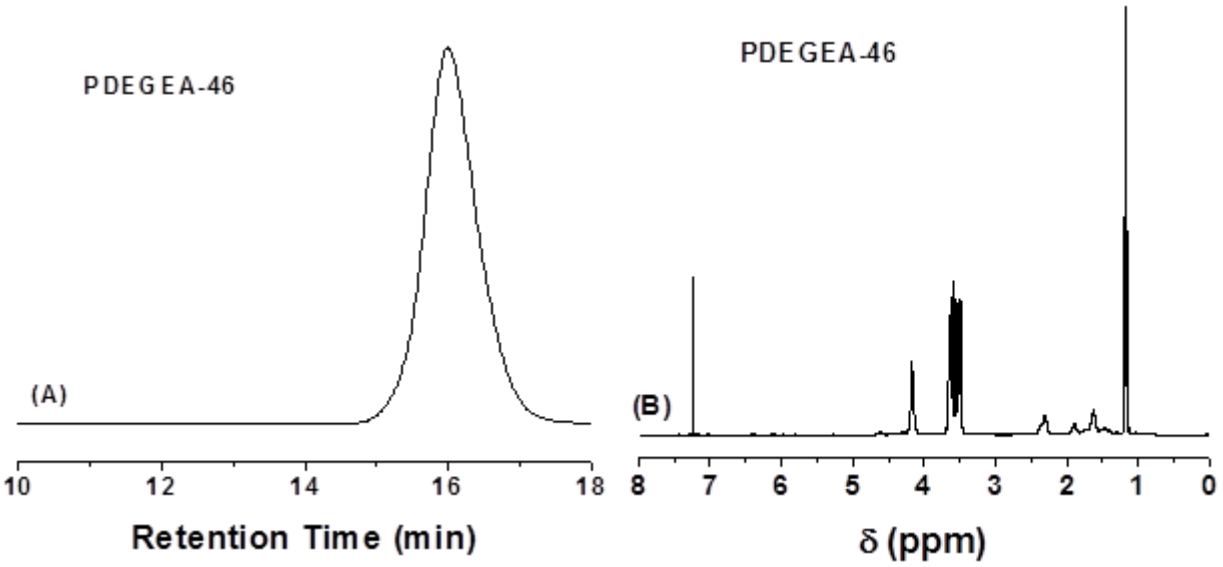

Figure C1. (A) SEC trace of PDEGEA side chains with a DP of 46 (PDEGEA-46) and (B) ^{1}H NMR spectrum of PDEGEA-46 in $CDCl_3$. SEC analysis was carried out on PL GPC-20 system using THF as carrier solvent.

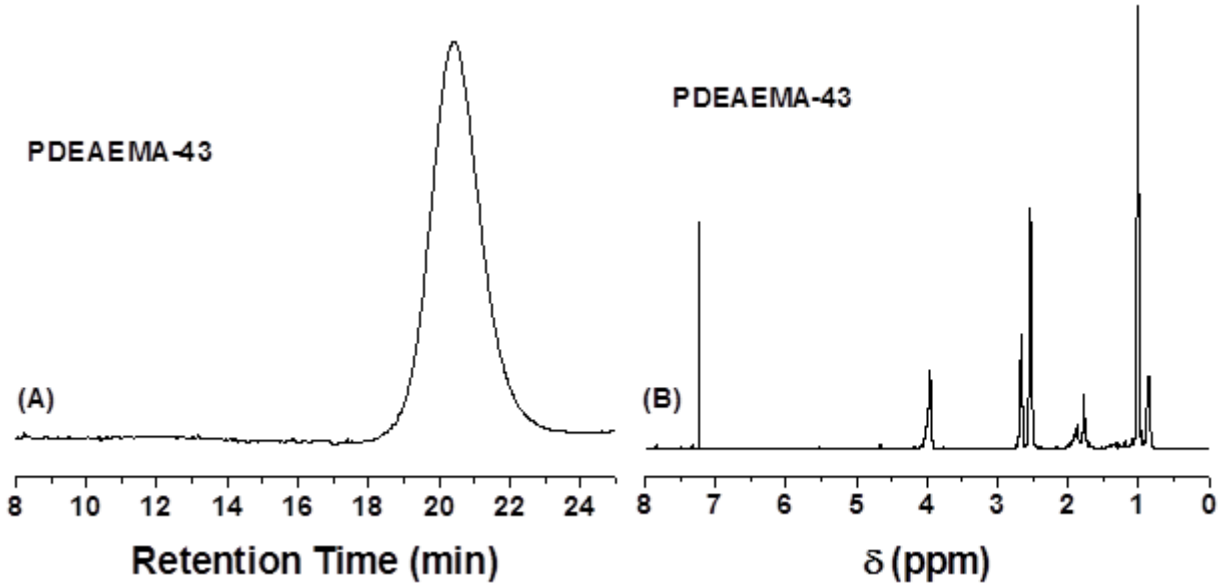

Figure C2. (A) SEC trace of PDEAEMA side chains with a DP of 43 (PDEAEMA-43) and (B) ^{1}H NMR spectrum of PDEAEMA-43 in $CDCl_3$. SEC analysis was carried out on PL GPC-50 Plus system with PSS GRAL columns using DMF containing 50 mM LiBr as carrier solvent.

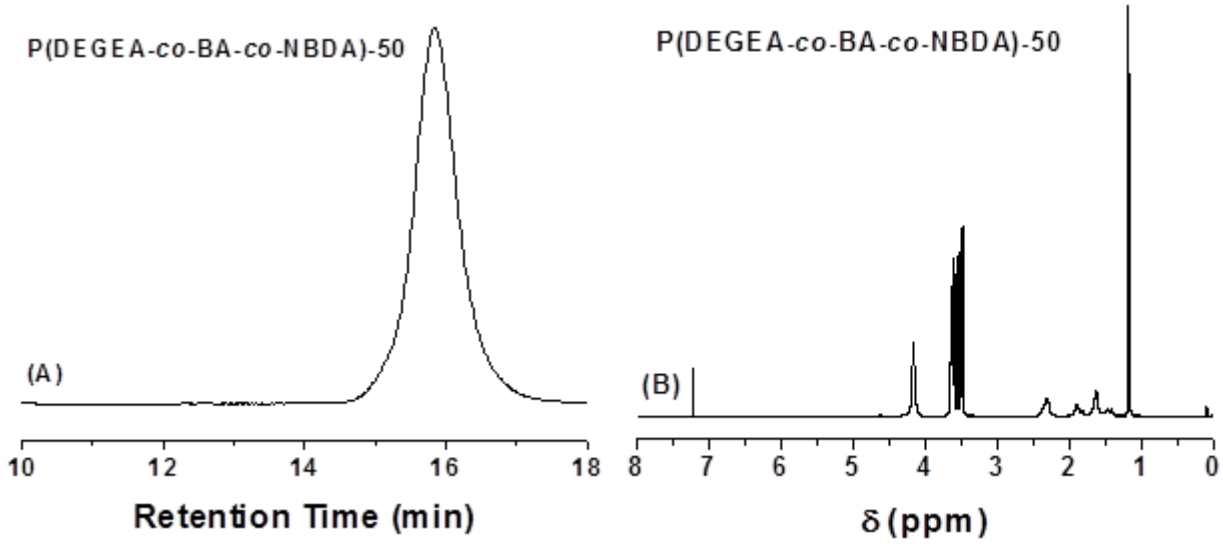

Figure C3. (A) SEC trace of P(DEGEA-*co*-BA-*co*-NBDA) side chains with a DP of 50 (P(DEGEA-*co*-BA-*co*-NBDA)-50) and (B) ^{1}H NMR spectrum of P(DEGEA-*co*-BA-*co*-NBDA)-50 in $CDCl_3$. SEC analysis was carried out on PL GPC-20 system using THF as carrier solvent

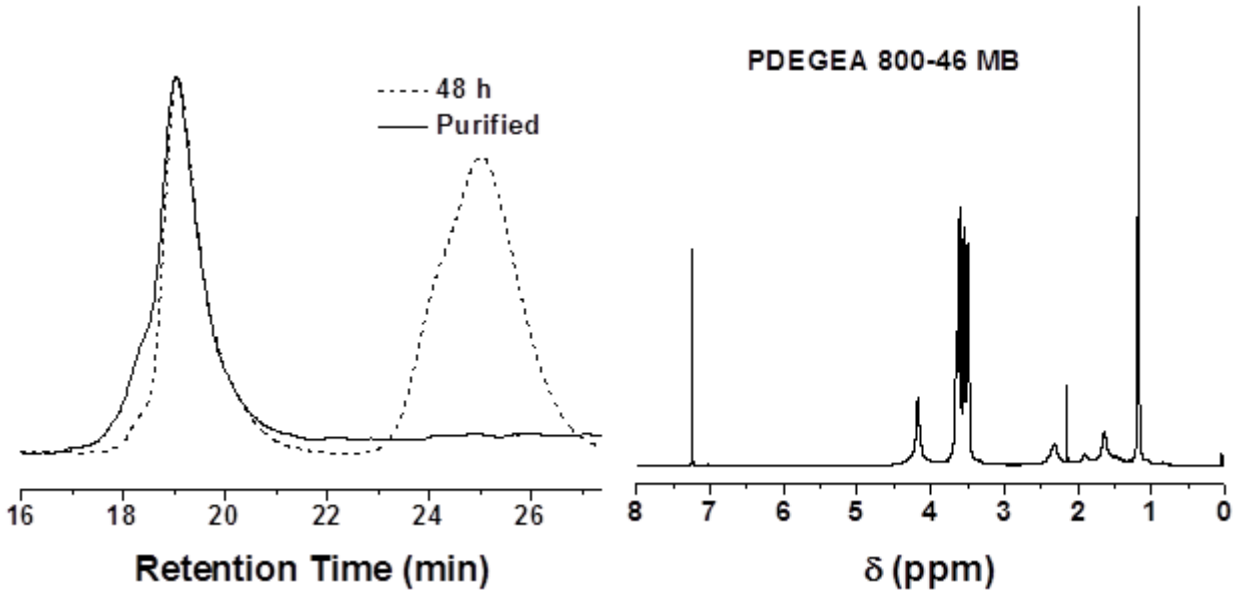

Figure C4. (A) SEC trace of PDEGEA MB-1 homografted molecular brushes prepared from $PTEGN_3MA$-800 backbone with PDEGEA-46 side chains before and after removal of unreacted side chains by fractionation. (B) ^{1}H NMR spectrum of PDEGEA 800-46 homograft molecular brushes in $CDCl_3$. SEC analysis was carried out on PL GPC-50 Plus system with Agilent Mixed-B columns using DMF containing 50 mM LiBr as carrier solvent. Before purification: $M_{n,\,SEC}$ = 1,086,000; PDI = 1.12. After purification: $M_{n,\,SEC}$ = 1,190,100; PDI = 1.14.

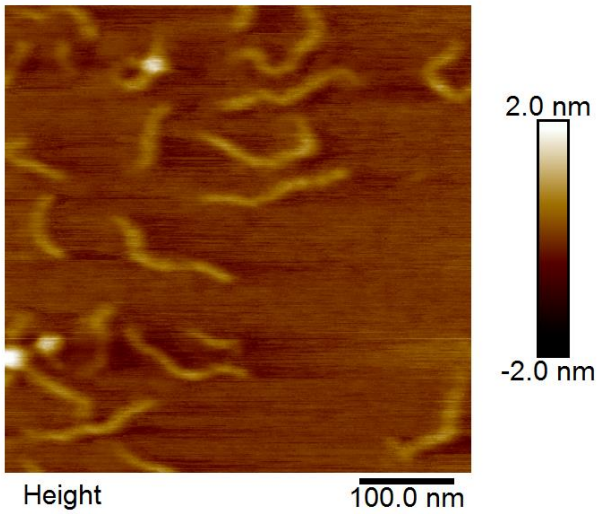

Figure C5. Additional AFM height image of PEO/DEGEA MMB-1 spin coated onto mica from an aqueous solution at 0 ^{o}C with a polymer concentration of 0.1 mg/g.

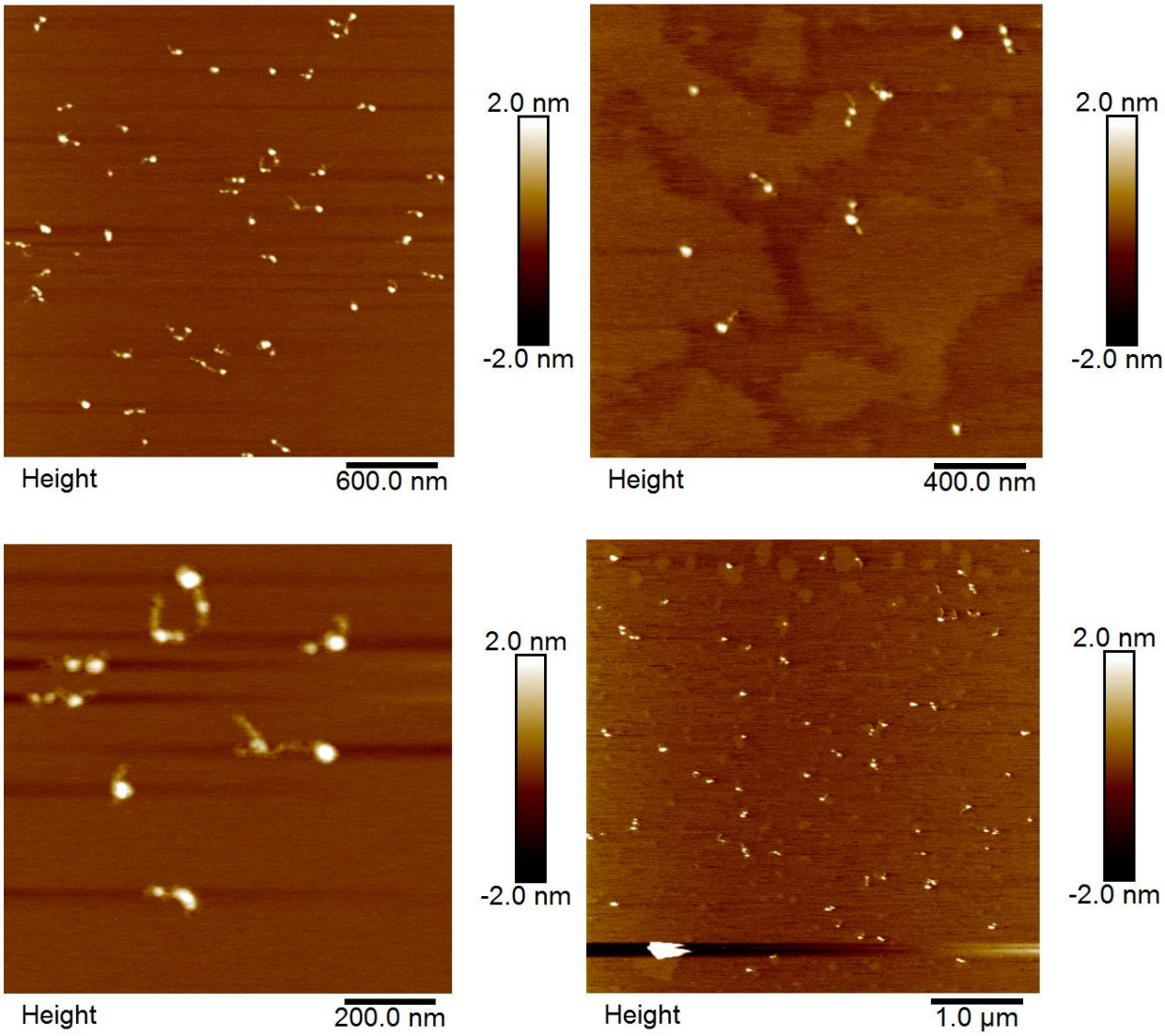

Figure C6. Additional AFM height images of PEO/DEGEA MMB-1 spin coated onto mica from an aqueous solution at 40 ^{o}C with a polymer concentration of 0.01 mg/g.

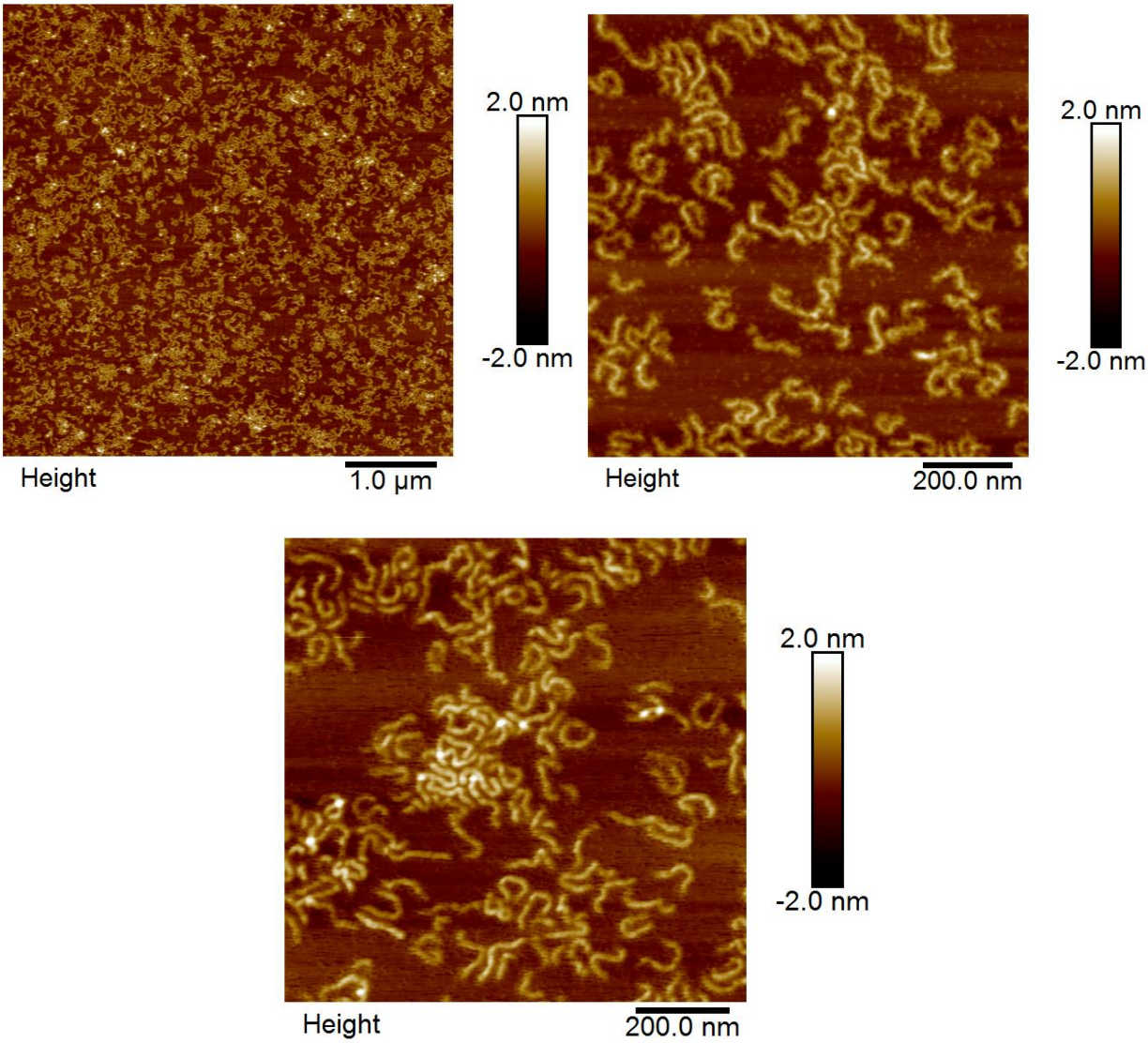

Figure C7. Additional AFM height images of PEO/PDEAEMA MMB-2 spin coated onto mica from an aqueous 1.25 mM KH_2PO_4 solution at pH = 4.99 with a polymer concentration of 0.05 mg/g.

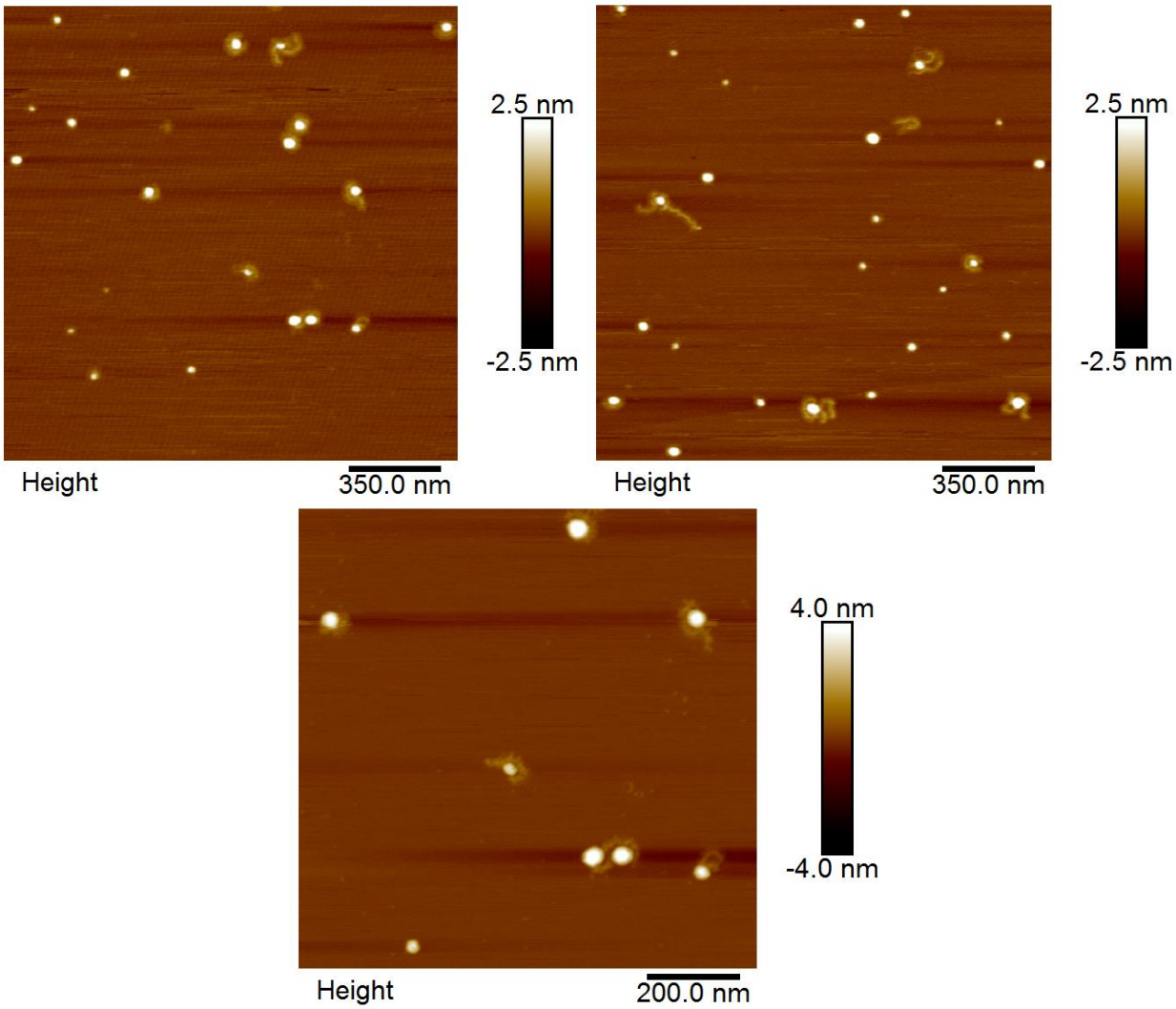

Figure C8. Additional AFM height images of PEO/PDEAEMA MMB-2 spin coated onto mica from an aqueous 0.5 mM KH_2PO_4 solution at pH = 9.79 with a polymer concentration of 0.01 mg/g.

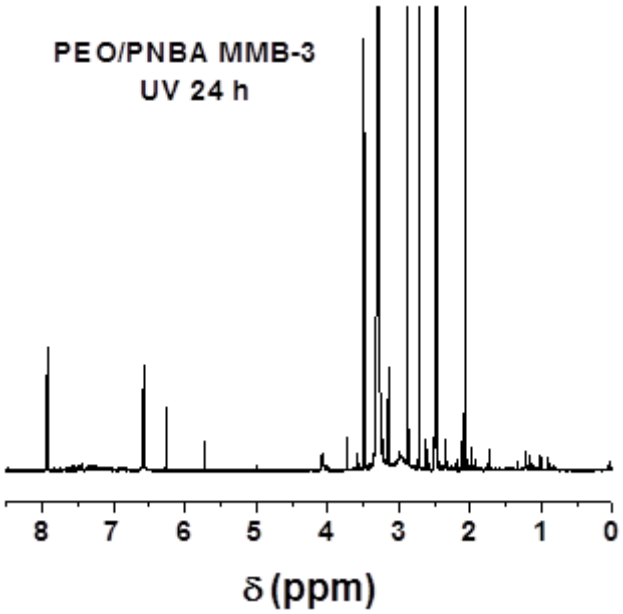

Figure C9. ^{1}H NMR spectrum of PEO/PNBA MMB-3 obtained from a 0.1 mg/g solution in water that was irradiated with 365 nm UV light for 24 h (DMSO-d_6 solvent for NMR).

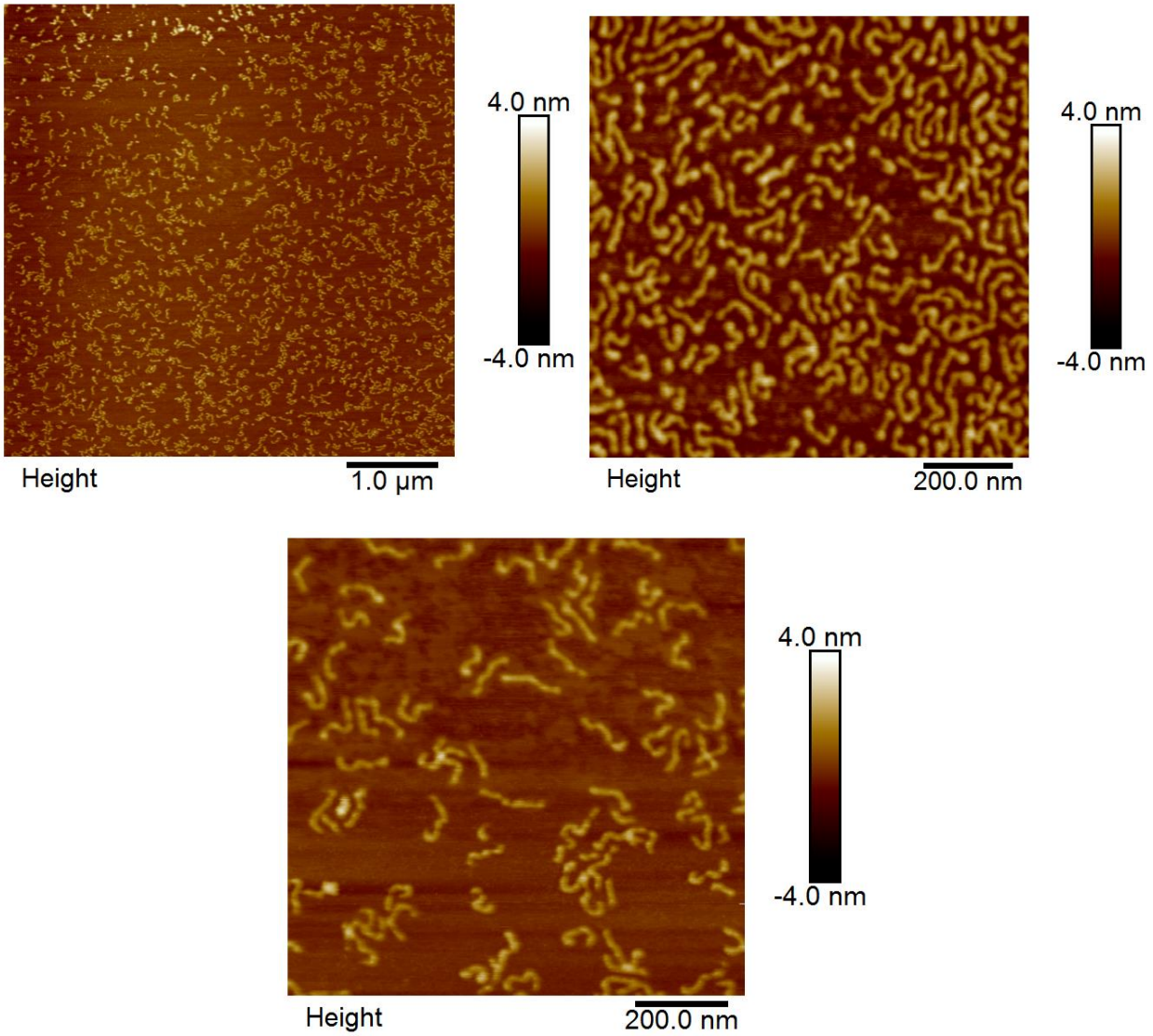

Figure C10. Additional AFM height images of PEO/PNBA MMB-3 spin coated onto mica from a 0.01 mg/g solution in chloroform.

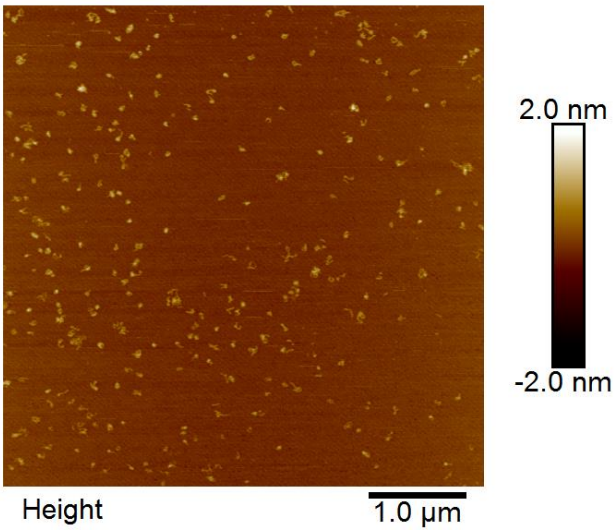

Figure C11. Additional AFM height image of PEO/PNBA MMB-3 spin coated onto mica from an aqueous 2 mM KH_2PO_4 solution at pH = 7.06 with a polymer concentration of 0.05 mg/g after 22 h of irradiation with 365 nm UV light.

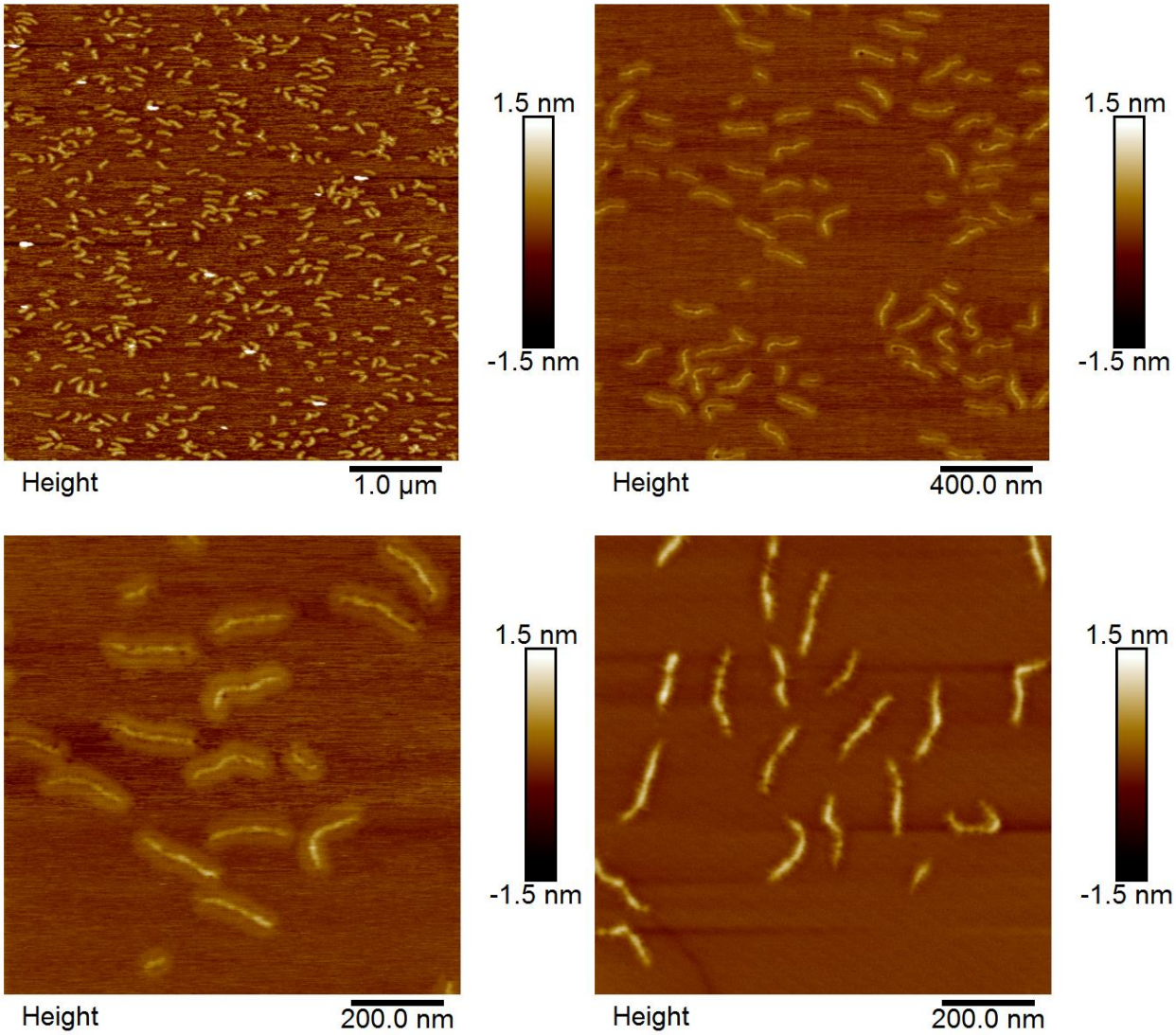

Figure C12. Additional AFM height images of PEO/P(DEGEA-*co*-BA-*co*-NBDA) MMB-4 spin coated onto mica from an aqueous solution at 0 ^{o}C with a polymer concentration of 0.05 mg/g.

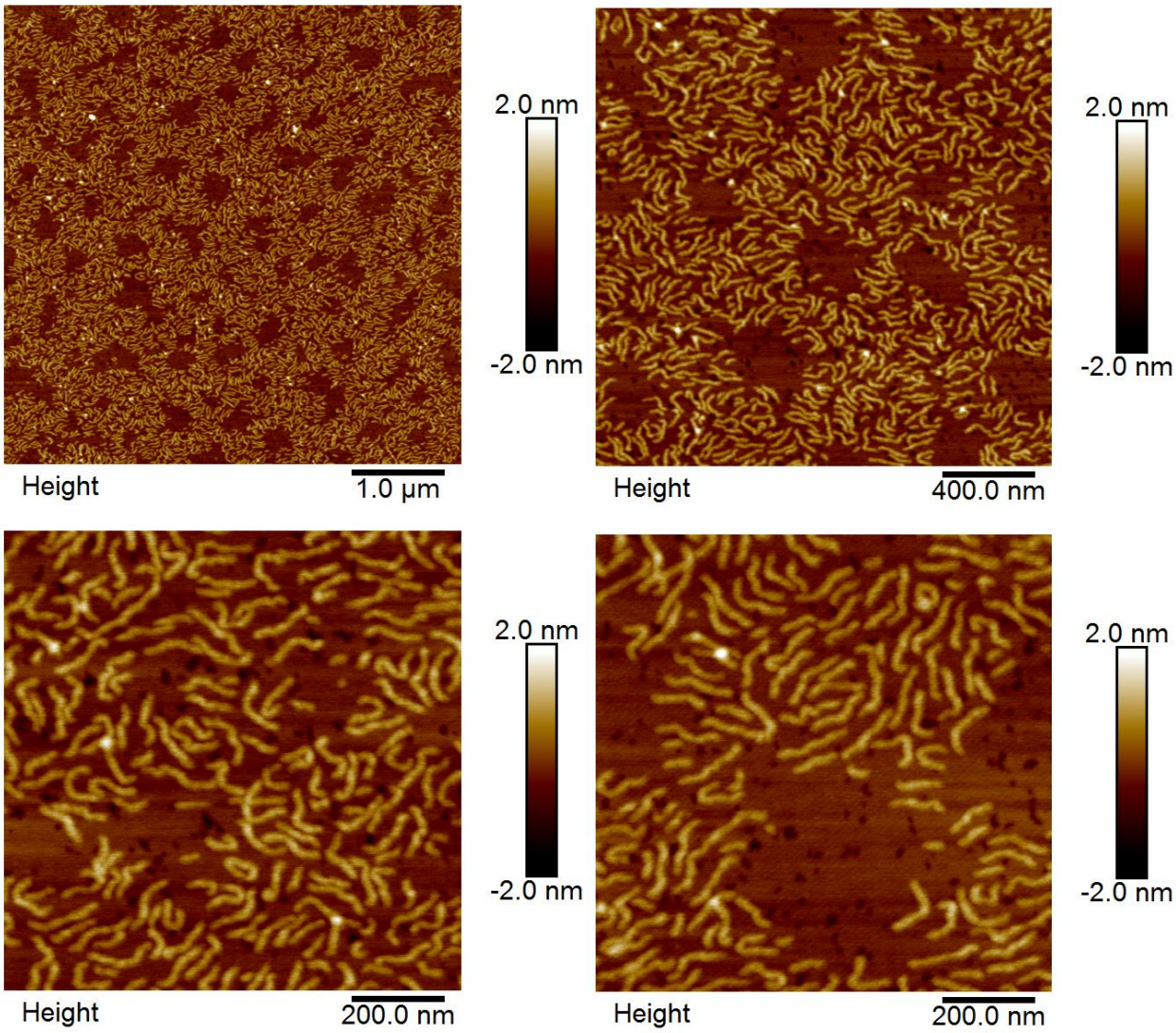

Figure C13. Additional AFM height images of PEO/P(DEGEA-*co*-BA-*co*-NBDA) MMB-4 drop cast onto mica-PS from an aqueous solution at 0 ^{o}C with a polymer concentration of 0.05 mg/g.

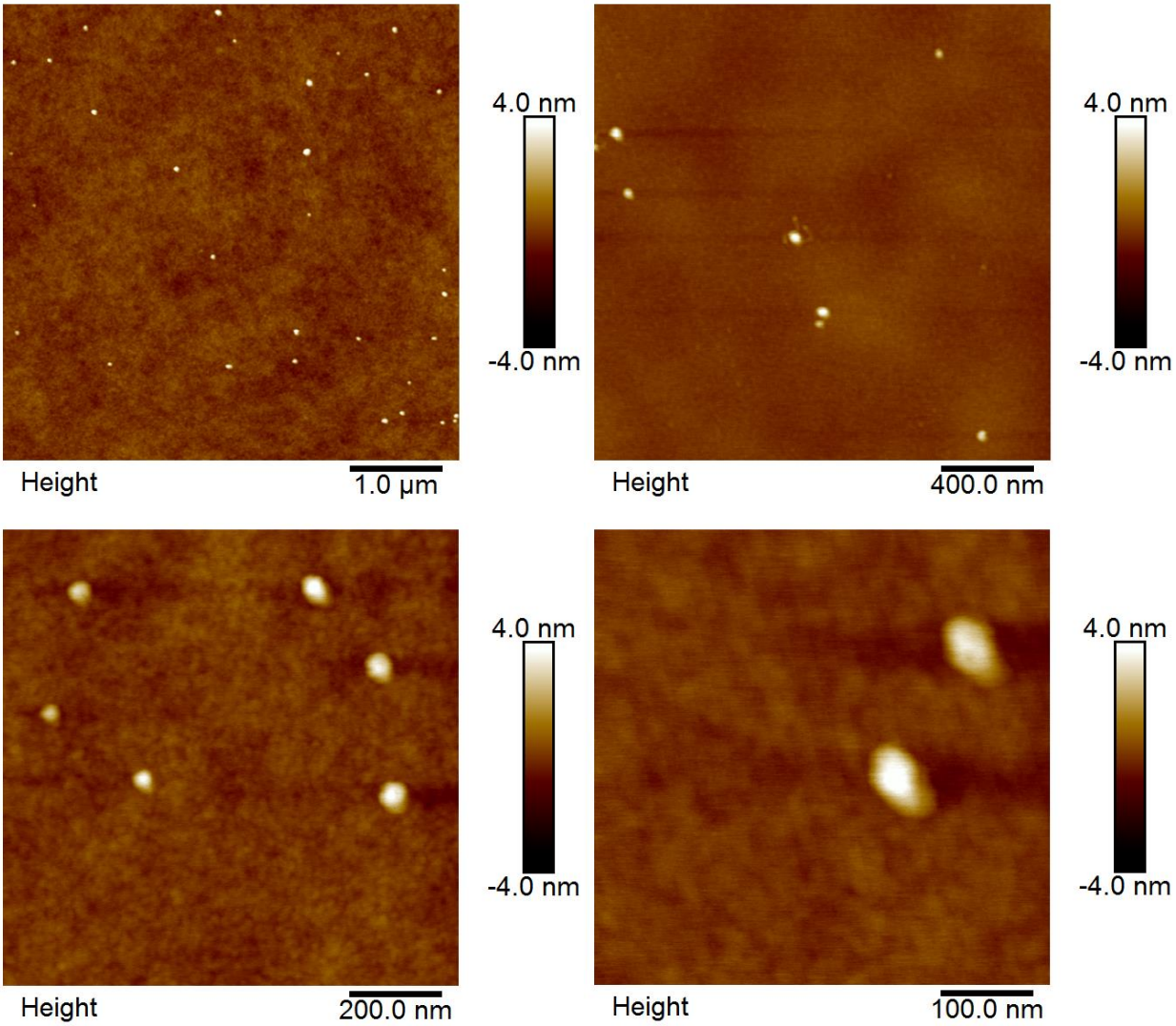

Figure C14. Additional AFM height images of PEO/P(DEGEA-*co*-BA-*co*-NBDA) MMB-4 drop cast onto mica-PS from an aqueous solution at 45 ^{o}C with a polymer concentration of 0.01 mg/g.

Chapter 5: Tertiary Amine-Containing Thermo- and pH-Sensitive Hydrophilic ABA Triblock Copolymers: Effect of Different Tertiary Amines on Thermally Induced Sol-Gel Transitions

Abstract

This Chapter presents the synthesis of a series of well-defined, tertiary amine-containing ABA triblock copolymers, composed of a poly(ethylene oxide) central block and thermo- and pH-sensitive outer blocks, and the study of the effect of different tertiary amines on thermally induced sol-gel transition temperatures ($T_{\text{sol-gel}}$) of their 10 wt % aqueous solutions. The doubly responsive ABA triblock copolymers were prepared from a difunctional poly(ethylene oxide) macroinitiator by atom transfer radical polymerization of methoxydi(ethylene glycol) methacrylate and ethoxydi(ethylene glycol) methacrylate at a feed molar ratio of 30 : 70 with ~ 5 mol % of either *N*,*N*-diethylaminoethyl methacrylate (DEAEMA), *N*,*N*-diisopropylaminoethyl methacrylate, or *N*,*N*-di(*n*-butyl)aminoethyl methacrylate. The chain lengths of thermosensitive outer blocks and the molar contents of tertiary amines were very similar for all copolymers. Using rheological measurements, we determined the pH dependences of $T_{\text{sol-gel}}$ of 10 wt % aqueous solutions of these copolymers in a phosphate buffer. The $T_{\text{sol-gel}}$ vs. pH curves of all polymers exhibited a sigmoidal shape. The $T_{\text{sol-gel}}$ increased with decreasing pH; the changes were small on both high and low pH sides. At a specific pH, the $T_{\text{sol-gel}}$ decreased with increasing the hydrophobicity of the tertiary amine, and upon decreasing pH, the onset pH value for the $T_{\text{sol-gel}}$ to begin to increase noticeably was lower for the more hydrophobic tertiary amine-containing copolymer. In addition, we studied the effect of different tertiary amines on the release behavior of fluorescein isothiocyanate-dextran (FITC-dextran, 40,000 g/mol) from 10 wt % micellar gels of different tertiary amine-containing thermosensitive ABA triblock copolymers in an acidic medium at 37 and 27 °C. The release profiles for three studied hydrogels at 37 °C were essentially the same, suggesting that the release was dominated by the diffusion of FITC-dextran. At 27 °C, the release was significantly faster for

the DEAEMA-containing copolymer, indicating that both diffusion and gel dissolution contributed to the release at this temperature.

5.1. Introduction

Moderately concentrated aqueous solutions of linear ABA triblock copolymers, composed of a permanently hydrophilic central block and stimuli-responsive outer blocks, have been shown to undergo reversible transitions from free-flowing liquids to free-standing gels upon application of external stimuli.[1-3] These triblock copolymers self-assemble in water, in response to environmental changes, into 3-dimensional networks with the central block forming bridges among micellar cores that consist of the outer blocks. Such stimuli-responsive micellar hydrogels have received growing interest because of their potential applications in controlled release of drugs, tissue engineering, etc.[2-8] This interest can largely be attributed to the fact that, compared with chemically crosslinked hydrogels, the in situ sol–gel transitions of these responsive micellar gels coupled with the nature of physical crosslinking allow for more convenient delivery and removal of polymers.[1-3] There are many reports on micellar hydrogels of stimuli-sensitive hydrophilic ABA triblock copolymers.[9-17] For example, using atom transfer radical polymerization (ATRP), Armes et al. synthesized a series of well-defined ABA triblock copolymers composed of a biocompatible phosphorylcholine-containing polymer as the central block and pH- or temperature-sensitive polymers as outer blocks.[9-13] These copolymers were capable of forming gels in water in response to either pH or temperature changes.

Our lab is especially interested in block copolymer hydrogels that can respond to multiple stimuli; such gels can provide greater design flexibility that is needed in many applications.[2-5,18-30] A number of multiresponsive block copolymer aqueous micellar gels can be found in the literature.[18-30] For instance, Li *et al*. synthesized thermo- and redox-sensitive ABA triblock copolymers from a difunctional initiator that contained a redox-sensitive disulfide bond by ATRP and demonstrated the gel formation and responsiveness.[18] Thermo- and pH-sensitive block

copolymer hydrogels have been intensively studied because the temperature and pH changes are particularly relevant to biomedical applications.[22--32] The block copolymers for such gels were usually prepared by either growing pH-sensitive blocks from or introducing pH-responsive groups onto the chain ends of ABA triblock copolymers that can form thermoreversible gels in water (e.g., poly(ethylene oxide)-*b*-poly(propylene oxide)-*b*-poly(ethylene oxide) (PEO-*b*-PPO-*b*-PEO)).[22-27] In addition, Suh *et al*. synthesized multiblock copolymers with carboxylic acid groups incorporated at the junction points by using pyromellitic dianhydride to couple PEO-*b*-PPO-*b*-PEO.[28] Schmalz *et al.* prepared doubly responsive star-block copolymers consisting of poly(*N*,*N*-dimethylaminoethyl methacrylate) (PDMAEMA) interior blocks and poly(methoxydi(ethylene glycol) methacrylate) (PDEGMMA) outer blocks using ATRP.[30] Above the lower critical solution temperature (LCST) of the PDEGMMA blocks, the star-block copolymers formed micellar gels in concentrated aqueous solution. The mechanical properties of the gels could be manipulated by varying the pH due to the pH-responsive PDMAEMA inner blocks.

Through the incorporation of a small amount of carboxylic acid groups into the thermosensitive outer blocks of ABA triblock copolymers, which allows the LCST to be modified by changing the solution pH, our lab recently showed that the sol-gel transition temperatures ($T_{\text{sol-gel}}$) of moderately concentrated aqueous solutions of these polymers can be reversibly tuned over a wide temperature range.[31,32] Note that for the carboxylic acid-containing ABA triblock copolymers, the $T_{\text{sol-gel}}$ of their aqueous solutions increased with increasing pH. It is known that the diseased tissues often exhibit unusually acidic pH values.[33] Thus, to use our injectable hydrogels as drug delivery systems for battling such diseases, it is necessary to employ weak bases with appropriate pK_a values for making doubly responsive ABA copolymers, which would allow the drugs loaded into the gels to be released at a greater rate at lower pH values. It should be noted

that the release rate of a drug from an injectable hydrogel depends on many factors,[4-6,11] including the nature of the drug (e.g. hydrophilic or hydrophobic), the architecture and the composition of the block copolymer, the solubility of the polymer in water, etc.

In this work, we synthesized a series of ABA triblock copolymers with the thermosensitive outer blocks incorporated with ~ 5 mol % of different tertiary amine groups by ATRP from a difunctional PEO macroinitiator with a molecular weight of 20 kDa (Scheme 5.1) and examined the sol-gel transitions of their 10 wt % aqueous solutions as a function of pH. In the absence of pH-responsive moieties, the thermosensitive polymer making up the outer blocks should have a cloud point of ~ 10 °C in order to form a gel at room temperature, because the typical $T_{\text{sol-gel}}$ values of 10 wt % aqueous solutions of this kind of ABA triblock copolymers are approximately 10 °C above the LCST of the outer blocks as shown in our prior work.[31,32] PDEGMMA and poly(ethoxydi(ethylene glycol) methacrylate) (PDEGEMA) are a new class of thermosensitive water-soluble polymers with cloud points in water of 26 and 4 °C, respectively.[34-37] We chose to copolymerize DEGMMA and DEGEMA with a feed molar ratio of 30 : 70, which should lead to a thermosensitive copolymer with a cloud point of 10.6 °C in water according to a linear relationship between the compositions and the cloud points of copolymers of two monomers reported in the literature.[2,3,37] The pH sensitivities of ABA triblock copolymers were imparted through the incorporation of ~ 5 mol % of either *N*,*N*-diethylaminoethyl methacrylate (DEAEMA), *N*,*N*-diisopropylaminoethyl methacrylate (DPAEMA), or *N*,*N*-di(*n*-butyl)aminoethyl methacrylate (DBAEMA) into the thermosensitive outer blocks. The pK_a values of the homopolymers of DEAEMA, DPAEMA, and DBAEMA in water have been reported to be 7.4, 6.3, and 5.1, respectively,[33] which represent a pH range that is of interest to the development of injectable

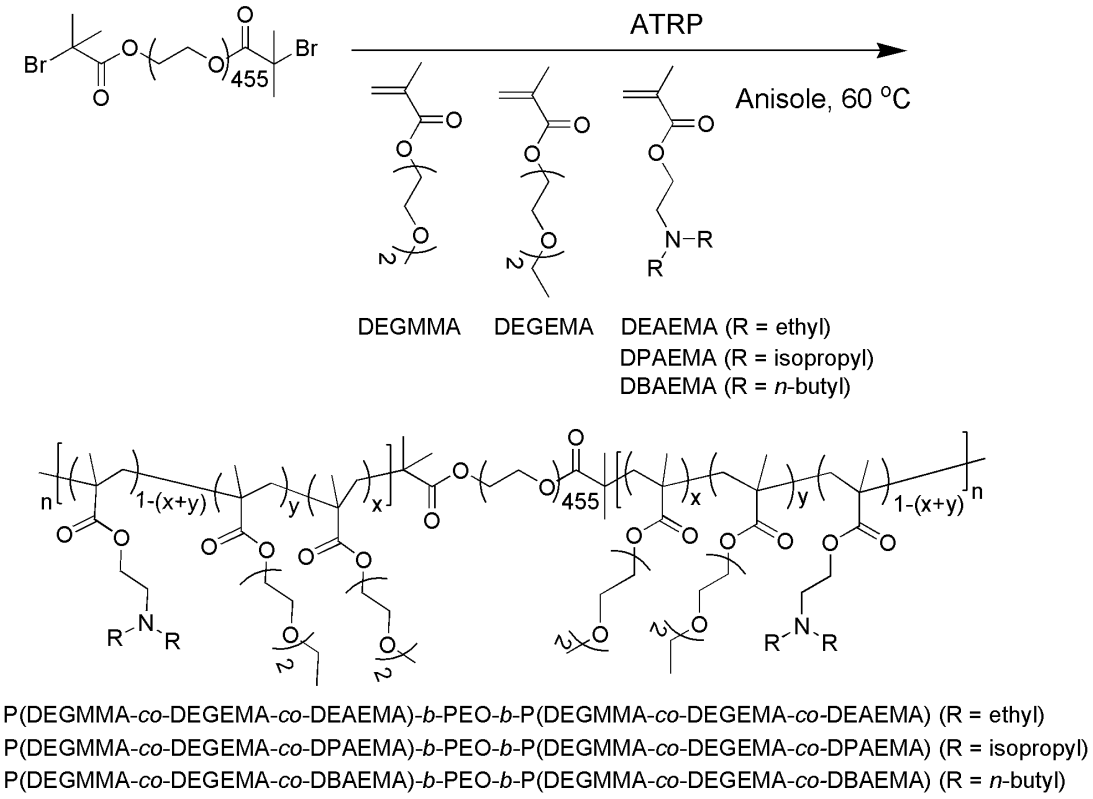

Scheme 5.1. Synthesis of Tertiary Amine-Containing, Thermo- and pH-Sensitive Hydrophilic ABA Triblock Copolymers by Atom Transfer Radical Polymerization (ATRP)

thermo- and pH-responsive block copolymer micellar hydrogels capable of releasing drugs at a greater rate at low pH values.

5.2. Experimental Section

5.2.1. Materials

Methoxydi(ethylene glycol) methacrylate (or di(ethylene glycol) methyl ether methacrylate, DEGMMA) was purchased from TCI and purified by vacuum distillation over calcium hydride. Ethoxydi(ethylene glycol) methacrylate (di(ethylene glycol) ethyl ether methacrylate, DEGEMA) was synthesized via the reaction of di(ethylene glycol) monoethyl ether (> 99.0%, TCI) and methacryloyl chloride (95%, Acros) in dry methylene chloride in the presence of triethylamine (99%, Acros). The product was purified by column chromatography and vacuum distillation, and the molecular structure was confirmed by ^{1}H NMR spectroscopy. *N*,*N*-Diethylaminoethyl methacrylate (DEAEMA, 99%, Aldrich) and *N*,*N*-diisopropylaminoethyl methacrylate (DPAEMA, 97%, Aldrich) were passed through a basic alumina column to remove the inhibitor prior to use. *N*,*N*-Di(*n*-butyl)aminoethyl methacrylate (DBAEMA) was synthesized from *N*,*N*-di(*n*-butyl)aminoethanol (99%, Aldrich) and methacryloyl chloride using triethylamine as catalyst. The product was purified by column chromatography and vacuum distillation, and its molecular structure was confirmed by ^{1}H NMR spectroscopy. Poly(ethylene glycol) (HO-PEO-OH, MW = 20000 g/mol, Aldrich) was end-functionalized with an ATRP initiator via the reaction with 2-bromoisobutyryl bromide according to a procedure described in the literature,[31,32] yielding the difunctional PEO macroinitiator (Br-PEO-Br). 1,1,4,7,10,10-Hexamethyltriethylenetetramine (HMTETA) was purchased from Aldrich and used as received. CuBr (98%, Aldrich) was stirred in glacial acetic acid overnight, filtered, and washed with absolute ethanol and ethyl ether. The

solid was then collected, dried under vacuum, and stored in a desiccator. Fluorescein isothiocyanate-dextran (FITC-dextran, 40,000 g/mol) was purchased from Aldrich and used as received. All other chemicals were purchased from either Aldrich or Fisher and used as received.

5.2.2. General Characterization

Size exclusion chromatography (SEC) was carried out at ambient temperature using a PL-GPC 50 Plus (an integrated GPC/SEC system from Polymer Laboratories, Inc.) with a differential refractive index detector, one PSS GRAL guard column (50 × 8 mm, Polymer Standards Service-USA, Inc.), and two PSS GRAL linear columns (each 300 × 8 mm, molecular weight range from 500 to 1,000,000 according to Polymer Standards Service-USA, Inc.). The data were processed using Cirrus^{TM} GPC/SEC software (Polymer Laboratories, Inc.). *N*,*N*-Dimethylformamide (DMF) was used as the carrier solvent at a flow rate of 1.0 mL/min. The system was calibrated by using polystyrene standards (Polymer Laboratories, Inc.). ^{1}H NMR (300 MHz) spectra were recorded on a Varian Mercury 300 NMR spectrometer and the residual solvent proton signal was used as the internal standard.

5.2.3. Synthesis of P(DEGMMA-*co*-DEGEMA-*co*-DEAEMA)-*b*-PEO-*b*-P(DEGMMA-*co*-DEGEMA-*co*-DEAEMA) (ABA-DEA-1)

The following is the procedure for the synthesis of P(DEGMMA-*co*-DEGEMA-*co*-DEAEMA)-*b*-PEO-*b*-P(DEGMMA-*co*-DEGEMA-*co*-DEAEMA) (ABA-DEA-1). The other ABA triblock copolymers were prepared via similar procedures. Difunctional PEO macroinitiator Br-PEO-Br (0.701 g, 0.0345 mmol) was weighed into a two-necked round bottom flask with a stir bar, followed by the addition of DEGMMA (1.179 g, 6.27 mmol), DEGEMA (2.932 g, 14.5 mmol), DEAEMA (0.207 g, 1.12 mmol), CuBr (5.8 mg, 0.040 mmol), and anisole (6.006 g). The mixture was degassed by three freeze-pump-thaw cycles, placed in a 60 °C oil bath, and stirred for

several minutes to dissolve the Br-PEO-Br. HMTETA (10.0 μL, 0.0368 mmol) was injected via a microsyringe, and the mixture changed from yellow to light green in color. The reaction was monitored by SEC. After 375 min the polymerization was stopped by removing the flask from the oil bath, opening it to air, diluting the mixture with THF, and passing the solution through a basic/neutral alumina column with a mixture of THF and $CHCl_3$ (1:1, v/v) as eluent. The polymer was purified by precipitation three times in a mixture of hexanes and ethyl ether (60:40, v/v), and then dried under high vacuum at 50 °C for 4 h. SEC analysis showed that the value of $M_{n,SEC}$ relative to polystyrene standards was 77.6 kDa and the polydispersity index (PDI) was 1.13. The numbers of DEGMMA, DEGEMA, and DEAEMA units in the polymer were 86, 164, and 13, respectively, calculated from ^{1}H NMR analysis.

5.2.4. Preparation of 10 wt % Aqueous Solutions of Tertiary Amine-Containing, Thermo- and pH-Responsive ABA Triblock Copolymers

The preparation of 10 wt % aqueous solutions of tertiary amine-containing ABA triblock copolymers follows the same general procedure; the following is the procedure for P(DEGMMA-*co*-DEGEMA-*co*-DEAEMA)-*b*-PEO-*b*-P(DEGMMA-*co*-DEGEMA-*co*-DEAEMA) (ABA-DEA-1) given as an example. ABA-DEA-1 was added to a small, pre-weighed vial and dried under high vacuum at 50 °C for 4 h. The mass of the dried polymer was 0.747 g. An aqueous KH_2PO_4 buffer solution with the salt concentration of 20 mM (6.728 g) was added into the vial along with a stir bar. The mixture was stored in a refrigerator (~ 4 °C) overnight and then stirred at 0 °C (in an ice/water bath) to ensure complete dissolution of the polymer. The pH was measured with a pH meter (Accumet AB15 pH meter from Fisher Scientific, calibrated with pH = 4.01, 7.00, and 10.01 standard buffer solutions) in an ice/water bath (0 °C). The pH of the solution was adjusted using 1.0 M HCl and 1.0 M KOH solutions, which are volumetric standards.

5.2.5. Rheological Measurements

Rheological experiments were conducted on a TA Instruments (Model TA AR2000ex) rheometer. A cone-plate geometry with a cone diameter of 20 mm and an angle of 2° (truncation 52 μm) was used, and the temperature was controlled by the bottom Peltier plate. Whenever possible, ~ 90 μL of the polymer solution was loaded onto the plate by a micropipette for each measurement. For extremely viscous solutions, the approximately same volume (~90 μL) of the polymer solution was loaded onto the plate using a metal spatula. The solvent trap was filled with water and a solvent trap cover was used to minimize water evaporation. Dynamic viscoelastic properties (dynamic storage modulus G' and loss modulus G'') of a sample were measured by oscillatory shear experiments[38,39] performed at a fixed frequency of 1 Hz in a heating ramp at a heating rate of 3 °C/min. The frequency dependencies of G' and G'' of a sample at selected temperatures were obtained by frequency sweep measurements from 0.1 to 100 Hz. A fixed strain amplitude of $\gamma = 1$ % was employed in rheological experiments.

5.2.6. Controlled Release of FITC-Dextran from 10 wt % Thermo- and pH-Responsive ABA Triblock Copolymer Hydrogels

The controlled release behaviors of fluorescein isothiocyanate-dextran (FITC-dextran, 40,000 g/mol) loaded into 10 wt % thermo- and pH-responsive ABA triblock copolymer micellar hydrogels in a 20 mM phosphate buffer solution with pH of 5.5 at different temperatures were investigated using fluorescence spectroscopy. The following is the procedure for studying the controlled release of FITC-dextran from a 10 wt % P(DEGMMA-*co*-DEGEMA-*co*-DEAEMA)-*b*-PEO-*b*-P(DEGMMA-*co*-DEGEMA-*co*-DEAEMA) (ABA-DEA-1) hydrogel at 37 °C given as an example. An aliquot of FITC-dextran stock solution (6.4 mg/g in DI water, 15.5 mg) was weighed into a small cylindrical dish (inner diameter = 1.3 cm, height = 6 mm) and dried under a

gentle stream of nitrogen. A 10 wt % aqueous solution of ABA-DEA-1 in a 20 mM phosphate buffer with a pH of 7.4 (0.104 g) was then added into the same dish. The solution was then mixed with a small spatula at 0 °C until homogenous. The FITC-dextran-containing polymer solution was equilibrated at 0 °C for 15 min, gelled at 37 °C, and then equilibrated at the same temperature for 10 min before being immersed in the release medium, a 20 mM phosphate buffer solution with pH of 5.5 (25.001 g), with the temperature maintained at 37 °C. The release medium was stirred at 600 rpm. Periodically, aliquots (~ 1 g) were taken from the release medium and replaced with an equal mass of the 20 mM phosphate buffer solution at a pH of 5.5. The cumulative percentages of FITC-dextran released from the hydrogel were calculated using the maximum fluorescence intensity (at 515 nm) from fluorescence emission spectra. Fluorescence measurements were performed on a PerkinElmer LS 55 fluorescence spectrometer equipped with a 20 kW xenon discharge lamp. The excitation wavelength was 490 nm, and the fluorescence emission spectra were recorded from 500 to 550 nm. Both the excitation and emission slit widths were 7.0 nm. Each measurement of fluorescence intensity was performed in triplicate and the three values were averaged.

5.3. Results and Discussion

5.3.1. Synthesis and Characterization of Tertiary Amine-Containing Thermo- and pH-Responsive Hydrophilic ABA Triblock Copolymers

By incorporating a small amount of pH-responsive tertiary amine groups with different chemical structures into the thermosensitive outer blocks, we designed and synthesized three thermo- and pH-sensitive ABA triblock copolymers in which the central B block was PEO (Scheme 5.1): P(DEGMMA-*co*-DEGEMA-*co*-DEAEMA)-*b*-PEO-*b*-P(DEGMMA-*co*-

DEGEMA-*co*-DEAEMA) (ABA-DEA-1), P(DEGMMA-*co*-DEGEMA-*co*-DPAEMA)-*b*-PEO-*b*-P(DEGMMA-*co*-DEGEMA-*co*-DPAEMA) (ABA-DPA-2), and P(DEGMMA-*co*-DEGEMA-*co*-DBAEMA)-*b*-PEO-*b*-P(DEGMMA-*co*-DEGEMA-*co*-DBAEMA) (ABA-DBA-3). The LCST transitions of the thermosensitive outer blocks are expected to increase with decreasing pH as the protonation of tertiary amine groups makes the outer blocks more hydrophilic, thus increasing the LCSTs.[40] These multiresponsive block copolymers were prepared from a difunctional PEO macroinitiator with a molecular weight of 20.0 kDa by ATRP at 60 °C of a mixture of DEGMMA, DEGEMA, and a tertiary amine monomer with a molar ratio of 30 : 70 : 5.4 (for DEAEMA and DPAEMA) or 5.3 (for DBAEMA) using CuBr/1,1,4,7,10,10-hexamethyltriethylenetetramine as catalyst and anisole as solvent. The polymerizations were monitored by SEC and were stopped when the molecular weights reached desired values. The obtained block copolymers were passed through a basic/neutral alumina column to remove the copper catalyst and purified by repetitive precipitation in a solvent mixture of hexanes and ethyl ether with a volume ratio of 60 : 40. The polymers were dried under high vacuum and analyzed by SEC and ^{1}H NMR spectroscopy.

Figures 5.1a, 5.2a, and 5.3a show the SEC curves of the difunctional macroinitiator Br-PEO-Br and the three ABA triblock copolymers. Clearly, the peaks shifted uniformly to the high molecular weight side and remained narrow, indicating that all three ATRP polymerizations were well-controlled. The values of $M_{\mathrm{n,SEC}}$ and PDI relative to polystyrene standards were 77.6 kDa and 1.13 for ABA-DEA-1, 80.8 kDa and 1.15 for ABA-DPA-2, and 75.5 kDa and 1.16 for ABA-DBA-3, respectively. The numbers of DEGMMA, DEGEMA, and the tertiary amine monomer units were calculated from ^{1}H NMR spectroscopy analysis; the ^{1}H NMR spectra of three block copolymers ABA-DEA-1**,** ABA-DPA-2**,** and ABA-DBA-3 are shown in Figures 5.1b, 5.2b, and 5.3b, respectively. We used the integral ratios of the peaks at 1.2 ppm (-OCH_2CH_3 from

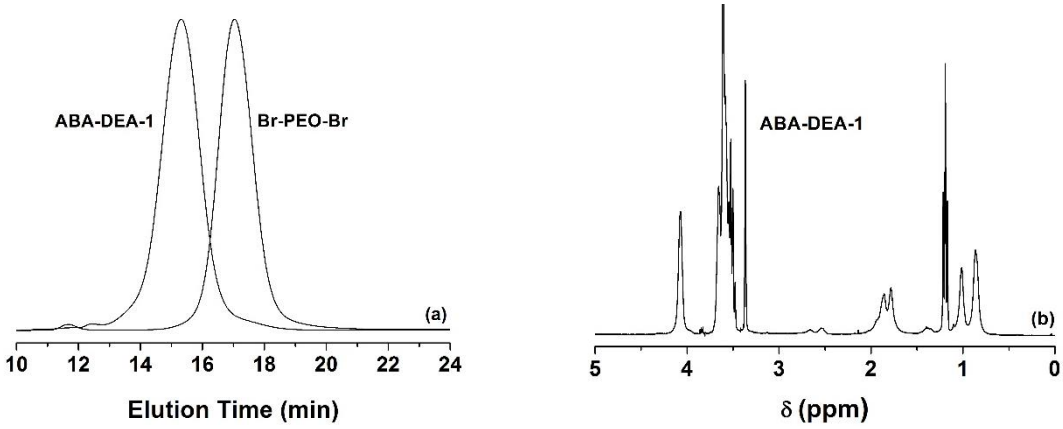

Figure 5.1. (A) SEC traces of difunctional macroinitiator Br-PEO-Br and P(DEGMMA-*co*-DEGEMA-*co*-DEAEMA)-*b*-PEO-*b*-P(DEGMMA-*co*-DEGEMA-*co*-DEAEMA) (ABA-DEA-1). (B) ^{1}H NMR spectrum of ABA-DEA-1 ($CDCl_3$ as solvent).

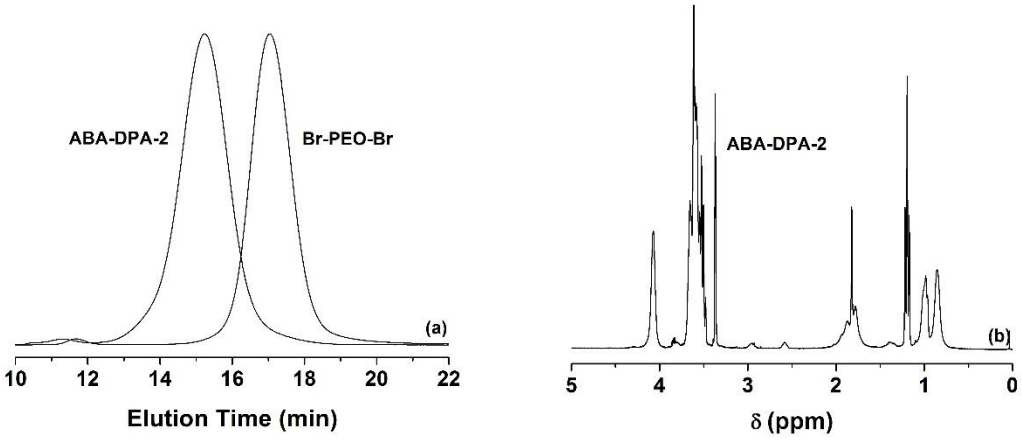

Figure 5.2. (A) SEC traces of difunctional macroinitiator Br-PEO-Br and P(DEGMMA-*co*-DEGEMA-*co*-DPAEMA)-*b*-PEO-*b*-P(DEGMMA-*co*-DEGEMA-*co*-DPAEMA) (ABA-DPA-2). (B) ^{1}H NMR spectrum of ABA-DPA-2 ($CDCl_3$ as solvent).

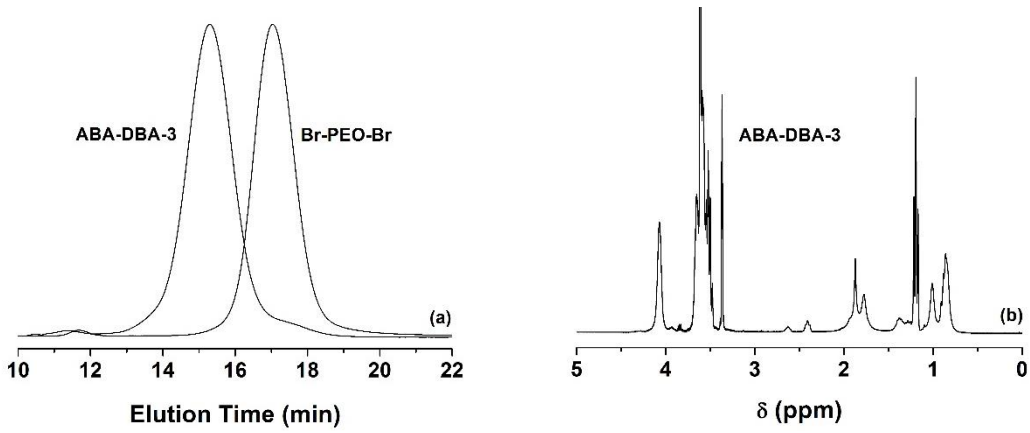

Figure 5.3. (A) SEC traces of difunctional macroinitiator Br-PEO-Br and P(DEGMMA-*co*-DEGEMA-*co*-DBAEMA)-*b*-PEO-*b*-P(DEGMMA-*co*-DEGEMA-*co*-DBAEMA) (ABA-DBA-3). (B) ^{1}H NMR spectrum of ABA-DBA-3 ($CDCl_3$ as solvent).

DEGEMA), 3.4 ppm (-OCH_3 from DEGMMA), 3.45 – 3.75 (-CH_2CH_2O- from PEO, -COOCH$_2$CH_2OCH_2CH_2OCH$_3$ from DEGMMA, and -COOCH$_2$CH_2OCH_2CH_2OCH_2CH$_3$ from DEGEMA), and 2.4 – 2.8 ppm (for ABA-DEA-1, -OCH$_2$CH_2N(CH_2CH$_3$)$_2$ from DEAEMA), or 2.5 – 3.05 ppm (for ABA-DPA-2, -OCH$_2$CH_2N(CHCH$_3$CH$_3$)$_2$ from DPAEMA), or 2.35 – 2.7 ppm (for ABA-DBA-3, -OCH$_2$CH_2N(CH_2CH$_2$CH$_2$CH$_3$)$_2$ from DBAEMA). The calculation results are summarized in Table 5.1 along with the SEC data and the feed molar contents of tertiary amine monomers. As can be seen from Table 5.1, the molar contents of the tertiary amine monomer units in all three ABA triblock copolymers are very close to those in the feeds and are similar to each other, allowing us to study the effect of different tertiary amine monomers on the thermally induced sol-gel transitions of their 10 wt % aqueous solutions.

5.3.2. pH Dependence of Sol-Gel Transition of 10 wt % Aqueous Solution of ABA-DEA-1.

We first studied the pH dependence of the sol-gel transition of a 10 wt % aqueous solution of ABA-DEA-1. The vacuum dried triblock copolymer ABA-DEA-1 was dissolved in a calculated amount of a 20 mM KH_2PO_4 in a refrigerator (~ 4 °C) and then stirred in an ice/water bath to ensure complete dissolution of the polymer, yielding a 10 wt % clear solution with a pH of 7.57, measured at 0 °C using a pH meter. The polymer solution was a liquid in an ice/water bath, but turned into a clear gel at room temperature that remained immobile when the vial was inverted. This thermally induced sol-gel transition was reversible; placing the vial into an ice/water bath converted the gel into a sol, consistent with the expected behavior of a thermosensitive hydrophilic ABA triblock copolymer in water at a concentration of 10 %. The pH of the solution was adjusted using either a 1.0 M HCl or a 1.0 M NaOH solution (volumetric standards) and measured with a pH meter at 0 °C before rheological measurements were performed.

Table 5.1. Characterization Data for Tertiary Amine-Containing, Thermo- and pH-Sensitive Hydrophilic ABA Triblock Copolymers

Polymer Number	$M_{n,SEC}$ and PDI [a]	n_{DEGMMA}, n_{DEGEMA}, and $n_{Amine\ Monomer}$ [b]	Molar Content of Amine Monomer in Outer Blocks of Polymer [c]	Molar Content of Amine Monomer in Feed
ABA-DEA-1	77.6 kDa, 1.13	86, 164, 13	4.9 %	5.1 %
ABA-DPA-2	80.8 kDa, 1.15	93, 172, 16	5.7 %	5.1 %
ABA-DBA-3	75.5 kDa, 1.16	82, 157, 12	4.8 %	5.0 %
ABA-DEA-4	82.1 kDa, 1.17	96, 176, 15	5.2 %	5.1 %
ABA-DPA-5	78.3 kDa, 1.14	89, 166, 18	6.6 %	5.0 %

[a] The values of $M_{n,SEC}$ and polydispersity index (PDI) were measured by size exclusion chromatography (SEC) using polystyrene standards for calibration. [b] The numbers of DEGMMA (n_{DEGMMA}), DEGEMA (n_{DEGEMA}), and tertiary amine monomer ($n_{Amine\ Monomer}$) units were calculated by ^{1}H NMR spectroscopy analysis. [c] The molar content of tertiary amine monomer units in the thermosensitive outer blocks of an ABA triblock copolymer was calculated by using equation $(n_{Amine\ Monomer}/(n_{DEGMMA} + n_{DEGEMA} + n_{Amine\ Monomer})) \times 100\%$.

Figure 5.4a shows the rheological data for the 10 wt % aqueous solution of ABA-DEA-1 with pH of 10.73, obtained from an oscillatory shear experiment in a heating ramp performed using a fixed frequency of 1 Hz, a strain amplitude of 1.0 %, and a heating rate of 3 °C/min. The dynamic storage modulus G' and loss modulus G'' at temperatures of < 9 °C were small. With the increase of temperature in the range of 9 – 13.0 °C, both G' and G'' increased rapidly; however, the value of G'' was larger than G', evidencing that the sample was a viscous liquid. Above 13.3 °C, G' became larger than G'', suggesting that the sample turned into a gel. If the crossover of two curves, i.e., $G' = G''$, is taken as the sol-gel transition temperature ($T_{\text{sol-gel}}$),[1,41] then for this particular sample (a 10 wt % aqueous solution of ABA-DEA-1 at pH = 10.73), the $T_{\text{sol-gel}}$ is 13.3 °C. Figure 5.4b shows the frequency dependences of G' and G'' of this sample at 21.9 °C (i.e., the normalized temperature $T/T_{\text{sol-gel}} = 1.03$,[32] where T and $T_{\text{sol-gel}}$ are expressed in kelvin), collected in a frequency sweep from 0.1 to 100 Hz at a strain amplitude of $\gamma = 1$ %. Both G' and G'' exhibited weak dependence on frequency, a characteristic of physically crosslinked hydrogels.

The pH of the 10 wt % aqueous solution of ABA-DEA-1 was then adjusted in an ice/water bath, and the sol-gel transitions at various pH values were determined by rheological measurements. The $T_{\text{sol-gel}}$ increased with decreasing pH, which is consistent with the expected behavior because of the gradual protonation of tertiary amine groups making the polymer chains more hydrophilic. As an example, the heating ramp for the 10 wt % aqueous solution of ABA-DEA-1 with pH of 5.18 is shown in Figure 5.5a. The sol-gel transition occurred at 38.1 °C, significantly higher than that at pH = 10.73 ($T_{\text{sol-gel}}$ = 13.3 °C). Compared with the heating ramp in Figure 5.4a, a noticeable feature of Figure 5a is that the transition is broader. This is consistent with our previous observation for the sol-gel transition of carboxylic acid-containing thermosensitive ABA triblock copolymer solutions,[32] presumably because the LCST transition of

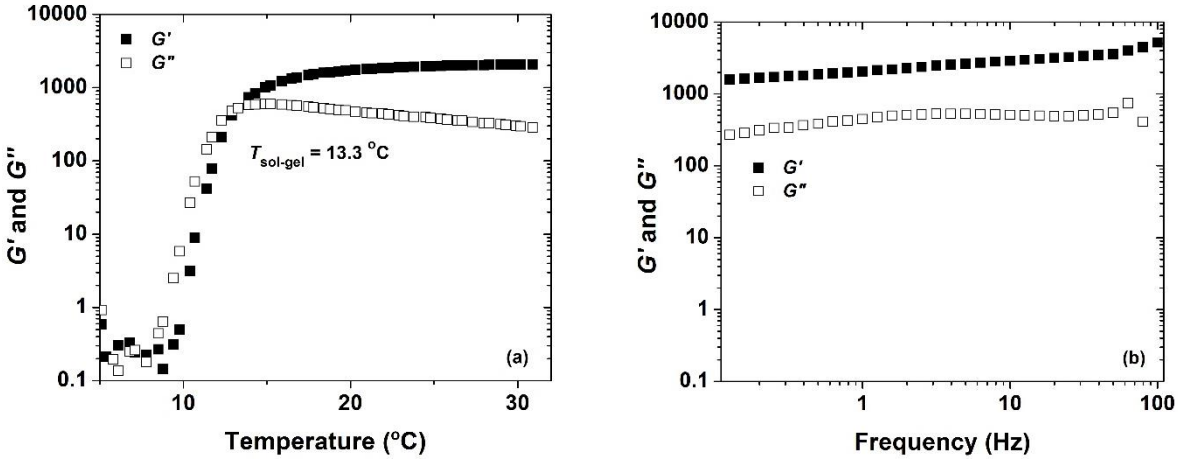

Figure 5.4. (A) Plot of dynamic storage modulus *G′* (■) and dynamic loss modulus *G″* (□) versus temperature for a 10 wt % aqueous solution of ABA-DEA-1 with pH of 10.73. The data were collected from a temperature ramp experiment performed by using a fixed frequency of 1 Hz, a strain amplitude of 1 %, and a heating rate of 3 °C/min. (B) Frequency dependences of *G′* (■) and *G″* (□) at 21.9 °C of the gel formed from the sample with pH of 10.73, collected using a strain amplitude of 1 %.

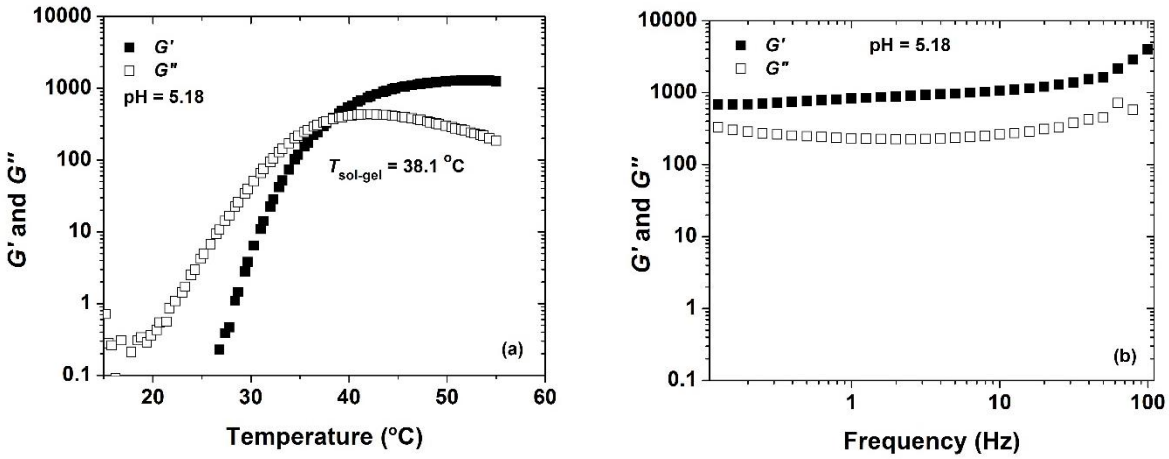

Figure 5.5. (A) Plot of dynamic storage modulus *G′* (■) and loss modulus *G″* (□) versus temperature for a 10 wt % aqueous solution of ABA-DEA-1 with pH of 5.18. The data were collected from a heating ramp experiment performed at a frequency of 1 Hz, a strain amplitude of 1 %, and a heating rate of 3 °C/min. (B) Frequency dependences of *G′* (■) and *G″* (□) of the gel from the sample with pH of 5.18 at 47.4 °C, collected using a strain amplitude of 1 %.

the thermosensitive hydrophilic polymer that carries a small amount of charges is weaker and broader. Similar to the gel at pH = 10.73, the G' and G'' of the sample with pH of 5.18 at the normalized temperature of 1.03 ($T/T_{sol\text{-}gel}$ = 1.03, where T and $T_{sol\text{-}gel}$ are expressed in kelvin), i.e., 47.4 °C, exhibited weak dependence on frequency (Figure 5.5b).

The pH dependence of $T_{sol\text{-}gel}$ of the 10 wt % aqueous solution of ABA-DEA-1 is shown in Figure 5.6. In the pH range of 10 – 11.5, the $T_{sol\text{-}gel}$ did not change much. With decreasing pH, the sol-gel transition temperature gradually increased and the sharpest change was observed in the pH range of 8.7 to 6.0. Below pH = 6.0, the change in $T_{sol\text{-}gel}$ became noticeably slower. The curve exhibited a sigmoidal shape. To further examine the pH dependence of $T_{sol\text{-}gel}$, we fit the data points to a Boltzmann equation:[42]

$$y = \frac{A_1 - A_2}{1 + e^{(x - x_0)/dx}} + A_2$$

in which A_1 and A_2 are the Y limits, x_0 is the inflection point (half amplitude) and dx is the width (the change in x corresponding to the most significant change in Y values – also shown as rate in sigmoidal fit tool). The black smooth curve in Figure 5.6 is the fitted curve. The fitted values of A_1, A_2, x_0, and dx are included in Table 5.2. The inflection occurs at pH = 7.21.

5.3.3. pH Dependences of $T_{sol\text{-}gel}$ of 10 wt % Aqueous Solutions of ABA-DPA-2 and ABA-DBA-3 and Comparison with ABA-DEA-1

Similarly, we studied the pH dependences of $T_{sol\text{-}gel}$ of 10 wt % aqueous solutions of ABA-DPA-2 and ABA-DBA-3 in a 20 mM phosphate buffer by rheological measurements. Typical heating ramps for ABA-DPA-2 and ABA-DBA-3 at a lower and a higher pH value can be found in Appendix D. The results are summarized in Figure 5.6. Both polymers exhibited the same trend as ABA-DEA-1: the $T_{sol\text{-}gel}$ increased with decreasing pH and all curves had a sigmoidal

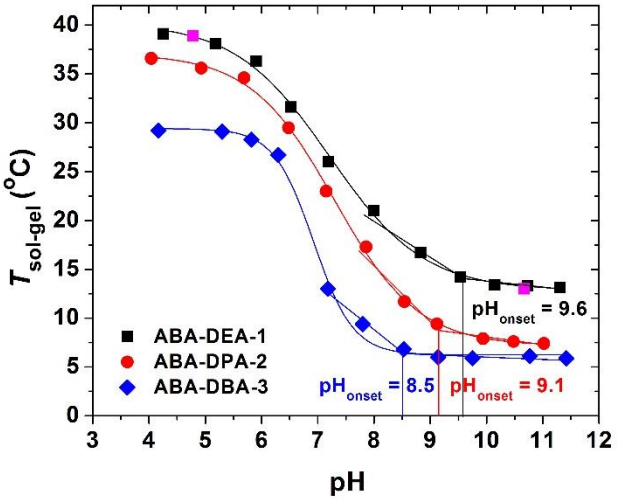

Figure 5.6. The sol-gel transition ($T_{sol-gel}$) of the 10 wt % solution of ABA-DEA-1 (■), ABA-DPA-2 (●), and ABA-DBA-3 (♦) in the 20 mM phosphate buffer as a function of solution pH fitted to a Boltzmann function as well as the $T_{sol-gel}$ values at pH = 3.78 and 10.67 of a 10 wt % aqueous solution of ABA-DEA-1 after storage at room temperature and pH = 3.20 for 8 months (■). The two $T_{sol-gel}$ values at pH = 3.78 and 10.67 for ABA-DEA-1 were not included in the fitting.

Table 5.2. The Fitted Values of A_1, A_2, x_0, and dx from Fitting the pH Dependences of $T_{sol\text{-}gel}$ for ABA Triblock Copolymers Using Boltzmann Function

Parameter [a]	ABA-DEA-1	ABA-DPA-2	ABA-DBA-3	ABA-DEA-4	ABA-DPA-5
A_1	40.27	37.07	29.41	40.14	38.22
A_2	12.85	7.15	6.24	12.21	5.99
x_0	7.21	7.29	6.92	7.11	7.35
dx	0.84	0.74	0.35	0.79	0.70

[a] The data points of $T_{sol\text{-}gel}$ as a function of pH were fitted to a Boltzmann equation shown in the text. A_1 and A_2 are the Y limits, x_0 is the inflection point (half amplitude) and dx is the width (the change in x corresponding to the most significant change in Y values – also shown as rate in sigmoidal fit tool).

shape. We fitted the data points to a Boltzmann function and the values of four parameters are included in Table 5.2.

A closer examination of data points and fit curves in Figure 5.6 revealed a number of trends for the three ABA triblock copolymers incorporated with different tertiary amine groups into the thermosensitive outer blocks. (1) At any pH value, the sol-gel transition temperatures of the 10 wt % polymer solutions decreased from ABA-DEA-1 to ABA-DPA-2 to ABA-DBA-3, which is particularly clear at the higher and lower pH values where all three curves either changed slowly or leveled off. Because the chain length of the thermosensitive outer blocks and the content of the tertiary amine monomer are about the same for three triblock copolymers, this observation is attributed to the hydrophobicity of the incorporated tertiary amine increasing from DEAEMA to DPAEMA and to DBAEMA. The more hydrophobic substituents (e.g., *n*-butyl in DBAEMA) suppressed the LCST transition of the thermosensitive outer blocks to a greater extent and thus decreased the sol-gel transition as the $T_{\text{sol-gel}}$ is largely governed by the LCST transition of the thermosensitive outer blocks. (2) At higher pH values, the $T_{\text{sol-gel}}$ for all three block copolymers was essentially independent of the solution pH. Upon decreasing pH, the sol-gel transition began to increase; the onset pH values at which the $T_{\text{sol-gel}}$ increased appreciably were 9.6, 9.1, and 8.5 for ABA-DEA-1, ABA-DPA-2, and ABA-DBA-3, respectively (Figure 5.6). This is consistent with the order of pK_a values of the homopolymers of three tertiary amine monomers reported in the literature (the pK_a values of PDEAEMA, PDPAEMA, and PDBAEMA are 7.4, 6.3, and 5.1, respectively).[33] However, all three onset pH values are significantly higher than the reported pK_a values of the corresponding homopolymers (by 2.2 to 3.4 pH units). This observation suggested that the $T_{\text{sol-gel}}$ was very sensitive to the charges on the thermosensitive outer blocks. (3) The sharpness of the $T_{\text{sol-gel}}$ change with pH increased in the order of ABA-DEA-1 < ABA-DPA-2 <

ABA-DBA-3, which can be seen from the fitted values of the width dx from Boltzmann fitting (0.84, 0.73, and 0.35 for ABA-DEA-1, ABA-DPA-2, and ABA-DBA-3, respectively). This correlates with the order of increasing hydrophobicity from DEAEMA to DPAEMA to DBAEMA. The transition tends to be sharper for a more hydrophobic thermosensitive water-soluble polymer, i.e., the thermosensitive polymer with a lower LCST.

(4) The difference between $T_{\text{sol-gel}}$ values for ABA-DEA-1 and ABA-DBA-3 on the low pH value side was only slightly wider than that on the high pH value side. The curve for ABA-DPA-2 was quite interesting. The gap between the curves of ABA-DEA-1 and ABA-DPA-2 was significantly larger on the high pH side than that on the low pH value side. On the other hand, the difference between the curves of ABA-DPA-2 and ABA-DBA-3 is smaller on the high pH value side than that at the lower pH values. This is likely caused by the slightly higher tertiary amine monomer content in ABA-DPA-2 (5.7 mol % in contrast to 4.9 and 4.8 mol% for ABA-DEA-1 and ABA-DBA-3, respectively). When nonprotonated, a higher content of a hydrophobic monomer would suppress the LCST to a greater extent and thus the sol-gel transition. When protonated, the charges on the outer blocks would make the thermosensitive blocks slightly more hydrophilic, resulting in a higher LCST and a greater $T_{\text{sol-gel}}$. (5) The inflection point, the point at which the half magnitude of the change occurred from Boltzmann fitting, was 7.21 for ABA-DEA-1, 7.29 for ABA-DPA-2, and 6.92 for ABA-DBA-3. While the inflection point for ABA-DEA-1 is close to the pK_a of PDEAEMA (7.4), the inflection points for the other two triblock copolymers are significantly different from the pK_a values of the corresponding homopolymers. In addition, the inflection point for ABA-DPA-2 occurred at a slightly higher pH value (7.29) than that for ABA-DEA-1 (7.21), which was unexpected. Despite this, the ABA-DPA-2 curve is always lower than the ABA-DEA-1 curve. It should be noted here that the pK_a is defined as the pH at which half

of the tertiary amine groups are protonated, while the inflection point is the pH at which the half magnitude of the $T_{sol\text{-}gel}$ change occurs and $T_{sol\text{-}gel}$ is related to the mechanical properties of the gel. Thus, it is not obvious how the inflection point is correlated with the pK_a value of the homopolymer of the incorporated tertiary amine monomer. A further investigation is needed to gain better understanding of this observation.

Nevertheless, we stress here that the results are reproducible. We synthesized two additional DEAEMA- and DPAEMA-containing thermosensitive hydrophilic ABA triblock copolymers (ABA-DEA-4 and ABA-DPA-5, respectively) using essentially the same polymerization conditions as those for ABA-DEA-1 and ABA-DPA-2. The SEC traces and ^{1}H NMR spectra can be found in Appendix D; the characterization data are summarized in Table 5.1. The overall molecular weights and the chain lengths of the thermosensitive outer blocks are similar to those of ABA-DEA-1, ABA-DPA-2, and ABA-DBA-3. The only noticeable difference is the tertiary amine content in ABA-DPA-5 (6.6 mol %), slightly higher than in other copolymers. The pH dependences of $T_{sol\text{-}gel}$ of 10 wt % aqueous solutions of ABA-DEA-4 and ABA-DPA-5 in a 20 mM phosphate buffer were determined and are shown in Figure 5.7 along with the results from ABA-DEA-1, ABA-DPA-2, and ABA-DBA-3 for comparison. Clearly, the two curves are similar to their respective ABA triblock copolymers and are centered at similar pH values. The data points for ABA-DEA-4 on the high pH side are slightly lower than those of ABA-DEA-1 (e.g., by ~ 0.7 °C at pH = ~ 10), likely because of the slightly higher DEAEMA content. The results for ABA-DPA-5 are particularly interesting in that the ABA-DPA-5 curve is lower than that of ABA-DPA-2 on the high pH side (e.g., by 1.4 °C at pH = ~ 10.5), but higher on the low pH side (e.g., by 1.5 °C at pH = ~ 4.9), in line with our explanation for the aforementioned point (4). We attributed this difference to the slightly higher tertiary amine content in ABA-DPA-5, 6.6 mol % in contrast to

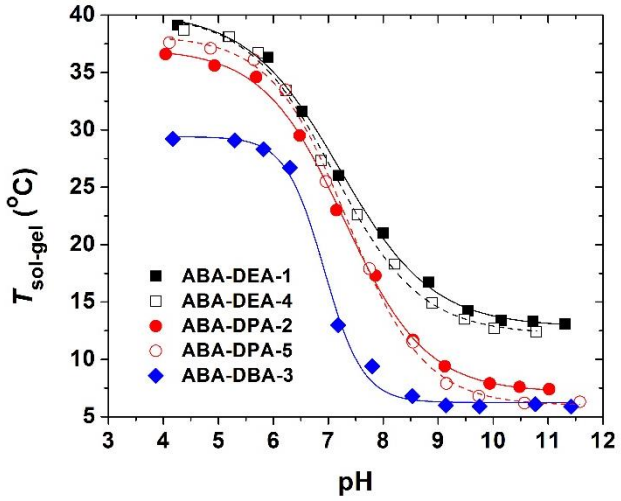

Figure 5.7. The sol-gel transition ($T_{sol-gel}$) of the 10 wt % aqueous solution of ABA-DEA-1 (■), ABA-DEA-4 (□), ABA-DPA-2 (●), ABA-DPA-5 (○), and ABA-DBA-3 (♦) in the 20 mM phosphate buffer as a function of solution pH fitted to a Boltzmann function. The data for ABA-DEA-1 (■), ABA-DPA-2 (●), and ABA-DBA-3 (♦) are from Figure 5.6.

5.7 mol % in ABA-DPA-2. The higher content of hydrophobic DPAEMA suppressed the LCST and thus the $T_{sol\text{-}gel}$ to a greater extent at higher pH values and increased the LCST and the $T_{sol\text{-}gel}$ to a larger degree when protonated. We fitted the data points to a Boltzmann function, and the fitted values of A_1, A_2, x_0, and dx are included in Table 5.2. They are comparable to those for the respective ABA triblock copolymers.

5.3.4. Controlled Release of FITC-Dextran from 10 wt % Thermo- and pH-Responsive ABA Triblock Copolymer Micellar Hydrogels of ABA-DEA-1, ABA-DPA-2, and ABA-DBA-3

As shown in Figure 5.6, 10 wt % aqueous solutions of ABA-DEA-1, ABA-DPA-2, and ABA-DBA-3 exhibited different thermally induced sol-gel transition temperatures at different pH values, which can be exploited to design pH-responsive hydrogel delivery systems. For a demonstration study, we loaded water-soluble, fluorescein isothiocyanate-labelled dextran (FITC-dextran) with a molecular weight of 40000 g/mol, a hydrophilic model drug, into 10 wt % hydrogels of ABA-DEA-1, ABA-DPA-2, and ABA-DBA-3 and examined the release behaviors of FITC-dexan in a 20 mM phosphate buffer with pH of 5.5.

FITC-dextran was mixed with a 10 wt % aqueous solution of each ABA triblock copolymer in a 20 mM phosphate buffer solution with pH of 7.4. After the gel (~ 0.10 g) was formed at 37 °C in a small cylindrical dish and equilibrated for 10 min, it was immersed in a 20 mM phosphate buffer with pH of 5.5 (25.0 g) and the temperature was maintained at 37 °C. The release rate of FITC-dextran was measured by fluorescence spectroscopy. The cumulative percentages of the released FITC-dextran at various time intervals were calculated and plotted against the time as shown in Figure 5.8a. Although the sol-gel transition temperatures of 10 wt % aqueous solutions of three block copolymers at pH = 5.5 are different (37, 34, and 29 °C for ABA-DEA-1, ABA-DPA-2, and ABA-DBA-3, respectively), the release rates of FITC-dextran were essentially the

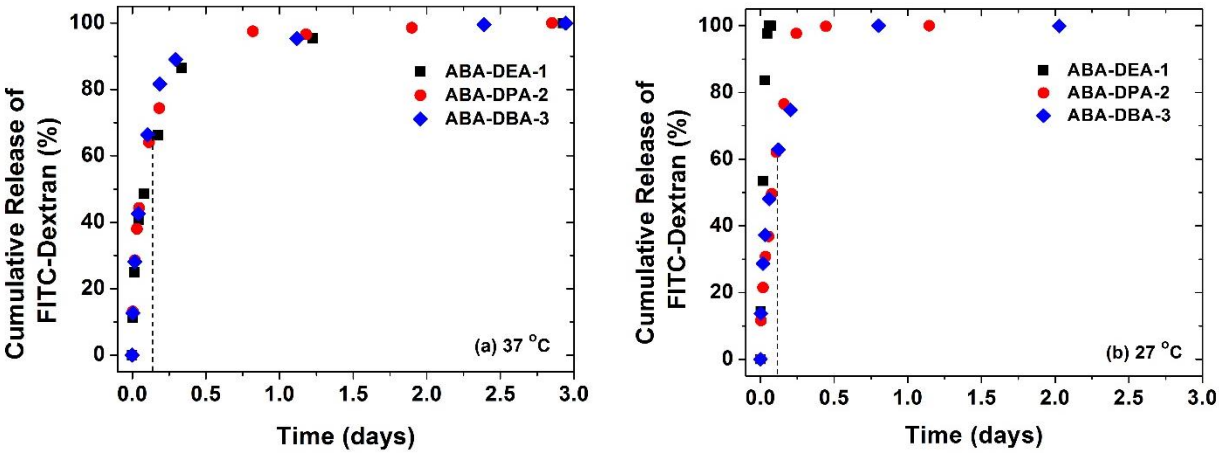

Figure 5.8. Cumulative release of FITC-dextran (%) over time from 10 wt % ABA-DEA-1 (■), **A**BA-DPA-2 (●), and ABA-DBA-3 (♦) micellar hydrogels at 37 °C (a) and 27 °C (b).

same for the three gels; nearly all FITC-dextran was released into the surrounding medium after one day with little noticeable dissolution of either gel during that time. It appeared that the diffusion of FITC-dextran from the hydrogels to the release media was the dominant process and the dissolution rates of hydrogels had little contribution to the release of FITC-dextran. Most likely, this is because the size of dextran is smaller than the mesh size of the micellar hydrogels of all three polymers.

We then examined the release behavior of FITC-dextran from three micellar gels at 27 °C; the data are shown in Figure 5.8b. While the release rates of FITC-dextran from ABA-DPA-2 and ABA-DBA-3 gels were similar to those at 37 °C as indicated by the dash lines in Figure 5.8a and 5.8b, the release of dextran from the ABA-DEA-1 was significantly faster and was complete within 1.5 h. Apparently, for ABA-DEA-1, the dissolution of the gel and the diffusion of FITC-dextran both contributed to the release of FITC-dextran. As mentioned earlier, the sol-gel transitions of 10 wt % aqueous solutions of ABA-DEA-1, ABA-DPA-2, and ABA-DBA-3 at pH 5.5 were ~ 37, 34, and 29 °C, respectively, which were estimated from rheological data (Figure 5.6). Because these values are all above the release temperature of 27 °C, the observations for ABA-DPA-2 and ABA-DBA-3 hydrogels are somewhat unexpected. We speculate that the dissolution rates of these two gels at 27 °C were smaller compared with the diffusion rate of FITC-dextran. Consequently, the release of dextran at this temperature was still dominated by the diffusion. In addition, we believe that the dissolution rates are not only related to the sol-gel transition temperatures, but also depend on the hydrophobicity of the thermosensitive outer blocks of ABA triblock copolymers. Indeed, we observed no noticeable changes for the gels of ABA-DPA-2 and ABA-DBA-3 at 27 °C after 45 min, but the gel of ABA-DEA-1 dissolved appreciably after the same period of time and had completely dissolved after 1 h 25 min. For ABA-DPA-2 at 27 °C, noticeable gel dissolution

occurred after 1 h 20 min, and the gel was completely dissolved after 10 h 40 min. No noticeable dissolution of the ABA-DBA-3 gel at 27 °C had occurred after 2 days.

5.3.5. Stability of a 10 wt % Aqueous Solution of ABA-DEA-1 at Low pH

Ester groups are known to be susceptible to hydrolysis in aqueous solution, especially at extreme pH values. To test the stability of the ester moieties in the ABA triblock copolymers towards hydrolysis, we prepared a 10 wt % aqueous solution of ABA-DEA-1 in the 20 mM phosphate buffer and adjusted the pH to 3.20 with 1.0 M HCl. The solution, a viscous sol at room temperature, was stored at room temperature for eight months. The pH was then adjusted with 1.0 M KOH, and the sol-gel transition was examined at pH = 4.78 and pH = 10.67. $T_{\text{sol-gel}}$ was found through rheological measurements to be 38.9 and 13.0 °C at pH = 4.78 and 10.67, respectively. As shown in Figure 5.6, the two $T_{\text{sol-gel}}$ values lie right on the original $T_{\text{sol-gel}}$ vs. pH curve for ABA-DEA-1. The transition from a clear sol to a clear gel was observed visually through gradual heating of the solution in a water bath, and optical photographs are shown in Figure 5.9. Both rheological measurements and vial inversion tests indicate that the storage at low pH for this amount of time had no effect on the sol-gel behavior of the ABA triblock copolymer. Furthermore, we dried a portion of the stored solution, and the ^{1}H NMR spectroscopy analysis showed that the ^{1}H NMR spectrum was essentially unchanged from the original spectrum, confirming the stability of the ABA-DEA-1 copolymer at low pH. The rheological data and the ^{1}H NMR spectrum can be found in Appendix D.

5.4. Conclusions

We synthesized a series of doubly responsive ABA triblock copolymers with the thermosensitive outer blocks incorporated with ~ 5 mol % of pH-responsive tertiary amine units.

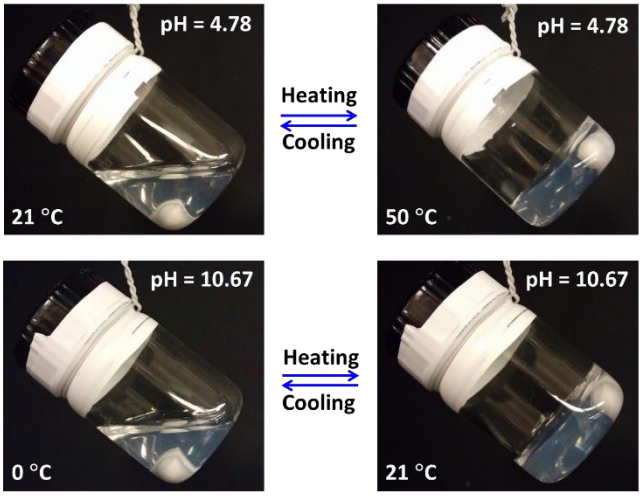

Figure 5.9. Optical photographs showing the sol-gel transitions at pH = 4.78 and pH = 10.67 of a 10 wt % aqueous solution of ABA-DEA-1 in a 20 mM phosphate buffer upon temperature changes. The solution had been stored for eight months at pH = 3.20 before the pH was adjusted to 4.78 and 10.67.

These copolymers were prepared from a difunctional PEO macroinitiator with a molecular weight of 20000 g/mol by ATRP of a mixture of DEGMMA, DEGEMA, and either DEAEMA, DPAEMA, or DBAEMA in anisole at 60 °C using CuBr/HMTETA as catalyst. The molecular weights and the chain lengths of the thermosensitive outer blocks of the obtained five ABA triblock copolymers were very similar, and so were the molar contents of tertiary amine units. Using rheological measurements, we investigated the effect of the incorporated different tertiary amine monomers on thermally induced sol-gel transitions of the 10 wt % aqueous solutions of these copolymers in a 20 mM phosphate buffer. For all ABA triblock copolymers, the $T_{\text{sol-gel}}$ vs. pH curves exhibited a sigmoidal shape. The $T_{\text{sol-gel}}$ increased with decreasing pH because of the gradual protonation of tertiary amine groups in the thermosensitive outer blocks; the changes were small on both high and low pH value sides. Furthermore, we found that at each pH value, the $T_{\text{sol-gel}}$ decreased with increasing the hydrophobicity of the incorporated tertiary amine monomer and that upon decreasing the solution pH, the onset pH value for the $T_{\text{sol-gel}}$ to begin to increase noticeably was lower for the more hydrophobic tertiary amine-containing copolymer. Using fluorescence spectroscopy, we examined the effect of the incorporated tertiary amine monomers on the release behavior of FITC-dextran from 10 wt % aqueous gels in an acidic medium at 37 and 27 °C. The release profiles for ABA-DEA-1, ABA-DPA-2, and ABA-DBA-3 at 37 °C were essentially the same, suggesting that the release was dominated by the diffusion of FITC-dextran. At 27 °C, the release of FITC-dextran was much faster for ABA-DEA-1, indicating that both diffusion and gel dissolution contributed to the release of FITC-dextran at this temperature. We also found that the polymer was stable after the 10 wt % aqueous solution of ABA-DEA-1 in a phosphate buffer with pH of 3.20 was stored at room temperature for eight months. The findings

from this study could be used for designing stimuli-responsive injectable hydrogel drug delivery systems.

References

1. Hamley, I. W. *Block Copolymers in Solution: Fundamentals and Applications*; John Wiley & Sons: Chichester, 2005.
2. Gil, E. S.; Hudson, S. M. *Prog. Polym. Sci*. **2004**, *29*, 1173–1222.
3. Dimitrov, I.; Trzebicka, B.; Müller, A. H. E.; Dworak, A.; Tsvetanov, C. B. *Prog. Polym. Chem.* **2007**, *32*, 1275–1343.
4. Joo, M. K.; Park, M. H.; Choi, B. G.; Jeong, B. *J. Mater. Chem*. **2009**, *19*, 5891–5905.
5. He, C. L.; Kim, S. W.; Lee, D. S. *J. Controlled Release* **2008**, *127*, 189–207.
6. Jeong, B.; Kim, S.W; Bae, Y. H. *Adv. Drug Delivery Rev*. **2002**, *54*, 37–51.
7. Yu, L.; Ding, J. *Chem. Soc. Rev*. **2008**, *37*, 1473–1481.
8. Ahn, S. -K.; Kasi, R. M.; Kim, S. -C.; Sharma, N.; Zhou, Y. *Soft Matter* **2008**, *4*, 1151–1157.
9. Li, C.; Tang, Y.; Armes, S. P.; Morris, C. J.; Rose, S. F.; Lloyd, A. W.; Lewis, A. L. *Biomacromolecules* **2005**, *6*, 994–999.
10. Li, C.; Buurma, N. J.; Haq, I.; Turner, C.; Armes, S. P. *Langmuir* **2005**, *21*, 11026–11033.
11. Ma, Y.; Tang, Y.; Billingham, N. C.; Armes, S. P. Lewis, A. L. *Biomacromolecules* **2003**, *4*, 864–868.
12. Castelletto, V.; Hamley, I. W.; Ma, Y.; Bories-Azeau, X.; Armes, S. P.; Lewis, A. L. *Langmuir* **2004**, *20*, 4306–4309.
13. Madsen, J.; Armes, S. P.; Bertal, K.; Lomas, H.; MacNeil, S.; Lewis, A. L. *Biomacromolecules* **2008**, *9*, 2265–2275.
14. Mortensen, K.; Brown, W.; Jørgensen, E. *Macromolecules* **1994**, *27*, 5654–5666.
15. Hietala, S.; Nuopponen, M.; Kalliomaki, K.; Tenhu, H. *Macromolecules* **2008**, *4*1, 2627–2631.

16. Kirkland, S. E.; Hensarling, R. M.; McConaught, S. D.; Guo, Y.; Jarrett, W. L.; McCormick, C. L. *Biomacromolecules* **2008**, *9*, 481–486.

17. Iatridi, Z.; Mattheolabakis, G.; Avgoustakis, K.; Tsitsilianis, C. *Soft Matter* **2011**, *7*, 11160–11168.

18. Li, C.; Madsen, J.; Armes, S. P.; Lewis, A. L. *Angew. Chem., Int. Ed.* **2006**, *45*, 3510–3513.

19. Sun, K. H.; Sohn, Y. S.; Jeong, B. *Biomacromolecules* **2006**, *7*, 2871–2848.

20. Vogt, A. P.; Sumerlin, B. S. *Soft Mater* **2009**, *5*, 2347–2351.

21. Woodcock, J. W.; Wright, R. A. E.; Jiang, X. G.; O'Lenick, T. G.; Zhao, B. *Soft Matter* **2010**, *6*, 3325–3336.

22. Anderson, B. C.; Cox, S. M.; Bloom, P. D.; Sheares, V. V.; Mallapragada, S. K. *Macromolecules* **2003**, *36*, 1670–1676.

23. Determan, M. D.; Guo, L.; Thiyagarajan, P.; Mallapragada, S. K. *Langmuir* **2006**, *22*, 1469–1473.

24. Shim, W. S.; Yoo, J. S.; Bae, Y. H.; Lee, D. S. *Biomacromolecules* **2005**, *6*, 2930–2934.

25. Shim, W. S.; Kim, S. W.; Lee, D. S. *Biomacromolecules* **2006**, *7*, 1935–1941.

26. Dayananda, K.; Pi, B. S.; Kim, B. S.; Park, T. G.; Lee, D. S. *Polymer* **2007**, *48*, 758–762.

27. Park, S. Y.; Lee, Y.; Bae, K. H.; Ahn, C. H.; Park, T. G. *Macromol. Rapid Commun.* **2007**, *28*, 1172–1176.

28. Suh, J. M.; Bae, S. J.; Jeong, B. *Adv. Mater.* **2005**, *17*, 118–120.

29. Huynh, D. P.; Nguyen, M. K.; Kim, B. S.; Lee, D. S. *Polymer* **2009**, *50*, 2565–2571.

30. Schmalz, A.; Schmalz, H.; Müller, A. H. E. *Soft Matter* **2012**, *8*, 9436–9445.

31. O'Lenick, T. G.; Jiang X. G.; Zhao, B. *Langmuir* **2010**, *26*, 8787–8796.

32. O'Lenick, T. G.; Jin, N. X.; Woodcock, J. W.; Zhao, B. *J. Phys. Chem. B.* **2011**, *115*, 2870–2881.

33. Zhou, K. J.; Wang, Y. G.; Huang, X. N.; Luby-Phelps, K..; Sumer, B. D.; Gao, J. M. *Angew. Chem., Int. Ed.* **2011**, ***50,*** 6109–6114**.**

34. Han, S.; Hagiwara, M.; Ishizone, T. *Macromolecules* **2003**, *36*, 8312−8319.

35. Ishizone, T.; Seki, A.; Hagiwara, M.; Han, S.; Yokoyama, H.; Oyane, A.; Deffieux, A.; Carlotti, S. *Macromoleucles* **2008**, *41*, 2963–2967.

36. Li, D. J.; Jones, G. J.; Dunlap, J. R.; Hua, F. J.; Zhao, B. *Langmuir* **2006**, *22*, 3344–3351.

37. Lutz, J.-F.; Hoth, A. *Macromolecules* **2006**, *39*, 893–896.

38. Jin, N. X.; Morin, E. A.; Henn, D. M.; Cao, Y.; Woodcock, J. W.; Tang, S. C.; He, W.; Zhao, B. *Biomacromolecules* **2013**, *14*, 2713–2723.

39. Jiang, X. G.; Jin S.; Zhong, Q. X.; Dadmun, M. D.; Zhao, B. *Macromolecules* **2009**, *42*, 8468–8476.

40. Feil, H.; Bae, Y. H.; Feijen, J.; Kim, S. W. *Macromolecules* **1993**, 26, 2496–2500.

41. Noro, A.; Matshushita, Y.; Lodge, T. P. *Macromolecules* **2009**, *42*, 5802−5810.

42. Zhao, B.; Moore, J. S. *Langmuir* **2001**, *17*, 4758–4763.

43. The work presented in this chapter has been published as an article:

    Henn, D. M.; Wright, R. A. E.; Woodcock, J. W.; Hu, B.; Zhao, B. *Langmuir* **2014**, *30*, 2541-2550.

Appendix D

for

Chapter 5: Tertiary Amine-Containing Thermo- and pH-Sensitive Hydrophilic ABA Triblock Copolymers: Effect of Different Tertiary Amines on Thermally Induced Sol-Gel Transitions

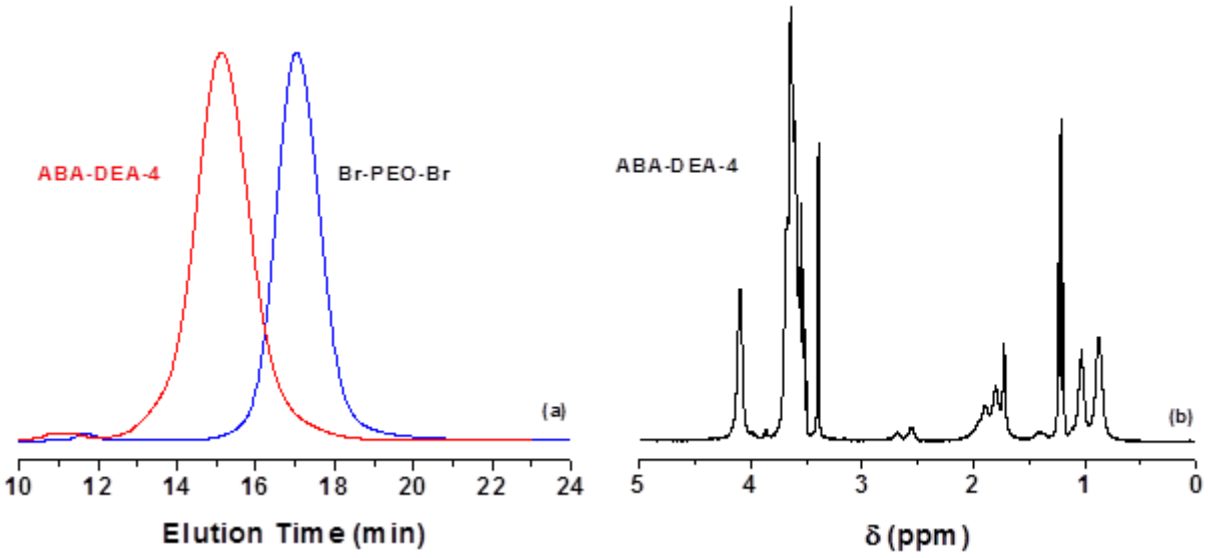

Figure D1. (A) SEC traces of difunctional macroinitiator Br-PEO-Br and P(DEGMMA-*co*-DEGEMA-*co*-DEAEMA)-*b*-PEO-*b*-P(DEGMMA-*co*-DEGEMA-*co*-DEAEMA) (ABA-DEA-4). (B) ^{1}H NMR spectrum of ABA-DEA-4 ($CDCl_3$ as solvent).

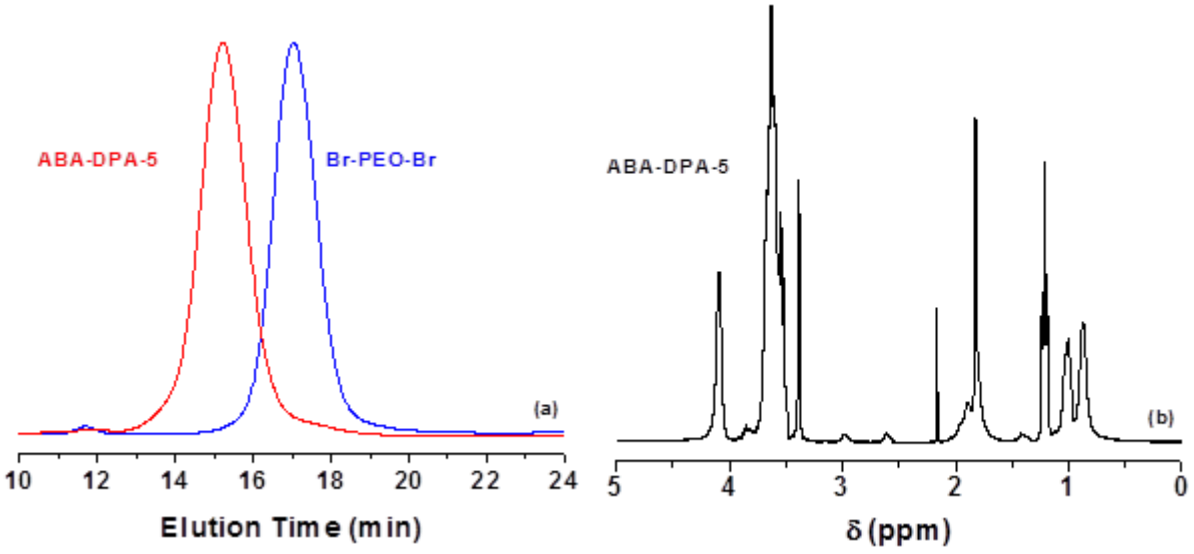

Figure D2. (A) SEC traces of difunctional macroinitiator Br-PEO-Br and P(DEGMMA-*co*-DEGEMA-*co*-DPAEMA)-*b*-PEO-*b*-P(DEGMMA-*co*-DEGEMA-*co*-DPAEMA) (ABA-DPA-5). (B) ^{1}H NMR spectrum of ABA-DPA-5 ($CDCl_3$ as solvent).

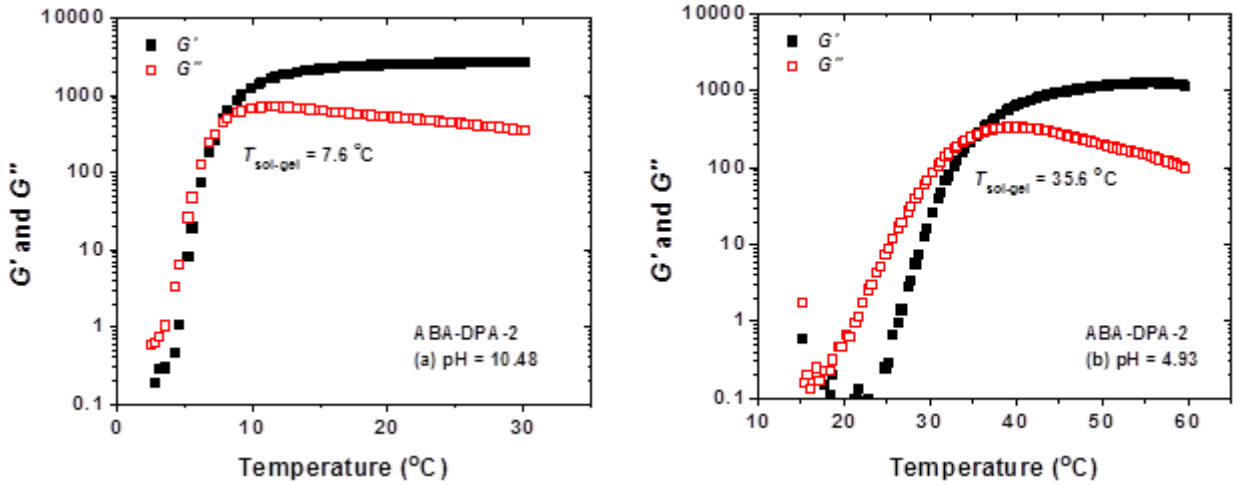

Figure D3. Plot of dynamic storage modulus *G'* (■) and dynamic loss modulus *G''* (□) versus temperature for a 10 wt % aqueous solution of ABA-DPA-2 with (a) pH = 10.48 and (b) pH = 4.93. The data were collected from temperature ramp experiments performed by using a fixed frequency of 1 Hz, a strain amplitude of 1.0 %, and a heating rate of 3 °C/min.

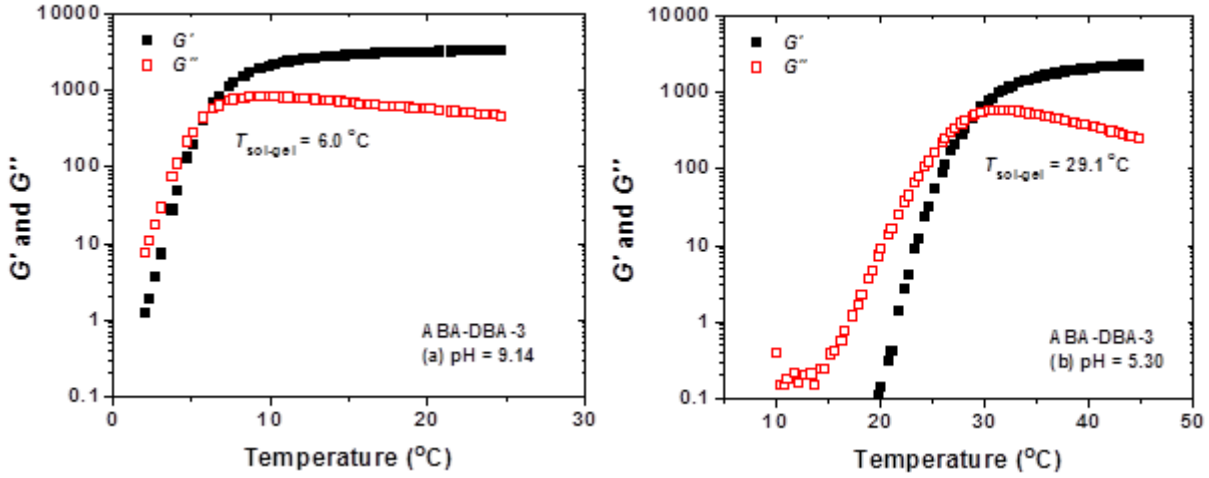

Figure D4. Plot of dynamic storage modulus *G'* (■) and dynamic loss modulus *G''* (□) versus temperature for a 10 wt % aqueous solution of ABA-DBA-3 with (a) pH = 9.14 and (b) pH = 5.30. The data were collected from temperature ramp experiments performed by using a fixed frequency of 1 Hz, a strain amplitude of 1.0 %, and a heating rate of 3 °C/min.

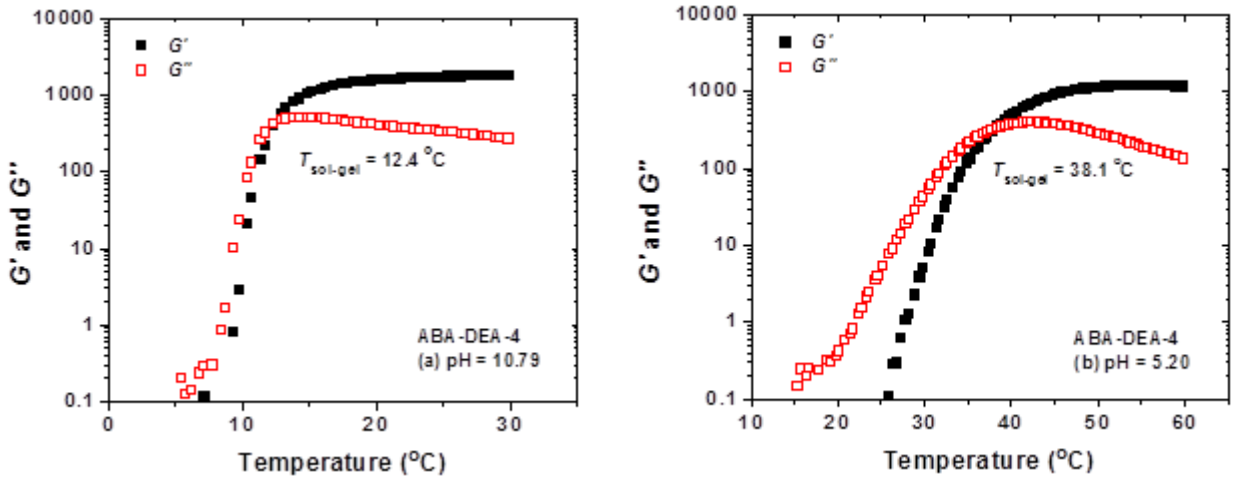

Figure D5. Plot of dynamic storage modulus *G'* (■) and dynamic loss modulus *G''* (□) versus temperature for a 10 wt % aqueous solution of ABA-DEA-4 with (a) pH = 10.79 and (b) pH = 5.20. The data were collected from temperature ramp experiments performed by using a fixed frequency of 1 Hz, a strain amplitude of 1.0 %, and a heating rate of 3 °C/min.

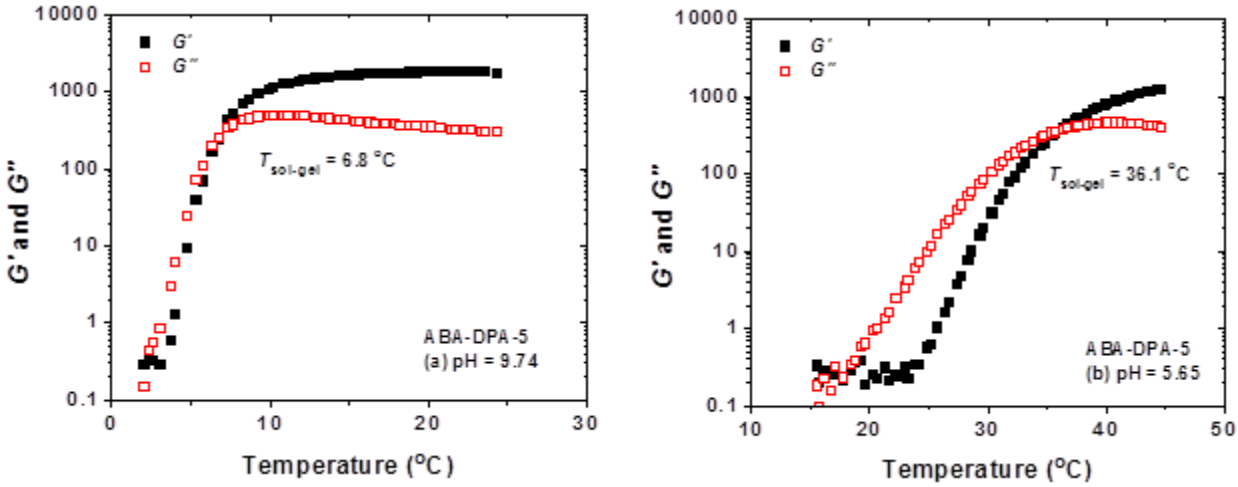

Figure D6. Plot of dynamic storage modulus *G'* (■) and dynamic loss modulus *G''* (□) versus temperature for a 10 wt % aqueous solution of ABA-DPA-5 with (a) pH = 9.74 and (b) pH = 5.65. The data were collected from temperature ramp experiments performed by using a fixed frequency of 1 Hz, a strain amplitude of 1.0 %, and a heating rate of 3 °C/min.

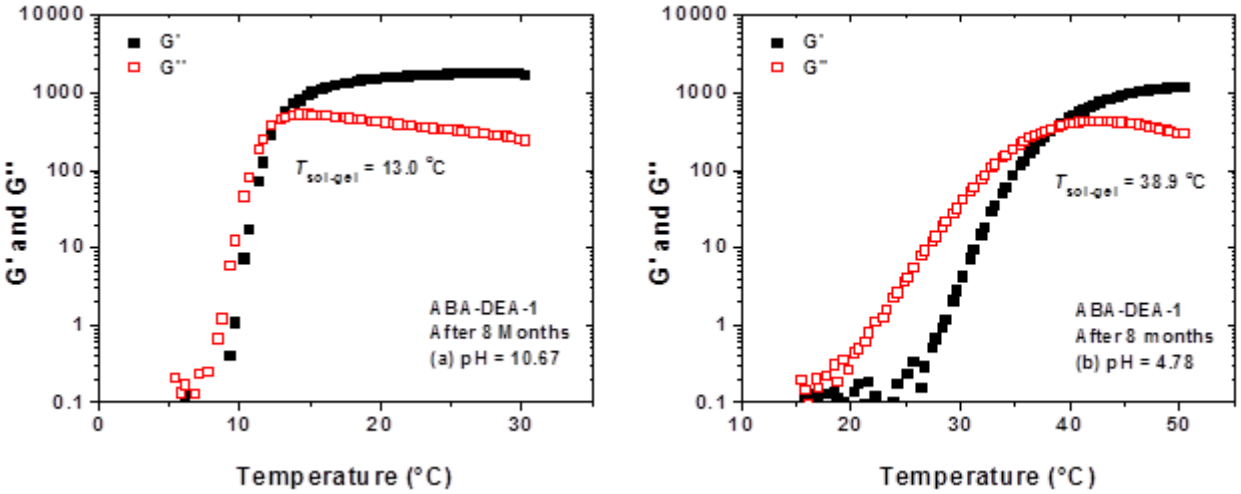

Figure D7. Plot of dynamic storage modulus *G'* (■) and dynamic loss modulus *G''* (□) versus temperature for a 10 wt % aqueous solution of ABA-DEA-1 with (a) pH = 10.67 and (b) pH = 4.78 after storage at pH = 3.20 and room temperature for eight months. The data were collected from temperature ramp experiments performed by using a fixed frequency of 1 Hz, a strain amplitude of 1.0 %, and a heating rate of 3 °C/min.

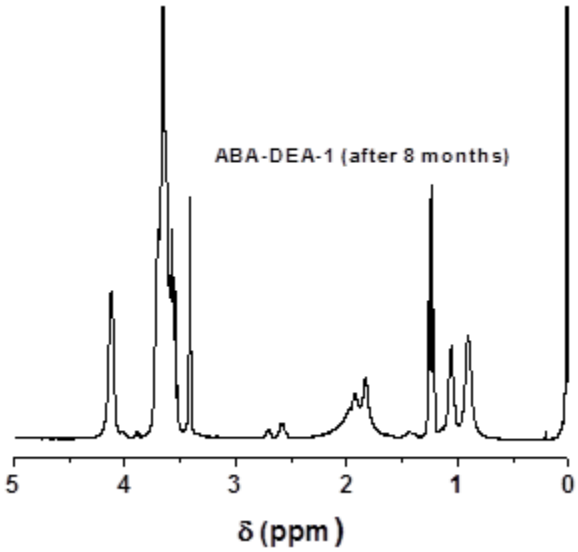

Figure D8. ^{1}H NMR spectrum of ABA-DEA-1 from a 10 wt % aqueous solution of ABA-DEA-1 in a 20 mM phosphate buffer after storage at pH = 3.20 and room temperature for eight months ($CDCl_3$ as solvent).

Chapter 6: Conclusions and Future Work

This dissertation work focused on the synthesis and behavior of stimuli-responsive linear molecular brushes with an emphasis on stimuli-induced morphological changes of single brush molecules in dilute aqueous solution. A “grafting to” method was developed in Chapter 2 using a combination of “living”/controlled polymerization techniques and CuAAC “click” coupling reactions, which was extended to the synthesis of stimuli-responsive homografted (Chapter 3) and binary heterografted (Chapter 4) molecular brushes. Their stimuli-responsive properties in dilute aqueous solution were investigated using visual inspection, DLS, and AFM. Chapter 5 shifted the focus away from molecular brushes with a study of thermally induced sol-gel transitions of moderately concentrated aqueous solutions of thermo- and pH-responsive hydrophilic ABA triblock copolymers.

Of the three strategies available for the synthesis of molecular bottlebrushes, namely “grafting from,” “grafting to,” and “grafting through,”[1,2] the “grafting to” strategy is desirable due to the ability to readily prepare brushes of different compositions depending on the identity and relative amounts of side chains added to the reaction feed. For this reason, we set out in Chapter 2 to develop a robust grafting to method that could later be used for the synthesis of stimuli-responsive molecular brush of varying types. A new azide-containing backbone polymer with a triethylene glycol spacer was prepared by ATRP of a silyl ether protected monomer, followed by deprotection, tosylation, and finally substitution with sodium azide. Two backbone polymers with DPs of 527 and 800 were prepared with high degrees of azide functionality. Well-defined molecular brushes were prepared by CuAAC “click” reactions between the azide-containing backbones and alkyne end-functionalized PEO homopolymers with molecular weights of 2 and 5 kDa as model side chains. High grafting densities were achieved when an approximately 1 : 2 molar ratio of backbone monomer units to side chains was used, and the grafting density could be

reduced by lowering this ratio. The synthesis of densely grafted “worm-like” molecular brushes was directly confirmed by AFM.

This “grafting to” methodology was utilized in Chapter 3 to synthesize homografted stimuli-responsive molecular brushes with side chains composed of either thermosensitive poly(di(ethylene glycol) ethyl ether acrylate) (PDEGEA), thermo- and light-responsive poly((di(ethylene glycol) methyl ether acrylate)-*co*-(*o*-nitrobenzyl acrylate)) (P(DEGMA-*co*-NBA)), or pH-responsive poly(*N*,*N*-diethylaminoethyl methacrylate) (PDEAEMA). The same azide-functionalized backbone polymers with DPs of 527 and 800 that were prepared in Chapter 2 were used. Either ATRP or RAFT polymerization was employed to prepare alkyne end-functionalize side chains from an alkyne-functionalized initiator or chain transfer agent. High grafting densities could be achieved even for these more sterically-hindered stimuli-responsive polymers, although brushes composed of PDEAEMA, a methacrylate, were less densely grafted compared to PDEGEA and P(DEGMA-*co*-NBA), both acrylates. From a series of PDEGEA brushes, we showed that the side chain length did not have a large effect on grafting density when a molar ratio of backbone monomer units to side chains was approximately 1 : 2, and similar to PEO brushes, lowering this ratio resulted in lower grafting densities. Stimuli-responsive properties of PDEGEA, P(DEGMA-*co*-NBA), and PDEAEMA molecular bottlebrushes were investigated by visual inspection and DLS. For more concentrated (~1 mg/g) solutions of PDEGEA and P(DEGMA-*co*-NBA) brushes in water, a clear-to-cloudy transition was observed upon increasing the temperature above the LCST of side chains. More dilute solutions (0.2 mg/g) underwent unimolecular collapse without aggregation as observed by DLS as the temperature was increased. The transition temperature of P(DEGMA-*co*-NBA) brushes was increased by 16 °C upon photocleavage of the hydrophobic *o*-nitrobenzyl groups with longwave UV light. PDEAEMA

brushes in 5 mM KH_2PO_4 buffer solution exhibited a decrease in size as the pH was increased but underwent aggregation and precipitation even at very low polymer concentrations (0.002 mg/g).

In Chapter 4, we expanded the scope to binary heterografted molecular brushes that contained water-soluble PEO (2 kDa) as well as either thermosensitive PDEGEA, pH-responsive PDEAEMA, or light-responsive PNBA side chains randomly distributed along the backbone. Only the longer azide-functionalized backbone with a DP of 800 was employed in order to achieve high aspect ratio brushes for which stimuli-induced shape transitions would be more readily observed. A feed molar ratio of approximately 0.6 : 0.4 for PEO to the other (stimuli-responsive) side chain polymer was used, and the composition of the purified brushes was very closed to that of the feed, except for the PEO/PDEAEMA brush, which exhibited a higher amount of PEO and a slightly lower grafting density. Compared to homografted brushes described in Chapter 3, the collapsed state of heterografted brushes was found to be stabilized by the PEO side chains as designed and expected. Stimuli-induced size changes were studied by DLS, and we used AFM to directly observe shape transitions for each brush sample from the extended worm-like morphology to the collapsed, globular state by changing environmental conditions. Finally, we demonstrated the ability to exploit these stimuli-induced morphological transitions to control molecular interactions between binary heterografted molecular brushes and their environment. PDEGEA side chains were incorporated with a small amount of a biotin-containing monomer (BA) and a fluorescent monomer (NBDA), and binary heterografted molecular brushes were synthesized using PEO (5 kDa) and P(DEGEA-*co*-BA-*co*-NBDA) side chains. Aqueous solutions of PEO/P(DEGEA-*co*-BA-*co*-NBDA) molecular brushes and rhodamine-labelled avidin, which is known to strongly complex biotin, were heterografted at 40 °C such that the biotin-containing side chains were collapsed and shielded from the environment by the PEO corona. Using a decrease in temperature

to trigger "unraveling" of the brushes, an immediate significant increase in binding between avidin and the extended biotin-containing brushes was observed by fluorescence spectroscopy.

Finally, Chapter 5 departs from the theme of molecular brushes to stimuli-responsive hydrogels based on ABA triblock copolymers, composed of a PEO central B block and thermo- and pH-sensitive outer A blocks.[3] A series of tertiary amine-containing ABA triblock copolymers were prepared from a difunctional PEO macroinitiator by ATRP of methoxydi(ethylene glycol) methacrylate (DEGMMA) and ethoxydi(ethylene glycol) methacrylate (DEGEMA) and a small amount of either DEAEMA, *N*,*N*-diisopropylaminoethyl methacrylate (DPAEMA), or *N*,*N*-di(*n*-butyl)aminoethyl methacrylate (DBAEMA). The effect of pH on the sol-gel transitions of 10 wt % aqueous solutions of the copolymers in a phosphate buffer was investigated using rheometry. The effect of different tertiary amines on the release behavior of FITC-dextran from micellar hydrogels of these copolymers in acidic media was also studied.

Stimuli-responsive polymers offer exciting opportunities for the design of functional soft materials.[4-9] This dissertation work illustrates how stimuli-responsive molecular bottlebrushes provide a unique framework for synthetic soft organic materials whose molecular structures can be precisely controlled to exhibit morphological changes in response to environmental triggers. Future work along this direction could include a study of the effect of the relative amounts of water-soluble and stimuli-responsive side chain polymers in binary heterografted molecular brushes on the stimuli-induced morphological transitions. For example, the work presented in Chapter 4 showed that similar amounts of PEO and the other side chain polymer resulted in stimuli-induced worm-to-sphere transitions. Perhaps a relatively low amount of stimuli-responsive side chains would result in inward collapse of the responsive chains upon application of the stimulus without a significant change in overall morphology. In this case, one could imagine a cylindrical

hydrated brush with small hydrophobic “pockets” composed of the collapsed responsive chains. Other future prospects include studies on the synthesis and behavior of non-linear stimuli-responsive brushes, such as star or cyclic brushes.

References

1. Sheiko, S. S.; Sumerlin, B. S.; Matyjaszewski, K. *Prog. Polym. Sci.* **2008**, *33*, 759-785.
2. Lee, H.; Pietrasik, J.; Sheiko, S. S.; Matyjaszewski, K. *Prog. Polym. Sci.* **2010**, *35*, 24-44.
3. Henn, D. M.; Wright, R. A. E.; Woodcock, J. W.; Hu, B.; Zhao, B. "Tertiary Amine-Containing Thermo- and pH-Sensitive Hydrophilic ABA Triblock Copolymers: Effect of Different Tertiary Amines on Thermally Induced Sol-Gel Transitions", *Langmuir* **2014**, *30*, 2541-2550.
4. Jin, N. X.; Morin, E. A.; Henn, D. M.; Cao, Y.; Woodcock, J. W.; Tang, S. C.; He, W.; Zhao, B. "Agarose Hydrogels Embedded with pH-Responsive Diblock Copolymer Micelles for Triggered Release of Substances", *Biomacromolecules* **2013**, *14*, 2713-2723.
5. Hu, B.; Henn, D. M.; Wright, R. A. E.; Zhao, B. "Hybrid Micellar Hydrogels of a Thermosensitive ABA Triblock Copolymer and Hairy Nanoparticles: Effect of Spatial Location of Hairy Nanoparticles on Gel Properties", *Langmuir* **2014**, *30*, 11212-11224.
6. Wright, R. A. E.; Hu, B.; Henn, D. M.; Zhao, B. "Reversible Sol-Gel Transitions of Aqueous Dispersions of Silica Nanoparticles Grafted with Diblock Copolymer Brushes Composed of a Thermosensitive Inner Block and a Charged Outer Block", *Soft Matter* **2015**, *11*, 6808-6820.
7. Hu, B.; Wright, R. A. E.; Jiang, S. S.; Henn, D. M.; Zhao, B. "Hybrid Micellar Network Hydrogels of Thermosensitive ABA Triblock Copolymer and Polymer Brush-Grafted Nanoparticles: Effect of LCST Transition of Polymer Brushes on Gel Property", *Polymer* **2016**, *82*, 206-216.

8. Wright, R. A. E.; Henn, D. M.; Zhao, B. “Thermally Reversible Physically Crosslinked Hybrid Network Hydrogels Formed by Thermosensitive Hairy NPs”, *J. Phys. Chem. B* **2016**, *120*, 8036-8045.

9. He, L.; Hu, B.; Henn, D. M.; Zhao, B. “Influence of Cleavage of Photosensitive Group on Thermally Induced Micellization and Gelation of a Doubly Responsive Diblock Copolymer in Aqueous Solutions: A SANS Study”, *Polymer* **2016**, *105*, 25-34.

Vita

Daniel Mark Henn was born in Charlotte, North Carolina, U.S.A. in 1987. In May 2011, he received his B.S. degree in Chemistry from the University of Tennessee, Knoxville. He continued his education at UTK by enrolling as a graduate student in August of that year and soon joined Professor Bin Zhao's research group. His research work focused on the synthesis and behavior of stimuli-responsive linear molecular bottlebrushes as well as responsive block copolymer hydrogels. He received a Doctor of Philosophy Degree in Chemistry from the University of Tennessee, Knoxville in December, 2016.